

**Asymmetrical Flow Field-Flow-Fractionation in
Pharmaceutical Analytics**

-

**Investigations in Aggregation Tendencies of
Pharmaceutical Antibodies**

Dissertation

zur Erlangung des Doktorgrades der
Fakultät für Chemie und Pharmazie der
Ludwig-Maximilians-Universität München

vorgelegt von

Wolfgang Fraunhofer
aus Weiden i.d. Opf.

München 2003

Erklärung

Diese Dissertation wurde im Sinne von § 13 Abs. 3 und 4 der Promotionsordnung vom 29. Januar 1998 von Herrn Prof. Dr. G. Winter betreut.

Ehrenwörtliche Versicherung

Diese Dissertation wurde selbständig und ohne unerlaubte Hilfe angefertigt.

München, 6. Juni 2002

(Wolfgang Fraunhofer)

Dissertation eingereicht am:	10. Juni 2003
1. Berichterstatter:	Prof. Dr. G. Winter
2. Berichterstatter:	Prof. Dr. W. Friß

Tag der mündlichen Prüfung:	8. Juli 2003
-----------------------------	--------------

ACKNOWLEDGMENTS

Foremost, I wish to express my deepest appreciation to my supervisor, Prof. Dr. Gerhard Winter. I am much obliged to him for his professional guidance and his scientific support. On a personal note, I especially want to thank him for inspiring my interest in protein pharmaceuticals, for teaching me so much, and for keeping me on the straight and narrow.

I am extremely grateful to the Department of Pharmaceutical Development and Parenterals of Abbott GmbH & Co. KG, Ludwigshafen, Germany, for financial support. I would like to acknowledge Dr. Krause as well as Frau Baust, Dr. Dickes, Dr. Martin and Dr. Tschoepe for rendering every assistance and providing the basis for my feeling of being “within the team”, though I was working some miles apart from Ludwigshafen.

Postnova Analytics Europe, Landsberg/Lech, Germany, is acknowledged for assistance in the realm of field-flow fractionation. I am indebted to Dr. Klein for his steady support (which was requested short-term in most cases).

In addition, thanks are extended to Wyatt Technology Deutschland GmbH, Woldert, Germany, for enabling me to gain hands-on experience in light scattering. Special thanks to Dr. Roessner for introducing me into the secrets of MALS. I also enjoyed the philosophical discussions on our view of today’s world.

Furthermore, I would like to acknowledge Dr. Schuch, who is with the Department of Colloids and Surfaces at BASF AG, Ludwigshafen, Germany, for the practical introduction in field-flow fractionation and multi-angle light scattering at the early stages of this work.

I would like to thank Klaus Hellerbrand, who is with Scil Biomedicals GmbH, Martinsried, Germany, for his valuable advice during the microcalorimetric experiments.

Dr. Coester is acknowledged for providing me an insight into research on nanoparticles. Many thanks to Jan and Klaus for their support during the experiments on nanoparticle characterization. Jan, thanks to you for being considerate of my needs of AF4 seizure.

I am indebted to Christoph Mueck for introducing me into the Coulter technique. Christoph, I really enjoyed our collaboration during your four months’ stay in Munich.

Thanks are also extended to Prof. Dr. Bracher, PD Dr. Dirsch, Prof. Dr. Frieß, Prof. Dr. Reimann and Prof. Dr. Wagner for serving as members of my thesis advisor committee.

I enjoyed immensely working at the Department for Pharmaceutical Technology and Biopharmaceutics of the Munich Ludwig-Maximilians-University, what was mainly due to the cooperative and most convenient atmosphere. Anke, Sassie, Fritz, Ingo, Matthias, Ralf, Roland, and all the others, it was a pleasure to work with you. Maria, thank you so much for furnishing me with all the literature. Special thanks are extended to Silke, who had to cope with my bustling activity and nevertheless payed back with organization of laboratory, schedules and bureaucracy. Silke, I am joyfully looking forward to the reunions you most likely will arrange.

Table of Contents

Chapters	Page
THEORETICAL SECTION	
1 Introduction	1
1.1 Background	1
1.2 Rationale of this work	2
1.3 Organization of this thesis	3
2 The family of field-flow fractionation (FFF) techniques	4
2.1 Introduction and underlying principles	4
2.2 FFF techniques and modes of operation	7
2.3 Asymmetrical flow field-flow fractionation (AF4)	10
2.3.1 Channel set-up	11
2.3.2 Consideration of theoretical principles	13
2.3.3 Operational procedures	17
2.3.4 Applications of AF4	19
3 Protein aggregation in liquid protein pharmaceuticals	23
3.1 Introduction	23
3.2 Chemical instability	23
3.3 Aggregation - a consequence of physical instability	28
3.3.1 Random walks	28
3.3.2 Thermodynamics	29
3.3.3 The aggregation process	32
3.3.4 Theories on aggregation	34
3.3.5 Quantification of the aggregation rate	39
4 Multi-angle light scattering (MALS) in protein analytics	43
4.1 Introduction	43
4.2 Theoretical aspects	44
4.3 MALS in laboratory practice: online combination with FFF or HPLC	48
5 Summary	51
EXPERIMENTAL SECTION	
6 AF4 as analytical tool in protein aggregation analytics	53
6.1 Introduction	53
6.2 Evaluation of general AF4 applicability in protein analytics	53
6.2.1 Materials and methods	53
6.2.2 Results	56
6.3 Parameters of fractionation	61
6.3.1 Sample recovery	61
6.3.2 Elution order	66
6.4 Fractionation of protein specimen	71
6.4.1 Monomers, oligomers, soluble aggregates	71
6.4.2 High-molecular weight aggregates and precipitates	75
6.5 Characterization of protein solutions by AF4 and SE-HPLC: a comparative study	78
6.6 Summary	85

7 Analytics of pharmaceutical antibody solutions in siliconized syringes	88
7.1 Introduction	88
7.2 Analysis of syringe volumes by light obscuration	90
7.3 Detection of soluble aggregates	92
7.4 Development of AF4 application: aqueous silicone oil emulsions	95
7.5 Analysis of syringe volumes	99
7.6 The effect of silicone oil detachment on syringe frictional drags	108
7.7 Can protein drugs vanish within a syringe?	111
7.8 Summary	116
8 Characterization of gelatin nanoparticles by AF4	118
8.1 Introduction	118
8.2 Materials and methods	120
8.3 Analytics of gelatin raw material	121
8.4 Size-determination of unloaded/loaded nanoparticles	126
8.5 Determination of nanoparticle loading efficacy via AF4	129
8.6 Summary	133
9 Particulate matter in parenterals: a case study	135
9.1 Introduction	135
9.2 Background	136
9.3 Providing evidence of particulate matter	137
9.4 Investigations by SE-HPLC and SDS-PAGE	139
9.5 Microcalorimetric experiments	143
9.6 Particulate matter analysis by AF4/MALS and filtration	147
9.7 Summary and evaluation	153
10 Minimizing aggregation in antibody pharmaceuticals: a laboratory case study	155
10.1 Introduction	155
10.2 Formulation/stabilization of liquid protein pharmaceuticals: a short review	155
10.3 General experimental procedures	161
10.4 Evaluation of pH optimum	162
10.5 Stabilization by excipients	165
10.5.1 Surfactants	165
10.5.2 Polyols	169
10.5.3 Salts	173
10.6 Summary and discussion	174
11 Summary, conclusions and prospective	176
12 References	180
13 Publications and presentations associated with this work	213
14 Curriculum Vitae	215

**To my parents,
for their continued love**

1 Introduction

1.1 Background

It would be interesting to know whether S. H. Cohen and H. W. Boyer anticipated the impact of their 1973's discovery, that genes can be combined and arranged in new order in vitro, on today's spectrum of modern pharmaceuticals. Since then, the development of protein pharmaceuticals has undoubtedly been boosted by the advent of recombinant DNA technology. Thereby, the large-scale production of recombinant DNA based vaccines, antibodies, functional regulators, enzymes and the like became possible. And the scientific world is still in move: in June 2000, U.S. President Clinton announced the completion of the first survey of the entire human genome. As a consequence, a better understanding of the molecular basis of diseases and the disclosure of new targets for proteinic drugs took center stage of pharmaceutical scientists' hopes and expectations. Under these conditions, biopharmaceutical technology is considered to enjoy a magnificent prospect. The world market in recombinant drugs – struggling for US\$ 1.2bn in 1985 – totaled US\$ 27bn in 2001 and is forecasted to almost double to US\$ 50bn in 2010.

However, this growth phenomenon would level to a minor degree if the ground has been less well prepared: tremendous effort was put on the fields of pharmaceutical analytics and protein drug stabilization during the last two decades. High-sophisticated analytical methods accompany drug development and are a prerequisite to appropriate drug's R&D programs.

Both areas, protein analytics and protein aggregation interfere with each other in a most exciting way: on the one hand, the identification of intrinsic and extrinsic factors that contribute to the stabilization of protein drugs has provided valuable information for stabilizing protein pharmaceuticals (Wang, 1999). On the other hand, insufficient stabilization, facilitating aggregation processes, has to be unveiled in earliest stages in order to commence adequate counter measurements. Hence, pharmaceutical industries try to implement advanced up-to-date analytical techniques in aggregation identification and quantification.

The major obstacle to an overall quantification of protein aggregates is obvious: protein aggregates can be soluble or insoluble in nature, and most commonly – and for the pharmaceutical analyst most challenging – they do exist in parallel. Due to the underlying principles of the methods applied in aggregation analysis, either the soluble or the insoluble aggregate fraction can be separated and quantified. Quantification of insoluble aggregate specimen – often subsumed under particulate matter – is commonly performed by turbidity measurements or particle counting techniques, e.g., via light obscuration or Coulter principle. Moreover, filtration and centrifugation procedures may be applied to separate insoluble aggregates from soluble, native protein.

Referring to soluble aggregates, (polyacrylamide) gel electrophoresis (PAGE) and high pressure liquid chromatography (HPLC) are state-of-the-art techniques. While accurate determination of the aggregate amount subsequent to PAGE separation via densitometric detection is delicate, HPLC proved to be a sound method for soluble aggregate analysis. In case of aggregate determination based on size, the size-exclusion (SE) mode of HPLC is to be applied, whereas in reversed-phase (RP) mode isoforms of aggregates or covalent and non-covalent aggregates can be differentiated (Perlman and Nguyen, 1992; Shahrokh et al., 1994). However, both methods lack the possibility to analyze dissolved samples aside undissolved samples.

Almost coevally, the field-flow fractionation (FFF) technique entered the analytical stage in the 1960s, but with by far less success (Giddings, 1966). Considering the FFF's low recognition, the development that has taken place since then resulting in a diversity of different FFF methods – albeit promoted by only a few supporters – is all the more remarkably (Coelfen and Antonietti, 2000). That range of various FFF techniques was established in the early years, by this extending the assortment of sample components amenable to FFF separation considerably, i.e., encompassing a width from the lowest nm range up to ~100 μm . Given the sample dimensions in the arena of pharmaceutical protein drugs - varying between 1 – 10 nm by native state peptides and proteins, the two-digit nm range of soluble aggregates and several microns of insoluble aggregates –, FFF may be considered as ideal candidate for analysis of complex protein samples. However, only recently the optimization of FFF methodology and instrumentation, most notably of the subtechnique asymmetrical flow FFF (AF4) has taken place and should pave the way for a broader application in the pharmaceutical industry.

1.2 Rationale of this work

The major aim of this work was to comprehensively evaluate the applicability of AF4 in pharmaceutical protein analytics. Soluble and insoluble protein aggregates were to be separated from native protein monomers in a reproducible way in one single run. For a rational assessment of the results, AF4 data were compared to established methods in protein aggregation analysis, mainly SE-HPLC and light obscuration technique. To gain maximum information on the fractionated specimen, AF4 was to be coupled on-line with multi-angle light scattering (MALS).

Furthermore, the general applicability of AF4 in other closely related fields of pharmaceutical analytics was to be investigated and the provided data were to be assessed. Therefore, separation tasks in the field of parenterals and nanocolloids were approached presently considered to be impractical or, at least, highly challenging.

The investigations in protein aggregation analysis were augmented with an approach to optimize the liquid formulation of a therapeutic antibody. Via adequate selection of stabilizers

and assessment of appropriate excipient concentrations aggregation tendencies of the antibody were to be minimized.

1.3 Organization of this thesis

This thesis is divided into two main sections. The THEORETICAL SECTION starts with a general FFF overview in **Chapter 2**. In particular, inherent AF4 parameters and separation principles are presented. In **Chapter 3** the phenomenon of protein aggregation is reviewed. Besides, prevalent theories on aggregation are discussed and means of aggregation quantification are set out. **Chapter 4** focuses on the application of multi-angle light scattering in protein analytics and extensively surveys the theoretical aspects. The theoretical section is summarized in **Chapter 5**.

Chapter 6, which illustrates and exemplifies the evaluation of AF4 applicability in protein aggregation analytics, launches the EXPERIMENTAL SECTION. The following chapters present exclusive examples of how AF4 can be favorably applied to selected tasks in pharmaceutical analytics, e.g., analytics of antibody solutions in siliconized syringes (**Chapter 7**), gelatin nanoparticle characterization (**Chapter 8**), and particulate matter identification in parenterals (**Chapter 9**). The subject protein aggregation is specifically targeted by a laboratory case study described in **Chapter 10**. Besides a short review on formulation strategies of liquid protein pharmaceuticals an approach to reduce aggregation biases of a therapeutic antibody is presented. **Chapter 11** summarizes the experimental outcome, aims for appropriate conclusions and puts the results into perspective. **Chapter 12** is addressed to listen special and continuative literature referred to in the thesis.

2 The family of field-flow fractionation (FFF) techniques

2.1 Introduction and underlying principles

FFF occupies an unique niche in the field of analytical fractionations because it is the only technique being capable to separate materials over the entire colloidal size range with high resolution (Giddings, 1993). However, FFF operators agree that one major obstacle to a widespread FFF utilization is due to its greatest asset. That asset is its versatility, and – as in daily life – versatility comes with a price: there is no simple formula for choosing the proper FFF technique for a given application. Moreover, one has to understand the underlying mechanisms of the fractionation to approach successfully a separation problem by means of FFF (Jonsson, 2001). The fundamental principle of FFF is illustrated in Fig. 1.

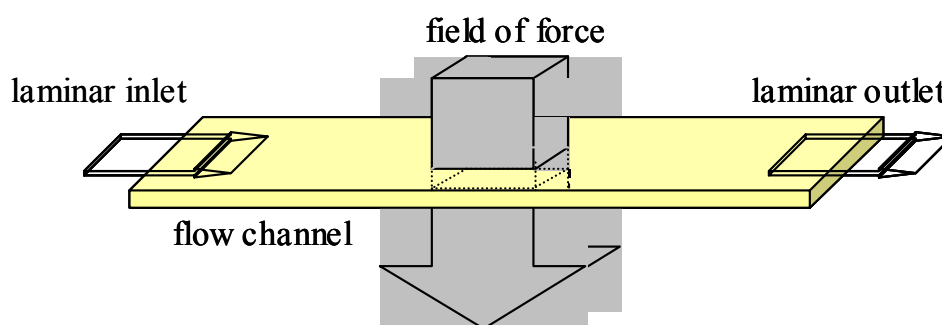


Fig. 1. Schematic separation principle of FFF.

An external field forces the sample components to accumulate at different levels in a channel. Since the flow velocities of the carrier liquid streaming through that channel correlate with those level heights, the sample components are transported with different speed, resulting in a component separation. However, this view would simplify matters in an unjustifiable way.

The sample separation is performed inside a narrow ribbon-like channel. This channel typically reveals dimensions of ± 50 cm in length and ± 2 cm in width, whereas the channel height can vary between $50 \mu\text{m}$ and $500 \mu\text{m}$. From the inlet, a carrier liquid is pumped through the channel, establishing a parabolic flow profile (laminar Newtonian flow) as in a capillary tube, propelling the samples towards the outlet (Huang, 1999; Bos and Tijssen, 1995). Perpendicular to the direction of the carrier liquid flow an external field is applied, forcing the sample components to accumulate at one of the channel walls, termed accumulation wall. Under “normal mode” or “Brownian mode” conditions, the sample components can be considered as non-interacting point masses, with their center of gravity near to the accumulation wall (van Asten, 1995). Due to the established concentration gradient, a diffusion flux in reverse direction, i.e., back into the interior of the channel, is induced according to Fick’s law. As a consequence of the two rivaling parameters – the exerted field of force and the opponent diffusion flux – a steady-state profile is

generated, and the equilibrium distributions of the sample components across the channel can be expressed by a mean layer thickness x , as illustrated in Fig. 2 (Coelfen and Antonietti, 2000; Giddings, 1991). Those analytes (like **a**) with distributions nearest to the accumulation wall are positioned in the slowest flow laminae of the parabolic laminar flow. Accordingly, they gradually separate from analytes (like **b**), which are positioned at more elevated levels in the channel, therefore eluting with faster laminae.

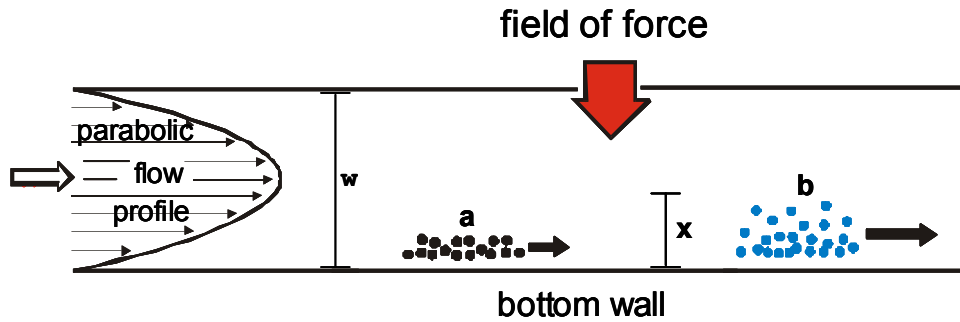


Fig. 2. Schematic representation of the separation of two components **a** and **b** via FFF across the parabolic flow profile within the channel.

Consequently, FFF can be considered as a hybrid of chromatography and field-driven methods such as electrophoresis and ultracentrifugation (Pauck and Coelfen, 1998; Li et al., 1990). Like chromatography, FFF is an elution technique with inherent differential flow displacement phenomena. On the other hand, like ultracentrifugation, FFF separation is based on an applied gradient or field of force.

Since that field of force is opposed by sample diffusion processes, the sample concentration c (relative to the wall concentration c_0) approaches an exponential function of the mean layer thickness x remote from the accumulation wall (Martin and Williams, 1992)

$$c = c_0 \exp\left(\frac{-x|U|}{D}\right) \quad (1)$$

where U represents the drift velocity of the sample induced by the external field. The diffusion coefficient D can be related to the frictional coefficient f by the Stokes-Einstein relationship

$$D = \frac{kT}{f} \quad (2)$$

where k is Boltzmann's constant and T is the temperature. The drift velocity U is correlated to the force F , which is exerted on the sample, by $U = F/f$. Furthermore, the parameter $l = D/|U|$ is introduced, with l representing the average sample-wall distance. Consequently, the relationship

$$l = \frac{kT}{F} \quad (3)$$

can be derived, expressing that the samples will be positioned proximate to the accumulation wall (low l) when exposed to vigorous forces. In order to provide optimal values of l , i.e., to guarantee appropriate sample levels for FFF experiments, the intensity of the external field can be varied. Accordingly, F can be altered proportionally and the precedent condition to ensure efficient FFF operations can be met: $w \gg l$. As the FFF accessories kits available provide almost any “ w ”, the wide application range of FFF becomes evident. Eq. (3) can be extended by the dimensionless parameter λ , leading to

$$\lambda = \frac{t_0}{t_r} = \frac{V_0}{V_r} = \frac{l}{w} = \frac{kT}{Fw} \quad (4)$$

where λ is a synonym for the retention ratio R , i.e., the retention time of an unretained sample component t_0 to the retention time of a retained sample component t_r , or equivalently in terms of retention volumes V_0/V_r . It is important to refer to the relationship $t_r = F$ given by Eq. (4), thereby implicating that the retention time of sample components can be assessed as desired by exerting expedient force intensities. Large analytes with inherent low values of their diffusion coefficients D will offer only slight resistance to exerted force intensities. In contrast, smaller analytes such as peptides or low molecular weight (lmw) proteins will counterbalance even extensive force fields, due to their high D values. This explains why it is usually more delicate to separate small sample specimen via FFF than to fractionate larger samples. As it will be shown in the experimental section, F can be increased to a level at which the elution of high molecular weight (hmw) samples is totally blocked. By monitoring of the channel effluent by adequate detection systems, the retention times of the analytes can be determined and sample compositions can be elucidated by straightforward FFF experiments.

The magnitude of F , which can be applied on the sample specimen, depends on the experimental arrangements of the various FFF techniques, i.e., the kind of field that is installed. Primarily four prominent FFF fields, introduced in Chapter 2.2, have become most relevant for scientific research - and are applied to an increasing extent in industrial practice (Janca, 1992). The common feature of all FFF subtechniques is the parabolic flow profile of the carrier liquid as the driving parameter of separation.

To keep up with completeness: a significant number of FFF techniques have been developed. However, some of those – although justified by special applications – attract scant attention or are to be qualified as “exotic”. Therefore, these techniques are described in the literature only sporadically, e.g., acoustic or photophoretic FFF (Coelfen and Antonietti, 2000).

2.2 FFF techniques and modes of operation

Since the theoretical fundament of **Sedimentation FFF** (SFFF) was grounded in the late 1960's and put into practice shortly thereafter, SFFF may be deemed one of the oldest FFF techniques (Yang et al., 1974; Berg and Purcell, 1967). SFFF experiments are performed in a channel constituted by two closely spaced parallel surfaces. When this channel is rotated in a centrifuge, dissolved and suspended analytes - which are more dense than the ambient mobile phase - are forced to migrate towards the outer wall. Correspondingly, if the sample is less dense than the ambient liquid, "floating" phenomena are to be observed, and those sample components accumulate at the inner wall, as illustrated in Fig. 3.

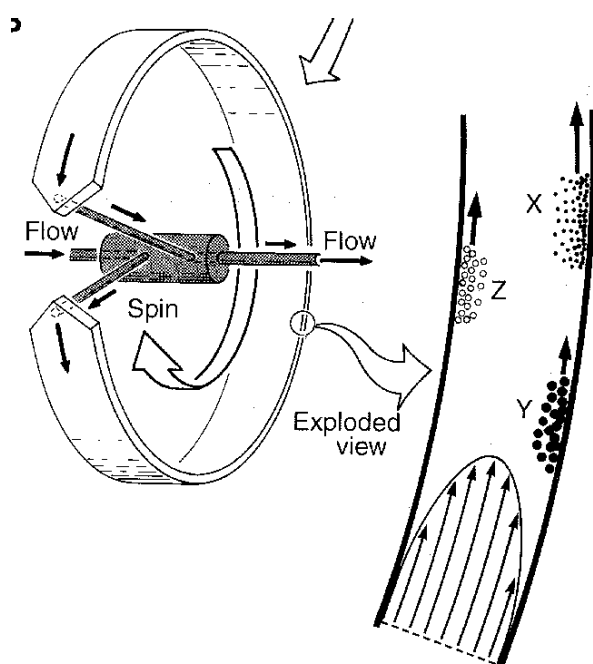


Fig. 3. Sedimentation FFF: Due to ultra-centrifugation, the separation is based on density differences between analyte specimen and the carrier liquid. Note that "floating" analytes (z) opposite the bands of denser samples (x, y), enabling fractionation of "floating" and "sinking" components simultaneously.

The limiting particle size for retention in SFFF depends on the maximum speed of the centrifuge, i.e., on the gravitational field exerted, and on density differences. Via modern SFFF equipment with inherent gravitational forces exceeding 100,000 g a broad range of materials of biological and industrial interest can be characterized. Furthermore, the aqueous carrier density can be varied towards lower densities by adding organic liquids. Vice versa, the density will increase if salts or sugars are added to aqueous liquids or if water is added to organic fluids, resp. (Moon, 2000; Kirkland et al., 1983). The theoretical principles of SFFF are summarized by Eq. (5)

$$F = \frac{\pi d_H^3 G |\Delta\rho|}{6} \quad (5)$$

with G symbolizing the centrifugal/gravitational acceleration, $|\Delta\rho|$ the density differences between the sample components and the solvent used, and d the effective spherical diameter of the sample component. Due to the high resolution potential of SFFF, typical applications are the

characterization of soil and sediment colloids, the separation of biopolymers and macromolecules, or cell sorting (Williams et al., 2002; Chen and Beckett, 2001; Kirkland et al., 1980).

Thermal FFF (ThFFF), is considered to be the oldest of all FFF methods. As a matter of fact, research in thermal diffusion started in 1856, when Ludwig observed the selective migration of compounds towards colder regions (Tyrell, 1961). In the 1960's, ThFFF was at first applied for the separation of polystyrenes; its broad applicability for the fractionation of various polymers was demonstrated in 1978 (Thompson et al., 1967; Giddings et al., 1978). The channel design of ThFFF is shown in Fig. 4.

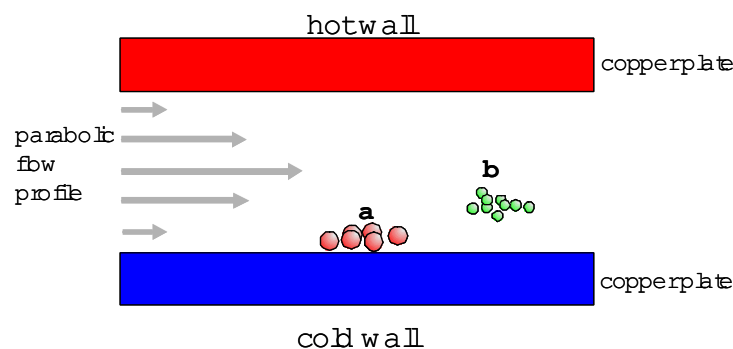


Fig. 4. Basic illustration of an ThFFF channel. Note that the sample components, e.g., lipophilic polymers, accumulate at the cold channel wall.

By exerting a large temperature difference across the channel the thermal diffusion effect is employed to concentrate the sample components – typically polymers and colloids – at the cold wall. Under normal operation, this temperature difference between the hot wall, heated with electric cartridges, and the water-cooled cold wall encompasses 100 °C. The applicability of ThFFF in aqueous systems is restricted due to the weak thermal diffusion of polymers in water. Therefore, particles and lipophilic polymers are favorably characterized in organic media (Schimpf, 2000a). Given the background of the numerous assumptions and approximations inherent to ThFFF, this method is judged to be the most complicated FFF subtechnique, though the effective driving force $|F|$ per analyte can be defined by the basic correlation

$$|F| = kT \frac{D_T}{D} \frac{dT}{dx} \quad (6)$$

where D_T is the thermal diffusion coefficient (Coelfen and Antonietti, 2000). Although considerable effort is invested in the subject, e.g., by the development of micro-channels with increased speed and resolution power, ThFFF will not gain acceptance in pharmaceutical analytics because of its inherent drawbacks due to the underlying principles. However, ThFFF occupies a niche in the spectrum of hmw polymer characterization, what is to be attributed to its unique separation mode (Lou, 2003; Janca, 2002; Sibbald et al., 2000).

In terms of its analytical properties, the **electrical FFF** (eFFFF) is discussed controversially. The prevalent eFFFF channel design utilizes two graphite plates, which serve a dual role of both channel wall and electrode, separated by a Teflon spacer (Caldwell and Gao, 1993). Exposing the $\sim 150\ \mu\text{m}$ wide channel to only a few volts gives rise to substantial effective field strengths in the order of $100 - 200\ \text{Vm}^{-1}$. To achieve fields of comparable strength in capillary electrophoresis, $20 - 30\ \text{kV}$ are to be provided. Moreover, electrophoretic separations lack the possibility to differentiate between particles of different size, but with similar surface charge density (Tri and Caldwell, 2000).

Since the electrical field E is related to the drift velocity U of a sample component with the electrophoretic mobility μ_e by $U = \mu_e E$, the force F exerted on the sample can be expressed as

$$\lambda = \frac{D}{\mu_e E w} \quad (7)$$

with regard to Eq. (3). What speaks in favor of the method is the simplicity of applying and programming E , as does the absence of any moving parts. The other side of the eFFFF medal is labeled with two major disadvantages: the electrode polarization limitates the carrier solutions which can be applied and, as a consequence, the sample materials that can be characterized by the technique (Caldwell, 2000a). Additionally, conductivity differences between the analytes and the carrier liquid influence the retention, what means, that sample concentration affects the data obtained (Palkar and Schure, 1997a; Palkar and Schure, 1997b; Coelfen and Antonietti, 2000). A trend is evident, that more effort will be put into further development of other FFF subtechniques.

The significant difference between **Flow FFF** (FIFFF) and the FFF subtechniques introduced above is that the separation field of force is established by a second stream of carrier liquid, pumped in vertical direction to the axial flow stream, as illustrated in Fig. 5.

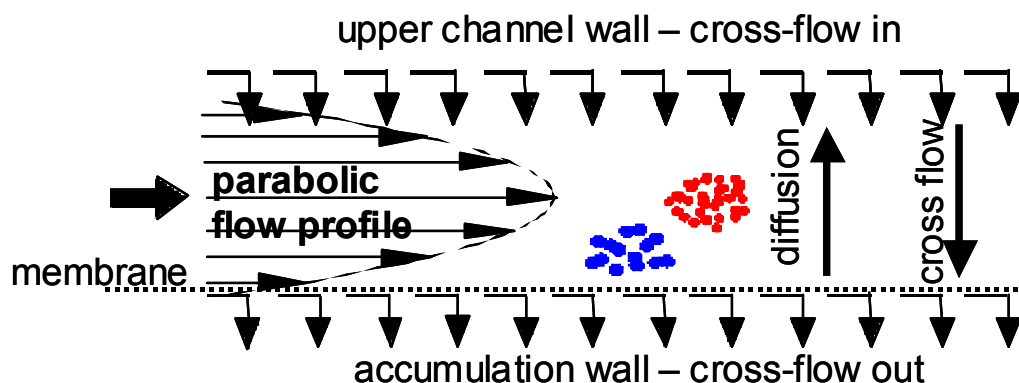


Fig. 5. Schematic representation of a Flow FFF channel. The position of sample specimen is determined by two independent flow streams, i.e., the axial carrier liquid flow and the vertical cross flow, propelling the sample components towards the accumulation wall.

In SFFF, TFFF and eFFFF, the sample separation is induced by external physical or chemical fields. Contrarily, in FIFFF this field is to be characterized as “internal”. The FIFFF experiments are performed in a symmetrical set-up, in which the channel walls consist of two porous frits. This “symmetrical” system was developed in the mid1970s (Giddings et al., 1976). The lower wall is covered by an ultrafiltration membrane, permeable only by carrier liquid, not by sample components. Provided by a separate pump, the cross flow enters the channel via the upper channel wall, crosses the channel interior and finally passes the accumulation wall, subsequent to passing an ultrafiltration membrane.

As the separation only relies on differences in diffusion coefficients, FIFFF is the most applicable FFF subtechnique. The wide applicability was demonstrated in characterizations of analytes ranging from solutes with inherent molar masses of ~ 500 g/mol and dimensions of < 2 nm up to particles with dimensions of $100 \mu\text{m}$ (Dycus, 1995). The lower size limit is determined by the molecular weight cut-off of the ultrafiltration membranes (~ 1 kDa), whereas the upper size limit is assessed by a threshold of about 20% of the channel height w (Williams, 2000).

The driving force of FIFFF separations, exerted on the analytes by the cross flow, can be mathematically expressed as

$$|F| = f|U| = 3\pi\mu d|U| = \frac{kT|U|}{D} \quad (8)$$

with d_H being the hydrodynamic diameter of the sample, and where the linear cross flow velocity $|U|$ can be classified as an experimental parameter. Eq. (8) reveals that – since U is exerted on each compound with identical intensity – the separation of sample components is only due to their inherent dimensions, i.e, their diffusion coefficients D .

The theoretical FIFFF principles were introduced in 1976 and, in the subsequent years, a broad variety of samples was exemplarily separated by means of FIFFF, covering polystyrene latexes, various proteins, viruses and macromolecules (Lee and Lightfoot, 1976; Giddings et al., 1977; 1978b; 1978c). In retrospect, the further development of FIFFF seems predicted, confirming the golden rule of science: new techniques attract more successful experiments, successful experiments attract more users, more users contribute new ideas. In case of FIFFF, Wahlund and Giddings helped to get a new idea accepted: the idea of an asymmetrical FIFFF channel set-up.

2.3 Asymmetrical flow field-flow fractionation (AF4)

The first approach to the AF4 principle was ventured in 1986, but due to technical “teething troubles” of that system, the actual break-through of AF4 can be set to 1987 (Granger et al., 1986; Wahlund and Giddings, 1987). AF4 draws a significant distinction to FIFFF in

revealing only one permeable wall, so that the carrier liquid can leave the channel solely via the accumulation wall to generate a cross flow.

2.3.1 Channel set-up

In contrast to symmetrical FIFFF, the upper wall in AF4 consists of transparent plexiglas (polymethylmethacrylate, PMMA), nonpermeable to the solvent (Fig. 6). The transparency of the upper wall allows visual observation of the channel interior, helping to cope with troubleshooting during experiments or enabling visual monitoring of colored sample separation. Due to the obvious differences between upper and bottom wall, “asymmetrical” was prefixed to the term AF4.

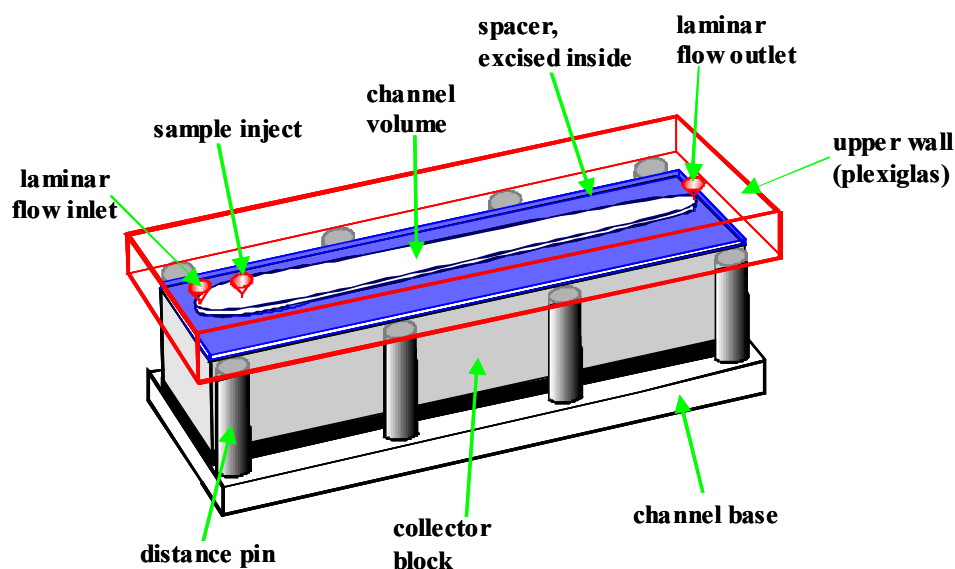


Fig. 6. Schematic presentation of the AF4 channel assembly.

Consequently, the cross flow rate through the accumulation wall – comprising a ceramic frit covered by an ultrafiltration membrane – is induced by the constant loss of axial flow occurring with the transport of carrier liquid along the channel. This leads to a continuous decrease in the volumetric flow rate, i.e., the flow velocity, of the horizontal flow while approaching the outlet of the rectangular channel (Wahlund, 2000). In case of using very thin channels with low volumetric capacities in order to speed up separations, applying high cross flow rates results in fatal low outlet flow rates. During separation, this phenomenon has to be taken into account in order to avoid mis-assigning of sample characteristics due to the observed elution times. To compensate these undesired effect, a trapezoidal channel geometry was innovated, where the breadth decreases ongoing towards the channel outlet (Fig. 6). Within short time, the trapezoidal channel proved superior to the traditional rectangular geometry, and is almost exclusively applied now (Litzén and Wahlund, 1991; Coelfen and Antonietti, 2000).

Due to the variety of material qualified for channel composition, AF4 – as the other FFF subtechniques – can be operated with aqueous and organic solvents. The suitability of wall materials such as polycarbonate, polyethylene, aluminium or stainless steel have been examined (Kirkland, 1992). Appropriate holes for both carrier inlet and outlet and sample injection tubing can be drilled easily through the walls. The introduction of modern materials such as PMMA not only broadened AF4 applicability, but also initiated the development of innovative channel construction: traditionally, spacers were sandwiched between both walls, dimensioning a definite channel height due to their gage. Channel shape, e.g., rectangular or trapezoidal, was assessed by an outline cut in the spacer material, for instance polyester like mylar, teflon or polyimide (Miller, 1996). Contrarily, the new way of channel construction is as simple as effective: via engraving an appropriate cavity - with desired depth and geometry - direct into the upper wall, the required channel volume capacity is provided. The wall block, with the cavity underside, is placed on the ultrafiltration membrane, which overlies the ceramic frit. Accordingly, fumbling with spacers becomes redundant – an agreeable way how rationalization meets analytical practice.

The minimum usable spacer thickness, i.e., the cavity depth, is determined by the compressibility of the ultrafiltration membrane (Jensen et al., 1996; Giddings et al., 1992). When the channel is bolted together, the membrane is compressed in regions direct contacting the spacer and the upper wall, respectively. On the other hand, in unaffected areas the membrane maintains its original thickness and now protrudes into the channel. Amplified by membrane swelling phenomena, this determines a threshold for spacer thickness minima (Williams, 2000).

As outlined before, thin channels normally advance separation. Referring to this, applying thin channels is afflicted with a severe drawback, namely the increased probability of interferences with the laminar forward flow profile as a consequence of membrane corrugations. As illustrated in Fig. 7, the process of separation happens in immediate vicinity of the membrane.

Considering that in normal mode separations the analyte specimen are positioned in lamina levels not exceeding 5 μm distance off the membrane, the importance of smooth, unruffled membrane surfaces becomes evident.

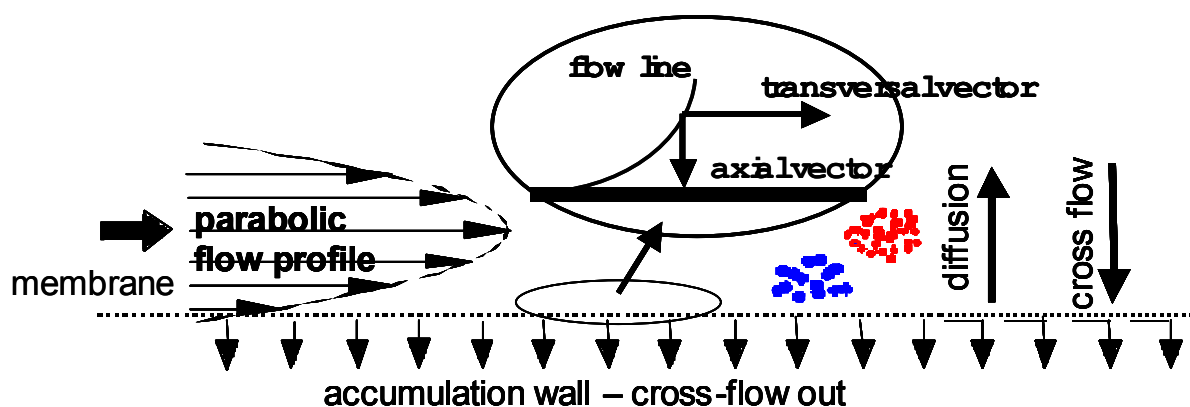


Fig. 7. Schematic representation of AF4 flow conditions close to the ultrafiltration membrane.

During separation, the sample components are subjected both by an axial flow vector – as a result of the laminar forward flow – and by a transversal flow vector, arising from the cross flow (Wittgren, 1997). If the sum of the vector net effect is falsified by sterical – and referring to AF4 principles, also theoretical - barriers, reproducibility, accuracy and power of the fractionation process is critically corrupted. This, in combination with the imperative of sample-membrane compatibility, led to a rushing demand for various membrane materials. The prevalent ultrafiltration membranes have meanwhile to withstand fierce competition by microporous membranes, since the latter provide a flat surface, marginal compressibility, high flux and low cost.

Proper selection of membrane material is a condition precedent to sufficient AF4 separation. The most popular materials are cellulose derivatives, poly(ether)sulfone, polycarbonate, polyamide, acrylic copolymers, fluoropolymers, polyethylene and polypropylene.

Since the samples are prevented from leaving the channel with the cross flow by the membrane, its cut-off properties crucially influence potential sample loss and sample recovery. It is known that the nominal cut-off value only refers to an estimation of the smallest analyte retained by the membrane, far apart from a precise specification. Consequences arising therefrom can be for good or for bad: sample specimen with molar masses as low as 6.5 kDa have been observed to be retained by membranes with declared nominal pore sizes of 50 nm (Benincasa and Giddings, 1992). Otherwise, membrane permeability may provide optimal conditions in the analysis of lipoproteins and pharmaceutical colloids, where co-analytes like lmw plasma proteins present aside would interfere analytics, but are displaced from the samples by passing the membrane (Li and Giddings, 1996).

2.3.2 Consideration of theoretical principles

Due to the rectangular channel geometry in FIFFF, the velocity U of the cross flow stream can be related to the cross flow rate V_c by

$$U = \frac{V_c}{bL} \quad (9)$$

where b represents the width and L the length of the channel. Given the background that both V_{in} - i.e., the carrier liquid volume entering the channel - and V_{out} values may accurately be assessed via flowmeater measurements, V_c is experimentally accessible via $V_c = V_{in} - V_{out}$. Unfortunately, matters in AF4 are complicated by asymmetrical channel design and trapezoidal channel geometry associated with non-uniform flow velocities.

To obtain U in the vertical x -direction in AF4, the basic Eq. (9) has to be rewritten to

$$U = -|u_0| \left(1 - \frac{3x^2}{w^2} + \frac{2x^3}{w^3} \right) \quad (10)$$

where $|u_0|$ is the cross flow velocity at the accumulation wall and x is the sample-wall distance. A constant cross flow provided, the mean flow velocity $\langle v \rangle$ in the horizontal z -direction can be expressed in rectangular AF4 channels via

$$\langle v \rangle = \langle v \rangle_0 - \frac{|u_0|}{w} z \quad (11)$$

where $\langle v \rangle_0$ is the flow velocity of the carrier liquid at the channel inlet. In trapezoidal channels, the area of the accumulation wall $A(z)$ from the inlet up to z - with $b(z)$ representing the channel width at z - is dispositive for both t_0 and the channel volume V_0 , alias the void volume. With b_0 and b_L as the channel widths at 0 and L , $b(z)$ is assessed by

$$b(z) = b_0 - \frac{z(b_0 - b_L)}{L} \quad (12)$$

Accordingly, $A(z)$ can be expressed as

$$A(z) = \int_0^z b(z) dz = b_0 z - \frac{z^2(b_0 - b_L)}{2L} \quad (13)$$

and the horizontal average flow velocity results in

$$\langle v \rangle = \frac{V_{in} - |u_0| A(z)}{wb(z)} \quad (14)$$

Utilizing Eq. (4) and Eq. (13), t_0 can be calculated by

$$t_0 = \frac{V_0}{V_c} \ln \left(1 + \frac{V_c}{V_{out}} \left[1 - \frac{A(z') - y}{A_{tot}} \right] \right) \quad (15)$$

where z' is the distance from the inlet to the focusing point, V_c the cross flow, V_{out} the outlet flow rate, V_0 the void volume and y the area excluded by the tapered inlet end. Given the known parameters t_0 , V_c , V_0 and w , furthermore the experimentally assessed t_r , and assuming the approximation $R = 6\lambda$, the diffusion coefficient D can be obtained directly via

$$D = \frac{t_0 V_c w^2}{6 t_r V_0} \quad (16)$$

Moreover, by applying the Stokes-Einstein relationship - referred to in Eq. (3) - the hydrodynamic diameter d_H of sample specimen can be assessed

$$d_H = \frac{2kTV_0}{\pi\eta V_c w^2 t_0} t_r \quad (17)$$

where η is the solvent viscosity.

Therefore, AF4 not only enables the fractionation of sample components, but also can be utilized for concomitant size determination of the fractionated specimen. These AF4 features can be applied for the characterization of complex samples, for instance, to separate and size-determine 70S ribosomes of *Escherichia coli* and the analogous 30S and 50S subunits (Nilsson et al., 1996). However, since the truth of the t_r values determined has always to be scrutinized, e.g., due to sample-membrane interactions potentially biasing AF4 data, the assessment of sample dimensions by means of AF4 theory per se took a back seat in recent years. Other sophisticated size-assessing detection systems, such as multi-angle light scattering (MALS), are to be preferred (Wyatt, 1993).

All mathematical considerations outlined above apply exclusively for what is often referred to as the “normal” or “Brownian” mode of FFF: sample specimen behave as point masses whose sizes are insignificant compared to the dimensions of the sample specimen zone. Consequently, sample retention becomes a unique reflection of the size, i.e., the hydrodynamic radius, and the diffusion coefficient (Caldwell, 2000b).

The larger the sample specimen, the less valid this approach becomes. In case particle sizes increase to a level where they are no longer negligible compared to the channel height, their retention has to be considered as a reflection of their inability to approach infinitely closely to the accumulation wall (Giddings, 1978d). Because the centers of gravity of large particles can approximate the wall not closer than the particle radius, the net result of this protrusion into the parabolic flow profile is that migration becomes forwarded in relation to particle size (Fig. 8).

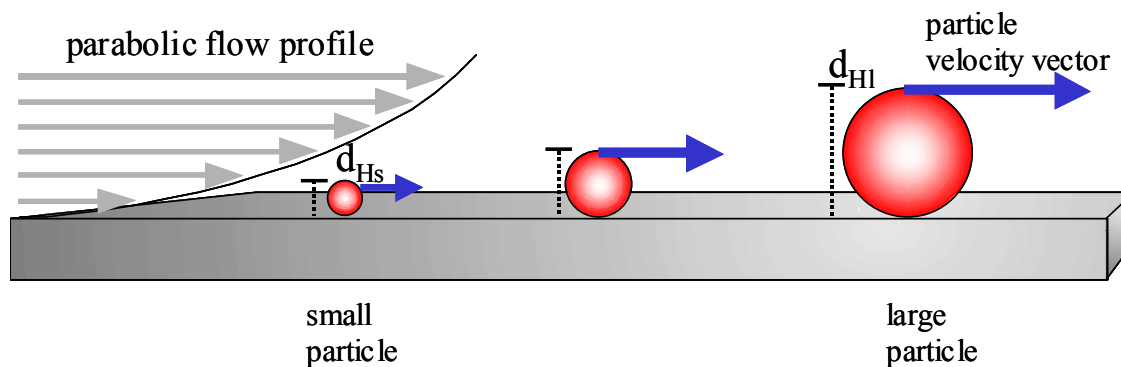


Fig. 8. Schematic representation of the steric mode FFF principle. Sample specimen are prevented from approaching the accumulation wall closer than half of their hydrodynamic diameter d_H . Due to their greater migration velocity vector, larger particles elute prior to smaller particles.

Thus, the order of separation is reversed, and that phenomenon is called “steric” mode effect (Min et al., 2002). The transition between normal and steric FFF mode depends on both particle size and channel height and is to be assessed for standard separation parameters at $\sim 1 \mu\text{m}$.

(To leave the Ariadne’s thread of AF4 matters for reasons of correctness: this steric exclusion observed in areas adjacent to walls is an important parameter in other separation

contexts, e.g., hydrodynamic chromatography or in size exclusion chromatography, where it accounts for the Casassa model (Dos Ramos and Silebi, 1993; Casassa and Tagami, 1969)).

However, that is only half of the truth: it has been discovered early, that steric particles do not migrate with direct contact to the wall surface – due to their high sensitivity to driving forces of the vertical field of force - but are positioned at elevated levels due to the role of hydrodynamic lift forces (Caldwell, 1979). These results were substantiated by data revealing that large diameter particles are migrating at levels more distant from the accumulation wall than smaller particles, eluting in steric mode, too (Moon et al., 1999). The situation in which steric mode is combined with hydrodynamic lift forces is termed hyperlayer mode. Fig. 9 depicts the forces affecting a sample eluting in hyperlayer mode.

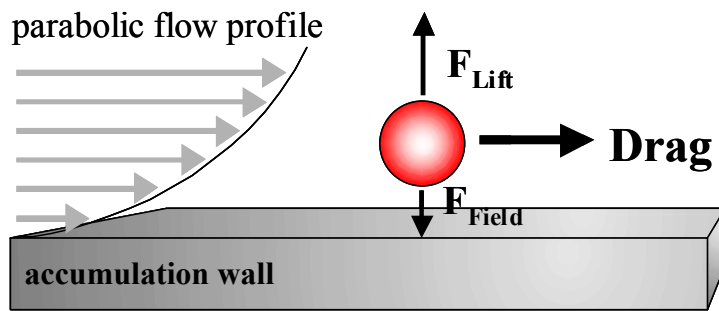


Fig. 9. Schematic representation of the forces affecting a large particle eluting in hyperlayer mode. The traction towards the wall due to the vertical field of force is opposed by hydrodynamic lift forces F_{Lift} . The laminar parabolic flow drags the particle at hyper-layered levels towards the channel outlet.

It is to be noted that the hyperlayer mode does not change the elution order of the steric mode, i.e., larger hyper-layered particles do elute prior to smaller hyper-layered particles, which in turn elute prior to steric particles very proximate to the accumulation wall.

These matters may be associated with the ascending force of airplanes due to the wing airfoils, what can be interrelated to those phenomena. Particles under laminar flow in thin tubes have long been known to experience velocity-dependent hydrodynamic lift forces directed away from the tube wall (Caldwell, 2000b). Early observations of this phenomenon include the so-called Fahraeus-Lindquist effect, which describes the depletion of blood cells from areas proximate to the endothel during the blood-flow through capillary vessels (Fahraeus, 1929).

However, the nature of hydrodynamic lift forces and hyperlayer mode are still only poorly understood. The expedient, although oversimplified, Eq. (18) relates the retention ratio R in steric mode FFF to the particle size d_H :

$$R = \frac{t_0}{t_r} = \frac{3\gamma_s d_H}{w} \quad (18)$$

where γ_s represents a steric correction factor related to the hydrodynamic lift forces. It can be derived from Eq. (18) that the retention time of sample specimen is decreased by thinner channels, like in normal mode separations.

2.3.3 Operational procedures

Basically, the AF4 experiment can be divided into three stages: sample injection, sample focusing, and the fractionation step. Identical to conditions in HPLC, the sample volume designated to AF4 analysis is gauged by using sample loops with inherent loop volumes spanning 10 – 100 μl . Considering prevalent AF4 channel capacities ranging between 200 and 1000 μl , to inject 100 μl sample entails that a considerable part of the channel volume will be replenished by the sample, not to mention void volumina of the injection capillaries. In a worst case scenario, the injected sample would fill the channel completely. Starting fractionation subsequently would implicate a situation, in which some of the sample components were positioned directly adjacent to the flow inlet and the sample injection port, while the rest of the sample would populate areas towards the flow outlet. Fractionations based on those preliminary conditions would suffer insufficiency and peak broadening (Fig. 10).

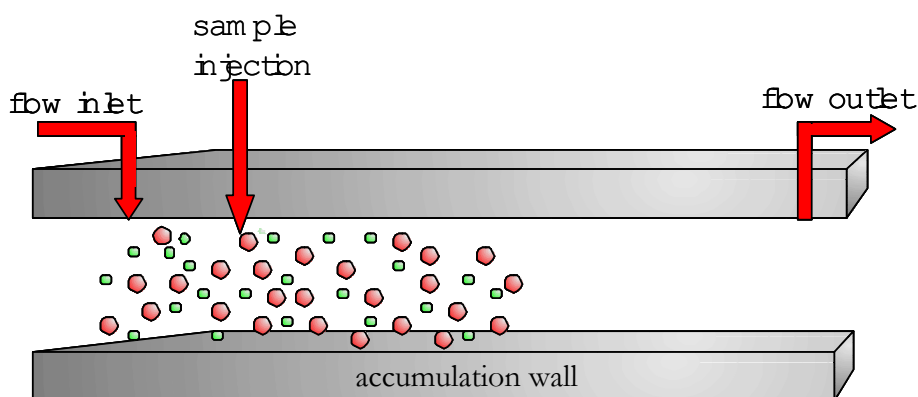


Fig. 10. Sample distribution within an AF4 channel subsequent to the injection step.

Furthermore, the sample specimen are to be positioned in their steady-state equilibrium levels before being eluted, in order to optimize fractionation quality. Referring to that, in virtually any FFF subtechnique a focusing step – often termed focusing/relaxation step – must be performed prior to separation. Due to this focusing/relaxation process, sample material that is distributed widely throughout the channel interior is forced into a narrow “band” from which proper separation is possible (Giddings, 1990). Unlike other forms of FFF, the field of force in AF4 can not be controlled independently of the axial flow. Therefore, sample focusing to narrow bands – to minimize band broadening of the detection signals – and sample arrangement in steady-state equilibrium profile has to be achieved simultaneously.

To meet this premise, an opposing stream of carrier liquid is pumped into the channel from the outlet end additionally to the flow through the inlet port. As a consequence, the sample specimen are focused at a predetermined point in the vicinity of the sample injection port and the carrier liquid exits the channel via passing the membrane (Fig. 11, Fig. 12). A position ~ 5 mm downstream from the inlet port is deemed an adequate location for sample focusing, since otherwise, one has to accept the consequences of flow inhomogeneities: surface protuberances of both flow inlet port and sample inlet port may interfere with the axial parabolic flow profile and may foster artifacts (Wahlund, 2000).

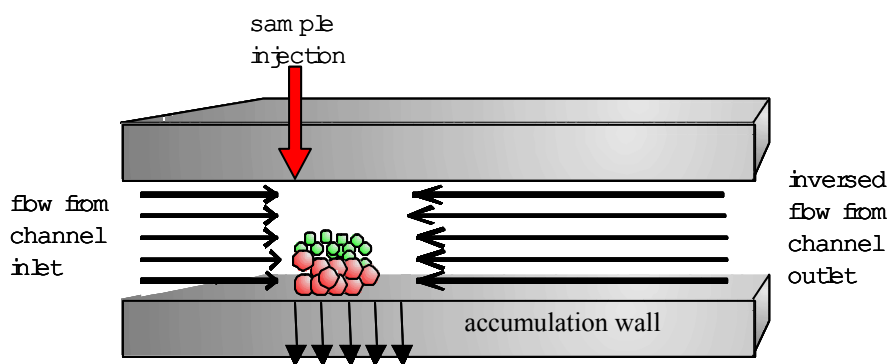


Fig. 11: Schematic diagram of sample specimen arrangement subsequent to focusing/relaxation. Note that analytes are focused to a narrow band and arrange at level heights related to their diffusion coefficients.

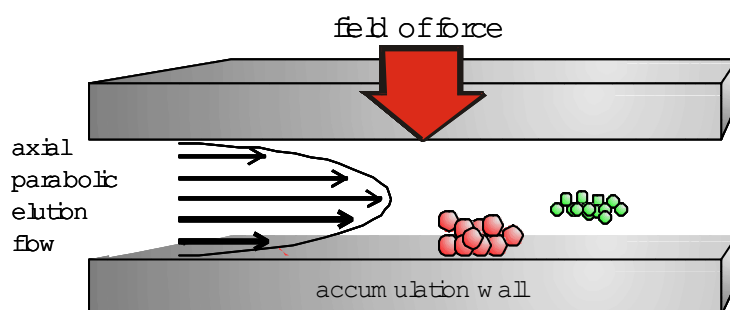


Fig. 12. Situation in the channel at an early stage of separation: since sample components arrange at different lamina levels after focusing/relaxation, sample specimen disband right from separation start.

Referring to Fig. 11 and Fig. 12, the dependence of successful AF4 separation on optimal focusing/relaxation becomes evident. Although the assessment of necessary focusing/relaxation times was approached inhere some uncertainties due to the necessity of assumptions (Moon and Myers, 2000). Therefore, for quality monitoring of focusing/relaxation, the utilization of colored macromolecular samples such as cytochrome-c and ferritin is feasible (Wittgren et al., 1996). Besides, the ideality of flow lines and channel leakage can easily be controlled by color indicator substances like bromophenol blue (BPB).

Set to action concomitantly, the intensities of both axial forward flow and cross flow determine the retention time of analytes. If samples to be fractionated are very polydisperse, a high cross flow must be applied in order to separate the least retained analytes, e.g., to counterbalance their high diffusion coefficients. As a consequence, well-retained specimen would elute after an excessively long period (Coelfen and Antonietti, 2000).

In contrast to separation methods with rather stringent separation modes like (SE-) HPLC, the cross flow intensity in AF4 can be changed and programmed arbitrarily during separation. This programming consists of intentionally and systematically varying the cross flow rate – and commensurate herewith, the axial forward flow rate also has to be adapted. Already in the first paper, the concept of programming FFF runs was proposed and implemented shortly afterwards (Giddings, 1966; Thompson et al., 1969).

Recently, the delivery of facts in terms of programming by FFF practitioners was increasingly accompanied by the concepts of theoreticians – a fruitful symbiosis: not only were FFF data evaluated in terms of matching available theories, but were applied to create new ones. Those in turn gave rise to technical innovations, e.g., a trapezoidal channel geometry. By means thereof, experimental facts were set, again demanding for appropriate underlying principles. From this “who was first: hen or egg”-race a wide mathematical arsenal evolved, including step, linear, parabolic and exponential functions, a special class of power functions capable of yielding almost constant relative resolutions, and data analysis algorithms (Moon et al., 2002; Williams et al., 2001; Williams and Giddings, 1994).

The actual cross flow intensity is simply to quote %-values. For instance, the term 10% cross flow means, that 10% of the elution medium entering the channel are pumped off through the ultrafiltration membrane. Therefore, if the laminar flow profile at the channel outlet is set to be 1.0 mL/min, consequently a flow volume of 1.1 mL/min has to enter the channel via the flow inlet in order to enable a 10% cross flow rate. Moreover, basically all state-of-the-art detection systems applied in monitoring elution of fractionated analytes – i.e., spectrophotometry, refractive index, light scattering and fluorescence detection units – are prone to artifact measurements due to (rapid) change of system parameters, i.e., discharge shifts of cell flow. Referring to that, the channel outlet flow volume has to be maintained constant during the whole experiment.

In this manner, even complex AF4 fractionation conditions can be expressed both comprehensively and briefly.

2.3.4 Applications of AF4

Confronted with the task to review AF4 applications, it is to be accentuated that AF4 is not a state-of-the-art method, neither in industries nor in scientific research. A general survey of the

published literature, e.g., in terms of AF4 in protein analysis, is completed within short time, revealing a low two-digit number of extensive scientific publications. In contrast, to perform the same in terms of SE-HPLC means to become assailed with thousands of articles. This indicates that AF4 applications mainly originate for special – not to say unusual – analytical tasks. Due to the lacking of package material within the channel, fractionations are performed under moderate conditions, avoiding both shear stress and high system pressures. This predestines AF4 for characterization of hmw analytes, prone to artifacts due to experiment conditions, e.g., shear degradation and upper exclusion limit of the separation technique applied.

Referring to this, AF4 was mainly employed to study conformational changes, aggregation tendencies and hmw ratios of macromolecules, which are utilized in pharmaceutical and chemical industries, such as ethylhydroxyethyl cellulose, carrageenans and starch polysaccharides (Andersson et al., 2001; Roger et al., 2001; Wittgren et al., 1998). Furthermore, AF4 was employed to characterize amphiphilic polymers, where the usefulness of SE-HPLC is limited because of interactions between hydrophobic polymer segments and the stationary phase. Consequently, the aggregation of amphiphilic graft copolymers, essential for the stabilization of interfacial structures, was analyzed via AF4 as well as the aggregation of pullulan derivatives (Wittgren et al. 1996; Duval et al., 2001).

The second main field of AF4 application represents the analysis of dissolved sample components aside undissolved particles. Moreover, the size limit of samples amenable to AF4 separation can be risen to the μm range, allowing the separation of nanoclusters, nanocolloids, microparticles and even cells.

In case of nanocolloids, AF4 was used for analysis of polyorganosiloxane nanoparticles dispersed in a complex mixture in the presence of excess surfactant (Jungmann et al., 2001). Additionally, the FFF potential for degradation-free separation was applied to provide analytes with extremely narrow size distributions for subsequent high-precision measurement of analyte dimensions via MALS. In this respect, the superiority of AF4/MALS over established methods like transmission electron microscopy (TEM) was shown (Wyatt and Villalpando, 1997).

The challenging task to separate dissolved and undissolved sample components via AF4 was repeatedly performed, e.g., by examining the distribution of a lipophilic drug within human plasma or when characterizing lipoproteins originating from human blood (Madorin et al., 1997; Li and Giddings, 1996). In particular, the potential of AF4 was demonstrated in the separation of lipoprotein particles of coronary artery disease patients (Park et al., 2002).

Without doubt, the exertion of AF4 in vaccine control is one of the most promising applications. The surface features of deactivated bacteria or viruses affect the immunoresponse to bacteria- or virus-associated antigens. Therefore, sorting and characterization of deactivated bacteria or viruses is an important way of quality control for whole-cell bacterial or viral vaccines and was demonstrated by using AF4 only recently (Fraunhofer et al. 2003, Reschiglian et al.,

2002). In this context, also the separation of plasmids and plasmid fragments, and the determination of acid phosphatase in cultivation media via AF4 have to be subsumed (Wahlund and Litzén, 1989; Litzén et al., 1994).

Furthermore, the amounts of ribosome and ribosome subunits were determined via AF4 as well as the assessment of tRNA levels in bacterial cells (Nillson et al., 1996; Arfvidsson et al., 2003).

The general acceptance of HPLC in protein characterization reduces the significance of AF4 therein. Although a variety of proteins have been analyzed by means of AF4, almost without exception the aim of those studies was to demonstrate the basic applicability of AF4 in protein separation rather than to approach and elucidate an analytical problem in particular (Fraunhofer et al., 2001; Giddings, 1993). The characterization of wheat flour protein by SE-HPLC and AF4 is one of the few examples of an extensive case study, wherein AF4 was applied. Unfortunately, AF4 data were not comparable to SE-HPLC data, as samples were either characterized solely via SE-HPLC or AF4 (Ueno et al., 2002).

Conversely, due to their unimodal mass-distributions, protein monomers are considered ideal systems to control AF4 set-up or evaluation.

Commensurate with the nowadays increased ecological awareness, AF4 is employed accumulatively in analytics of environmental particles and macromolecules. This development is instanced by the characterization of humic substances and the separation of colloidal organic matter from river waters (Benincasa et al., 2002; Benedetti et al., 2002).

An extensive register of AF4 applications, encompassing published results prior to 1999, can be found in the literature (Coelfen and Antonietti, 2000; Jonsson, 2000).

To predict some future trends of AF4 applications is delicate, since there are reasons legitimizing a pessimistic as well as an optimistic rating.

The main argument of the “bears” is the low recognition of the brand itself. Within the vast majority of analytical laboratories, the term AF4 is not associated with a powerful separation technique with wide applicability, but more with a black box. Consequently, the routine analysis of samples is performed with state-of-the-art methods, resulting in data which can be assessed in correlation with data formerly obtained by the same established methods. Moreover, allowing new methods to take roots is synonymous with additional expenses on time, employees and money. Finally, present established methods are subject to constant optimization, be it propelled by the users or by the manufacturers. The outcome is an increase in accuracy and applicability of present established analytical methods.

Falling into line with the “bulls”, the increasing demand for new analytical methods may fertilize AF4 development. Three trends may be anticipated. One is certainly to combine AF4 with absolute detection techniques like MALS or other methods like inductively coupled plasma

(ICP) or electrospray mass spectroscopy. Thereby, a convenient identification of the separated analytes by assessment of molar mass, hydrodynamic radius or chemical composition is possible.

Another development with much potential is to couple several FFF separation mechanisms to a kind of multidimensional FFF. Since this technique combines the assets of several FFF methods, all possible data of each individual FFF technique would contribute to sample information obtained from one single experiment.

Probably the greatest potential for AF4 progress lies in the development of advanced membranes. Sample specimen are brought in immediate vicinity to the membrane during separation, facilitating possible sample-membrane interaction. Bearing in mind the low sample concentrations of many biotechnological products, there is a tremendous need for new technologies of protein compound identification and quantification. In this regard, the development of immunoassay-membranes, masked with antibodies that are highly specific to the target compound within the sample, is highly promising. Since those membranes can be tailored in any desired way, the high potential of such kind of membranes in interacting with specific organic (and anorganic) analytes becomes evident. Consequently, accuracy, sensitivity and applicability of AF4 may be boosted.

Considering that FFF was introduced to analytical science in the late 1960s and was long kept in a rather shadowy existence, by regarding the development in the last decade it is to be assumed that diversity and potential of FFF methods probably will experience an upturn in the years ahead.

3 Protein aggregation in liquid protein pharmaceuticals

3.1 Introduction

Products of modern pharmaceutical biotechnology represent a very significant fraction of today's total pharmaceutical market. The rapid development not only of simple replacement proteins, e.g., recombinant insulins and blood factors, but also engineered protein pharmaceuticals was particularly facilitated by technical innovations in molecular biotechnology and protein chemistry. Thus far, some 88 recombinant proteins/monoclonal antibody-based products have gained marketing approval within the European Union (EU), accounting for a 36% share of all new EU drug approvals since 1995 (Walsh, 2003). As the vast majority of protein drugs are administered through injection, the stability of proteins in dissolved state is a critical concern. Committed to the development of elegant formulations as well as patient acceptance, pharmaceutical scientists increasingly offer protein drugs in liquid formulations, thereby avoiding costly lyophilized products.

Subsequent to application, the protein drug still is opposed to an environment that is predominantly aqueous: a typical cell contains 70-85% water and the extracellular space of most tissues is composed of 99% thereof. Even the brain, with its complex arrangement of cells and myelinated structures, comprises a ~80% water content (Saltzman, 2001). Consequently, to accommodate protein drugs with a broad portfolio of stabilizing parameters may be considered the formulator's task. Therefore, sufficient protein stability in liquid formulations is a criterion of utmost importance. Unfortunately, protein drugs don't care about that.

Instability of peptides and proteins can be originated by two pathways: chemical and physical. Chemical instability can be deemed to take center stage in relevant scientific articles reviewing protein instability (Wang, 2000; Wang, 1999; Schoeneich et al., 1997; Cleland et al., 1993; Manning et al., 1989). In many cases, chemical degradation reactions can proceed simultaneously in proteins, thus complicating the revelation of one prime chemical degradation reaction. Contrarily, the prevalent scientific opinion hallmarks aggregation to be the most common process of physical instability (Wang, 1999; Cleland et al., 1993). Consequently, this chapter focuses on the protein aggregation phenomenon.

3.2 Chemical instability

Notable progress has been made in elucidating the link between protein structure and chemical instability. Basically, chemical instability can be defined as any process which comes along with protein modification by bond formation (e.g., oxidation) or – most commonly - by bond cleavage (e.g., hydrolysis).

In the majority of cases, hydrolytic reactions in proteins affect the side-chain amide groups of asparagine (Asn) and glutamine (Gln), and the peptide bond on the C-terminal side of an aspartic acid (Asp) or a proline (Pro) residue, when it is in the penultimate position from the N-terminal end (Goolcharran et al., 2000a). As Asn residues deamidate generally more rapidly than Gln residues, Asn hydrolysis is exemplified below in detail (Schoeneich et al., 1997). Acidic conditions provided ($\text{pH} < 4$), the prevalent reaction with an Asn residue involves direct attack of water on the side-chain amide carbonyl carbon resulting in the formation of an Asp residue. On the other hand, at neutral or basic conditions ($\text{pH} > 6$) the predominant reaction with an Asn residue involves cyclic imide formation with subsequent attack of water on one of the two carbonyl carbon atoms, yielding Asp and isoaspartic acid residues in an approx. 1 to 4 ratio (Fig. 13) (Patel and Borchartd, 1990).

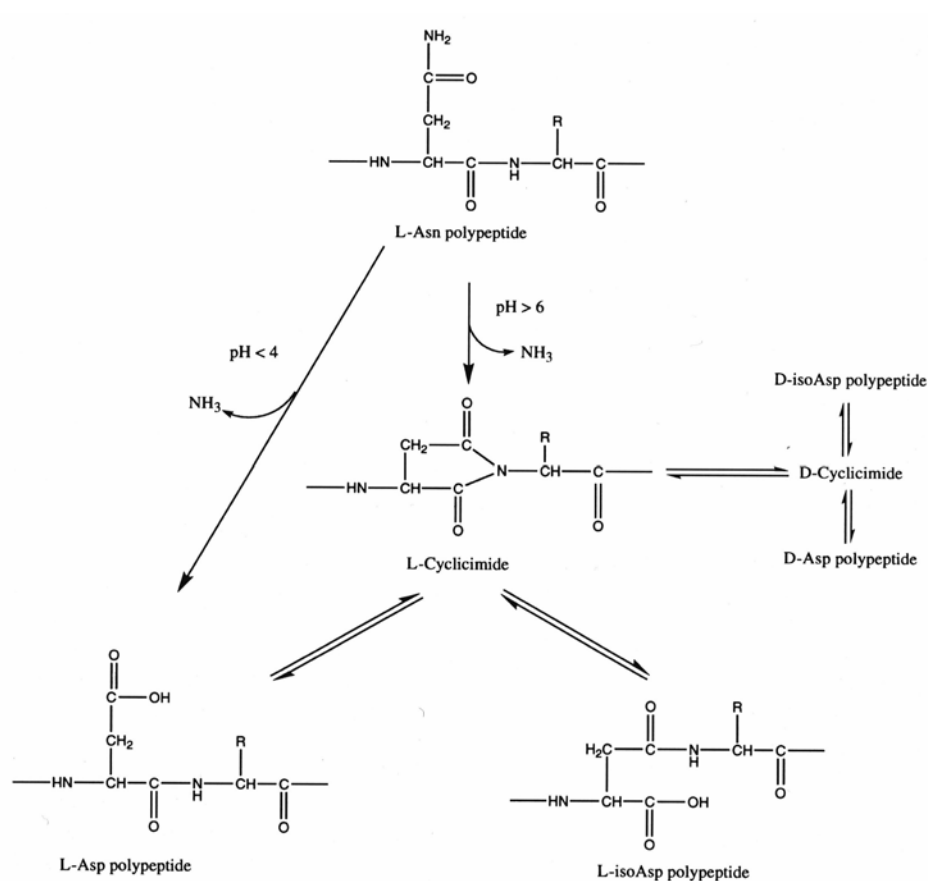


Fig. 13. Schematic representation of Asn residues deamidation pathways.

The exogenous factors influencing the deamidation rate are of dazzling array: besides temperature, buffer specimen, buffer concentration and ionic strength are critical parameters. Bicarbonate and glycine buffers appear to catalyze deamidation as well as buffers based on phosphate in a 0 – 20 mM range (Tyler-Cross and Schrich, 1991; Tomizawa et al, 1995). On the contrary, a thorough analysis revealed that the deamidation rate of Val-Asn-Gly-Ala was not influenced by the variation in buffer component concentration, encompassing a 0 – 50 mM range of phosphate and carbonate (Lura and Schrich, 1988). The list of investigations dealing with the

relationship between buffer components and deamidation rate may be prolonged arbitrarily (Goolcharran et al., 2000b; Tomizawa et al., 1995b, Capasso et al., 1991). Anything provided by experiments, science still misses a golden rule regulating this matter and, consequently, room for speculation prevails. One theory suggests, that phosphate ions, or other buffer ingredients, could act on the aqueous solvent to increase basicity of water molecules without forming free hydroxide ions, thereby affecting deamidation (Brennan and Clarke, 1995). However, data corroborating this hypothesis has not yet been published.

Equally, the effects of ionic strength on deamidation appear to resist easy generalizations. In protein solutions with neutral or alkaline pH, ionic strength effects on deamidation are evident: e.g., the catalytic activity of phosphate is decreased in the presence of salts (Johnson and Aswad, 1995; Tomizawa et al., 1995b). Interestingly, NaCl has been shown to protect less against deamidation than salts like LiCl and Tris HCl.

Other exogenous factors influencing deamidation include the effect of organic cosolvents, e.g., ethanol and glycerol, for obvious reason: embedded in a medium with reduced dielectricity, the protein or peptide bond nitrogen would be less likely to ionize. As the anionic bond nitrogen is necessary in the formation of the cyclic imide, a low dielectric medium is considered to retard the progress of deamidation (Bummer and Koppenol, 2000). This topic was approached in recent years, employing a hexapeptide (Brennan and Clarke, 1993). As expected, the lower dielectric constant media resulted in clearly lower deamidation rates of the Asn residue.

Furthermore, the deamidation rate is affected by endogenous factors, e.g., by the primary sequence of the protein. It was found early that Asn residues seem more prone to deamidation than Asp (Robinson and Rudd, 1974). In this regard, amino acid residues on the amino side of Asn have only minimal effect, regardless of parameters like charge and size. Otherwise, characteristics of the carbonyl side residues are decisive for the deamidation rate. Increasing both size and branching of the residue side chain minimizes the deamidation rate, in some cases as much as 70-fold relative to a Gly residue. Consequently, Asn-Gly is considered the most labile sequence (Powell, 1996). It is hypothesized that bulky residues succeeding Asn may inhibit sterically the formation of the succinimide intermediate in the deamidation reaction. Additionally to deamidation, proteins may undergo other non-enzymatic hydrolysis pathways, e.g., degradation of proteins yielding a diketopiperazine (DKP) and a truncated protein (Fig. 14).

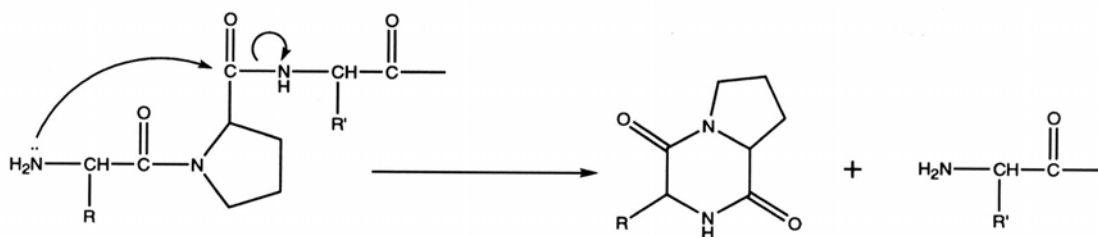


Fig. 14. Diketopiperazine formation resulting in degradation of N-terminal sequences with inherent penultimate Pro residues.

The mechanism of DKP formation commences with a nucleophilic attack of the N-terminal nitrogen on the carbonyl carbon of the peptide bond between the second and the third amino acid residues in the primary sequence. A precedent condition for this degradation process is Pro representing the penultimate residue in N-terminal sequences. This intramolecular aminolysis reaction was observed for a number of pharmaceutical proteins and is catalyzed in both acidic and basic conditions (Goolcharran et al., 2000c; Straub et al., 1995; Battersby et al., 1994). In the latter case, the DKP cyclization can be minimized by avoiding general base catalysts such as phosphate or acetate buffers.

Degradation of Asp residues represent the third major hydrolytic protein degradation pathway. Principally, the Asp stability is conditioned by its position in the primary sequence (Ota and Clarke, 1989). One degradation pathway takes place via Asp-to-isoAsp interconversion, propelled by a cyclic imide intermediate state similar to that represented in Fig. 13. The other pathway proceeds via amide bond hydrolysis of Asp and adjacent amino acids. Under moderate acidic conditions, the rate of peptide bond hydrolysis next to the Asp residue is by at least two orders of magnitude greater than the hydrolysis of other peptide bonds, where Asp is not involved (Oliyai and Borchardt, 1993; Goolcharran et al., 2000a). Although the impact of the primary sequence on Asp degradation is considerable, it is short of the effect on Asn residue deamidation. Nevertheless, the greater the steric bulk of the amino acid adjacent to Asp, the more the hydrolysis rate is decreased. For instance, in terms of cyclic imide formation at pH 7.4, the half-life of a sequence containing Asp-Ala exceeds that of the Asp-Gly analog by factor 7 (Stephenson and Clarke, 1989).

Besides hydrolysis, oxidation is the other major pathway of protein degradation. Facing a broad variety of possibilities to initiate oxidation, the formulator's assignment may be compared to the task of Sisyphos: even excipients like the polyether surfactant polysorbate 80 – without doubt one of the most utilized stabilizing agents in liquid protein formulations – have been convicted of releasing peroxide, a potent oxidizing protein cross-linking agent (Ha et al., 2002; Jaeger et al., 1994).

In general, protein oxidation is to be attributed to photochemical, metal ion catalyzed, high energy γ -radiation, or organic additive sources. Even sonication appears to promote the generation of reactive oxygen specimen (Bummer and Koppenol, 2000; Riesz and Kondo, 1992). Protein oxidation is – due to its importance - topic of intense research, and yet new information trickles scarcely.

Independent of the cause of oxidation induction, the basic principle implicates the interconversion of oxygen to (few) key reactive oxygen specimen, which react with the protein. The most potentially oxidizable sites of proteins are the side chains of His, Met, Cys, Trp, Arg and Tyr (Daniel et al., 1996; Stadtman, 1993). For instance, Met residues are easily amenable to oxidation by atmospheric oxygen in vials containing only 0.4% oxygen (Richards, 1997).

Metal catalysis is the most instanced oxidation phenomenon, as many pharmaceutical processes such as protein/peptide synthesis and subsequent purification, bulk storage and dosage form storage may provide conditions which facilitate metal-catalyzed oxidation (Cleland et al., 1993; Manning et al., 1989). Trace levels of metal ions such as Fe(III) and Cu(II) are often implemented unintentionally to pharmaceutical systems, e.g., via buffer reagents (Li et al., 1995). Reduced by prooxidants, the metal ions then provide reactive oxygen specimen via interaction with oxygen. Prooxidative agents present in formulations may be buffer component contaminants or excipients added originally in antioxidative terms, e.g., ascorbic acid (Li et al., 1995b). Even the victim is to be convicted complicity, since side-chains of the amino acids Tyr, Trp and Cys may operate as prooxidants (Timmins et al., 1982).

Both photooxidation and autooxidation are minor sources for fostering protein degradation.

As only few pharmaceutical proteins are photosensitive, little is published dealing with light-induced protein oxidation. Amino acids found to be most susceptible of photooxidation are His, Trp, Met and Cys (Halliwell and Gutteridge, 1989). Of more interest are the photosensitizing features of stabilizing excipients. For instance, the photolytic degradation of proteins such as antibodies has been observed in the presence of non-ionic surfactants (Lam et al., 1997; Brot and Weissbach, 1991). In case of polysorbate 20, it was concluded that the excited polysorbate may initiate photooxidative reactions via interaction with oxygen to form singlet O_2 , resulting in a met sulfoxide formation (Duenas et al., 2001).

Autooxidation as direct reaction between ground state oxygen in triplet state and singlet ground state proteins and peptides is unlikely, as both components differ in the appropriate electron spin directions. Assuming air-saturated and metal- and peroxide-free buffers, the approximate half-life of the most labile amino acid residues was calculated to be 80 years for Cys and over 10^7 years for Met (Schoeneich et al., 1997). Referring to his, many of the so-called cases of autooxidation observed for proteins are most likely due to metal-catalysis or other sources (Goolcharran et al., 2000a).

Other chemical pathways of protein degradation are of lower importance, although a broad portfolio may be compiled by searching the literature. Instances thereof encompass isomerization, succinimidation, non-disulfide crosslinking, beta-elimination, conversion, racemization or more circuitous pathways like deglycosylation and maillard reactions. Further information on the mechanisms and consequences of chemical protein degradation is provided by the review articles cited in the introduction of this chapter.

3.3 Aggregation – a consequence of physical instability

3.3.1 Random walks

Proteins successfully cope with even harsh conditions in order to maintain stability: in nature they can be found at conditions ranging from $-40\text{ }^{\circ}\text{C}$ to $115\text{ }^{\circ}\text{C}$ and from ~ 1 pH to 11 pH, respectively (Jaenicke, 1991).

Referring to this, the pharmaceutical formulator's task to make long-term stability data of protein drugs available - covering 12 months at minimum at drug submission - seems simple: at $30\text{ }^{\circ}\text{C} \pm 2\text{ }^{\circ}\text{C}$ and 65% rh, valid for most territories (ICH Draft, 2002). However, unequally challenging tasks account for unequal facilities. Whereas the formulator basically has to rely on his experience, proteins *in vivo* are provided with a sophisticated quality control system in order to guarantee proper folding and stability subsequent to synthesis (Fig. 15).

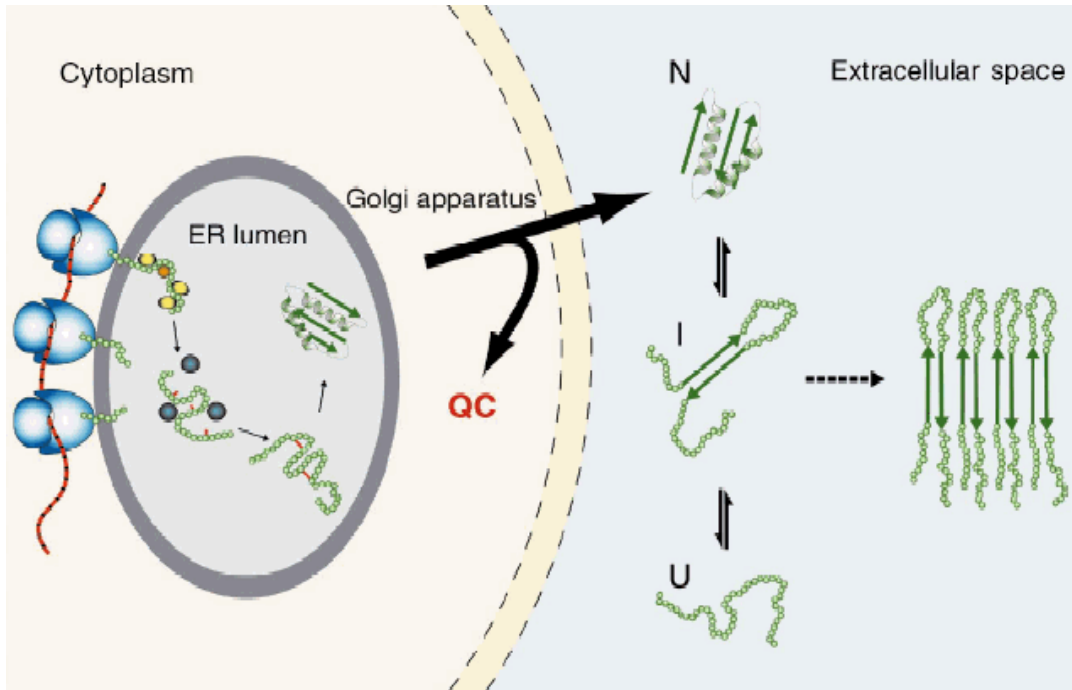


Fig. 15. Cell situation scheme of a globular protein. After synthesis on the ribosome, the protein is assumed to fold in the endoplasmic reticulum (ER) and to be secreted from the cell. Under certain conditions, proteins may at least partially unfold and become prone to aggregation. N, I and U refer to native, partially folded (intermediate) and unfolded protein states, respectively. QC refers to the quality control systems which prevent incompletely folded proteins being secreted from the ER, mainly comprising chaperones and proteases. Chaperone binding and release of folding intermediates allows proteins to reach their native conformation. As aggregated proteins are relatively resistant to proteolysis, chaperones promote proteolysis indirectly by maintaining misfolded proteins in an unaggregated state (Wickner et al., 1999) (illustration with friendly permission of Oxford Center for Molecular Sciences, UK).

Despite these cellular controls, a range of debilitating human diseases is associated with protein misfolding events that result in the malfunctioning of the cellular machinery. Most attention has been focused on a group of diseases where proteins or protein fragments convert from their soluble forms with intact helical folding to insoluble fibrils or plaques. The final forms of these aggregates often reveal a well-defined fibrillar nature, known as amyloids (Fig. 16).

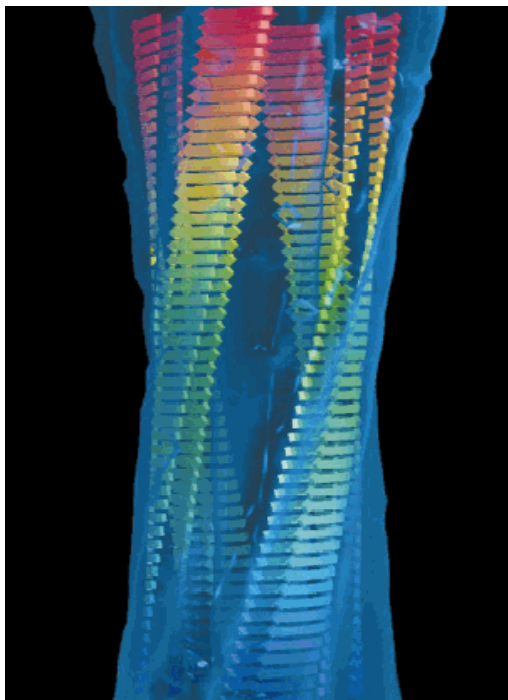


Fig. 16. Molecular model of an amyloid fibril derived from the SH3 module of PI3 kinase via cryo electron microscopy. Amyloid fibrils are known to be rich in β -structure, giving rise to the α -helix-to- β -sheet transition of proteins with originally largely helical conformation. The fibril consists of four twisted “protofilaments”, forming a hollow tube with approx. 60Å in diameter, and reveals a characteristic cross- β -structure, generally considered to be requisite for protein aggregates subsumed to amyloids. Today, some 20 human proteins have been found to form amyloids, which are associated with diseases like Creutzfeldt-Jakob, Alzheimer’s, Huntington’s, or Parkinson’s diseases (illustration with friendly permission of Dobson, 1999).

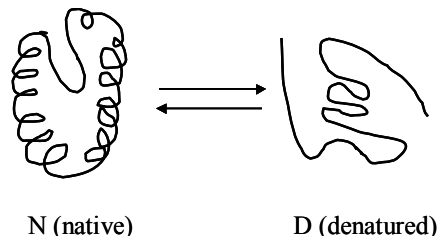
One remarkable protein feature – considering the dependence of native conformation on function – is that the native state is only marginally stable relative to denatured states, facilitating subsequent aggregation phenomena. As this is valid for proteins *in vivo* and in pharmaceutical dosage forms, to understand the basic principles of denaturation and aggregation is of crucial importance for the formulator in order to minimize or – at best – to avoid negative consequences concerning drug formulation.

3.3.2 Thermodynamics

Unlike small pharmaceutical drugs, where physical instability is rarely encountered except for poorly water-soluble compounds, proteins, because of their unique ability to adopt three-dimensional forms, tend to undergo a number of structural changes, independent of chemical modifications (Akers and Defilippis, 2000). Thereby, the tertiary structure of proteins is conveyed by two kinds of noncovalent interactions: hydrophobic interactions, which mainly represent hydration effects of nonpolar groups, and electrostatic interactions, e.g., ion pairs, weak polar interactions, H bonds and van der Waal forces (Anderson et al., 1990). Bearing in mind that the free energy change for the unfolding/denaturation reaction of proteins is minimal – 5-10

kcal/mol – the impact of even slight changes of enthalpic and entropic parameters on protein stability becomes evident (Pace et al., 1996; Jaenicke, 1990).

In order to approach this matter, most articles are predicated on a trivial two-state model with an inherent equilibrium between the native (N) and the denatured states (D).



Physiological conditions provided, the equilibrium constant K for unfolding can be expressed as $K = [D]/[N]$ and utilized for the derivation of the change in Gibbs free energy (irrespective of intermediate state specimen):

$$\Delta G = (G_D - G_N) = -RT \ln K \quad (19)$$

wherein R represents the gas constant and T the absolute temperature. K may be inserted in the van't Hoff equation, yielding the temperature coefficient of the equilibrium constant via

$$\frac{d \ln K}{dT} = \frac{\Delta H}{RT^2} \quad (20)$$

Consequently, by combination of Eq. (19) and Eq. (20) the change in Gibbs free energy can be related to the temperature:

$$\Delta G = \Delta H - T\Delta S \quad (21)$$

where ΔH and ΔS symbolize enthalpic and entropic changes (typically 50 – 200 kcal), respectively, at the same temperature at which ΔG is evaluated. Since the small changes in free energies associated with the transition from N to D are the difference of large values, the difference in free energy is very sensitive to small perturbations in the attractive and repulsive intermolecular interactions (Bummer and Koppenol, 2000). The temperature dependence of ΔH and ΔS is defined by the heat capacity change, ΔC_p , between native and denatured states. For most proteins, ΔC_p reveals a large value, reflecting the restructuring of solvent subsequent to protein unfolding (Robertson and Murphy, 1997).

Combining Eq. (20) and Eq. (21) in terms of ΔC_p , Eq. (22) can be derived, generally referred to as the modified Gibbs-Helmholtz equation.

$$\Delta G = \Delta H^\circ - T\Delta S^\circ + \Delta C_p \left[(T - T_0) - T \ln \frac{T}{T_0} \right] \quad (22)$$

Accordingly, the value of ΔG is the fundamental stability parameter of a protein. As Eq. (22) is based on the two-state model, values derived therefrom are only valid for proteins lacking

stable folding intermediates. However, most small globular proteins were shown to correspond to this prerequisite, as they usually fold within milliseconds or even less (Kristjánsson and Kinsella, 1991; Lumry et al., 1966).

On the other hand, definite conditions provided, unfolded state intermediates may be stable for considerable time and reveal significant amounts of residual secondary structure. This was shown to be the case for some pharmaceutically relevant proteins, e.g., human growth hormone (Bam et al., 1996). (In this regard, scientists successfully gave proof of their sense for neologisms: striving towards denomination of those intermediates, the term “molten globule state” was coined, thus avoiding the oxymoron “durable intermediates”.) (Shortle, 1996; Goto and Fink, 1989)

In order not to lose the plot of thermodynamics: the large and positive ΔC_p observed in protein denaturation is primarily due to exposure of nonpolar groups. Over 80% of the nonpolar side chains such as Ala, Val or Phe are buried in the interior of the intact folded protein and are exposed to the surface after unfolding (Pace, 2001).

The molar enthalpy of protein denaturation, ΔH , may be either positive or negative at low temperatures, but increases notably with temperature. As the propulsive power for protein unfolding is the increased conformational entropy in aqueous solution, ΔS is expected to be positive. Consequently, $-T\Delta S$ forces the Gibbs free energy ΔG to become negative and thus forwards unfolding.

In this respect, the special situation of $\Delta G=0$ deserves attention: in that case, 50% of the protein molecules are unfolded, and the correlative temperature is defined as the unfolding or melting temperature T_m . For the majority of proteins, T_m values range between 45 °C and 70 °C (Wang, 1999). Extreme high T_m values are exhibited by proteins in hyperthermophilic bacteria, where T_m can exceed 100 °C (Jaenicke, 1996).

Two important caveats are to be noted in the use of T_m , often prompting misunderstandings. The first discord is that proteins are assigned specific T_m values, which characterize the proteins individually – what is not correct per se. For human and bovine albumin, two T_m values can be determined, indicating the existence of a molten globule state. Contrarily, dog and rabbit albumin reveal only one transition (Kosa et al., 1998). Moreover, the parameters temperature, pH or the analytical technique used can influence the number of transitions obtained, exemplified by differential scanning calorimetry (DSC). Prior to DSC deconvolution, two protein melting transitions may be yielded, whereas subsequent to deconvolution three unfolding transitions can be determined, accounting for three individual protein domains (Remmele et al., 1998).

The second misunderstanding refers to the relationship between T_m and general protein stability, represented by the Gibbs free energy ΔG . It is widely assumed that any change of structure which leads to increased T_m should result in a commensurate gain in general stability.

E.g., in case of the pharmaceutical protein rt-plasminogen activator T_m was found to be about 66 °C. In the presence of arginine, which stabilized the protein in solution, T_m shifted to 71 °C (Pearlman and Nguyen, 1992). Yet, thermodynamics – substantiated by experimental data - does not evaluate any particular relationship between T_m and ΔG at a given temperature (Knapp et al., 1998; Dill et al., 1989).

However, both rise and decrease of temperature may lead to a shift of ΔG (Fig. 17).

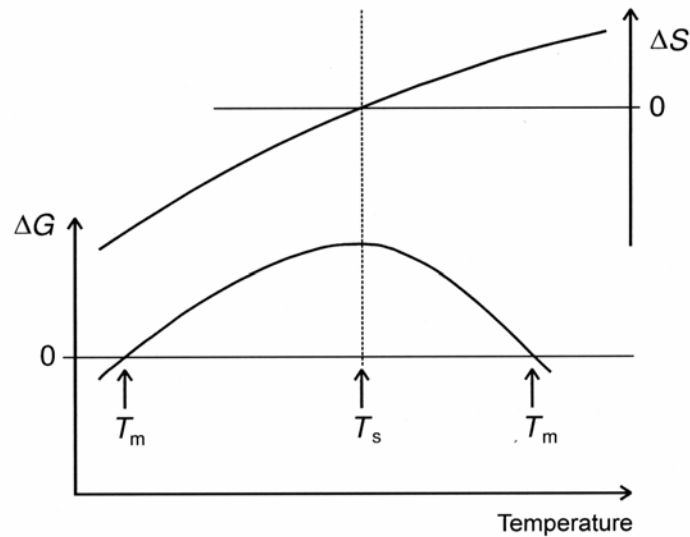


Fig. 17. Scheme of changes in entropy (ΔS) and Gibb's free energy (ΔG) of protein unfolding as a result of temperature alteration. T_m is the temperature at which the free energy difference between the native and the unfolded state is zero, and represents the cold and heat denaturation temperature. At T_s , the native state stability is maximal and ΔS is zero.

Whereas unfolding due to heat is driven principally by the loss of polar contacts and a gain in conformational entropy of the protein chain, cold denaturation is based on the weakening of the hydrophobic effect upon cooling (Privalov and Gill, 1988). For the overwhelming majority of proteins, the temperature of cold denaturation is far below the freezing point of aqueous solutions. As a practical matter, at the temperature of maximal stability (T_s), generally between – 10 °C and 35 °C, protein unfolding entropy is zero and the native structure is solely stabilized by the enthalpy factor (Pace and Laurents, 1989).

3.3.3 The aggregation process

The formation of soluble and insoluble protein aggregate specimen is based on either covalent or non-covalent interactions. Covalently linked protein dimers or specimen of higher order are due to chemical reactions between the protein molecules. Because the aggregate origin is generally not evident, unfortunately the term “aggregation” is employed to describe this process, which should rather be termed “polymerization”. As protein aggregates often represent

a potpourri of various covalently and non-covalently bound components, the term “aggregation” is universalized (Constantino et al., 1994).

Furthermore, the terms denaturation, aggregation, precipitation and coagulation – although describing closely linked phenomena – have to be specified. Denaturation refers to both reversible and irreversible structural changes in native proteins resulting in altered solubility properties. However, the primary structure stays intact. If denaturation occurs far away from the isoelectric point (IP), the denatured protein remains in solution with only slight tendency to form aggregates.

Generally, the item aggregation is used to differentiate between association or assembly with regard to quaternary structure formation on the one hand, and side reactions due to kinetic partitioning between correct folding and incorrect scrambling of subunits, on the other (Jaenicke, 1995). The macroscopic equivalent of aggregation is precipitation (Manning et al., 1989). Precipitation may be brought intentionally by either complex formation or multi-component solutions, e.g., by salting out with salts or fractionation with mixed solvents.

Coagulation of proteins is defined as an increase in particle size caused by denaturation and subsequent separation from the solution or gelation, often by means of elevated temperature (Jaenicke, 1997).

Protein aggregation can occur from a conformational intermediate or from more extensively unfolded (completely denatured) protein molecules, where hydrophobic residues are exposed to the aqueous solvent. The initial stages of aggregation are quite specific in the sense that they involve the interaction of structural subunits of one molecule with “corresponding” hydrophobic surface areas of structural subunits of a neighboring molecule. Two sites can be sufficient, in which case the aggregation most likely propagates in a linear fashion forming long fibres. Anyhow, the process will yield larger aggregates, whose sizes will eventually exceed the solubility limit (Brange, 2000). Hydrophobic interaction, i.e., the reluctance of nonpolar groups to be exposed to water, is prevalently deemed the *primum mobile* for protein unfolding and subsequent aggregation (Franks, 2002).

A variety of physical parameters can contribute to the aggregation process, as they facilitate the exposure of hydrophobic protein sites. The fragile balance of exposed and buried hydrophobic sites – propelling unfolding and aggregation if outbalanced - may be interfered by temperature, ionic strength, shaking, ultrasound or exposure to interfaces (Patro and Przybycien, 1996).

Basically, there is a continuous kinetic competition between refolding into the protein native state and reactions towards high-order aggregates. As aggregation is generally concentration-dependent, and since at higher concentrations aggregation dominates over refolding, there is obviously a sword of Damocles hanging over high-concentrated formulations. However, it is to be noted that the risk of product loss due to potential adsorption phenomena

on packaging material increases at low drug concentrations, i.e., <1 mg/mL. Hence, a statistically greater portion of protein drug has access to the adsorptive surface area of the package container (McLeod et al., 2000).

Moreover, in event of highly dosed liquid protein formulations not only the aggregation rate, but also the size of protein aggregates may increase, resulting in possible precipitation phenomena (Roefs and De Kruif, 1994). If so, the aggregate nuclei have grown into primary particles, which may agglomerate and result in visible particulate matter. These primary particles, typically with dimensions ranging between 100 and 200 nm, correspond to approximately 1000 protein molecules, according to protein molecular weight (Glatz, 1992).

Aggregation reversibility and nature – i.e., covalent or non-covalent – can be characterized by means of denaturants such as GdnHCl, urea and sodium dodecyl sulfate (SDS). Principally, aggregation is irreversible and due to covalent processes if the protein aggregates can not be solubilized in those agents (Allison et al., 1996; De Young et al., 1993).

An aggregate feature often in the fore is the formation of long fibres, especially if aggregation is due to thermal denaturation. In this case, the aggregates reveal an intermolecular hydrogen-bonded, antiparallel β -sheet structure, comparable to that illustrated in Fig. 16 (Dong et al., 1995). The thermally induced α -helix-to- β -sheet conversion was verified early on the basis of poly-L-lysine and subsequently demonstrated for a variety of proteins such as calcitonin, fibronectin or other proteins whose native folds are largely helical (Timasheff et al., 1967; Dong et al., 1995; Sunde and Blake, 1997).

3.3.4 Theories on aggregation

In contrast to the detailed information about proteins, relatively little is known about the thermodynamics of the aggregated protein state and the kinetics and mechanisms of its formation (Randolph et al., 2002). However, many theories on aggregation have been proclaimed, were expanded and upgraded, and some of them were binned.

Most theories assume imperative protein denaturation prior to aggregation. Historically, research on protein aggregation first led to the proposal that protein aggregates originate from the totally unfolded, denatured state. It was found that (thermally induced) protein aggregates feature an antiparallel β -sheet structure, regardless of the initial secondary structural composition of the native proteins (Dong et al., 1995). Consequently, proteins have to unfold completely, i.e., to abandon their secondary structure, before aggregation occurs.

The next historical leap in insight into aggregation involved “molten globule” protein intermediates. Associated herewith is the maintenance of secondary protein structure, albeit the tertiary structure is vastly perturbed due to destabilizing ambience. Effectually high

concentrations provided, e.g., >1 mg/mL, molten globules readily form aggregates (Uversky et al., 2001). This implicates that aggregation may eventuate from only partially unfolded states.

To confuse the matter further on, most recently it was found that even under solution conditions not disrupting tertiary structure and thermodynamically greatly favoring the native state, proteins can aggregate and even precipitate (Kim et al., 2000). Accordingly, the native conformation is accredited a dynamic structure, such that at any instant in time an ensemble of specimen exists with a distribution of structural expansion/compaction. Aggregates derived thereof arise from components which reveal an expanded structure, compared to the most compact conformations present.

This conclusion is substantiated by the status of proteins in thermophilic bacteria, generally considered practically unsusceptible to aggregation. Here, a slightly denser packing in native proteins is observed compared to the density of ubiquitary proteins (De Decker et al., 1996).

These renewed efforts to define theories and to determine aggregation processes were both permitted and fueled by the demonstration that aggregation proceeds through specific pathways (Speed et al., 1996). Thereby, a rationale for repudiation of the nonspecific coaggregation dogma has been provided and the conceptual bias that aggregation is a random process has been removed.

The theory, that the native protein conformation has a dynamic structure is supported by the energy landscape theory and the folding funnel concept, respectively (Fig. 18).

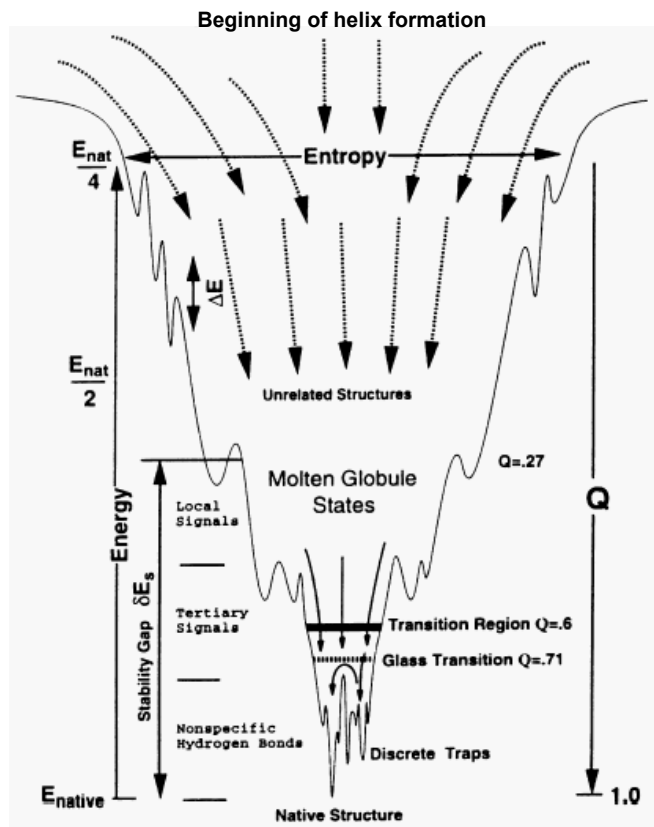


Fig. 18. „Rugged energy landscape“ of protein folding for a small protein site with a preferred directionality towards an unique native state. E and Q refer to the solvent-averaged energy and the fraction of native-like contacts, respectively. The fluctuations ΔE and the stability gap δE_s between the misfolded or molten globule states and the native state are functions of the order parameters. Unique folding is assessed by local secondary and tertiary contacts as well as hydrogen bonds within the stability gap. If correct folding is opposed, the directionality is inverted and the proteins reveal denatured states, prone to aggregation phenomena (Jaenicke, 1999).

There is evidence from NMR data that even under extreme denaturing conditions a certain amount of native residual protein structure prevails (Wilson et al., 1996). As a consequence, the denatured state comprises a large number of noticeably different conformations in rapid equilibrium with each other. In the framework of folding delineation as the descent in an energy landscape, native protein sites would populate the tapered terminal area of the landscape. Each native protein state is assigned a specific trap, with minimal distances between stabilizing secondary and tertiary contacts. Conversely, unfolded and aggregated protein sites would populate sub-states in the funnel-part of the landscape that are characterized by distances between stabilizing sites in the range of many Ångstroms (Chahine et al., 2002).

One major obstacle in establishing a universally valid aggregation theory can be ascribed to the heterogeneity of aggregation peculiarities. Aggregation can be characterized as an unimolecular/intramolecular process (e.g., β -elimination) as well as a multimolecular/intermolecular process (Chang et al., 1996). Consequently, aggregation may or may not follow first-order-kinetics, as proved by experimental data (Wang, 1999; Pikal et al., 1991). However, this matter is still discussed controversially, exemplified by the investigations on pancreas RNase: thermally induced inactivation was found to be strictly of first order or unimolecular kinetics. The researchers assigned protein aggregation in general a necessarily first-order kinetic and a polymolecular pathway. As a consequence, they innately ruled out aggregation as the cause of inactivation (Ó Fágáin, 1995).

A quite simple, though target-oriented, attempt is to approach underlying principles of protein aggregation by employment of colloidal aggregation models. Accordingly, both native protein monomers and denatured aggregates are considered to act like colloids, with inherent diameters between 1 and 1000 nm and dispersed in solution (De Young et al., 1993b).

Basically, the DLVO theory accounts for steric and electrostatic repulsions and van der Waals attractions between particles in solution. Referring to this, DLVO provides a simple framework for describing the thermodynamics and kinetics of colloidal stability and aggregation (Russel et al., 1989). According to the Smoluchowski theory, the kinetics of protein aggregation depends on the diffusion coefficient, particle number and particle radius (Rosenqvist et al., 1987). This theory has been successfully employed to model protein aggregation (Fig. 19).

Considerable progress has been made in terms of understanding protein aggregation by introducing theories which draw a comparison between parameters contributing to protein stability and parameters forwarding protein unfolding and aggregation, respectively. The mean-field lattice theory posits an equilibrium between denatured and aggregated states of proteins (Fields et al., 1992). The lattice model implicates the aggregate state to be composed of amorphous protein polymer plus solvent, and that the driving forces are hydrophobic interaction, advancing aggregation, and conformational and translational entropies, which foster

disaggregation. The theory predicts that at sufficiently high protein concentration precipitation proceeds, whereby the solubility limit represents the lowest concentration at which this occurs.

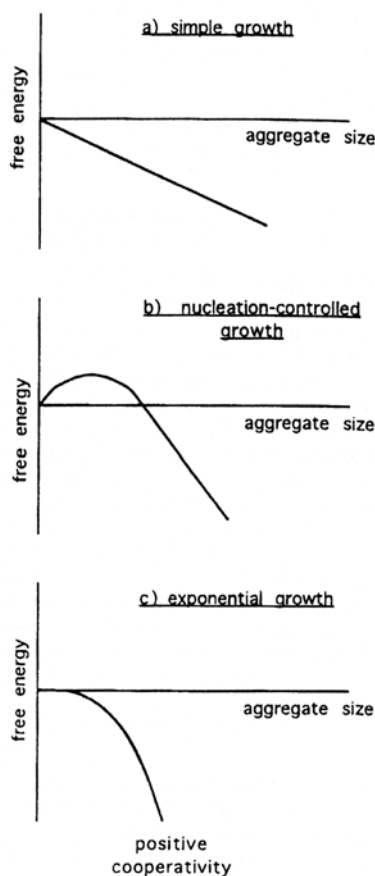


Fig. 19. Free energy dependence on aggregate size. Pursuant to Smoluchowski theory, protein particles stick so strongly to the aggregate that the rate-limiting step is diffusion of the particles to the aggregate cluster. In this regard, it is important how one monomer attachment influences the next, and whether aggregate growth is (a) simple, (b) nucleation controlled or (c) exponential. Simple growth (a) occurs when each monomer addition is favorable to about the same degree, independent of the size of the growing aggregate. The free energy per added monomer is negative (favorable) and is of comparable amount for each monomer. Larger aggregates are favored but smaller ones are also populated, particularly at early times. In nucleation controlled growth (b), e.g., protein crystallization, the free energy of adding monomers is positive when the aggregate is small. Consequently, small aggregates are unfavorable. In exponential growth (c), the addition of each unit is more favorable than for the preceding unit, e.g., the Ca^{2+} -induced aggregation of α -casein occurs via exponential aggregation kinetics followed by Smoluchowski aggregation (De Young et al., 1993).

An integral part of the lattice model is the determination of upper and lower temperatures, assessing dissolved-undissolved protein phase boundaries. For instance, cooling at low temperatures leads to a loss of the translational entropy, favoring aggregation. More important at low temperatures is the weakening of the hydrophobic interaction upon cooling, what forwards dispersion of the protein polymer in the solvent. Hence, principally, proteins could be dissolved by cooling at adequate temperatures. However, this temperatures are predicted to be below the freezing point of water. Due to the temperature dependence, the phase boundaries can undergo remarkably large shifts with very small changes in copolymer composition. The practical consequence of this is that the change of a single amino acid of a protein can cause precipitation or can cause an insoluble protein to become soluble, vice versa (Fields et al., 1992).

Two years ago, the manifold ensemble of theories was enriched by an article of Pace, causing a stir within the prevalent point of view of most researchers (Pace, 2001). According to Pace, the burial of an polar amide group is deemed to contribute more to protein stability than the burial of an equivalent volume of nonpolar $-\text{CH}_2-$ groups. Since about 1960, the latter parameter was considered to contribute the lion's share to protein stability (Kauzmann, 1959). However, Pace construed several studies as the desolvation penalty for burying peptide groups to

be considerably smaller than thought hitherto. Contrarily, hydrogen bonding and van der Waals interactions of peptide groups in the tightly packed interior of folded proteins are more favorable. The fraction of space occupied by atoms is 0.75 in protein interiors – outranging the 0.71 packing of close packed spheres – and regions containing hydrogen-bonded polar groups may be more tightly packed than regions containing nonpolar side chains. As a consequence, van der Waals interactions among groups in the interior of a folded protein will be more favorable than the interactions of the same groups with water in the unfolded protein (Fleming and Richards, 2000; Honig, 1999). Therefore, improved van der Waals interactions have a large share in the enthalpy of protein folding. This theory was supported by investigations demonstrating that protein stability can not be increased by replacing groups forming a buried hydrogen bond by different combinations of hydrophobic residues (Maxwell and Davidson, 1998).

Given the background of the low solubility of glycine peptides, it may be concluded that water is a relatively poor solvent for the peptide backbone. This raises the question of whether solvophobicity of the backbone in water has been overlooked as a contributor to the collapse and folding of proteins – all the more, because reduced packing density and increased solvophobicity of the protein backbone facilitate protein aggregation subsequent to unfolding phenomena. At present, science is digesting these notions, as neither Pace nor the supporters of the contribution of nonpolar group burial to protein stability have published further arousing details.

The accumulating number of observations of three-dimensional protein domain swapping has prompted speculations as to its impact on aggregation phenomena (Fig. 20).

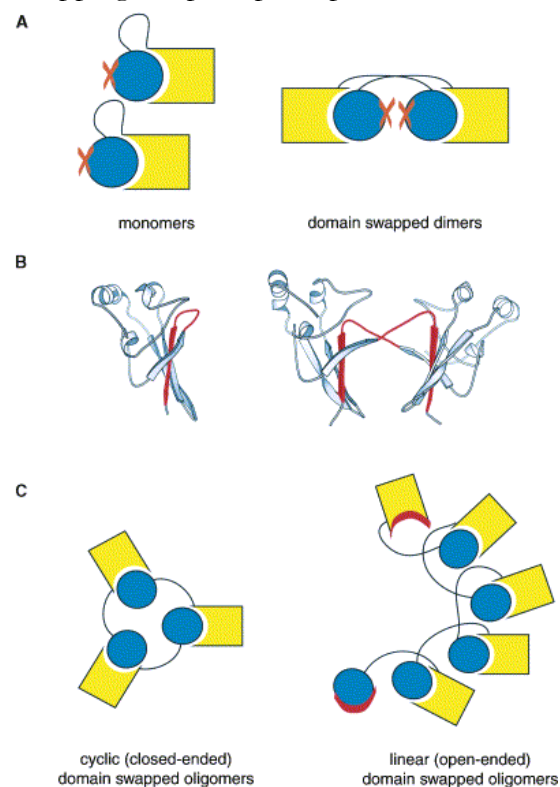


Fig. 20. Basic principles in domain swapping. The term domain is not used in a strict sense, as proteins have been reported to swap entire tertiary globular domains as well as domain elements such as α -helices or β -sheet strands. (A) Simplified representation of a protein monomer and a domain-swapped dimer. The exchanging parts of the structure form a new interface in a domain-swapped oligomer, highlighted in red. (B) Structures of monomer and domain-swapped dimer; the domain swapping C-terminal β -strand and the hinge loops are shown in red. (C) Illustration of open-ended and close-ended domain swapped oligomers, exemplifying aggregation processes induced by domain swapping (with friendly permission of Rousseau et al., 2003).

Originally proposed to be a mechanism for the emergence of polymeric proteins, an increasing amount of data solidify its potentiality to foster misfolding and aggregation. Basically, three-dimensional domain swapping – the term was introduced in 1994 - is a process by which one protein molecule exchanges a domain with an identical partner (Bennet et al., 1994).

Referring to this, transient aggregation was observed during refolding of several proteins, and was ascribed due to domain swapping (Silow et al., 1999). Additionally, a correlation between domain swapping propensity and the rate of heat aggregation of proteins was stated (Rousseau et al., 2001). Domain swapping is also attributed to play a role in the processes of prion and amyloid formation, substantiated by crystallization data of prion protein, for instance (Knaus et al., 2001). As research strongly focuses on understanding protein aggregation due to self-association, it is to be expected that domain swapping will gain increasing attention (Rousseau et al., 2003).

Considering the diversity of theories available, the development of an overall theory in terms of aggregation is to be deemed unlikely. If at all, this theory will be a patchwork of several theories available, and each protein aggregation problem will have to be approached individually.

3.3.5 Quantification of the aggregation rate

“To be aggregated or to be unfolded” seems to be the Hamlet’s question for protein samples analyzed in terms of physical instability. As protein aggregation involves precedent unfolding, a definite classification of techniques in methods monitoring the unfolding/denaturation process and methods quantifying the aggregation rate is not always unambiguously.

This inherent method ambiguity can be exemplified by (fourier transform) infrared spectroscopy (FT-IR). Today, FT-IR is the most widely employed technique in order to assess the secondary structure of proteins (D’Auria et al., 1997). The investigated parameter is the C=O stretching vibration of the peptide moiety, which is weakly coupled with the in-plane N-H bendings and the C-N stretching vibrations (Takeda et al., 1995). Induced by different secondary structures, e.g., α -helix, β -sheet or loops, C=O stretching vibrations are covered by the amide I region ($1620 - 1690 \text{ cm}^{-1}$). In order to increase IR resolution and assess secondary protein structure more accurately, fourier self-deconvolution and second or fourth derivation have been applied (Goormaghtigh et al., 1994). On the other hand, intermolecular hydrogen-bonded β -sheet structures are a common characteristic of protein aggregation, mainly represented by a low-frequency band around 1620 cm^{-1} (Dong et al., 1995b). This structural composition occurs regardless of the pristine composition of the secondary structure of native proteins. Therefore, this band can be used - among other bands – to quantify protein aggregation in both aqueous and solid states (Wang, 1999). Moreover, FT-IR can be applied to estimate protein T_m values via analysis of amide I band intensities (Bischof et al., 2002; Chehin et al., 1998).

As regulatory authorities generally limit the potential consequences of protein aggregation - e.g., particulate matter contamination –, the formulation scientists usually focus on aggregation rate determination rather than to analyze unfolding phenomena. Furthermore, inactivation of proteins may occur without disruption of the tertiary structure and proteins highly prone to unfolding phenomena do not necessarily exhibit a pronounced tendency to aggregate (Cowan, 1997). Thus, aggregation per se is generally scrutinized by the scientists more intensively than protein unfolding. Among the various methods applied in aggregate quantification, PAGE and SE-HPLC are the most widespread techniques. Both techniques monitor the increase of protein size during aggregation.

The popularity of SE-HPLC is based on its high reproducibility, simplicity of operation and the ability to satisfactorily estimate protein molecular weight averages (Olivia et al., 2001). For instance, newly cloned proteins, especially those generated subsequent to large-scale sequencing, may exist in solution optionally in monomeric or oligomeric forms. By means of SE-HPLC the solution consistence may easily be verified (Wen et al., 1996). Unfortunately, protein or aggregate size can be overestimated by SE-HPLC if the protein is not spherical - e.g., but highly-coiled - and its Stokes radius exceeds that of a globular protein (Kuhlman et al., 1997). While SE-HPLC assesses the total amount of aggregates based on size, reversed phase HPLC (RP-HPLC) can intergrade covalent and non-covalent aggregates or differentiate between various isoforms of protein aggregates (Sharokh et al., 1994; Perlman and Nguyen, 1992). However, filtration or centrifugation of the samples prior to HPLC analysis imposes the significant constriction of HPLC to be limited for the determination of soluble aggregates.

Referring to PAGE, the distinction between covalently and non-covalently (ionic) bound soluble aggregates is possible via reducing and non-reducing PAGE (Reubsæet et al., 1998). E.g., by reducing SDS-PAGE the covalent binding of G-CSF was shown to be primarily due to disulfide linkages via intermolecular disulfide scrambling (Bartkowski et al., 2002). Both reducing and non-reducing SDS-PAGE can be combined in two-dimensional electrophoresis, where the first dimension is a non-reducing run and the second dimension is a reducing one. Quantification of the separated aggregate fractions is usually performed densitometrically (Petruccioli and Anon, 1995). Though, this method lacks accuracy, as the utilized dyeing agents, e.g., Coomassie Blue, reveal an affinity for both proteins and gel material.

As the two methods complement one another, SE-HPLC and SDS-PAGE frequently are employed in parallel for meanwhile three decades (Maekawa et al., 2003; Skjelkvale and Duncan, 1975).

Light obscuration and Coulter technique are state-of-the-art methods for subvisible particle counting in protein parenterals with inherent lower detection limits of $\sim 1 \mu\text{m}$ and $\sim 0.4 \mu\text{m}$, respectively. As the aggregation process theoretically can run the gamut from nm range – at early stages of the aggregation process – to the subvisible μm range, maybe resulting in visible

association/precipitation products, particle counting techniques disclose protein instability tendencies relatively late – compared to methods like SE-HPLC or PAGE. In this regard, analysis of particulate matter in protein parenterals via light obscuration mainly is targeted on particles due to surface abrasion of package material during the manufacturing process rather than on protein particles due to aggregation processes (Borchert et al, 1986). On the other hand, Coulter-based measurements were successfully applied in analysis of hemoglobin aggregation and assessing size distributions of protein particles due to precipitation (NcNulty et al., 1994; Rohani and Chen, 1993). Generally, data of aggregation processes obtained by light obscuration closely correlate with data derived from Coulter technique, as both methods detect aggregation tendencies in protein shelf-life studies concomitantly with identical sensitivity (Fraunhofer et al., 2003).

The turbidimetric method is used to estimate the amount of protein aggregate by measuring the optical density of a sample based on light scattering in the near UV or visible region, where proteins do not reveal any absorption (Kelley and McClements, 2002; Wang et al., 1996). Given the background that soluble aggregates do not necessarily lead to opalescent or turbid protein solutions, whereas smallest amounts (<1%) of insoluble aggregates may cause turbidity with subsequent particulate matter, neither particle counting techniques nor turbidity measuring enables accurate quantification of aggregation rates (Hoffmann, 2000). One further aspect that has to be taken heed of is the potential intrinsic turbidity of highly-concentrated protein solutions, e.g., antibody formulations, which can exhibit protein concentrations exceeding 100 mg/ml. Additionally, opalescence/turbidity of liquid protein pharmaceuticals may be due to packing material such as siliconized rubber closures (Gebhardt et al., 1996). Thus, solution turbidity may not automatically be equated with protein aggregation.

In the last decade, a variety of new experimental techniques have been introduced in protein aggregation monitoring. However, many of those techniques still have to provide evidence of their general applicability in aggregation analytics. E.g., antibody mapping can be employed to detect early aggregation intermediates and to assess aggregation intensity (Betts and al., 1999). Referring to this, quasi-elastic light scattering (QELS) was shown to be also suited for resolving initial stages of the aggregation process and aggregate quantification (Walsh et al., 1997). Whereas fluorescence spectroscopy (FS) per se is prevalently used to investigate protein unfolding, FS can be applied to assess the aggregation intensity in combination with dying agents such as bis-anilino naphthalene sulfonic acid (BIS-ANS) (Azuaga et al., 2002; James and Bottomley, 1998). Besides the aggregation rate, by means of ANS fluorescence also structure and conformational plasticity of protein aggregates can be determined (Kundu and Guptasarma, 2002). However, as the exposure of hydrophobic core surfaces in the course of aggregation processes does not essentially correlate with the aggregation rate, this method reveals a major drawback - folding events can potentially be mistaken as aggregation events (Finke and Jennings,

2001). Moreover, the temperature dependent ANS fluorescence may only be observed in case of measurable turbidity of protein solutions (Andersen, 2002).

Analytical ultracentrifugation (AUC) may also provide valuable results in terms of protein aggregation (Arakawa et al., 1999). Besides identification of individual aggregated protein specimen, AUC can be applied to quantify the aggregation rate (Whittingham et al., 2002; Liu and Shire, 1999). Further methods applied in the evaluation of aggregation intensities encompass atomic force microscopy and electron diffraction (Nichols et al., 2002; Serpell et al., 2000).

In reviewing the information above, the conclusion arrives that present established methods of protein aggregate quantification inhere one major restriction: they enable the quantification of only soluble aggregates, thereby jettisoning insoluble aggregates or vice versa. Given this background, one candidate with great potential for aggregate quantification is AF4, as this method can analyze both aggregate specimen.

The separation of protein monomer from oligomers and soluble low molecular weight aggregates via AF4 was principally demonstrated in 1993 (Litzén et al., 1993). Subsequently, AF4 was shown to be capable of analyzing soluble high molecular weight aggregates of glutenin (Wahlund et al., 1996). Only recently, the overall-applicability of AF4 in protein analytics was successfully demonstrated by comparative studies addressing soluble aggregate quantification and particulate matter analysis – compared to SE-HPLC and light obscuration, respectively (Fraunhofer, 2002d). However, research still lacks an extensive study on the use of AF4 in protein analytics – comprising relevant parameters such as sample recovery and elution order. Consequently, Chapter 6 attends to those matters.

Finally, it should be stressed that instability/aggregation studies of pharmaceutical proteins generally are accompanied by activity assays. Yet, bioassays inhere several drawbacks, e.g., low reproducibility, labor-intensity, inability in detecting only slight activity alterations. Furthermore, in many cases a tailor-made bioassay is to be created based on the protein's function (Wolfbeis et al., 2002; Hsu et al., 1995). In practice, bioassays therefore are employed in combination with other analytical techniques to assess protein stability such as SE-HPLC for soluble aggregate quantification and light obscuration, seizing insoluble aggregates and particulate matter, respectively.

4 Multi-angle light scattering (MALS) in protein analytics

4.1 Introduction

Light scattering is an everyday occurrence of our life, that becomes apparent for instance in the color of the blue sky, red sunsets or the phenomenon of rainbows. Simplifying the latter, the raindrops function as scattering angular filters, and due to the properties of water there is enough angular spread ending up in colorful visions. Light scattering analytics has found its way into branches of science and research with an impact only scarcely imaginable some years ago, e.g., pharmaceuticals, medicine, bioengineering and meteorology (Hodgson, 2000). The upturn of light scattering appliance was fueled by the plethora of analyte information accessible, comprising molecular weight, radius of gyration, hydrodynamic radius, size distribution, shape and internal structure and even analyte interactions.

Two general techniques employing light scattering exist: dynamic light scattering (DLS), often referred to as PCS or quasi-elastic light scattering (QELS), and static or so-called classical light scattering (SLS). In DLS a laser is focused into the solution volume containing the (in most cases colloidal) analytes and the scattered light is collected over a small angle. Both phase and polarization of the light scattered are determined by size, shape and conformation of the analyte molecule (Brown, 1993). Thereby, the fluctuation of the scattered light intensity determined by the detector is closely related to the extent of random Brownian motion and, consequently, temperature-dependent (Hodgson, 2000). From these fluctuations an autocorrelation function is derived, which is inverted for assessment of analyte diffusion coefficient and analyte size, in case that the analytes are spherical. The use of DLS for off-line batch characterizations has extensively been reviewed in the literature (Borcovec, 2002; Will and Leipertz, 2001; Finsy et al., 1992). Although the application of DLS as on-line detection method during chromatographic sample separations was approached, this procedure inheres a major drawback: the DLS measurement normally fails to keep pace with the rate of sample specimen elution. Thus, unfavorable stop-flow modes of the separation method have to be accepted (Claes et al., 1992).

On the other hand, SLS is targeted on quantification of the scattered light intensity as a function of the scattering angle. By spacing several discrete photo-detectors around the flow-cell in a multi-angle geometry, measurements can be performed over a broad range of angles, resulting in a SLS-subtechnique called multi-angle light scattering (MALS) (Fig. 21). Thereby, both molecular weight and size of analytes can be determined absolutely, i.e., independently of the elution volume and without the need of calibration or assumptions concerning chemical and steric structure of the analyte. Furthermore, the light scattering intensity is monitored in the microsecond time range, thus drawing a major distinction to DLS, where monitoring is performed in second time range. Hence, SLS is applicable to on-line detection subsequent to

fractionation processes. In contrast to the rather low resolution of DLS in analyzing bi- or multimodal systems, MALS was shown to accurately resolve analyte subpopulations that differ by much less than a factor of two in mean size (Korgel et al., 1998). Due to its ability to elucidate the steric structure of sample components, MALS is increasingly applied to investigate conformation, unfolding, and both glycosylation and aggregation rate of proteins (Filenko, 2000). Assets and drawbacks of SLS and MALS, respectively, have repeatedly been published (Wyatt, 1998; Hallett, 1996; Schnablegger and Glatter, 1993).

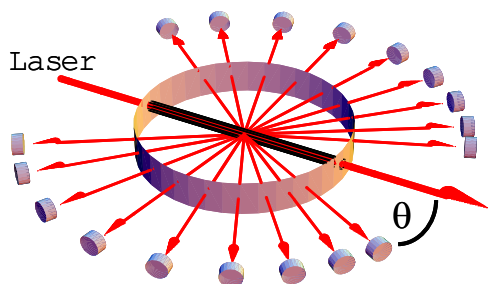


Fig. 21: Schematic principle of MALS detection. Several photo-diodes are spaced around a flow-cell, which is irradiated by laser light. The multi-angle geometry of the diodes enable a simultaneous detection of scattered light over a wide range of scattering angles (θ), typically varying from 10° to 160° .

Generally, the theory governing the light scattering process resembles the theory underlying the scattering by X-rays and neutrons, even though light and X-rays are electromagnetic radiation with different wavelengths while neutrons hold mass (Chu and Liu, 2000). Thus, besides SLS and DLS, similarly sophisticated techniques arise in protein analytics such as small-angle X-ray scattering (SAXS), wide-angle X-ray diffraction (WAXD) and small-angle neutron scattering (SANS), which can be applied in conformational studies of putatively fully unfolded protein states (Millet et al., 2001; Koch et al., 2001).

4.2 Theoretical aspects

The theoretical cornerstones of light scattering were developed early by Raman, Debye, Mie, Lorenz and Zimm (Raman, 1927; Zimm, 1948; Wriedt, 1998). Even Einstein addressed the light scattering phenomenon during his time as associate professor at Zurich by explaining light scattering from pure liquids as a result of density fluctuations (Einstein, 1910, 1911).

The fundamental equation relating the intensity of scattered light and molar masses of analytical scatterers was pioneered by Zimm in 1948,

$$\frac{Kc}{R(\theta)} = \frac{1}{M_w} + 2A_2c \quad (23)$$

where θ is the angle between the incident and the scattered rays and R_0 expresses the excess Rayleigh ratio of the light scattered from a dilute solution/suspension of analytes, i.e., the excess of scattering of the molecular solution/suspension above that scattered by the solvent itself.

Pertaining to that, R_θ is proportional to the fraction of incident light that is scattered by the pure solute without interference. A_2 represents the second virial coefficient and M_w indicates the molar mass of the analyte. At low concentrations c , the term $2A_2c$ in Eq. (23) may be negligible. K represents a physical constant according to

$$K = \frac{4\pi^2 n_o^2 (dn/dc)^2}{N_A \lambda_0^4} \quad (24)$$

where n_o is the refractive index of the solvent, N_A marks Avogadro's number, dn/dc signifies the refractive index increment of the analyte in solution or suspension, and λ_0 indicates the vacuum wavelength of the incident light. In analytical practice, the refractive index increment is easily amenable via use of refractive index detection systems. Basically, Eq. (23) is valid for any type of analyte, provided that the radial axis of the analyte does not exceed $\sim 20\%$ of the wavelength of the incident light. If the analyte reveals larger dimensions, the scattering emanating from various parts of the analyte will exhibit a difference in phase and the isotropic scattering profile will shift towards anisotropic behavior (Fig. 22).

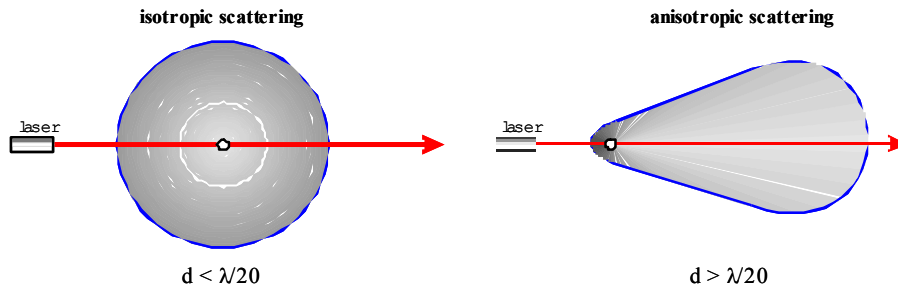


Fig. 22: Dependence of analyte size on light scattering characteristics: if the analyte diameter (d) exceeds $\lambda/20$, the light scattering profile is modified towards anisotropic scattering, i.e., light is scattered particularly in forward direction. As a consequence, at lower angles (θ) the intensity of scattered light increases.

Thereby, the extent of the phase difference depends on the scattering angle and intensifies when the observation angle is increased – while the difference remains unchanged at $\theta = 0$ (Wittgren and Wahlund, 1997b). In order to compensate Eq. (23) for the decrease in scattering power due to phase difference phenomena, a special form factor $P(\theta)$ is introduced (Zimm, 1945),

$$P(\theta) = 1 + \frac{16\pi^2 \langle r_G^2 \rangle}{3\lambda_0^2} \sin^2(\theta/2) \quad (25)$$

where $\langle r_G^2 \rangle^{1/2}$ represents the root mean square radius. This quantity is often referred to as radius of gyration, although it has no connection with any rotation or moment of inertia. By employing the form factor $P(\theta)$, Eq. (23) changes into

$$\frac{Kc}{R_\theta} = \left[\frac{1}{P(\theta)} \right] \left[\frac{1}{M_w} + 2A_2c \right] \quad (26)$$

Consequently, by assessing the scattering intensity at different angles and analyte concentrations, via Eq. (25) and Eq. (26) MALS can provide information about molecular mass, the radius of gyration and the second virial coefficient of analyte components.

It is important to emphasize that in case of small analytes with inherent diameters $< \lambda/20$ - e.g., immunoglobulin monomers of the subclass G reveal diameters of 5.2 nm - the detection of scattered light intensity at one single angle is sufficient for accurate molar mass determination. According to Fig. 22, antibody monomers scatter light in all directions with identical intensity, regardless of the detection angle. Referring to this, the form factor $P(\theta)$ may be applied as “scattering function” in order to describe the dependence of scattered light profile on the angle of detection. In case of small analytes, this dependence can be expressed in a straight line, indicating an isotropic mode of scattering (Fig. 23). Since the line slope is closely correlated to the scatterer’s diameter and as the scattering functions are to be extrapolated towards conditions with $\theta = 0$, one single detector placed at an optional angle enables accurate mass determination. However, in case of larger analytes - e.g., hmw protein aggregates with diameters exceeding $\lambda/20$ - the scattering function is to be expressed by higher-order functions. As a consequence, several breakpoints are to be assessed to determine the scattering function and to render extrapolation towards a $\theta = 0$ situation possible. Thus, several photo-detectors have to be placed at various angles.

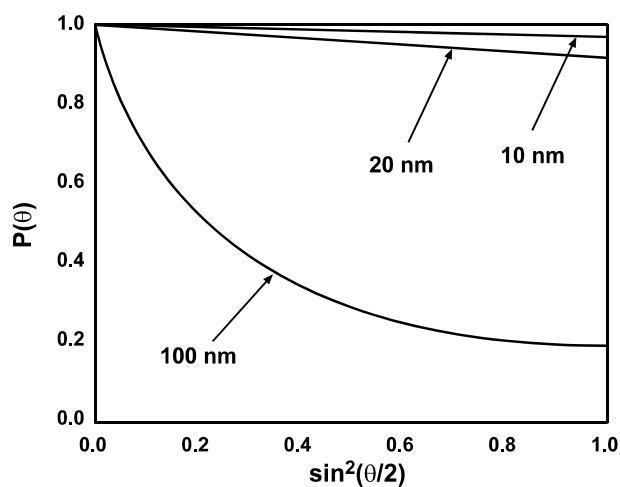


Fig. 23: Dependence of the form factor $P(\theta)$, often referred to as scattering function, on scattering analyte dimensions. The larger the analyte, the greater the angular variation of the scattered light intensity. Note that $P(0^\circ) = 1$ is imperatively.

If MALS is combined with separation systems such as HPLC or AF4, the theory outlined above may be applied to gain further information. As this modus operandi enables to gauge the scattering intensity in each small slice i of the fractionated sample via

$$\frac{Kc_i}{R_{\theta_i}} = \left[\frac{1}{P(\theta)_i} \right] \left[\frac{1}{M_i} + 2A_2c \right] \quad (27)$$

parameters such as molecular mass distribution, radius of gyration distribution and different averages of the molecular mass are made accessible (Shortt et al., 1996). Furthermore, the

concentration in each individual slice is different and the number of slices may be considered to be discretionary, thus, the amount of analyte in every slice is guaranteed to be low (Wittgren and Wahlund, 1997). Consequently, the term $2A_2c$ in Eq. (27) and Eq. (23) may be neglected, thereby improving accuracy of the calculated data.

A graphical representation of the extrapolation of Eq. (27) can be achieved by plotting Kc/R_θ versus $\sin^2(\theta/2)$ for each (θ, c) point measured (Fig. 24). The extrapolation towards $\theta = 0$ yields $1/M$ at the point of ordinate intersection, whereas the slope of the fitted straight line expresses the root mean square radius per Eq. (25).

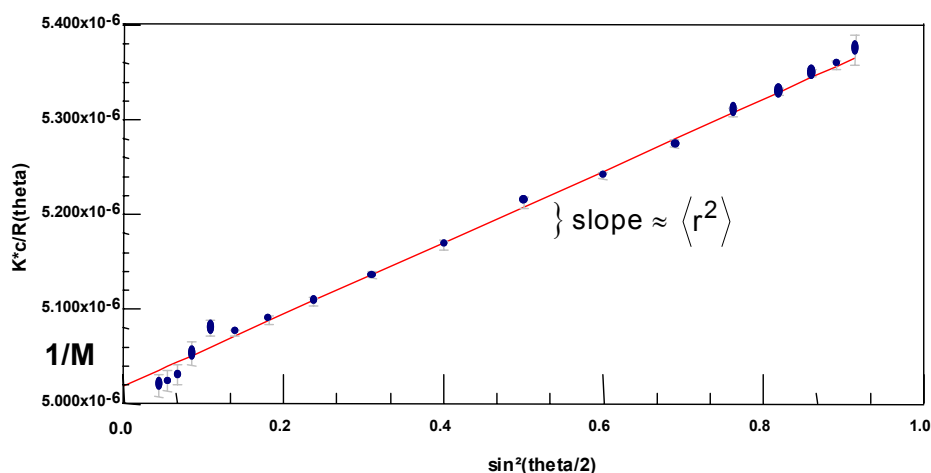


Fig. 24. A Zimm plot derived from a MALS experiment with simultaneous assessment of the scattered light intensity at 18 individual angles. The ordinate intersection indicates the reciprocal molar mass value, and the line slope represents the root mean square radius of the analyte.

Principally, the standard data reduction equipment required is a straight edge, a pencil and a firm eraser. As a matter of fact, this was the state-of-the-art treatment of data when Zimm originally developed that technique (Wyatt, 1993). In case of assessing small analytes with inherent low molecular weights, data treatment applying a Zimm plot is prevalently esteemed: the extrapolation towards $1/M$ is then targeted on high values, what is conducive for data interpretation verity. Vice versa, analyzing large sample components – i.e., sample specimen beyond 100 nm in diameter and thus exceeding $\lambda/20$, since established wavelengths of MALS instruments average ~ 600 nm – involves a reciprocal Zimm plot, generally termed Debye plot (Debye, 1944; 1947).

Thereby, R_θ/Kc is plotted versus $\sin^2(\theta/2)$. Accordingly, the extrapolation towards $\theta = 0$ yields $M/1$ – and as M represents a large value, even unprecise extrapolation results in only slight aberrations concerning experiment fidelity.

For further particulars it is to be referred to reviewed literature (Buchholz and Barron, 2001; van de Hulst, 1996; Wyatt, 1993).

As outlined in Chapter 3, the protein drug formulation scientist is strongly interested in early-stage detection of protein aggregation. In this regard, light scattering can be deployed as reconnaissance tool: the presence of even slightest amounts of (hwm) aggregates in the formulation is reflected by a disproportional intense light scattering signal. This gives the formulator a competitive edge (Fig. 25).

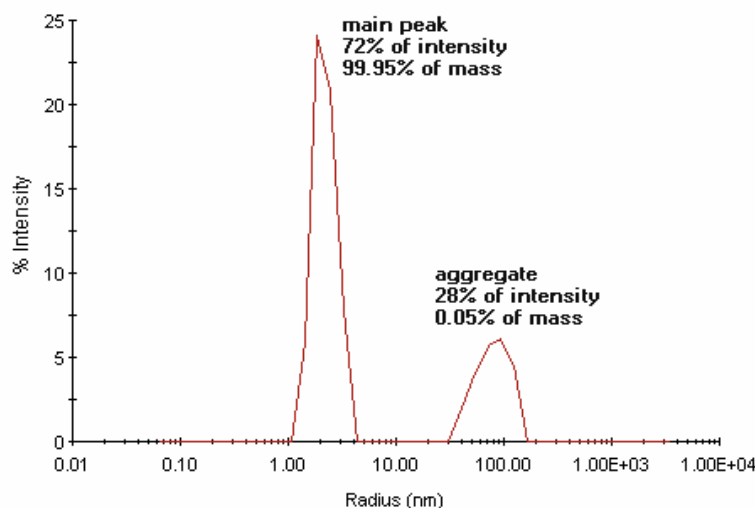


Fig. 25: Relationship of protein aggregate mass ratio and according share of the total scattered light. The protein monomers reveal a 2.2 nm diameter and account for 99.95% of the protein mass present in the sample. On the contrary, the average size of aggregate specimen is assessed to be ~80 nm. Though the aggregates total to solely 0.05% of protein mass present, they cause 28% of the intensity of overall scattered light, thus underlining the sensitivity of the method (illustration with kind permission of Alliance Protein Laboratories, CA, USA).

Therefore, the coupling of MALS with (semi-)chromatographic separating techniques such as SE-HPLC enables a highly sensitive detection of aggregate specimen in protein solutions. As demonstrated in Chapter 10, this feature of SE-HPLC/MALS can facilitate early-stage detection of protein instabilities in different protein drug formulations.

4.3 MALS in laboratory practice: on-line combination with FFF or HPLC

It is generally accepted that light scattering is the method of choice for assessing the size of analyte ensembles, provided that all analytes reveal exactly the same size (Wyatt, 1998). In that case, the ensemble of identical analytes generate a light scattering pattern the same as that of a single analyte molecule, but amplified proportional to the particle number present in the investigated scattering volume. Until analytical samples could be separated, e.g., by HPLC, light scattering measurements assessed solely weight average molecular weights and number-average square radii. The often underestimated pitfalls inherent to that limitation are reflected by one

issue of *Applied Optics*, that was (almost exclusively) devoted to light scattering (Bohren and Hirleman, 1991).

For FFF/MALS coupling basically any FFF subtechnique is qualified. The pioneering experiment was performed in 1991, when MALS was combined with Sd-FFF (Wyatt, 1991). Later on, the first successful coupling of MALS with Flow-FFF was performed in order to determine molar mass distributions of polystyrene particles and dissolved dextrans (Roessner and Kulicke, 1994). The results were compared to SE-HPLC/MALS data, thus demonstrating the general applicability of FFF/MALS to separate sample components in the range where SE-HPLC fails due to the existence of an exclusion boundary. These findings were substantiated by the characterization of ultra-hmw polymers via SE-HPLC, Th-FFF and MALS, as SE-HPLC per se was demonstrated to consistently underestimate the molecular weight of the samples (Lee and Kwon, 1995). Even in connection with MALS, the accuracy of molar mass determination via SE-HPLC was limited due to the deficiency of SE-HPLC to provide monodispersity in each data slice. Recent investigations performed by means of AF4/MALS aiming at the characterization of ultra-hmw components of synthetic and natural polymers may also be subsumed to this matter (Wahlund et al., 2002).

As a consequence, MALS is preferentially applied to characterize hmw and particulate sample specimen fractionated via precedent FFF separation. E.g., polystyrene latices and various swellable core-shell sub-micron particles were assigned (thermal) diffusion coefficients, surface structure and radii of gyration by associating MALS with Th-FFF and AF4, respectively (Mes et al., 2001; Frankema et al., 2002). A challenging analytical task was approached when molar mass distributions of polymer aggregates in solutions containing flocculants were evaluated via Flow-FFF and MALS (Hecker et al., 1999).

Pertaining to pharmaceuticals, MALS can be employed to accurately analyze colloidal and particulate systems running the gamut from nm to μm range. E.g., heterogeneous mixtures of cationic lipid-DNA colloids can be characterized in terms of shape and size distribution subsequent to separation via Flow-FFF (Lee et al., 2001).

As HPLC enjoys a state-of-the-art prevalence, a broad spectrum of applications in combination with MALS may be itemized. Most notably, synthetic polymers are characterized routinely in both aqueous and organic solvents (Himel et al., 2003). In particular, the characterization of block copolymers is to be quoted, as copolymers gain increasing importance in (colloidal) drug carrier design (Zhang et al, 2003; Liu and Tsiang, 2003). Referring to this, the successful determination of molar mass, polydispersity and storage stability of hyaluronan in commercial intra-articular injectable preparations may be instanced (Adam and Gosh, 2001).

Commensurate with AF4 applications in protein analytics, HPLC/MALS primarily is applied for characterization of aggregated hmw specimen (Southan and MacRitchie, 1999). In case of fibroblast growth factor, MALS contributed substantially to the elucidation of multimer

formation pathways due to varying oxidation conditions (Astafieva et al., 1996). Additionally, the characterization of proteins incorporated within colloidal drug carriers like liposomes or the analysis of liposomes per se was effectively approached applying MALS (Wang et al., 2002).

In order to add to the information provided, UV-spectrophotometry and refractive index (RI) detection are normally associated with MALS. With regard to protein analytics, assessment of protein concentration can easily be performed via UV-spectrophotometry, whereas the degree of glycosylation of proteins is advantageously determined by RI detection. This ternary detection set-up enabled the extensive evaluation of oligosaccharide conjugate vaccines by means of SE-HPLC/MALS (Jumel et al., 2002).

A more detailed listing of MALS applications comprising the period before 1999 – focusing on the coupling with FFF - can be found in the literature (Coelfen and Antonietti, 2000). In general, MALS is expected to have a cumulative stake in future analytics. Up to 1997, only few MALS applications were published, whereas there is an exponential increase ever since.

5 Summary

Despite more than two decades of intense research, the pharmaceutical formulation scientists still miss a generally-valid, rational procedure to ensure adequate protein drug stability. Thereby, protein stabilization is often hampered by a very subtle balance between native conformation and denatured states. The most prevalent outcome of physical instability is protein aggregation. In this regard, considerable progress has been made in understanding the complex combination of circumstances leading to aggregation, particularly facilitated by modern advanced analytical techniques capable of accurately assessing the rate of protein aggregation.

Field-flow fractionation (FFF) is introduced in **Chapter 2** as a family of analytical techniques with broad application range. Although pioneered almost four decades ago, FFF was adopted in analytical laboratories only recently to an increasing extent, mainly due to perfecting of inherent system parameters. The most prominent FFF subtechniques, their mode of operation and basic theoretical principles are expounded. A large subsection is devoted to AF4, the main technique applied in this thesis for assessing the degree of protein aggregation in liquid formulations and for approaching challenging tasks in pharmaceutical analytics. Besides the AF4 channel set-up, the individual separation steps involved in an AF4 experiment are outlined. Particularly with regard to applications presented in the Experimental Section, the basic modes of AF4 sample elution are described. In a concluding part, selected applications of AF4 are highlighted, thus offering a general survey of the published literature - though pharmaceutical applications are accentuated.

Chapter 3 attends to protein stability in pharmaceutical liquids. Introductorily, a description of the main chemical degradation pathways is presented – primarily hydrolysis and oxidation. The following section summarizes the wealth of information on protein aggregation available via a multiplicity of scientific articles. The aggregation phenomenon is elucidated in thermodynamical terms, thereby instancing caveats and misunderstandings which the matter inherently encounters. Consequently, the aggregation process per se is illustrated, dealing with issues such as molten globule states and fibre formation, for instance. Eminent emphasis is laid on reviewing prevalent aggregation theories extended in the literature. Contrarily to the dazzling array of theories being at the reader's disposal, little to no insight is provided in many articles on how the individual theory is to be put into correlation with other theories available. Accordingly, colloidal aggregation models are discussed in comparison to lattice models or domain swapping. Additionally, the controversial issue of polar group burial and nonpolar group burial, respectively, in the course of their contribution to protein stability and native state maintenance is reasoned. Finally, analytical methods commonly utilized in quantification of protein aggregation are

itemized and evaluated in terms of applicability, accuracy and inherent drawbacks. Thereby, one point of concern is the differentiation between methods capable of soluble aggregate analytics and insoluble aggregate/precipitate characterization, respectively.

Chapter 4 is a synopsis of multi-angle light scattering (MALS) in protein analytics. Initially, scope and underlying principle of both general light scattering techniques – i.e., dynamic and static mode - are defined. Given the background of its importance to analytical case studies outlined in chapters later on, the presentation of theoretical aspects of MALS is focused therein. The difference between isotropic scattering and anisotropic scattering and the employment of both scattering profiles in terms of absolute molar mass assessment and size determination are presented. Furthermore, the sensitivity of MALS concerning high-molecular weight or particulate specimen is explained. The chapter is completed with a list of exemplary MALS applications in combination with FFF and SE-HPLC, respectively.

Throughout the Theoretical Section strong emphasis was put on aligning the presented topic with scientific references. In order not to inappropriately outrange the scope of the thesis, an extensive reference list is provided in Chapter 12, indexing relevant special and continuative literature.

6 AF4 as analytical tool in protein aggregation analytics

6.1 Introduction

Considered more a bibelot of a few supporters rather than an effective separation method, FFF for long time was ascribed only minor importance in the arsenal of powerful analytical separation methods, especially when compared to popular techniques inhering similar application ranges, e.g., (SE)-HPLC and electrophoresis. Contrarily to the variety of distributors of HPLC equipment, in the field of FFF the analytical scientist for many years was dependent on one commercial manufacturer (FFFractionation LLC, Salt Lake City, USA). In many laboratories the standard FFF apparatus accounting for the development of new applications in most cases was a provisional do-it-yourself construction. However, things were on the move, and at present the analytical scientist is facing three manufacturers of commercially available FFF systems (Consensus GmbH, Ober-Hilbersheim, Germany; Postnova Analytics, Landsberg/Lech, Germany (merged with FFFractionation in 2001); Wyatt Technology Corp., Santa Barbara, USA).

Driven by the firms' impetus to increase the FFF technique's recognition, several articles were published, focusing thereby on the broad applicability of AF4 particularly in protein analytics and attending to the assets of AF4 compared to SE-HPLC (Wyatt Technology, 2002; Hansen and Klein, 2001; Jiang et al., 2000). Unfortunately, as with many other publications in this field, parameters such as reproducibility, sample recovery, elution order, etc., were not discussed in detail.

It is the aim of this chapter to comprehensively evaluate the general applicability of AF4 in protein analytics. Furthermore, new applications with the potential to have a considerable stake in the future are presented, including the possibility to invert the AF4 elution order in normal mode separations. Additionally, AF4 data on various proteins are compared to SE-HPLC data. As the discussion of experimental results often refers to figures or tables, the data are discussed extensively where appropriate. The chapter is concluded by a summarizing discussion.

6.2 Evaluation of general AF4 applicability in protein analytics

6.2.1 Materials and methods

All AF4 experiments presented in this thesis were performed with an HRFFF-10.000 AF4 system, comprising separation channel, pumps accounting for injection flow, forward flow and cross flow, in-line solvent filter (0.1 μm , PTFE), degaser (PN75) and autoinjection system (PN5200) (all from Postnova Analytics, Germany) (Fig. 26). Except stated otherwise, the channel height was 350 μm , the flow rate at the channel outlet was 1.0 mL/min, the sample loop held 100

μL and the applied ultrafiltration membrane consisted of regenerated cellulose with a 5 kDa cut-off (Postnova Analytics, Germany, and Nadir Filtration GmbH, Wiesbaden, Germany, resp.).

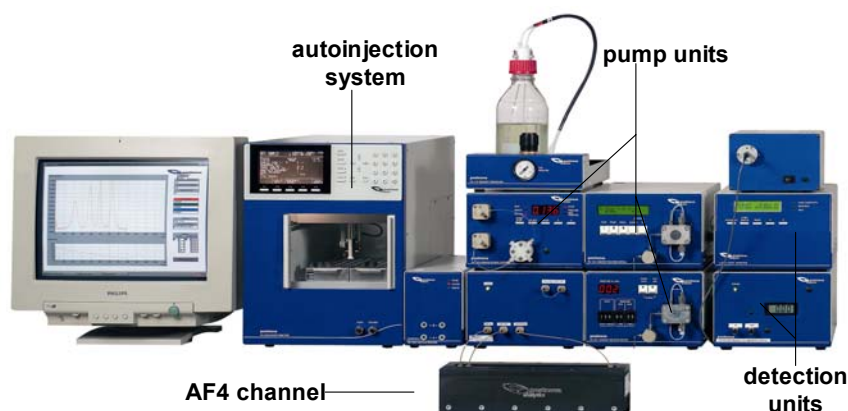


Fig. 26. AF4 system with channel, autoinjection system and detection units (UV, RI). Via pumps, the flow rates of forward flow, cross flow and sample injection flow are regulated.

The AF4 system was connected to a ternary detection system, combining MALS, UV-spectrophotometry and RI detection. MALS was performed by a miniDAWN[®]Tristar[™] with a 30 mW GaAs linearly polarized laser emitting 690 nm wavelength light and using three angles in order to detect scattered light (45°, 90°, 135°) (Wyatt Technology, USA). UV-spectrophotometry was performed at 280 nm wavelength (SpectraSystem UV 1000, Thermo Separation Products, Germany). Values of protein dn/dc were determined with a deflection type differential RI detector (Δn -1000, $\lambda = 620$ nm, WGE Dr. Bures, Dallgow, Germany). If not specified differently, the carrier medium consisted of 20 mM dibasic phosphate, pH 7.5.

Comparative study AF4 versus SE-HPLC: SE-HPLC was performed applying two different columns (column I: TSKgel G3000SW, Tosoh Biosep GmbH, Stuttgart, Germany, column pressure during operation 24 bar; column II: superose 6 HR 10/30, Amersham Biosciences Europe GmbH, Freiburg, Germany, column pressure during operation 7 bar), sample loop 20 μL , flow rate 0.5 mL/min, in-line degassing was performed (SCM1000, Thermo Separation Products, Germany). Due to overlapping of experiment time column I was connected solely to UV₂₈₀-spectrophotometry. AF4 parameters: channel height 500 μm ; an initial 80% cross flow rate was maintained for 20 min, then linearly minimized to 0% within 3 min; system pressure during 80% cross flow was 4 bar, without cross flow 2 bar; sample loop 100 μL , forward flow rate 0.6 mL/min. Carrier liquid for SE-HPLC and AF4 were identical to BSA solution medium (refer to Section 6.5), BSA samples were not diluted prior to injection, all experiments were performed in triplicate ($n=3$).

Prior to the AF4 fractionation steps, blue colored dextran was applied to monitor flow line ideality, contingent channel leakage, time-period of sample injection and focusing performance. As illustrated in Fig. 27, the intense color of the sample enables a convenient

control thereof. Subsequent to the focusing process, the elution step transports blue dextran in form of a colored band towards the channel outlet, visualizing the forward flow velocity. Blue dextran was shown to adsorb only moderately to capillary material, PMMA wall material and cellulosic membranes – thus, a consecutive short-time (<2 min) separation run with buffer liquid guarantees a total wash-out of the indicator analyte and provides immaculate channel surfaces.

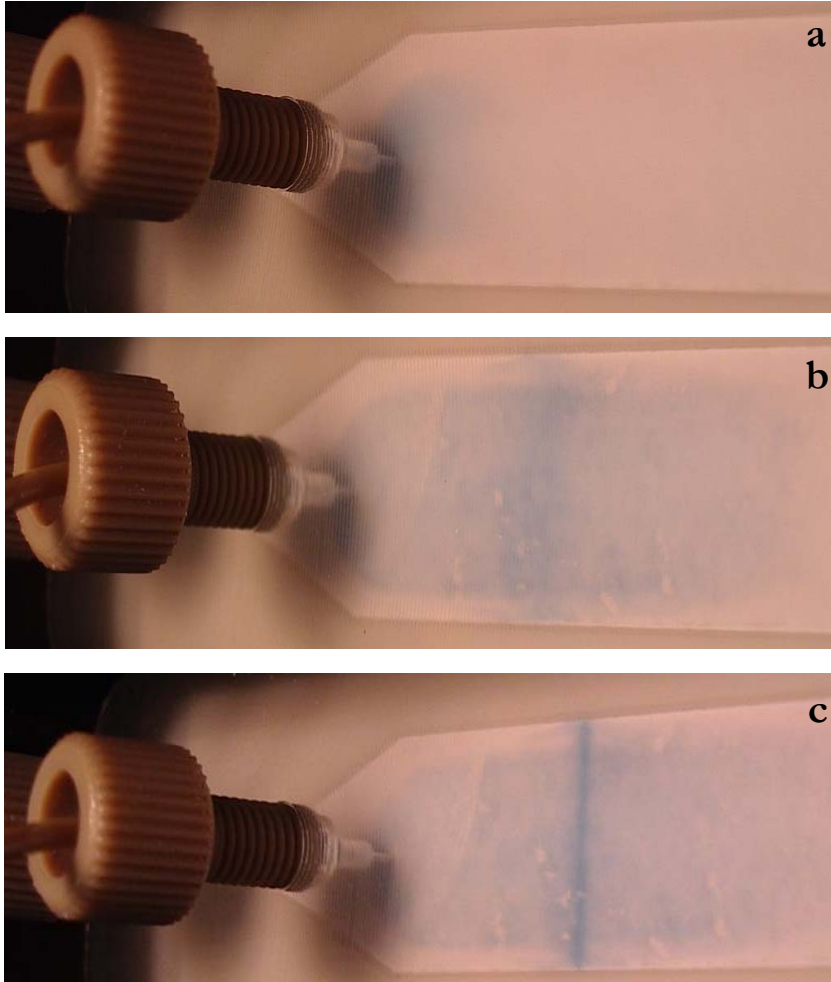


Fig. 27. Monitoring of sample injection and subsequent focusing of blue dextran in an AF4 channel; channel width 13 mm. **a)** Beginning injection via the sample injection port, blue dextran streaming towards the channel outlet. The forward flow inlet is placed at the end of the tapered channel, hidden by the brown fitting of the injection port. **b)** Initiation of sample focusing/relaxation. The densifying blue region in the middle of the picture indicates z' , used in Eq. (15). z' is assessed by the flow rate ratio of both focusing flows originating from channel inlet and channel outlet. **c)** Optimum of focusing/relaxation. The band representing blue dextran, extending over 80 mm prior to focusing, is narrowed to <1 mm.

Vice versa, the permeability of the applied ultrafiltration membrane may be demonstrated by means of colored lmw components such as bromophenol blue (BMP). During focusing, the BMP will gradually pass the membrane pores. Sufficient focusing time provided, the BMP will eventually vanish in total. Referring to this, a typical range for the focusing/relaxation time encompasses 30 – 180 s, whereas a representative injection time is 60 s using a 50 μ L injection

loop and a sample feed rate of 0.2 mL/min. The final fractionation step normally takes 10 – 30 min, although high-speed separations lasting <5 min have been described (Reschiglian et al., 2002). Often esteemed as linchpin of every successful AF4 experiment, the fractionation step simply leverages the accomplishments of the precedent focusing step, as far as the positioning of sample specimen in their steady-state equilibrium levels is concerned. In order to prove the quality of the channel configuration and the influence of different cross flow intensities on the analyte elution profile, the scrutiny via standard samples is well-established (Wahlund, 2000).

6.2.2 Results

The efficacy of an AF4 system can be investigated by monitoring the resolution of the different sample components, e.g., of accurately defined mixtures of polystyrene latex colloids or particles (Wright et al., 2001; Wahlund and Zattoni, 2002). Likewise, proteins represent ideal standard analytes, since the composition of each native monomer – concerning primary and secondary structure – is identical, thereby ensuring an unimodal size distribution. Based thereupon, the 440 kDa protein ferritin is often employed, as ferritin usually exhibits a constitution profile of monomers aside several oligomers (Wahlund, 2000). Equally, human or bovine serum albumin (HSA/BSA) may be used, due to its inherence of considerable amount of dimer (~10%) and higher-order oligomers/aggregates. Additionally, the amount of higher-order specimen can easily be increased by protein stressing, e.g., via 60 °C storage for 3 d of HSA lyophilisate, yielding accretions from 9.3% up to 29% for dimer and from 2.5% to 11.9% for trimer and higher-order specimen (Moreira et al., 1992). As illustrated in Fig. 28, HSA can favorably be employed to demonstrate the correlation between cross flow intensity and efficacy of resolution.

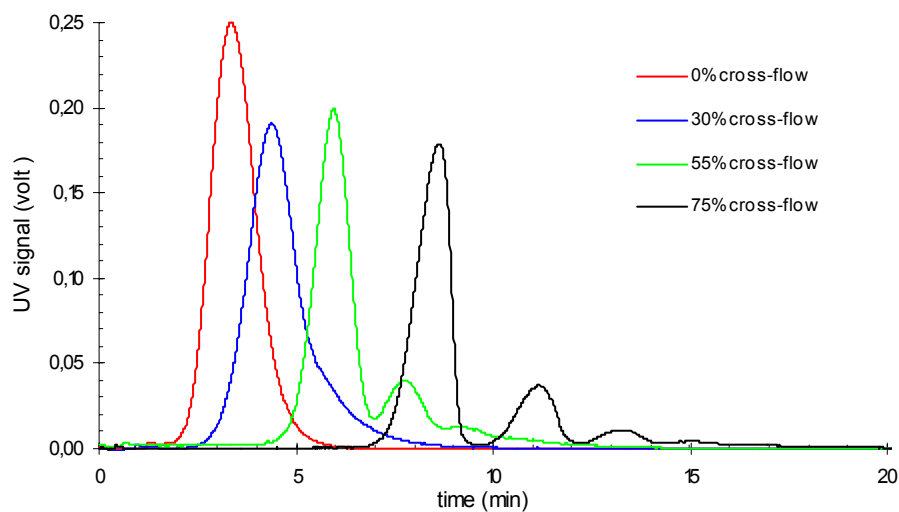


Fig. 28. Fractionation of HSA at different AF4 separation conditions. Note the correlation between increasing cross flow strength and prolonged elution time/resolution power.

When 0% cross flow is applied – i.e., no parameters provoke sample retainment – the HSA specimen are eluting concomitantly, unifying in one symmetric peak in subsequent UV₂₈₀ detection. Contrarily, when subjected to increasing cross flow intensities, the analytes elute more sluggishly and the peak symmetry changes towards a tailing profile. With 55% cross flow, sample elution is prolonged onward and analyte fractionation is performed, visualized by several UV₂₈₀ peaks. According to the theoretical principles of normal-mode separation, smaller analyte specimen elute prior to larger analytes – hence, it may be deduced, that the peaks derived from 75% cross flow conditions represent HSA monomer, dimer and trimer, eluting within 15 min. Subsequently, higher-order oligomers may be detected.

Fig. 28 gives rise to the question of both peak identification and the whereabouts of hmw aggregates. Referring to the first, the molecular weights of HSA specimen may be determined by PAGE; yet this involves the interpretation of data derived from different analytical techniques, facilitating potential data misinterpretation. On the other hand (knowledge on dn/dc values of the protein provided), each peak can be assigned the appropriate analyte molar mass via simultaneous MALS/UV-detection. Therefore, the HSA dn/dc value was determined off-line by RI analytics, applying concentrations in the range of 1-5 mg/mL. Via plotting $(n_i - n)/c_i$ versus c_i and extrapolating to zero concentration, dn/dc was determined to be 0.173 mL/g (with n_i being the refractive index at concentration c_i and n representing the refractive index of the carrier liquid). This value is in good agreement with formerly published data, where HSA dn/dc values were assessed 0.168 and 0.175 mL/g, respectively (Stuting and Krull, 1990). Accordingly, on-line molar mass determination of the fractionated specimen enables the unambiguous identification of analytes.

The sensitivity of larger analytes on high cross flow rates potentiates immobilization of hmw aggregates upon the ultrafiltration membrane. Thus, performing the experiment with 75% cross flow conditions even for long periods – e.g., for 10 hrs – renders no hmw aggregate elution. As a consequence, sample retainment is to be decreased by reducing the cross flow after elution of separated oligomers, i.e., after 20 min. Subjected to this separation conditions, HSA can be separated in monomer, dimer, trimer, tetramer and higher-order oligomers within 20 min. Subsequently, by gradually minimizing the cross flow rate within short time, the resolution power of the system is decreased and a soluble (hmw) aggregate fraction can be detected (Fig. 29).

Due to the possibility of flow programming, a broad repertoire of separation conditions is provided, comprising a broad molar mass application range (Fig. 29). The challenging aspect of AF4 flow programming is to maintain a delicate balance between optimal separation parameters – contributing to resolution power and low experiment times – and a “controlled system crash” – induced by irreversible sample immobilization on the membrane due to ultra-high cross flow rates. Optimizing a separation generally involves increasing the resolution of the analyte specimen and/or decreasing the analysis time. Unfortunately, in most prevalent analytical techniques –

including AF4 – resolution and analysis time are competing factors. As a consequence, the forward flow rate of the carrier can not be increased at random without sacrificing resolution. Therefore, a trade-off exists between resolution and analysis time (Schimpf, 2000c).

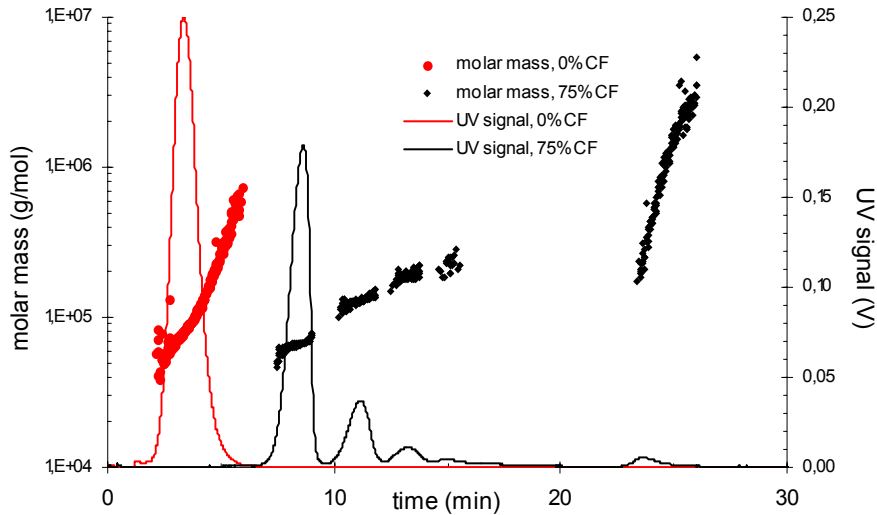


Fig. 29. Fractogram of HSA characterization applying 0% and 75% cross flow intensities, respectively. Minimizing the 75% cross-flow to 0% after 20 min enables elution of hmw aggregates, revealing molar masses of $>10^6$ Da. MALS enables convenient UV data interpretation, assigning calculated masses to the peaks of monomer (66.9 kDa), dimer (133.8 kDa) and trimer (204 kDa), matching the theoretical values. Note that the UV signal of 0% cross flow analysis unifies all HSA specimen, running the gamut from monomer to hmw aggregates. Due to the merger of scattered light from both hmw aggregate and lower-order specimen, the calculated mass maximum does not exceed 10^6 Da.

Ultimately, flow rates are limited by either pump specifications or the resulting rise of channel pressure. Low elution rates, e.g., <0.4 mL/min, imply the risk of peak broadening due to a growing impact of the well-known Eddy diffusion phenomenon (Giddings, 1960).

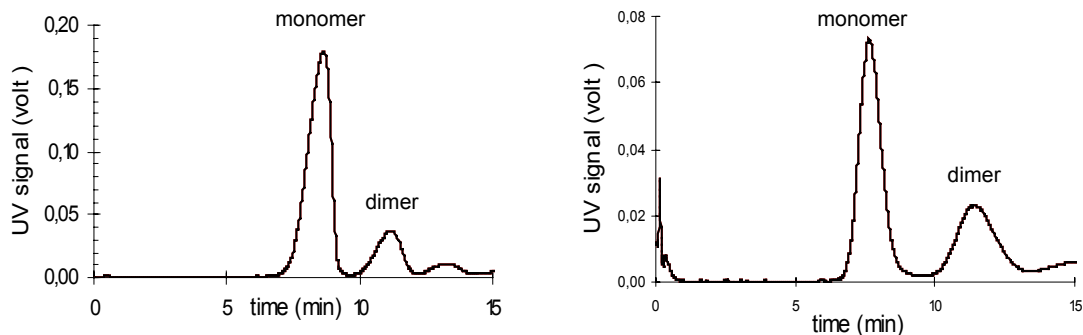


Fig. 30. Separation of HSA, applying 75% (left) and 85% cross flow rates (right). Although AF4 separation theory correlates intense cross flow rates with increased resolution, the dimer at 85% cross flow conditions is separated less efficacious from adjacent monomer and trimer than at less stringent conditions. This is mainly to be ascribed to sample-membrane interactions.

Furthermore, field strengths are finite due to the potential interaction of sample components with the ultrafiltration membrane as they are forced into more concentrated zones upon the membrane. Thus, increased cross flow rates do not necessarily lead to a gain in resolution power. In fact, if cross flow intensities exceed a definite threshold, this detracts from resolution, although sample retainment is prolonged (Fig. 30).

Besides resolution power, the amount of sample – either minimally required or maximally acceptable - amenable to AF4 separation appraises the applicability of AF4 in protein analytics. In general, a sample size of 1-50 μg is appropriate for most materials, whereas lower values are considered to be more favorable when the detection system inheres sufficient sensitivity (Moon and Myers, 2000). It is known that long-chain molecules are subject to considerable entanglement even at low mass concentration levels – thus making retention time and elution profiles dependent on concentration (Caldwell et al., 1988). On the other hand, anionic polymers were shown to reveal a tendency for high-loaded samples (30 μg) to elute earlier than small sample loads (5 μg) (Benincasa and Giddings, 1992). Consequently, the relationship protein load – elution profile was evaluated by analyzing 5 μg and 500 μg HSA, respectively (Fig. 31).

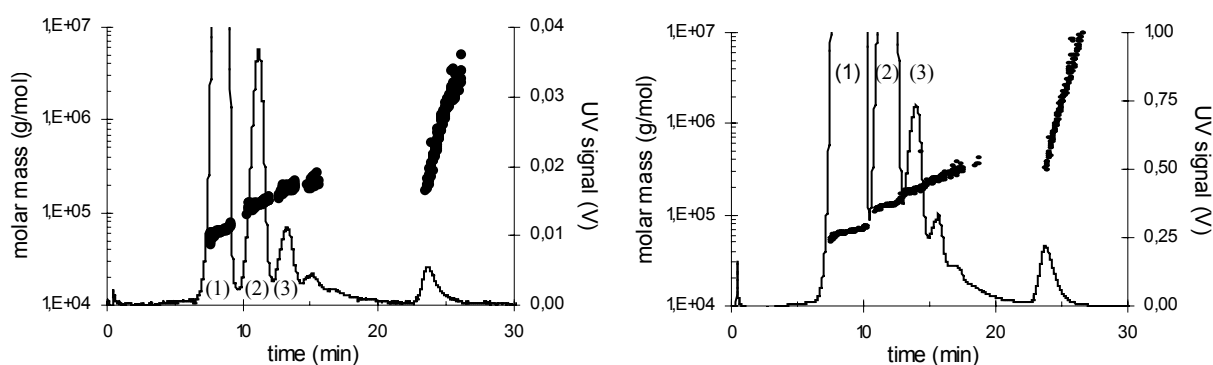


Fig. 31. Characterization of HSA samples with 5 μg load (left) and 500 μg load (right). In both experiments MALS assigned the monomer 67 kDa (1), the dimer 134 kDa (2) and the trimer 204 kDa (3). Concerning elution time, HSA specimen elute slightly differently: the 5 μg load trimer fraction finishes detector passage at 13.9 min, compared to 14.8 min of the 500 μg sample. Experiment conditions: 0.6 mL/min forward flow, 75% cross-flow (0-15 min, then linearly lowered to 0% at 22 min); UV-detector sensitivity dimmed by factor 2.5 in right figure.

As outlined above, the influence of sample load on elution time is discussed controversially. The findings in Fig. 31 are consistent with earlier work (Giddings et al., 1978c). Generally, because AF4 separation passes off in a very thin region with high sample concentration near the ultrafiltration membrane, the protein molecules may interact, what affects the diffusion coefficients, increases the viscosity and thus is regarded to prolong retention time (Benincasa and Giddings, 1992).

On the other hand, repulsion/interaction between analyte molecules can increase the area required for optimal separation – as a consequence, the equilibrium of distribution may be displaced towards higher, and therefore faster, flow laminae (Moon and Myers, 2000). Moreover,

the value of diffusion coefficients is deduced from infinite dilution, and as the fractionation of highly-loaded samples is involved with a more pronounced vertical concentration gradient, this additionally contributes to a more elevated steady-state position of the samples. Despite the variety of all theoretical scenarios, it is to be noted, that the elution profile of samples with concentrations varying by two orders of magnitude is in effect congruent, substantiated by the experimental data (Fig. 31).

As outlined in Table 1, the detected mass distribution among monomers, dimers and aggregates of high- and low-loaded samples vary, but can be assessed in reproducible way.

Thereby, high-loaded sample analysis is associated with inherent greater ratios of higher-order specimen, especially hmw aggregates. Since both samples were drawn from HSA stock solutions with concentrations of 50 $\mu\text{g}/\text{mL}$ and 5000 $\mu\text{g}/\text{mL}$, respectively, this discrepancy appears reasonable: the general dependence of the aggregation rate on protein concentration has been repeatedly reported (Wang, 1999).

mass distribution (%)	5 μg sample load	500 μg sample load
monomer	74.2	70.1
dimer	15.6	16.5
\geq trimer	8.6	10.3
hmw aggregates	1.6	3.1

Table 1. Mass distribution among HSA specimen in terms of 100-fold difference in sample load ($n=5$, S_{rel} for all data <2.3).

In summarizing the results, the applicability of AF4 in protein characterization appears feasible. Protein sample specimen can be separated with sufficient resolution in reproducible way. Furthermore, the coupling of AF4 with MALS, UV- and RI-detection facilitates both data interpretation and evaluation.

6.3 Parameters of fractionation

6.3.1 Sample recovery

The practicability of any separation method depends ultimately on its capability for the conversion of analyte specimen into separated fractions. In this regard, the evaluation of sample component recovery – i.e., the system’s ability to fractionate complex samples without a significant loss of content – is of utmost importance in order not to run the risk of a concomitant loss of information.

Principally, the term “absolute recovery” is to be differentiated from “relative” or “linear recovery”. The first is defined as the mass percentage of an injected sample that is recovered from the separation system (Williams and Giddings, 2000). In contrast, relative/linear recovery attends to the recovery of a sample component in amounts being proportional to – but not necessarily equal to – their levels in the original sample. It is obvious that without detection systems granting access to mass calculations – e.g., MALS – the absolute sample recovery can not be determined.

In case of AF4, sample loss may be the result of sample transport through the ultrafiltration membrane or of adsorption to the membrane (Beckett et al., 1988). As both phenomena are enhanced by direct contact and/or interaction of sample components with the ultrafiltration membrane, intensity and duration of cross flow and focusing step have a crucial impact on sample recovery. However, optimum conditions provided, the pursuit of absolute recovery values of almost 100% is not illusive (Fig. 32).

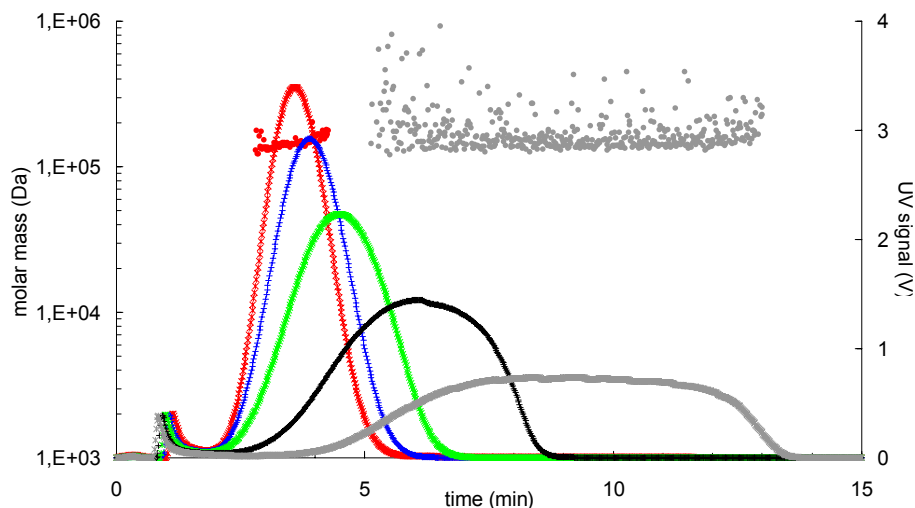


Fig. 32. Elution profiles of an immunoglobulin sample with >99.9% native monomer content in the original bulk solution. The color of the solid UV₂₈₀ lines and the MALS signals (dots) refer to cross flow intensities of 0% (red), 10% (blue), 20% (green), 30% (black) and 40% (grey). Ratio of AUC₂₈₀ 40% / AUC₂₈₀ 0% = 0.996; membrane cut-off 1 kDa; focus step was abandoned.

As demonstrated in Fig. 32, increasing cross flow rates do not mandatorily imply lower recovery rates due to adsorption processes and/or sample passage through the ultrafiltration membrane. The investigated 150 kDa immunoglobulin was shown to reveal a >99.9% native monomer content, demonstrated by RP-HPCL, SE-HPLC and circular dichroism analysis (Abbott, 2000). The impact of the exerted cross flow rates is reflected by prolonged elution times and peak broadening. MALS proves the immunoglobulin to exhibit unimodal mass distribution, regardless of the cross flow intensity applied. Because of the combination of concentration sensitive UV detection and molar mass sensitive MALS detection, sample recovery can be specified in terms of mass values. It is important to note that the AF4 system utilized was well-conditioned and potential adsorption effects were overcome due to constant operation: when analyzing polymers, the total adsorption of sample components on fresh membranes repeatedly was reported (Benincasa and Giddings, 1992). Though, subsequent experiments will yield increasing recovery rates, as the channel surface areas prone to adsorption are small and conditioning can be provided with minimal protein quantities, typically $\sim 10 \mu\text{g}$ (Coelfen and Antonietti, 2000; Towns and Regnier, 1991). The influence of the injected sample mass on absolute recovery rate is demonstrated in Table 2.

cross-flow intensity	0%	10%	20%	30%	40%
10 μg sample load	99.7	99.4	98.9	98.3	97.5
50 μg sample load	99.9	99.7	99.4	99.1	98.7
100 μg sample load	99.9	99.7	99.5	99.2	98.9

Table 2. Influence of sample load of a 147 kDa immunoglobulin on absolute recovery rate; membrane cut-off 1 kDa; $n = 5$, S_{rel} for all data < 0.89 ; experiment time 15 min, focusing step was abandoned.

As outlined, lower sample recoveries correlate to decreasing sample loads and intensified cross flow rates. Due to the relatively high molar mass of the immunoglobulin and the commensurate sensitivity on field strength, even moderate separation conditions entail notable retainment. Increasing the resolution power further on gives rise to complete sample immobilization upon the membrane. E.g., exerting 80% cross flow for 2 hrs yields recoveries of less than 10%. Referring to this, sample loss due to high field strengths was often reported as empirical fact (Jiang, 1994; Ratanathanawongs and Giddings, 1992; Li et al., 1990).

Besides adsorption, membrane parameters such as material and permeability influence sample recovery. In this realm, the affinity of proteins for membrane adsorption can often be attenuated by well-advised choice of carrier liquid, e.g., in terms of pH and both salt and surfactant content (Barman and Moon, 2000).

Contrarily, sample loss through the membrane can only be depleted by membrane cut-off specifications and not by so-called soft parameters such as carrier liquid composition. For

instance, a 15% loss of cytochrome C (13 kDa) or a 4% loss of BSA have been reported for cellulose membranes with 5 kDa cut-off, whereas 15% of a γ -globulin sample (160 kDa) passed a 100 kDa cut-off membrane (Williams and Giddings, 2000; Li et al., 1991). Based on that, the recoveries of a 147 kDa immunoglobulin versus membrane cut-off values were investigated (Table 3).

cross-flow intensity	0%	10%	20%	30%	40%
1 kDa cut-off	99.8	99.6	99.3	99.0	98.6
5 kDa cut-off	99.8	99.6	99.4	98.9	98.5
10 kDa cut-off	99.8	99.5	99.3	98.7	98.3

Table 3. Influence of regenerated cellulose membrane cut-off on absolute recovery of a 147 kDa immunoglobulin, $n = 5$, S_{rel} for all data < 0.95 , experiment time 15 min, focusing step was abandoned.

Referring to Table 3, only slight differences of the recovered sample masses can be detected. Subjected to low cross flow rates ($\leq 20\%$), the immunoglobulin is recovered always with identical rates, regardless of the applied membrane. However, increasing the field strength results in greater sample loss, which is maximal in case of 10 kDa cut-off membranes and in effect identical for membranes with 1 kDa and 5 kDa cut-off, respectively. The data appear reasonable, as the protein accumulation upon the membrane increases with greater flow rates – accordingly, the membrane with the greatest permeability reveals the most pronounced sample loss.

Whereas the impact of cross flow intensities on sample recovery already has been reported, no extensive study was performed investigating the influence of the focusing step thereon. Bearing in mind that during focusing the analyte specimen are concentrated within a narrow band with close contact to the membrane – as both opposing focus flows meet at the focusing point z' and mainly pass the membrane there – this appears remarkable. Furthermore, since both focusing length and intensity are attributed decisive influence on the quality of the subsequent separation, AF4 operators may tend to elongate the focusing step (Coelfen and Antonietti, 2000).

The theoretical membrane cut-off expresses a situation, where 90% of an analyte with a molecular weight identical to the cut-off value are retained by the membrane (Poeppelmeyer, 2002). Though, both effective membrane cut-off and membrane adsorption were characterized to be governed by analyte size, shape, surface charge and the solution conditions (Balakrishnan et al., 1993). Accordingly, proteins may differ in their recovery rates.

In order to approach that problem, identical mass amounts of several proteins were injected into the channel and subjected to various focusing periods. Since the influence of focus strength per se was attended, the subsequent elution step was performed without cross flow. As illustrated in Fig. 33, focusing notably affects protein recovery, whereby the lion's share of

protein loss is recorded during the initial stages of focusing (0-100 s). BSA (66.4 kDa), erythropoietin (EPO, 38 kDa) and γ -immunoglobulin (IgG, 147 kDa) are shown to yield the highest recovery rates. Given the background that those globular proteins are empirically characterized as very hydrophilic proteins, this appears rational. E.g., the adsorption of EPO on membranes made of regenerated cellulose was shown to be very low (Opatrny et al., 1998). Moreover, in contrast to granulocyte colony stimulating factor (G-CSF), EPO is a glycoprotein with an average carbohydrate content of $\sim 40\%$, thus revealing increased hydrophilicity (Narhi et al., 1991). In case of the less hydrophilic G-CSF (19.6 kDa), the increased sample loss may be ascribed to protein passage through the membrane, as the molar mass of G-CSF exceeds the membrane cut-off only 4-fold. However, facing a $\sim 40\%$ sample loss of interferon α -2a – IFN-2a, revealing a 19.4 kDa molar mass – after 300 s focusing, at least in terms of IFN α -2a adsorption appears to contribute more to sample loss than potential membrane permeation phenomena.

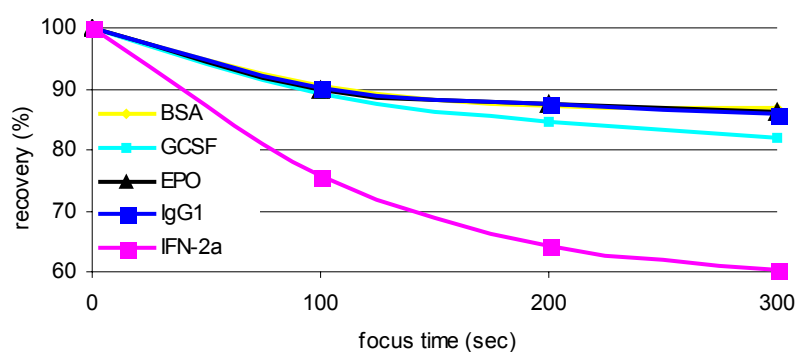


Fig. 33. Recovery rates of proteins depending on focusing time: BSA (66.4 kDa), granulocyte colony stimulating factor (G-CSF, 19.4 kDa), erythropoietin (EPO, 38 kDa), γ -immunoglobulin (IgG1, 147 kDa), interferon α -2a (IFN-2a, 19.4 kDa); AF4 parameters: focusing flow 0.8 mL/min, 15 min elution without cross flow, membrane cut-off 5 kDa, detection via MALS/UV₂₈₀, sample load 25 μ g each, $n=5$, S_{rel} for IFN-2a data >1.7 , for all other data <0.83 .

These experimental data is circumstantiated by former studies, showing interferon to adsorb readily not only to hydrophobic and hydrophilic surfaces but also to hydrophobic nanoparticles or proteins and other macromolecules (Nagaki et al., 2003; Lecomte et al., 2002; Ruzgas et al., 1992). Additionally, it is known that proteins of the IFN α -subtype generally inhere a flexible nature (Alkan and Braun, 1986). This (conformational) flexibility may facilitate – besides unfolding and aggregation – adsorption tendencies of IFN α -2a.

It is to be summarized that for all investigated proteins – except IFN α -2a – a 100 s focusing step results in acceptable recovery rates of $\sim 90\%$. However, in order to gain an increase in IFN α -2a recovery, the optimization of carrier liquid – e.g., by solvent effects – seems inevitable. The importance of solvent effects in protein analytics becomes evident, as proteins can be switched from positively to negatively charged polyelectrolytes by pH variation. Generally, the carrier pH should be chosen outside the range of the isoelectric point (IEP) to avoid

adsorption problems (Coelfen and Antonietti, 2000). Given a carrier pH of 7.4 and IEP values of the five proteins of 4.0-5.5, adsorption due to inadequate pH may not be an issue.

On the other hand, the use of nonionic surfactants in order to eclipse protein adsorption phenomena is state-of-the-art (Wang et al., 1995). In HPLC, nonionic surfactants are known to hydrophobically adsorb onto column surfaces to create a hydrophilic layer that will exclude proteins from the surface (Desilets et al., 1991). In this realm, Tween 20 was used in the fractionation of wheat proteins by Flow-FFF (Stevenson and Preston, 1997). Moreover, Tween 20 was demonstrated to displace adsorbed interferon specimen completely from both hydrophilic and hydrophobic surfaces (Ruzgas et al., 2003). As a consequence, in order to reduce IFN α -2a adsorption upon the ultrafiltration membrane, 0.01% (w/w) Tween 20 was added (Fig. 34).

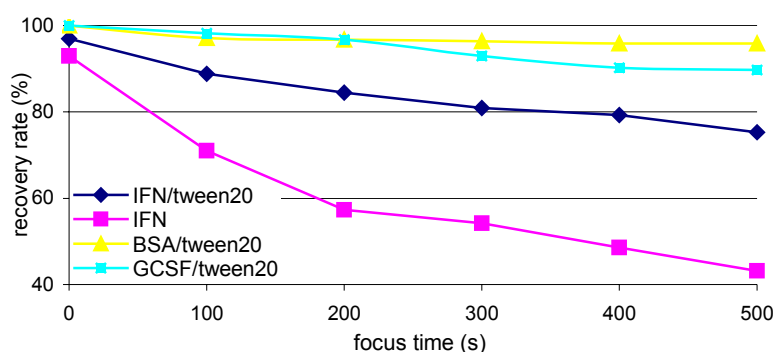


Fig. 34. Recovery rates of proteins depending on focusing time/carrier composition: BSA, G-CSF, IFN α -2a (carrier containing 0.01% Tween₂₀), IFN α -2a (carrier without Tween₂₀); AF4 parameters: focusing flow 0.8 mL/min, 15 min elution without cross flow, membrane cut-off 5 kDa, detection via MALS/UV₂₈₀, sample load 25 μ g each, $n = 5$, S_{rel} for IFN data >1.7 , for all other data <1.02 .

The addition of Tween 20 definitely increased the recovery of BSA, G-CSF and IFN α -2a. Compared to the humble gain in BSA and G-CSF recovery ($\sim 6\%$), the influence of Tween 20 on IFN α -2a recovery is notably. Whereas the impact of Tween 20 at conditions without focusing stays scarce ($\sim 3\%$), Tween 20 gives the IFN α -2a recovery a significant edge when the protein is subjected to 200 s focusing. Carrying the cross flow duration to the extremes (300 s), the recovery gain adds to $\sim 30\%$, demonstrating the importance of proper carrier choice in AF4 protein analytics. One explanation of the data may be that nonionic surfactants adsorb to both charged and neutral surfaces (Barman and Moon, 2000). Thus, when Tween 20 molecules adsorb on both protein and membrane surfaces and extend into the aqueous phase, they generate a steric barrier, inhibiting the close approach of protein molecules and membrane. It was shown via FT-IR assessments that Tween 20 binding does not induce any structural change upon binding to proteins. Moreover, the hypothesis for the inhibition of protein aggregation being due to steric effects caused by Tween binding on hydrophobic sites on protein surfaces was repeatedly published (Bam et al., 1998).

It is to be outlined that the presented data do not justify to enoble the addition of surfactants to carrier liquids as general procedure. E.g., minimal concentrations of surfactant (<0.001M SDS) were proven to cause protein precipitation during FFF separations (Stevenson and Preston, 1997). In order to retain the biological activity of the separated protein analytes, aqueous solutions based on phosphate buffered saline (PBS), Tris buffer or acetate buffer with ionic strengths in the range of 10-200 mM are typically used. For a detailed list of aqueous carrier liquids utilized in FFF analytics, it is referred to the literature (Li and Hansen, 2000).

6.3.2 Elution order

It seems likely that the IFN α -2a protein-membrane interplay initiated by the focusing step described in the previous chapter will influence the elution profile of the protein towards increased retainment. “Retention” in FFF refers to the fact that a zone of analyte is retained by its confinement to flow laminae revealing velocities lower than the average velocity of all flow laminae present in the channel (Schure et al., 2000). Thereby, the elution profile – i.e., analyte transport coefficients and analyte retention time - can be related to physicochemical parameters of the analytes. E.g., provided that parameters such as t_0 , V_c , V_0 and w are known (refer to Section 2.3.2), via determination of the retention time t_r the assessment of diffusion coefficients and hydrodynamic diameters is rendered possible (Eq. 16/17). Moreover, diffusion coefficients can directly be related to molar masses (M). Thus, in case of idealized spherical sample components – such as globular proteins –, a plot of $\log t_r$ versus $\log M$ was calculated to produce a straight line with a slope of 0.33 (Li and Hansen, 2000). Referring to this, a linear relationship between $\log t_r$ and \log protein M was published, substantiating this theoretical assumption (Liu et al., 1993). Consequently, that relationship may be applied as calibration curve to calculate the molecular weight of proteins, similarly to procedures in SE-HPLC technique (Harris, 1992).

However, this matter is based on the assumption that a monodisperse sample – such as a monomeric protein – reveals only one single set of transport coefficients, and therefore inheres only one characteristic retention time. Yet the elution profile of a monodisperse sample is not a delta function but rather Gaussian-shaped, spread over a range of retention times. Thereby, the dispersion in that profile is due to the slight diversity of each individual sample molecule concerning its position in axial flow laminae. Thus, there is a random variation in the velocities of the molecules around the average value, resulting in axial dimensioned zone spreading (Schimpf, 2000c). In the literature this phenomenon is referred to as random dispersion, column dispersion or band broadening (Weber and Carr, 1989).

Besides interaction with the cross flow – via the instrument diffusion coefficient -, the analytes’ retention times may decisively be influenced by sample-membrane interactions, as illustrated in Fig. 35. By subjecting IFN α -2a to 300 s focusing and a 80% cross flow, the protein

is immobilized upon the membrane, as no UV_{280} signal can be seized for 30 min elution with PBS. On the contrary, monomeric G-CSF – exhibiting similar molecular weight and diffusion coefficient – would elute at identical separation conditions within 6 min (data not shown). As outlined before, the addition of 0.01% Tween 20 dramatically decreases IFN α -2a adsorption intensity upon the membrane. Utilizing a carrier liquid enriched by Tween 20, in case of 70% cross flow IFN α -2a leaves the channel sluggishly, thereby inducing a broad, low-rising UV_{280} signal. It may be concluded that the IFN α -2a diffusion coefficient now exceeds the opposing parameters of cross flow and cohesive adsorption, thus unslaving the protein from immobilization. Minimizing the cross flow intensity rapidly from 70% to zero after 16 min experiment time enables an unimpeded protein elution of IFN α -2a, visualized by a sharp raise of the UV_{280} signal, pretending a symmetrical analyte peak. However, this UV signal unifies the complete set of protein specimen still present in the channel – monomers, dimers, oligomers and hmw aggregates.

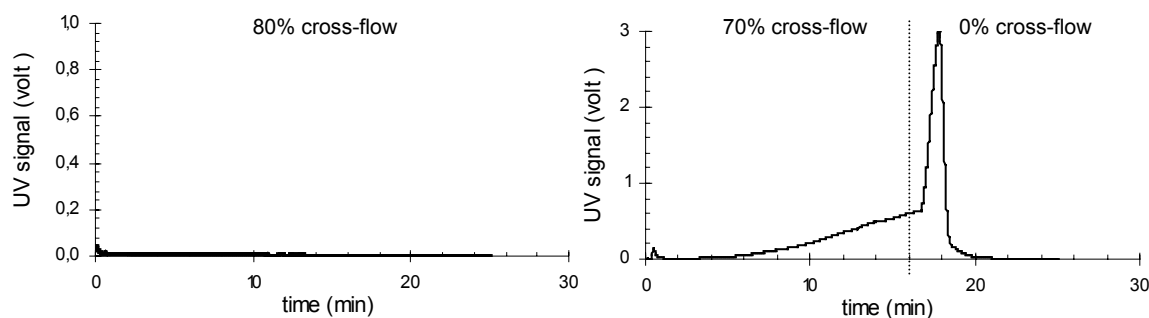


Fig. 35. Elution profile of IFN α -2a dependent on AF4 separation parameters; sample load 50 μ g, forward flow 0.6 mL/min, UV_{280} detection, PBS carrier, constant 80% cross flow and complete sample immobilization (left). PBS carrier plus 0.01% Tween 20, 70% cross flow, at $t = 16$ min minimized to 0% value. Retained elution is superseded by unrestricted protein wash-out (right).

As shown in Fig. 35, sample-membrane interactions – i.e., cohesive forces of membrane adsorption – can influence analytes' retention time. Although Tween 20 notably reduced the affinity of IFN α -2a to cellulose membrane material, adsorption was not annihilated totally, reflected by data from G-CSF separations. Furthermore, IFN α -2a experiments inherited low reproducibility. Referring to this, it is known that the evidence of adsorption typically comes in the form of irregularly shaped peaks and irreproducible elution profiles (Schure et al., 2000).

In order to eclipse IFN α -2a membrane adsorption onward, it was found in the literature that the amount of sample load may be harmlessly enlarged when the ionic strength of the carrier is concomitantly increased (Moon and Myers, 2000). This statement is substantiated by early observations revealing that the enhancement of channel overloading by the introduction of charge into analyte polymers may be most distinct at low ionic strengths (Giddings et al., 1978c). Additionally, in case of water-soluble polymers the double-layer thickness – commonly referred to as Debye length – decreases at high ionic strengths (Benincasa and Giddings, 1992). Hence, by

lessening the effective volume of a polymer molecule its diffusion coefficient increases – a factor generally considered to oppose the extent of adsorption. Finally, the potential energy of interaction between the channel surface and polydispersed colloidal analytes and thus adsorption was successfully minimized by changing the ionic strength of the FFF carrier solution (Karaiskakis et al., 2002).

The information clearly amounts to the utilization of a carrier with high ionic strength in order to approach reduced IFN α -2a membrane adsorption. Popular ionic strengths of carriers in both FFF and SE-HPLC technique range between 10^{-4} and 10^{-3} mM salt concentration. Facing notable IFN α -2a adsorption despite the presence of Tween 20, the NaCl concentration of the carrier was decided to be 20 mM NaCl.

Applying the revised carrier formidably ameliorates the IFN α -2a characterization via AF4/MALS (Fig. 36). Besides an enhanced recovery (>90%), the benefit of increased experiment reproducibility and peak symmetry are to be recorded.

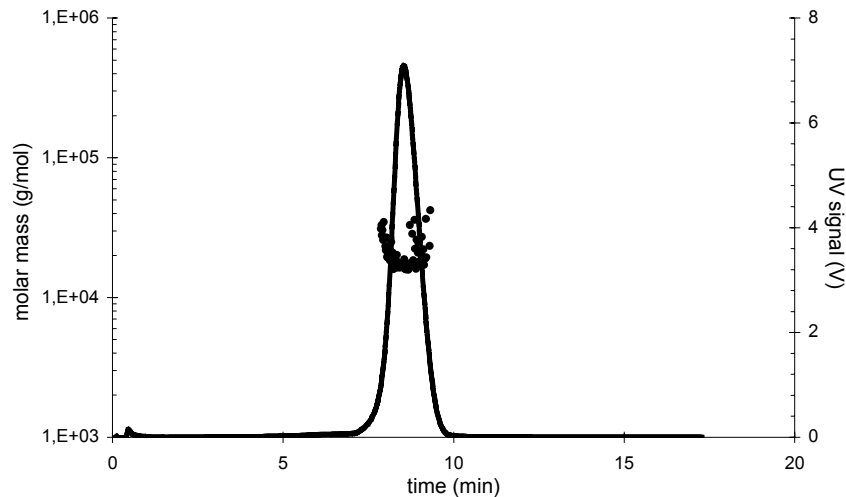


Fig. 36. Separation of IFN α -2a; the initial 65% cross flow was programmed to decrease linearly to 0% within 13 min, passing the 30% threshold after 7 min. MALS determined a 20.2 kDa molar mass of IFN α -2a. Due to the carrier composition (0.01% Tween 20, 20 mM NaCl), protein-membrane interactions were eclipsed and IFN α -2a eluted within a 3 min interval.

Interestingly, the increased ionic strength appears to unveil one characteristic feature of IFN α -2a: at cross flow rates beyond 30% the protein still inheres significant adsorption tendency, resulting in sample retainment and recovery loss. On the other hand, when subjected to field strengths below 30% IFN α -2a complies with the theoretical principles of FFF separation – i.e., IFN α -2a elution profiles resemble those of the equally-sized G-CSF. The high diffusion coefficient of IFN α -2a exceeds the retainment of 30% cross flow conditions, and the protein elutes apace.

However, this bivalent feature of IFN α -2a when being subjected to the cusp of the 30% cross flow threshold may prompt the AF4 operator to press home a significant advance: may both the characteristics of IFN α -2a and AF4 separation conditions facilitate the fractionation of proteins

with identical size? Up to now, no such successful FFF separation is described, reflecting the complicity of such a task.

The topic is examined by analyzing a sample containing IFN α -2a and a protein with similar diffusion coefficient such as G-CSF. Considering the proteins' minimal 200 Da difference in molar mass, the relationship $M \sim 1/D$ guarantees both G-CSF and IFN α -2a D values to be similarly $\sim 12 \cdot 10^{-7} \text{ cm}^2/\text{s}_{20^\circ\text{C,w}}$ (Saltzman et al., 1994).

Initially, the proteins' principal likeness in M and D values was verified by SE-HPLC, as separation in SE-HPLC is solely driven by discrepancies in analyte size. Optimal conditions ensured, G-CSF (19.6 kDa) should elute only marginally prior to IFN α -2a (19.4 kDa), if at all. As illustrated in Fig. 37, the proteins reveal similar retention times, indicating comparable D values.

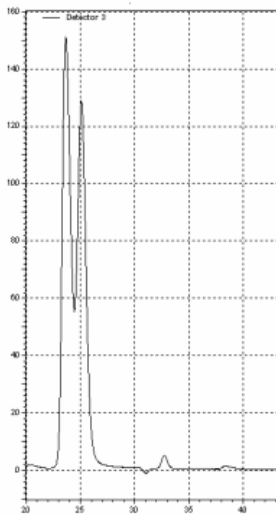


Fig. 37. SE-HPLC separation of G-CSF and IFN α -2a, with G-CSF eluting first. The low resolution reflects the similar hydrodynamic diameters of both proteins, indicating even D values. Experiment parameters: TSKgel G3000SWXL column (Tosoh Biosep GmbH, Stuttgart, Germany); detection via UV₂₈₀, mobile phase PBS pH 7.4, flow 0.5 mL/min.

The successful separation of G-CSF and IFN α -2a by means of AF4/MALS is depicted in Fig. 38. Since G-CSF exhibits no membrane adsorption tendency, its retainment is merely directed by the cross flow, which is linearly decreased within 13 min from 70% to 0%. Since G-CSF experiences higher cross flow rates, the protein reveals a broader UV₂₈₀ peak, compared to IFN α -2a. As the cross flow intensity passes the 30% threshold, IFN α -2a becomes exonerated from cohesive membrane adsorption and elutes readily within 2.5 min. Data interpretation was supported by MALS, assigning G-CSF a 21.8 kDa molar mass and IFN α -2a 20.2 kDa, respectively.

To carry the matter to the extremes, it can be investigated whether sample-membrane interactions may have an impact on AF4 elution order in normal mode separations. I.e., the cohesive and retaining forces of IFN α -2a adsorption may be deemed that effectual to invert the elution order imposed by the FFF theory. Thus, the underlying principles may apparently be infringed. However, this experiment approach is not heretical, as the standard FFF theory, developed for point masses at infinite dilution, in principle rules out a priori any effect on

retention behavior due to the amount of sample load or sample-wall and sample-sample interactions (Benincasa and Giddings, 1992).

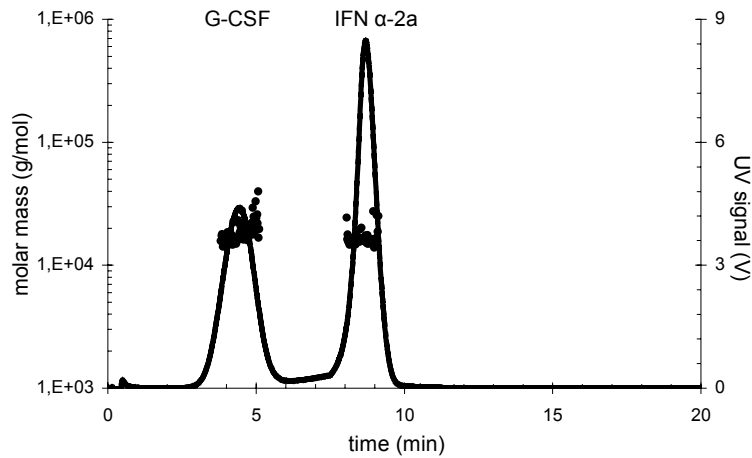


Fig. 38. AF4 separation of G-CSF and IFN α -2a. Injected protein load 50 μ g each, experiment conditions identical as described in Fig. 36. Due to IFN α -2a adsorption phenomena, which increases the protein's effective diffusion coefficient, both proteins are fractionated base-line, although inhering similar molar masses and diffusion coefficients.

Referring to this, the fractogram of EPO (38 kDa) and IFN α -2a is shown in Fig. 39.

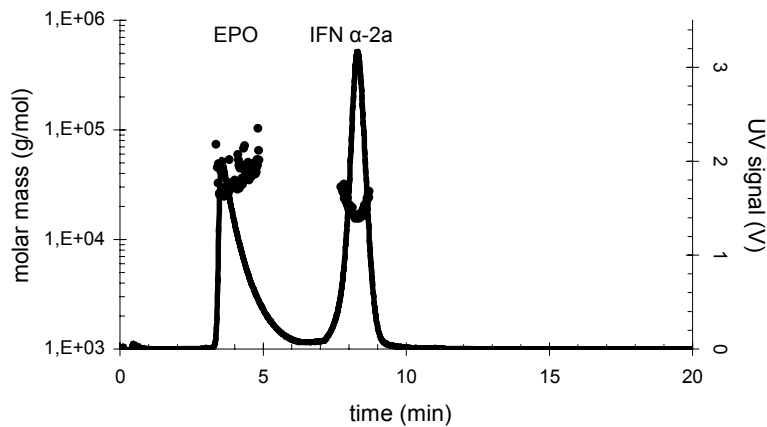


Fig. 39. Inversion of theoretical FFF normal mode elution order. Fractionation of EPO (38 kDa) and IFN α -2a. Injected protein load 25 μ g each, experiment conditions identical as described in Fig. 36. Although EPO doubles the molar mass of IFN α -2a, it elutes prior.

As long as the cross flow intensities exceed 30%, IFN α -2a is forced towards the ultrafiltration membrane and becomes in effect immobilized. Contrarily, EPO – assigned 42.6 kDa molecular weight by MALS – elutes earlier, obviously revealing no adsorption tendency. The data is consistent with the findings of investigations on EPO recovery rate, proving EPO to reveal hydrophilicity comparable to that of albumin and γ -immunoglobulins (refer to Fig. 33).

Hitherto, inversions of analytes' elution order were only monitored when the FFF conditions changed from normal mode to steric mode (Giddings, 1993). E.g., κ -carrageenan was

shown to alter the elution profile of low molecular weight specimen from normal mode to steric/hyperlayer mode after severe aggregation (Wittgren et al., 1998).

Facing an increasing share of analyte specimen with low hydrophilicity – e.g., protein complexes and lipoproteins – the problem of sample-membrane interactions will likely be on the rise in future pharmaceutical AF4 analytics (Li and Hansen, 2000). Yet, by proper choice of carrier liquid and taking advantage of analyte features which are at first glance obstructing, even challenging protein separation tasks may be successfully approached.

6.4 Fractionation of protein specimen

6.4.1 Monomers, oligomers, soluble aggregates

The acid test for any separation technique is providing greatest resolution within shortest time, thereby avoiding the generation of artifacts. Due to its equipment with field strength programming, FFF inherits the capability to considerably meet this standard. E.g., a six component latex mixture, ranging from 20 to 426 nm in size, was fractionated in normal mode Flow-FFF within 10 min (Botana et al., 1995). In terms of protein analytics, the size distribution of wheat proteins was investigated by separation of monomeric and polymeric specimen via Flow-FFF/MALS (Southan and MacRitchie, 1999).

Even multi-protein analysis was approached by AF4, managing the separation of four proteins within 20 min. Thereby, the scope of molar masses covered the range from 29 kDa (carbonic anhydrase) up to 669 kDa (thyroglobulin) (Moon and Hwang, 2001). However, the separation of samples containing two or more different proteins inherits one major pitfall: as proteins tend to take a variegated shape – comprising fragmented and oligomeric as well as unfolded forms – there may arise difficulties in assigning one single peak one separated component exclusively. E.g., G-CSF dimer (~39 kDa) may unify with the detection signal of EPO (38 kDa), as both specimen reveal identical molar masses, thus exacerbating correct data interpretation. The matter is exemplified by the fractionation of albumin solution containing a 147 kDa immunoglobulin (Fig. 40).

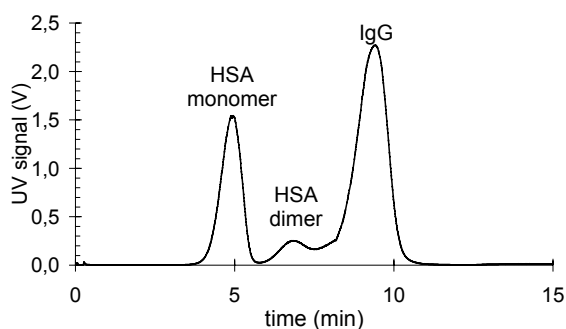


Fig. 40. Separation of HSA solution containing immunoglobulin. Due to the ~10% difference in molar mass between HSA dimer (133 kDa) and the antibody (147 kDa), a base-line separation is impeded, despite high-resolution conditions (75% cross flow). Thus, the overlap of UV₂₈₀ signals hampers data interpretation.

In order to demonstrate AF4 applicability in monitoring protein stability, G-CSF was exposed to short-time temperature stress (1 mg/mL in PBS pH 7.4, 1.0 mL in 1-mL polypropylene tubes, tubes were heated in borings of a 60 °C metal block and subsequently stored in 0 °C ice-water). Heat-induced aggregation of G-CSF was monitored via AF4/MALS (Table 4):

storage time (min)	0	2	4	6	8	10
monomer (%)	90.2	90.1	85.5	82.7	63.8	41.5
≥dimer	2.8	2.9	7.4	9.5	13.0	25.8
aggregates (%)	7.0	7.0	7.1	7.8	23.2	32.7

Table 4. Monitoring of temperature-induced aggregation of G-CSF via AF4/UV₂₈₀ (storage at 60 °C, conc. 1 mg/mL), n=3, S_{rel} for aggregate data <1.25, for all other data <0.7. % monomer relates the monomer AUC₂₈₀ to the AUC₂₈₀ of total protein; the term “aggregates” denotes protein hmw aggregates which are yielded as distinct fraction applying 0% cross flow.

As outlined in Table 4, subjecting the protein solution to heat induces notable aggregation, especially after ≥6 min storage, where the samples revealed a very slight turbidity. Besides, AF4 proves to be capable of detecting even a minor degree of protein instability, as demonstrated by a marginal increase of aggregate content in the primary stage of the stress test. To avert the simultaneous elution of G-CSF monomer and contiguously generated fragment specimen, the AF4 separation was started with initial high field-strengths (80%). Thus, protein monomer elution was delayed for ~5 min (Fig. 41).

Because of higher diffusion coefficients – compared to the monomers - protein fragments are expected to elute prior to intact G-CSF. Though, no fragments were detected, giving rise to the question whether fragments may have avoided detection by passing the ultrafiltration membrane, which revealed a 5 kDa cut-off. Since absolute recovery rates of all samples remained equal, fragment loss due to potential membrane passage could be excluded. Besides, the major denaturation pathway of proteins exposed to elevated temperatures is considered to be aggregation rather than fragmentation (Cleland et al., 1993).

As illustrated in Fig. 41a, a 80% cross flow rate was maintained for 10 min and then linearly lowered to 0% (t= 17 min). Due to that, G-CSF monomers and dimers could be seized as separated fractions. Additionally, an individual fraction of aggregates eluted when no cross flow was effective (Fig. 41b). According to the data, the unstressed G-CSF solution exhibits only little dimer and no multimers, but a considerable amount of hmw aggregates. This is consistent with results published in the course of an analytical case study of G-CSF/Neupogen[®], where also no fragments and no intermediate multimers have been observed, but only monomers and a notable aggregate fraction (Herman et al., 1996).

However, exposure to harsh thermal stress induces the formation of multimers – though outnumbered by the generation of a large fraction of soluble hmw aggregates. As illustrated in

Fig. 41, the tool of cross flow programming contributes substantially to the efficacious performance of AF4 in the fractionation of protein specimen. Thus, membrane adsorption/immobilization of larger aggregates can be circumvented.

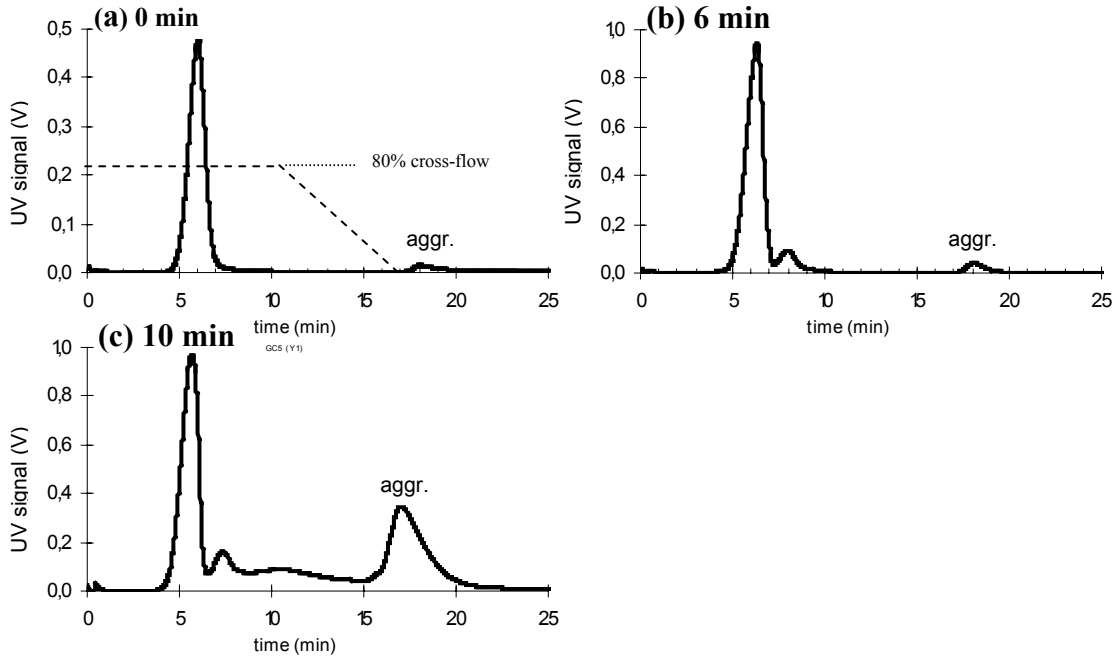


Fig. 41. Monitoring G-CSF instability due to storage at elevated temperature (60 °C) via AF4/UV₂₈₀. Minimizing the 80% cross flow linearly to 0% at $t = 17$ min enables to seize an individual fraction of aggregates (a). To scrutinize a potential impact of concentration, AF4 sample loads were varied (25 μ g in (a), 50 μ g each in (b) and (c), respectively).

Compared to SE-HPLC, adsorption phenomena in FFF may generally act a minor part, considering FFF channel surface areas of usually 30 cm² and SE-HPLC package material surface areas of $\geq 30,000$ cm² (Klein and Huerzeler, 1999). However, the cross flow induced analyte-membrane contact may somewhat annihilate this AF4 feature. In both techniques, the application of carrier liquids containing surfactants such as SDS or Tweens in order to reduce potential adsorption phenomena is popular (Barth et al., 1994).

As long as the concentration of carrier surfactants is assessed below their critical micelle concentration (CMC), this procedure can be deemed *lege artis*. On the other hand, surfactant concentrations beyond the CMC involves problems, since proteins will not enter the micelles, but may anyway be enriched in the micelle phase (Sivars et al., 1996). Consequently, protein specimen can avoid detection. According to the literature, the CMC of Tweens in water at room temperature is ~ 11 mM (Hillgren et al., 2002). Other investigations determined CMC weight percentage values of 0.006 for Tween 20 and 0.01 Tween 80 (Hoepfner et al., 2002).

In contrast to SE-HPLC, the use of surfactants in concentrations $> \text{CMC}$ is delicate, and concurrently the pro's of field programming turn into con's: micelles derived from polyoxyethylene-based surfactants like Tweens increase their size with concentration, temperature and decreased polyoxyethylene chain length, but their size distributions stay rather

narrow and constant at fixed conditions (Joensson et al., 1998). I.e., Tween micelles have to be considered as sample components in AF4 experiments, as the micelles are sensitive for cross flow. Thus, the micelle concentration in flow laminae in immediate proximity to the membrane will exceed the micelle concentration of more elevated laminae. Anyhow, as long as flow intensities remain unchanged, the micelle concentration of carrier leaving the channel and passing the detector cells will stay constant. Contrarily, a rapid decrease of the cross flow strength will force micelles hitherto accumulating at the membrane surface to elute, thereby inducing considerable detector response (Fig. 42).

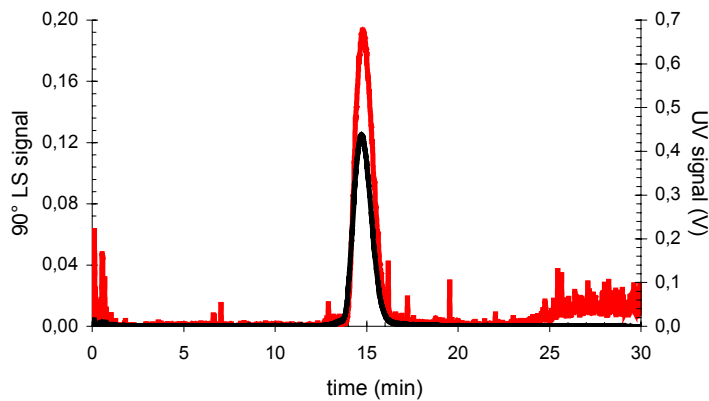


Fig. 42. „Stealth“ analyte signal induced by a rapid 70% to 2% change of cross flow intensity within 30 s, starting at $t=13$ min. No sample was injected, carrier liquid was PBS 7.4 containing 0.1% Tween 20. Due to the decreased retainment, Tween 20 micelles hitherto concentrated upon the membrane flood the detectors (MALS, UV_{220}).

Phenomena related to this context – where these surfactants were referred to as “stealth analytes” - have been reported before (Fraunhofer, 2002b). It is important to note, that stealth analytes are not to be subsumed to the experimental artifact of “ghost peaks” – here, a part of the sample analyte does not reach its steady-state concentration distribution and is thus transported with different velocity in the flow field, which can occur when high flow rates are exerted (Granger et al., 1986).

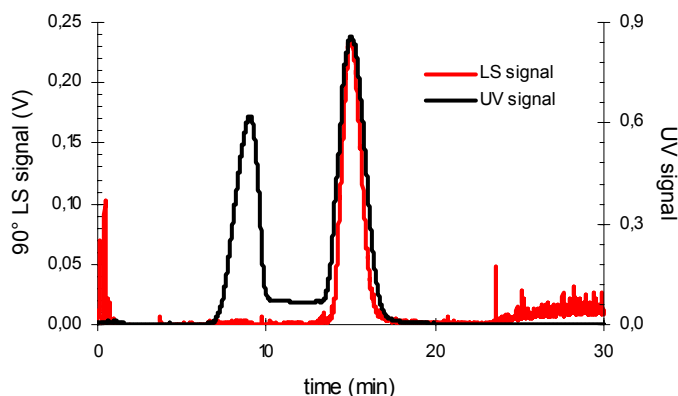


Fig. 43. Characterization of a sample containing G-CSF protein and 0.9% Tween 20. Due to low protein MW and low protein concentrations, MALS revealed only a very weak signal. Contrarily, UV_{220} detection responded well to both protein and Tween 20 micelles.

If solely the injected samples contain amounts of surfactants beyond the CMC, these phenomena are usually not observed, as the sample is diluted with carrier liquid during the injection/focusing process. However, micelles derived from samples with ultra-high concentrations of Tween 20 may ride out this dilution process, especially if the carrier liquid contains surfactants, too. Surfactants such as Twens are traditionally used for protein extraction

from lipophilic matrices or from apoprotein/lipoprotein complexes (Ikai, 1980). For instance, 0.9% Tween 20 was used to extract G-CSF from lipid implants based on tristearin matrices. Accordingly, sample analysis via AF4/UV₂₂₀ revealed two peaks, due to the presence of G-CSF protein and micelles of Tween 20 (Fig. 43).

6.4.2 High-molecular weight aggregates / precipitates

The absence of package material within the AF4 separation channel enables the characterization of insoluble analytes aside soluble specimen. Hence, AF4 may be predestined to the analysis of protein formulations containing soluble, insoluble or precipitated hmw aggregates. The general potential of AF4 for the separation of hmw aggregates and protein precipitates was demonstrated before (Litzén et al., 1993). Referring to this, wheat flour protein was characterized by means of Flow-FFF subsequent to various extraction methods only recently, where it was shown that the detected amount of polymeric and hmw protein depended on the extraction method used (Ueno et al., 2002).

In order to enable the FFF provision of protein sample solutions with predefined composition, G-CSF protein was heat-stressed until precipitation occurred (50 °C, 30 min, conc. 1 mg/mL in PBS pH 7.4). The precipitates were isolated via centrifugation (2500 rounds/min, 5 min, rotation radius 13 cm) and resuspended in PBS pH 7.4 via vortexing (120 rounds/min, 1 min, rotation radius 2 cm). A definite suspension volume was added to unstressed G-CSF solution and subjected to AF4 analysis (Fig. 44).

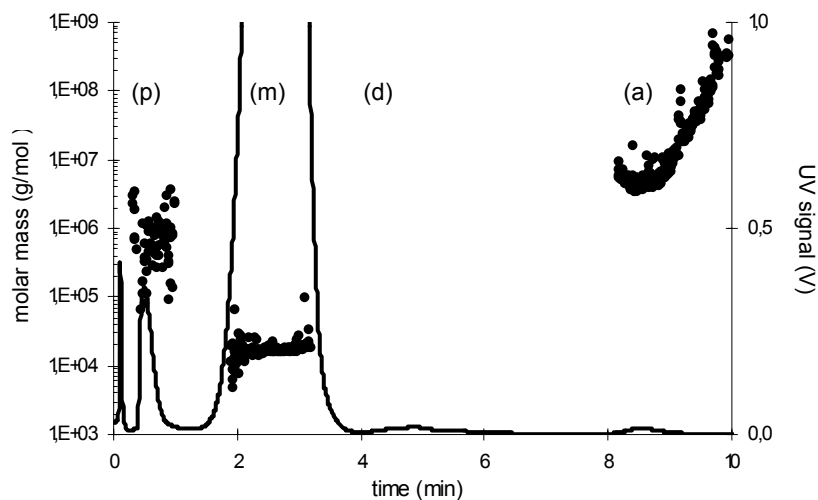


Fig. 44. Fractionation of G-CSF solution containing visible protein precipitates. Due to their size, precipitates (p) are separated in AF4 steric mode, thus eluting prior to the monomers (m) and minor fractions of dimer (d) and aggregates (a), which elute in normal mode order. MALS determines 20 kDa for monomer mass; hmw aggregate molar masses comprise $5 \cdot 10^6$ - 10^9 Da. MALS determination of precipitated protein is generally error-prone (referring to text); cross flow was linearly decreased from 50% to 0% within 8 min; UV₂₈₀ detection.

Because of their size, precipitated specimen are fractionated in accordance with the principles of the steric mode, thus eluting earlier than G-CSF monomers. The known absence of fragments enables the elution of the monomer fraction immediately afterwards, what is performed via moderate initial cross flow rates (50%). Thus, the individual separation of the protein specimen is rendered possible within relatively short time (10 min).

Whereas the assessment of molar masses for monomer (20 kDa) and hmw aggregates is trustworthy, MALS analysis of precipitated protein may be deemed unaccurate: the protein concentration is determined via UV₂₈₀-spectrophotometry, i.e., photodiodes gauge the difference of radiated and detected intensity of a monochromatic light beam – the difference is per definitionem ascribed to absorbing amino acids of the protein. However, when insoluble precipitates pass the detector cell, obscuration phenomena may account for a potential difference rather than absorption, thus pretending higher concentrations of protein than essentially present.

Given the background of both MALS theory and MW calculation via Zimm plot (Eq. 26/27), with the amount of scattered light $R_{(0)} \sim c * MW$, the consequence becomes evident: the calculated mass of analytes will be too low, in case of incorrect high concentration values assessed. As visualized in Fig. 44, the precipitates' MW is determined to be approximately 10^6 Da, well below the MW of soluble/insoluble hmw aggregates separated in normal mode.

Though, the applicability of AF4 to separate even insoluble hmw aggregate specimen and precipitates is substantiated. In order to comprehensively evaluate AF4 efficiency and reliability, the results are to be compared to data derived by techniques established in particulate matter analytics due to protein instability. In this realm, the utilization of light obscuration is state-of-the-art. Additionally, the assessment of protein aggregation may be performed via Coulter technique. E.g., Coulter counters were repeatedly used in stability monitoring of pharmaceutical immunoglobulin solutions (Mueck, 2002; Antonsen et al., 1994).

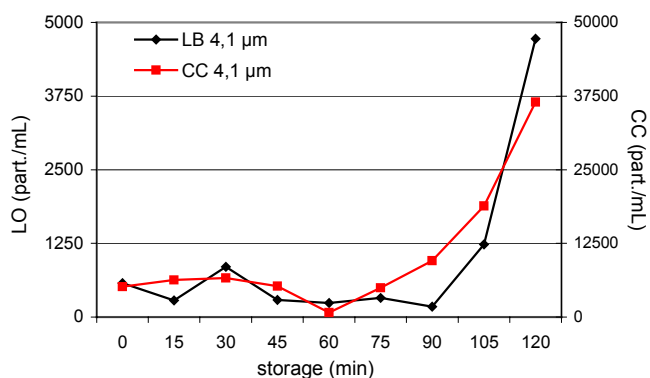


Fig. 45. Stability monitoring of afelimomab solution via Coulter technique (CC) and light obscuration (LO). Both methods detect a notable increase in particle content ($\geq 4.1 \mu\text{m}/\text{mL}$) at ~ 75 min and ~ 90 min, respectively, reflecting severe protein aggregation.

Consequently, light obscuration, Coulter technique and AF4 were employed in stability monitoring of two pharmaceutical immunoglobulines (SVSS-C⁴⁰, PAMAS GmbH, Rutesheim, Germany; MultisizerTM3, Beckman Coulter GmbH, Krefeld, Germany). Antibody solutions were subjected to elevated temperatures in order to induce protein aggregation (5 mL solution in 10R

glass vials, 2.5 mg/mL in PBS pH 6.8, solutions were heated in metal block borings and cooled in ice water). As illustrated in Fig. 45, the instability of afelimomab (40 °C storage, immunoglobulin fragment, ~100 kDa) is reflected by a notable rise in particulate matter contamination. Both methods assess the generation of particles $\geq 4.1 \mu\text{m}$ to commence not later than ~90 min experiment time.

Simultaneously, the afelimomab solution was characterized by AF4. As outlined in Fig 46, data correlation of AF4 and light obscuration technique excels. Similarly to light obscuration, AF4 assessed a remarkable increase of hmw aggregates at $t=90$ min. “% aggregates” denotes hmw aggregates which are yielded as individual fraction in AF4 separation when the cross flow is reduced to 0%.

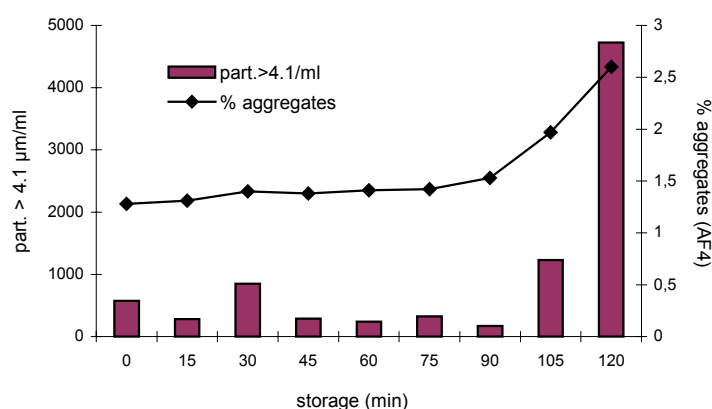


Fig. 46. Analysis of protein aggregation via light obscuration particle measurement ($\geq 4.1 \mu\text{m}/\text{mL}$) and AF4 (% aggregates relative to total protein $\text{AUC}_{\text{UV}280}$). Both techniques match in terms of aggregation onset determination at 90 min.

The correlation of AF4 and established particle counting techniques concerning the characterization of hmw aggregates and precipitates was circumstantiated by data derived from adalimumab experiments (immunoglobulin subclass G_1 , 147 kDa). Experiment design was identical to that of afelimomab, except for the storage temperature (60°C).

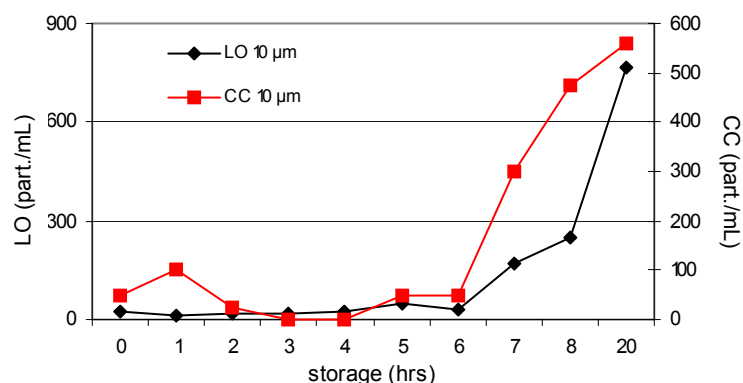


Fig 47. Stability monitoring of adalimumab solution via Coulter technique (CC) and light obscuration (LO). Protein instability is reflected by a gain in particles $\geq 10 \mu\text{m}/\text{mL}$ at 6 hrs storage at 60°C.

As outlined in Fig. 47, both particle counting techniques mark the onset of protein aggregation - reflected by a notable increase in particulate matter contamination - unambiguously at identical time. These results – backed by AF4 data shown in Fig. 48 – are consistent with the findings of afelimomab investigations.

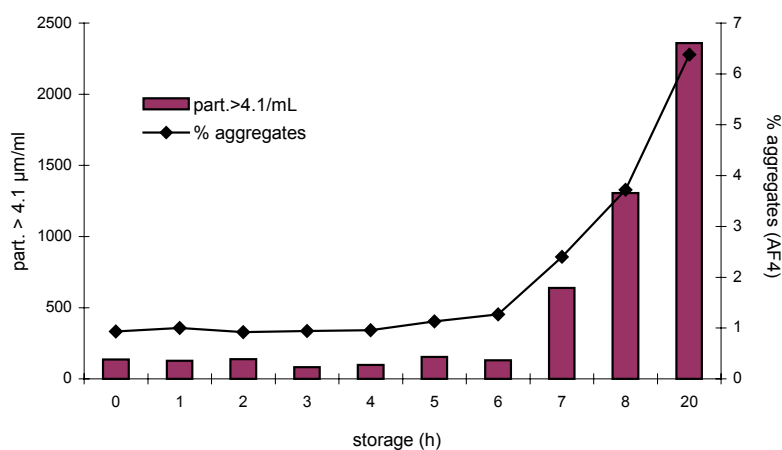


Fig 48. Correlation of AF4 and light obscuration data. Alike the 10 μm threshold, the aggregation process is visualized at 6 hrs storage by a notable increase in particles $\geq 4.1\mu\text{m}/\text{mL}$. Concomitantly, a gain in hmw aggregate content ($\%AUC_{UV280}$) is detected via AF4.

Basically, the time at which an increase in particulate matter contamination due to protein aggregation can first be assessed does not depend on the specification of the detection limit of particle counters. It was demonstrated in a comprehensive study that the commencement of protein aggregation – if monitored by light obscuration and Coulter counter – is to be assessed at identical time, regardless if the minimal detection limit is 0.7 μm or 10 μm (Mueck, 2002). Thus, the formation of insoluble protein aggregates was hypothesized to occur commensurately at various dimension levels, provided that the aggregation process proceeded beyond the cusp of insoluble – though subvisible – aggregate formation. Bearing in mind the capability of AF4 to quantify both soluble and insoluble aggregates, the data above is absolutely consistent with this theory. Otherwise, AF4 were to detect the formation of hmw aggregates at more primary stages of the aggregation process than light obscuration and Coulter counter, respectively. A caveat not to generally ascribe techniques like AF4 or SE-HPLC an inherent superiority in protein instability monitoring is to be noted. Due to the variety of aggregation pathways at hand, each protein may form aggregates in unique ways, thereby skipping the formation of hmw aggregates or totally eliding the genesis of multimers, as shown in the following chapter.

6.5 Characterization of protein solutions by AF4 and SE-HPLC: a comparative study

Even the most sophisticated techniques in protein analytics remain unconvincing and smack of inefficacy as long as they are not compared to general accepted state-of-the-art methods. Referring to quantification of protein aggregation, SE-HPLC certainly represents the gold standard in both industry and science.

Up to now, only two relevant comparative studies between FFF techniques and SE-HPLC have been performed. However, one study addressed the characterization of polystyrene standards in organic solvents by means of Th-FFF and was mainly aimed at compiling the particular theoretical principles of each method (Gunderson and Giddings, 1986). The other study correlated the results of both AF4 and SE-HPLC in terms of antibody analytics – solutions

of several immunoglobulins were stressed via rapid pH change and characterized subsequently. It was found that AF4 can give higher selectivity and greater resolution which is maintained over a wider molecular weight range than in SE-HPLC. Unfortunately, antibody samples were prepared individually for AF4 and SE-HPLC analysis, thus hampering accurate data correlation. Furthermore, different elution media for both techniques were chosen, and the study lacks recovery rate data (Litzén et al., 1993). Though, this study revealed the principal feasibility of AF4 in analysis of unprepared samples, allocating AF4 a greater application range and maybe more informational power.

Referring to the latter, this has to be affirmed, as demonstrated in the following case study of Neupogen[®] (a formulation of G-CSF protein). It was known to the formulation scientists that Neupogen[®] characteristically inheres a very small amount of hmw aggregate (<0.2%), while dimers solely occasionally can be detected. The hmw fraction was assigned a molecular weight of ~ 500 kDa by laser light scattering (Herman et al., 1996). The question, whether the hmw fraction is to be considered a native, stable component or if it is potentially prone to further accretion was of crucial interest. According to SE-HPLC data, the hmw fraction indeed constitutes a stable component, as no intermediate multimers have been observed between dimers and larger aggregates. It was hypothesized that those multimers are either bond irreversibly to the SE-HPLC column or that they are dissociated to monomer by the harsh conditions, thus avoiding detection.

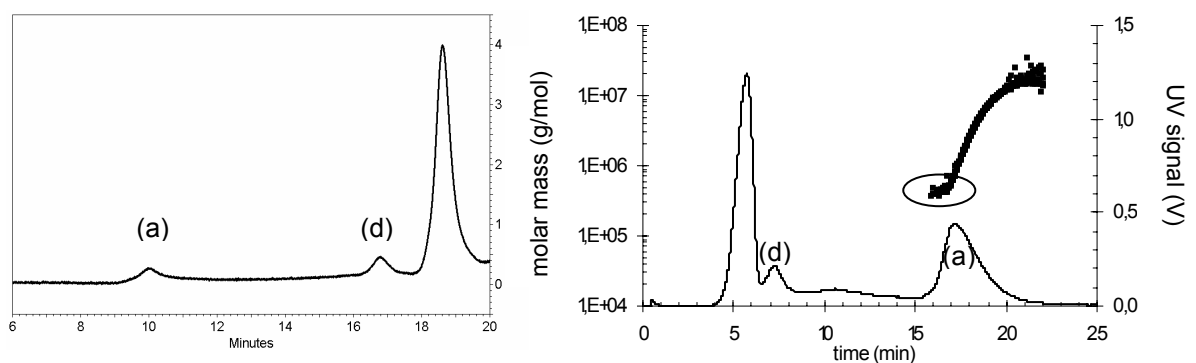


Fig. 49. Characterization of identical G-CSF samples by means of SE-HPLC (left) and AF4 (right). Due to inherent SE-HPLC parameters such as shear degradation, the hmw aggregate fraction (a) - accounting for 33% of total protein as assessed by AF4 – represents only $\sim 3\%$ AUC_{UV215} of total protein. Backing the literature data, the calculated lower MW limit of hmw aggregates is ~ 550 kDa (O). Additionally, AF4 seizes a humble fraction of multimers, by this linking the interstice between dimer (d) and hmw aggregates. AF4 separation conditions are equal to the conditions of Fig. 41.

Whereas the first speculation may be verified by monitoring of recovery and be approached by eluting the column with buffer medium containing SDS, eluate sampling and subsequent analysis via PAGE, the second assumption is Gordian. As illustrated in Fig. 49, the findings of Herman et al. are corroborated. Despite the G-CSF formulation was proved to have

undergone aggregation subsequent to 50 °C storage for 20 min – indicated by a notable increase in subvisible particulate matter – no multimers and only a sparse quantity of aggregates can be detected via SE-HPLC, substantiating the suspect of agglomerate/aggregate shear degradation.

On the other hand, the detection of oligomers and a large hmw fraction is amenable via AF4, assessing the content of hmw aggregates to be ~33%, compared to ~3% SE-HPLC data. Due to the absence of both sample preparation by centrifugation and shear effects in the AF4 channel, hmw aggregates can be seized. Equally to the light scattering results of Herman, a consistent fraction of hmw aggregates with ~550 kDa molar mass was analyzed; and this fraction appears to represent the low-limit barrier of the hmw aggregate fraction, which extends to over 10^7 Da.

It may be concluded that the primary driving forces of (thermally induced) G-CSF aggregation are mainly due to noncovalent hydrophobic interaction rather than decreased conformational and translational parameters because of the following arguments: (a) hmw aggregates are susceptible to abrasion and shear degradation, as outlined by SE-HPLC and AF4; therefore, aggregation is to be deemed a parameter of quaternary protein structure, which is consequently to be related with hydrophobic self-association (Kunitani et al., 1997). (b) lower-order specimen like multimers are also prone to shear degradation, thus thus objecting covalent oligomerization; (c) deamidation phenomena, a main factor facilitating subsequent covalent-based aggregation, have only been observed in G-CSF samples stored for extended periods at elevated temperatures, not during short-term stress; (d) G-CSF characteristically inheres a minimal amount of hmw aggregates (<0.2%, Herman et al., 1996). This meta-stable hmw aggregate cluster with ~550 kDa molecular weight can be observed in SE-HPLC, but mainly in AF4 analytics and is relatively sensitive to shear degradation. It may be assumed therefore, that once the protein aggregates have transcended this clustered state, a potential process of (physical) regression is contained at this definite cluster-state level. As a consequence, as soon as established, this G-CSF cluster may be reflected by a permanent difference in native monomer content assessed via abrasive techniques such as SE-HPLC and moderate methods like AF4. The difference is to be ascribed to abraded G-CSF cluster – what repeatedly was circumstantiated (Fig. 50).

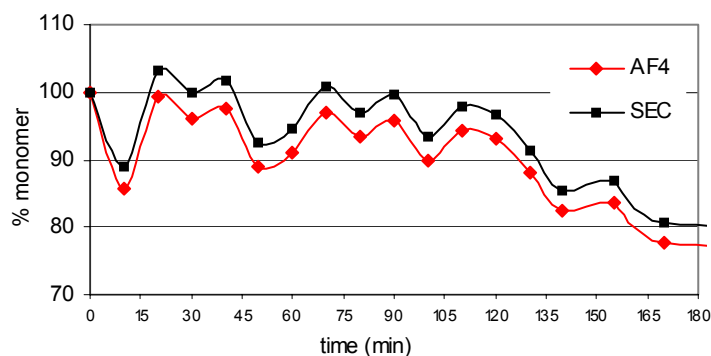


Fig. 50. Analysis of G-CSF solutions which were stressed via vacuum-drying for 180 min. Right from the start, a meta-stable aggregate cluster is formed, which is invariant at AF4 conditions but prone to SE-HPLC shear forces. The difference in AF4 and SE-HPLC AUC_{UV220} values of monomers accounts for the amount of meta-stable protein aggregates.

Thus, the delicate balance between native and aggregated state is interfered by a stable denatured form of quaternary structure, which is supportive of further destabilizing hydrophobic interaction rather than by the aggregation pathway of covalent dimerization – oligomerization – hmw aggregates. Even at extreme conditions, the dimer ratios of G-CSF solutions were comparable to the ratio of moderately stressed solutions. (refer to Fig. 41). This corroborates latest findings, which elucidate the dimeric G-CSF not to participate in the irreversible aggregation process (Sampathkumar, 2002).

Though, formulation scientists investigate heterogeneity, structural integrity and stability of protein drugs routinely. Hence, for evaluation of the benefits of analytical techniques they turn their attention to parameters such as efficiency, recovery rates, resolution power, and reproducibility. In order to compare AF4 and SE-HPLC characteristics in this realm, three protein model formulations were analyzed with both methods in the course of a benchmark study.

(Formulation parameters: a BSA stock solution was formulated by dissolving BSA in solution medium (conc. 10 mg/mL, BSA A-3059, lot 108H0881, Sigma Aldrich Chemie GmbH, Taufkirchen, Germany; solution medium was throughout 20 mM PBS, pH 6.8, containing 27 mM K_2SO_4). The stock solution was further diluted with solution medium to yield three formulations with concentrations of 0.125, 0.25 and 0.5 mg/mL, approximately, and subjected to sterile filtration (Minisart[®], 0.2 μ m, cellulose acetate, Sartorius GmbH, Goettingen, Germany). 2R glass vials were filled with 1.0 ml solution, plugged with teflon-coated bromobutyl closures, crimped, and stored for 12 hrs at 5 °C prior to analysis.

Chromatograms which are representative for the SE-HPLC separations of BSA are illustrated in Fig. 51.

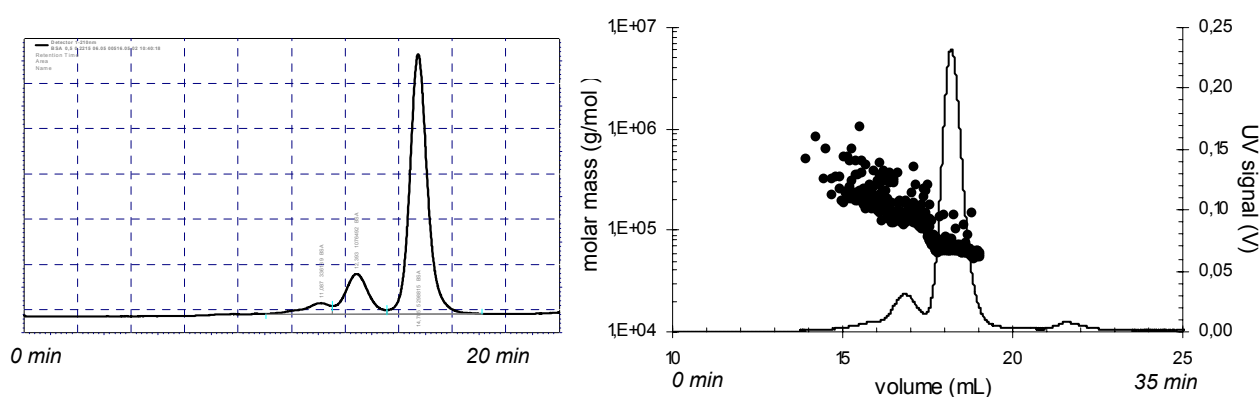


Fig. 51. SE-HPLC analysis of BSA, applying different columns. BSA formulation, conc. 0.25 mg/mL, separation with column I (left), separation with column II (right). Though a sufficient separation of BSA monomer and dimer is performed, the resolution power of column I exceeds that of column II slightly. Facing noisy MALS signals, molar mass calculation revealed values of ~68 kDa for BSA monomer and ~136 kDa for dimer and did generally not exceed 10^3 kDa.

Basically, the performance of the columns was identical, as both manage the fractionation of monomers and dimers with sufficient resolution. The base-line separation of dimers and higher-order oligomers was not possible, even if the flow rates were reduced to 0.3 mL/min. A comparison with corresponding AF4 data (Fig. 52) makes the consequences of the fundamental differences between both methods evident. According to the theoretical principles, AF4 is assigned a higher peak capacity and a greater selectivity (Jiang et al., 2000). Referring to theoretical AF4 selectivity values of 0.5-0.7 – versus 0.2 for SE-HPLC –, AF4 is considered to provide a much higher resolution, especially for samples with molar masses >100 kDa (Coelfen and Antonietti, 2000). Whereas SE-HPLC failed to resolve higher-order oligomers, AF4 rendered the fractionation of trimers and even tetramers possible, thereby guaranteeing high selectivity. E.g., the determination of the tetramers' molar mass via MALS assessed a value of ~268 kDa, exhibiting an <1% aberration from the theoretical value. Thus, the BSA components accounting for the tetramer UV₂₈₀ peak have to be almost exclusively tetramer specimen, reflecting the pronounced AF4 resolution power in concern of hmw analytes.

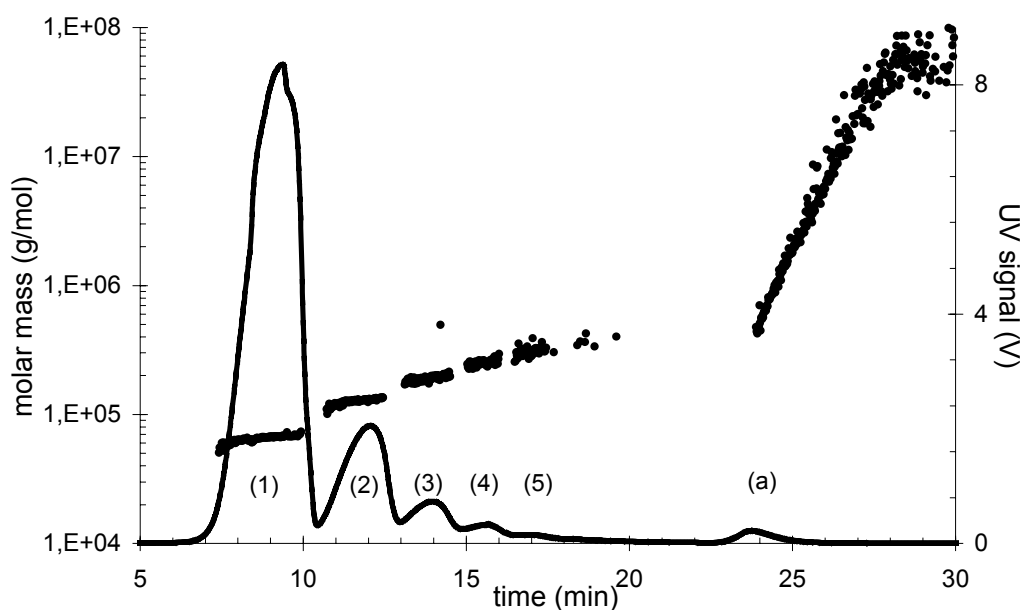


Fig. 52. AF4 fractionation of a BSA formulation, conc. 0.25 mg/mL. Exertion of 80% cross flow renders the separation of oligomer specimen possible, reflected by distinct UV₂₈₀ peaks. Additionally to monomer (1), dimer (2), trimer (3) and tetramer (4) as well as higher-order oligomers (≥ 5) can be separated. Ultra-hmw aggregates (a) elute >23 min, when no cross flow is applied. Due to the high sensitivity of MALS on hmw analytes, molar masses can be calculated up to values of $>10^7$ Da reliably, even if the analogical UV-signal reveals low concentrations ($<0.1\mu\text{g/mL}$).

Both separation methods exhibit similar experiment time – though, in contrast to SE-HPLC, the 100 s-focusing step adds to the time required for the AF4 separation process per se. On the other hand, both methods differ considerably in characterizing hmw aggregate fractions. By means of AF4, an individual fraction of hmw specimen can be separated, spanning a molar mass range from 500 kDa to over 10^4 kDa, thus indicating the presence of agglomerated components. Contrarily, the BSA analysis via column II lacks the detection of protein larger than

10³ kDa. Although the analysis with column I was not combined with MALS detection, a likewise situation is to be assumed: according to the column specifications, column I reveals a denser packing of the silica based packing material than column II – what is reflected by a ~16 bar difference in bed pressure during operation. Thus, BSA samples separated via column I may be exposed to even harsher conditions than exerted via column II. However, in both columns the hmw components are subjected to potential abrasion due to shear forces. Given the background that the BSA samples were not prepared – e.g., by filtration or centrifugation –, shear forces represent the only parameter accounting for the differences in aggregates' molecular weight, depending on the separation technique applied.

As far as data of sample consistency is concerned, both columns yielded similar results, though varying substantially from AF4 data (Table 5).

separation method	% monomer	% dimer	% ≥trimer	% recovery
column I	77.3 _{0.07}	16.4 _{0.08}	6.4 _{0.07}	-
column II	77.0 _{0.05}	16.5 _{0.08}	6.5 _{0.08}	97.8 _{2.07}
AF4	69.3 _{0.65}	16.5 _{0.76}	16.2 _{0.57}	88.5 _{3.65}

Table 5. Characterization of BSA formulation, conc. 0.5 mg/mL, via AF4 and SE-HPLC (two different columns); % content values indicate ratio of total detected AUC_{UV280}; the numbers in subscript refer to standard deviation values; % recovery refers to absolute recovery values. As column I was not combined with MALS detection, protein mass values could not be calculated, thus lacking recovery data.

Commensurate with the illustration via fractograms, the main difference in SE-HPLC and AF4 appears to be in quantification of hmw analytes. The aggregate values detected by AF4 – wherein trimers and higher-order protein specimen are to be subsumed – exceed the corresponding SE-HPLC data by nearly 10%. Due to column package, the protein (hmw-) aggregates undergo abrasion, thereby contributing to the yields of monomer and dimer. It is known that BSA is prone to the formation of non-covalent bonded aggregates, which may further interact hydrophobically and generate higher-order agglomerates (Zhu and Schwendeman, 1998; Nishimura and Goto, 1997). Thus - backed by the data of G-CSF analytics (Fig. 49) – the results can be explained reasonably.

Compared to SE-HPLC, the absolute recovery rates of AF4 are notably lower (~9%). This may be due to two parameters: the first addresses the void peak. Whereas considerable analyte losses due to pronounced void peak phenomena were reported, this study proved a 100 s focusing step to be sufficient to minimize AUC_{UV280} void peak values to <0.5% of AUC_{total} (Schimpf et al., 2000c). Generally, protein eluting in the void peak is not to be added on the mass of separated protein, if separation is based on normal mode. Additionally, the exerted high cross flow facilitates a close contact of BSA and membrane material – and immobilization of sample

material because of adhesive membrane effects may be the outcome. Facing no notable differences of standard deviation values of the individual fractions of monomer, dimer and higher-order specimen, a proneness of aggregates to particularly interact with the cellulose membrane can be excluded. Anyway, the low sample recoveries in AF4 analytics are reflected by higher standard deviation values, compared to SE-HPLC data. Referring to the SE-HPLC recovery being also notably below the optimum value, the ambitious effort to pit the determined recovery rates against the absolute recovery has to be outlined: protein masses, determined via UV_{280} /MALS analytics are related to the protein mass that is theoretically injected into the separation system, i.e., the theoretical volume of a sample loop assesses the maximum value. However, as inherent apparatus parameters as injection system or sample loop fidelity/specificity should be included into the evaluation of a technique designated for routine analysis, the absolute recovery rate was set the maximum standard. (To comprehensively attend that matter: relative recovery rates may be determined via conducting the sample loop content direct into the detection units, thus bypassing the separating units such as column or channel. In this case, for both SE-HPLC and AF4 recovery rates of >99.8% were assessed.)

The results are circumstantiated by the analysis data of 0.25 mg/mL formulation and 0.125 mg/mL, respectively (Tables 6 and 7).

separation method	% monomer	% dimer	% \geq trimer	% recovery
column I	79.0 _{0.05}	16.1 _{0.11}	4.9 _{0.08}	-
column II	78.9 _{0.09}	16.2 _{0.07}	4.9 _{0.12}	97.0 _{3.76}
AF4	69.3 _{0.83}	16.5 _{0.81}	16.2 _{0.75}	88.3 _{6.78}

Table 6. Characterization of BSA formulation, conc. 0.25 mg/mL, via AF4 and SE-HPLC (two different columns); captions and procedure are identical to Table 5.

separation method	% monomer	% dimer	% \geq trimer	% recovery
column I	81.2 _{0.09}	14.9 _{0.10}	3.9 _{0.05}	-
column II	81.1 _{0.07}	14.9 _{0.06}	4.0 _{0.08}	97.1 _{1.87}
AF4	72.1 _{0.57}	14.5 _{0.85}	13.4 _{0.64}	88.2 _{5.27}

Table 7. Characterization of BSA formulation, conc. 0.125 mg/mL, via AF4 and SE-HPLC (two different columns); captions and procedure are identical to Table 5.

It is to be noted that in both SE-HPLC and AF4 analytics the relative monomer contents of the samples increase with decreasing protein concentrations of the formulations. Consequently, the conclusion may be derived that the protein has undergone aggregation during

~12 hrs storage prior to analysis. Furthermore, the dependence of protein concentration on aggregation impetus is prevalent opinion (Wang, 1999).

As neither SE-HPLC – though revealing higher recovery rates – nor AF4 - exhibiting notably greater resolution – emerges from this comparative study unambiguously victorious, it is to be summarized that AF4 has the potential to be more than a promising alternative to SE-HPLC in the characterization of protein solutions.

Especially for laboratories which analyze a broad range of biopolymers on a routine basis, it is important to hold a technique that can be tuned to maximize the efficiency of each particular analysis. Whereas in AF4 the field strength is variable, in HPLC the column has to be changed. Although several SE-HPLC columns can be purchased for the price of one single FFF channel, the columns are to be replaced periodically as a result of degradation of the packing material.

In order to amplify the scope of SE-HPLC application to a range as broad as five orders of magnitude in weight and maintain accuracy, that, however, requires the connection of several columns in series, which significantly increases both run time and operating pressure, thereby facilitating artifacts (Coelfen and Antonietti, 2000).

Addressing the realm of an overall assessment, the possibility of AF4 to characterize unprepared samples gives AF4 a significant edge. E.g., for the purpose of quality control in pharmaceutical manufacturing this AF4 feature permits the native sample to be analyzed, without ignorantly removing the information sought (Litzén et al., 1993). In combination with sensitive techniques such as MALS even trace amounts of insoluble analytes can be quantified.

6.6 Summary

In this chapter, the general applicability of asymmetrical flow field-flow fractionation (AF4) in protein characterization was comprehensively evaluated. Furthermore, the impact of proper conduction of operational procedures such as focusing on subsequent fractionation efficiency has been demonstrated.

The unique AF4 feature to universally modulate the resolution power between two individual runs or even during one run was exemplified by the analysis of HSA: a progression of cross-flow intensity was directly correlated with a gain in resolution. Optimal system parameters provided, the fractionation of HSA into protein specimen such as monomer, dimer, trimer and tetramer can be considered state-of-the-art and was thereby implemented as control-parameter in the course of routine system check-ups during this study. Moreover, AF4 was proved to reveal reliable data when confronted with the task to analyze samples with varying concentrations – spanning a range of more than two orders of magnitude. Due to this robustness AF4 in this realm may be deemed superior to other analytical methods such as HPLC, where the risk of

potential column overloading effects demands the injection of appropriate sample amounts (Barth et al., 1994).

In general, parameters of fractionation like sample recovery and elution order was paid major attention. Hitherto, the exerted cross flow intensity was considered to account for the lion's share of contingent sample loss during an AF4 experiment because of protein adsorption phenomena upon the ultrafiltration membrane (Schimpf et al., 2000). However, it was demonstrated via analysis of several proteins with different hydrophilicity that focusing rather than the subsequent fractionation step may contribute considerably to sample loss. Additionally, the influence of adequate choice of membrane material and carrier liquid was exemplified by analysis of interferon (IFN α -2a), where the addition of surfactants to the carrier liquid was shown to notably enhance the recovery rates. Referring to this, potential pitfalls such as the detection of "stealth" effects as the basis of surfactant micell elution were elucidated.

Sample-membrane interactions, prevalently deemed to negatively influence AF4 efficiency, were thoroughly investigated. Adjustment of carrier additives, e.g., salts or surfactants, enabled not only to overcome this problem but were implemented to successfully approach analytical problems considered up to now impractical. Given the background that size differences of proteins – which account for differences in diffusion coefficients – are the driving force of an effective AF4 separation, it was shown that the retaining impact of membrane adhesion is to be deemed to practically add to size differences. As a consequence, proteins differing merely $\sim 1\%$ in molecular weight – e.g., G-CSF and IFN α -2a – could be fractionated.

In this concern, the possibility to invert the elution order in normal mode conditions was demonstrated. As the underlying normal mode theory categorically postulates the elution of smaller samples prior to larger samples, the accomplishment to elute 40 kDa analytes prior to 20 kDa analytes is to be considered new.

The possibility to subject nonprepared samples to AF4 analysis is a prerequisite for the quantification of high molecular weight aggregates, which is dealt with in a feasibility study. Because the channel lacks package material, hmw aggregates, which inhere a major sensitivity on abrasive shear forces, can be separated as individual fraction. Besides, (sub-)visible particulate matter such as protein precipitates is amenable to quantification. Due to this non-destructive character AF4 was proven to provide information on protein instability and to elucidate protein aggregation pathways. For instance, by means of AF4 G-CSF dimer was satisfactorily shown to be not involved in thermally induced irreversible aggregation, thus circumstantiating latest research in this field (Krishnan et al., 2002).

Chapter 6 is concluded with a comparative study of AF4 and SE-HPLC in routine analysis of protein solutions. Whereas SE-HPLC revealed higher recovery rates, AF4 substantially exhibited greater resolution, hence permitting a deeper insight into the effective situation. Data reproducibility was similar between both techniques, at high levels. Though, the combination

with advanced detection systems like multi-angle light scattering revealed SE-HPLC to induce artifacts in terms of hmw aggregate quantification. Hence, AF4 turned out to be more than a promising alternative to SE-HPLC in the routine analysis of protein pharmaceuticals.

This work provides a valuable code of practice for even advanced AF4 operators and demonstrates the usefulness of AF4 in protein analytics. Certain separation problems were successfully solved for the first time.

7 Analytics of pharmaceutical antibody solutions in siliconized syringes

7.1 Introduction

Traditional non-invasive delivery systems – administering drugs mainly via the oral route – are prevalently considered to be impractical for protein drugs. Enzymatic cleavage by proteolytic enzymes and denaturation due to HCl secretion by parietal cells would irreversibly damage the protein after drug release in the stomach or intestine (Patton, 1997). Hence, proteins are usually applied parenterally by injection. Although injections are a relatively recent form of therapy, the first recorded attempt to inject medication intentionally was in 1665 by Sir C. Wren. Unfortunately, the crude nature of the apparatus and the absence of pure, sterile drugs caused the practice to fall into disrepute. Later on, the work of Pasteur and Lister pointed out the need for the development of aseptic techniques – and things came into move rapidly: Simousin developed the first ampoule in the 1890s, and the “Luer-Syringe” was invented in 1896 by H. Walfing Luer, presenting a major step towards the disposable syringes used today. In 1923 it was demonstrated that the pyrogenic inducing bodies came from the water used to prepare the solutions, and care in using a pyrogen-free water eliminated the fever problem. This lead to the official acceptance of injectable solutions by the American Formulary in 1926, which is the true beginning of universal parenteral therapy (Frampton and Dean, 2000).

Today, disposable prefilled syringes for the parenteral application of drugs enjoy a great popularity among both patients and physicians, as they combine the function of a primary container with that of a conventional syringe, thus inhering several advantages: they enable the immediate administration of a gauged accurate dose from one item and offer reduced risks of errors in medication and contamination. Moreover, prefilled syringes can be used everywhere and provide easy handling, hence making patient’s drug self-application possible, e.g., with insulin in diabetes care or heparines in thrombosis prophylaxis (Kock et al., 1995). Additionally, such syringes provide convenient multi-dosing, enabling for instance the dispensing of epoetin- α at definite intervals to coincide with peritoneal dialysis (Naughton et al., 2003). In the course of an independent market research, physicians and nurses exhibited a 85% preference for prefilled syringes over vials/ampoules (Becton-Dickinson, 1998).

Prefilled syringes comprise several main components. The barrel consists primarily of glass or a sterilizable grade of polypropylene and the administration end is fitted with a standard medical luer tip or a needle. A plunger rod enables to move the piston up and down the barrel. In order to guarantee leak-proof syringes, a seal is made via circumferential ribs assembled on the plunger rod, which exert radial interference and thus affect the seal (Frampton and Dean, 2000).

In general, the special features of syringes are conferred by siliconization. Hereby, thin films of silicone oil – i.e., trimethylsiloxy endcapped polydimethylsiloxane, PDMS – are spread

from diluted aqueous silicone oil emulsions on the inner barrel surface and successively heat treated above 300 °C for ~30 min. As a consequence, lubricant films are generated which render a smooth gliding of the piston down the barrel possible. Furthermore, siliconization is required to reduce the adsorption of hydrophilic drug compounds via deactivation of glass walls and to increase the hydrolytic stability of the glass surface (Mundry, 1999).

However – as many pros often imply some cons -, even after heat curing besides an immobilized bound component a soluble silicone oil fraction is present. This soluble silicone oil is amenable to detachment, may permeate into the syringe volume and thereby result in (sub-)visible particulate matter via coalescence processes - thus potentially contravening regulatory standards. Dramatic increases in particle contamination of disposable siliconized syringes due to silicone oil detachment and potential interactions of drugs with silicone oil syringe coatings have repeatedly been reported (Jeandidier et al., 2002; Sendo et al.; 1995; Kobo, 1990; Bernstein, 1987).

Given that background, this chapter attends to an analytical case study of siliconized prefilled syringes. The solution of a pharmaceutical immunoglobulin (adalimumab, 147 kDa, 50 mg/mL) was formulated into siliconized disposable syringes. Subsequent to filling, the syringe production lots conformed to particulate matter regulations, i.e., the syringes were free of visible particulate matter and plainly met the subvisible particle limitations of maximal 6000 particles $\geq 10 \mu\text{m/mL}$ and maximal 600 particles $\geq 25 \mu\text{m/mL}$ (U.S. Pharmacopeia XXIII). During 5 °C storage the syringes sporadically developed visible particulates which can be characterized as whitish-gray fluff/droplets, revealing dimensions of 50-500 μm . Moreover, transparent, spheroidal, diminutive vesicles adhered to the barrel inner surface.

The question of the particulate matter origin was of crucial importance – and two main possibilities were considered. First, the particles may be attributed to denatured and aggregated protein drug, indicating insufficient protein stability. On the other hand, silicone oil may have detached off the barrel surface, this leading to particle formation due to coalescence. Bearing in mind the way of siliconization the syringes were subjected to, the latter hypothesis appeared rather causative: the syringe needles were fixed to the barrels (BD HypakTM 1 mL) with a thermolabile glue, thus ruling out heat curing subsequent to barrel treatment with silicone oil emulsions. Instead, siliconization was performed by a so-called strip-off procedure, whereby a definite volume of silicone oil emulsion is atomized via nozzles into the syringe barrel and peeled off after a definite time interval. It is generally accepted that silicone oil films maintain a considerable level of mobility when heat curing is avoided (Mundry, 1999). Thus, the migration of a mobile silicone oil fraction into the aqueous syringe volume may be facilitated and the detached fractions may merge to (sub-)visible particulate matter and clouding phenomena.

7.2 Analysis of syringe volumes by light obscuration

The assessment of particulate matter intensity in parenterals via light obscuration is state-of-the-art (Boom et al., 2000; Barber et al., 1992). Furthermore, subjective notions of human visible inspections can be transformed into objective values (Borchert et al., 1986). Hence, syringe volumes of the production lot revealing occasionally visible particulate matter are analyzed via light obscuration (SVSS-C⁴⁰, PAMAS GmbH, Rutesheim, Germany). More importantly, the mobility of silicone films on the surface of syringe barrels can be demonstrated by emptying the syringes in two different ways. A gentle – though alternative - manner to provide syringe volumes for light obscuration analysis is to remove the plunger backwards and draining the syringe content via the barrel aperture. The negative pressure arising thereby within the syringe is counterbalanced by air streaming through the needle into the container. Thus, artifacts associated with the movement of the piston down the barrel – commonly referred to as stiction – can be avoided (Capes et al., 1996). On the other hand, the traditional way of emptying siliconized syringes through a needle or LuerTM via piston movement involves (intense) reaming of the plunger exterior along the siliconized barrel surface. As a consequence, the silicone film can be abraded and be brushed along the barrel in a bow wave manner ahead of the plunger. Finally, droplets of abraded silicone oil may elute through the needle and may analytically be seized as particulate matter, visualized in Fig. 53 in case of siliconized syringe placebos.

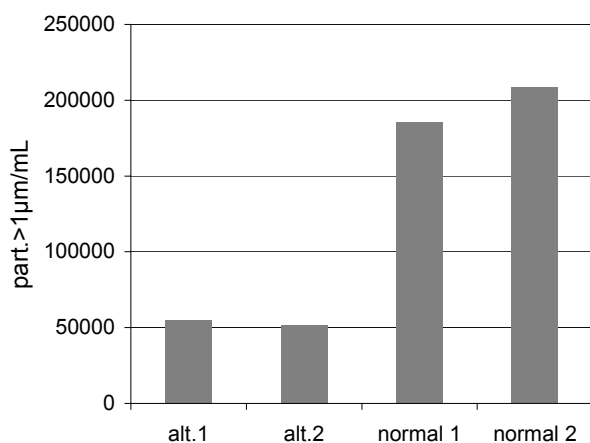


Fig. 53. Light obscuration data of four siliconized placebo syringe volumes, dependent on the way of syringe draining: removing the plunger backwards and draining the syringe content through the barrel aperture (alt.) vs. normal draining through the needle via plunger motion (normal), leading to partial abrasion of the silicone film and particulate matter (n=3, S_{rel} for all data <7.4).

Due to the generation of silicone oil droplets, the particle content of normally drained syringes exceeds the particle content of alternatively drained syringes by factor 4. Since the syringe containers and the filling process of placebo syringes were identically to the filling of adalimumab verum syringes – i.e., SCFTM filling: sterile, clean, ready to fill -, light obscuration data of verum were expected to corroborate the results of placebos. As illustrated in Fig. 54, the way of syringe draining also in case of verum had a decisive impact on the assessed degree of particulate matter contamination: draining the protein solution via the needle route led to a ~6-fold increase in particle content compared to draining via the opened barrel aperture. Hence, it

may be concluded that the layer of silicone oil on the syringe barrels is not irreversibly fixed, but exhibits a notable mobility: mechanical stress of plunger motion is sufficient to compel silicone oil to detach from its barrel locations.

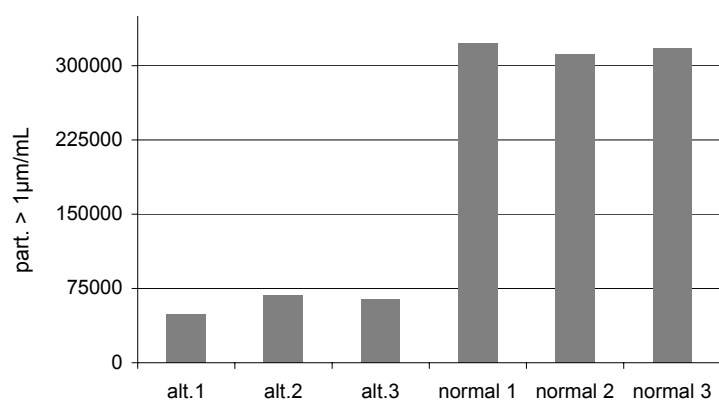


Fig. 54. Light obscuration data of verum syringe contents dependent on the way of syringe depletion: draining via opened barrel apertures (alt.) vs. draining through needles (normal), which adds abraded silicone oil droplets to particulate matter data ($n=3$, S_{rel} for all data <8.6).

These data are consistent with latest findings, which prove the heat curing process in siliconization of pharmaceutical glass containers to yield two qualities of silicone oil films: an irreversibly fixed silicone oil layer inhering covalent bonds between siloxane of the glass matrix and the organosilicon backbone of PDMS. This thin layer of covalent bound PDMS is overlaid by a thicker film of mobile silicone oil that adheres solely by hydrophobic interaction and can easily be removed by mechanical forces or suitable solvents (Mundry et al., 2000). Referring to that, the (partial) displacement of silicone oil films off glass surfaces by permanent sprinkling with water was demonstrated earlier (Steinbach and Sucker, 1975).

It is important to note that light obscuration analysis merely provides quantitative information on particulate matter and that a discrimination between particles originating by silicone oil detachment and particles due to adalimumab aggregation is not possible. This caveat can not be overemphasized. E.g., light obscuration analysis of a heat-stressed protein solution and a protein solution enriched by a small volume of aqueous silicone oil emulsion reveals similar data on particulate matter contamination, although the particle source is totally different (Table 8).

analyzed sample	particles/mL		
	$\geq 2 \mu\text{m}$	$\geq 10 \mu\text{m}$	$\geq 25 \mu\text{m}$
solution A: 5 mg/mL adalimumab in PBS pH 6.8, filtrated through 0.2 μm filter (PVDF)	62	0	0
solution A: 43 °C storage for 7 d	7 648	590	43
1.0 mL solution A: + 0.2 mL silicone oil emulsion	8694	275	63

Table 8. Analysis of particulate matter via light obscuration.

On that account, the provenience of (sub-)visible particles in individual adalimumab syringes can not automatically be ascribed to silicone oil detachment. Assumed that the visible particles are due to protein precipitation, adalimumab solution is deemed to exhibit substantial microheterogeneity, i.e., to reveal higher-order protein components such as oligomers and hmw

aggregates. The presence of protein precipitates as a consequence of protein denaturation is considered to be mandatorily associated with the presence of lower-order components aside monomers, which establish a thermodynamic and kinetic basis for (continuous) protein aggregation phenomena (Constantino et al., 1994b).

In order to elucidate that matter, adalimumab solution of turbid syringe volumes was subjected to state-of-the-art analysis targeted on characterization of protein oligomers and soluble aggregates.

7.3 Detection of soluble aggregates

Volumes of clear and turbid syringes were analyzed via SDS-PAGE (Laemmli method; NU-PAGE 10% Bis-Tris-gel, staining with colloidal blue, Invitrogen GmbH, Karlsruhe, Germany) (Fig. 55). SDS-PAGE is commonly used to characterize molecular weight and purity of pharmaceutical proteins as well as to evaluate protein stability over time during formulation and storage. Furthermore, the formation of covalent aggregates, e.g., through intermolecular disulphide bridges, can effectively be detected by performing the experiments under both reducing and non-reducing conditions (Nguyen and Ward, 1993).

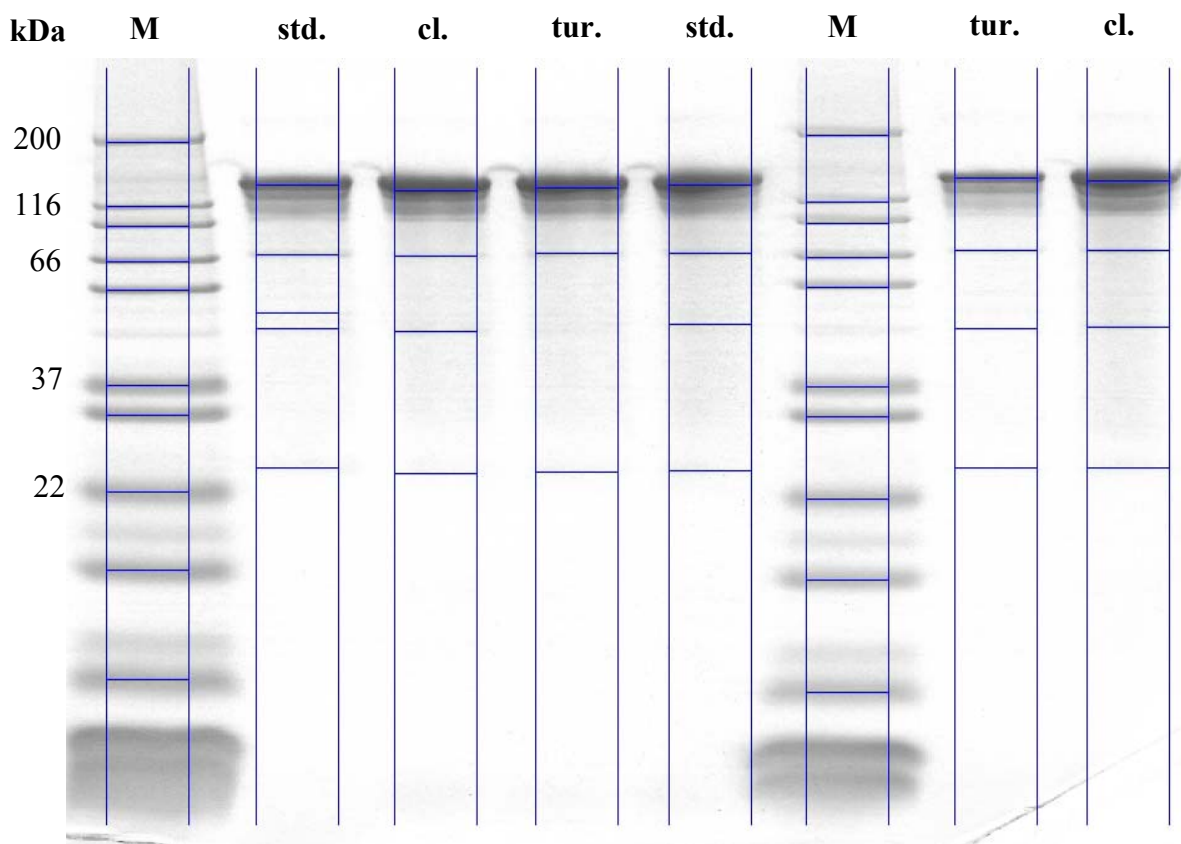


Fig. 55. SDS-PAGE analysis (reducing conditions) of syringe volumes. Application of molecular weight marker (M), adalimumab standard (std), volume of clear syringe (cl), volume of turbid syringe (tur). Distinct visible protein bands are marked by blue auxiliary lines.

As illustrated in Fig. 55, no difference is detectable between adalimumab solution derived from clear and turbid syringes, respectively. Concomitant investigations with protein bulk solution disclosed fragmentation as a major pathway of adalimumab degradation – reflected in PAGE analysis by three fragment fractions, which are detectable in all syringe volumes and reveal molar masses of some 70, 50 and 25 kDa, respectively. According to the marker proteins, adalimumab monomer with an assigned molecular weight of ~150 kDa represents the largest protein specimen within the syringe volumes. Although inconspicuous bands in the range of ~300 kDa suggest the possibility of present dimer, the intensity of dimer bands increased considerably in case of non-reducing conditions, disclosing dimerization via disulfide linkage to be a potential aggregation pathway. Again, no discrepancies between the syringe samples were to be monitored.

This is consistent with published data, revealing that antibody domains generally carry a highly conserved internal disulfide bond, connecting both β -sheets of the β -sandwich structure (Ramm et al., 1999). Immunoglobulines of subclass G like adalimumab were shown to dimerize via inter-heavy chain disulfide bridges at the N-terminal region, what substantiates the results of PAGE analysis (Krapp et al., 2003).

It may be hypothesized that detachment of silicone oil notably increases water-oil interfaces, thus fostering protein denaturation. E.g., fibrinogen was shown to rapidly denature and aggregate due to irreversibly interaction with silicon surfaces (Ortega-Vinuesa et al., 1998). As a consequence, provided the visible particulate matter in syringes to be due to silicone oil, the hydrophobic surface is deemed to pedal adalimumab protein towards aggregation. Nevertheless, PAGE analysis proved volumes of syringes to be free of noteworthy aggregate amount – corroborated by SE-HPLC analysis (Fig. 56). Storage at 5 °C for 12 m does not affect adalimumab stability, as there is merely a slight increase in aggregate content, resulting in <1% of total protein after 12 m; and no visible particulate matter was evident.

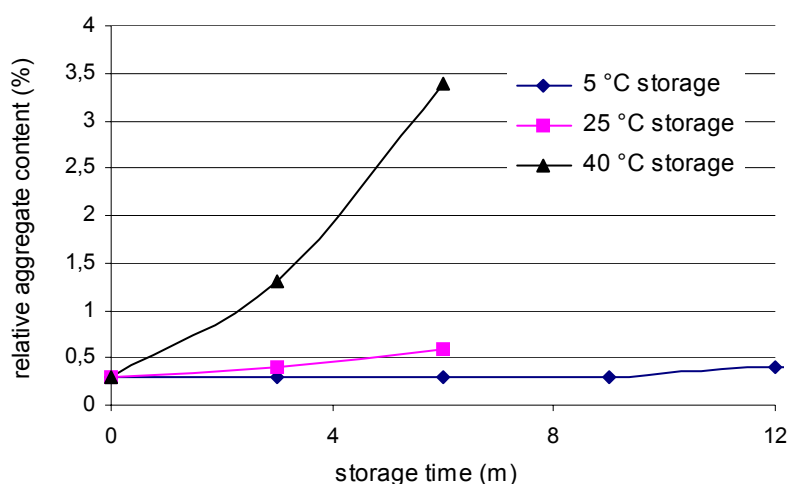


Fig. 56. Stability of adalimumab stored in syringes at various temperatures. 40 °C storage for 6 m leads to a notable increase of aggregates. Conversely, the aggregate content does not exceed 1% after 12 m storage at 5 °C.

The situation in terms of aggregate content in syringe volumes exhibiting severe particulate contamination is on the same lines: low (<0.3%) amount of aggregate, outnumbered

even by adalimumab fragments (Fig. 57). According to MALS, the fragment fraction exhibits a micro-homogeneity, i.e., the fragments were shown to inhere no multimodal mass distribution but may consist of two subfractions, each revealing molar mass uniformity. This is supported by PAGE, which confirmed adalimumab fragmentation to obey a certain regularity, as distinct fragment bands were to be observed. The staining would result in smearing bands, given the lack of a fragmentation pattern. Whereas the calculation of adalimumab monomer molar masses yields veritable data of ~ 148 kDa – with $<1\%$ difference from the theoretical value –, in case of fragment analysis MALS faces a worst case scenario: low concentrations and low molar masses, and both parameters are known to detract from MALS accuracy (Eq. 27).

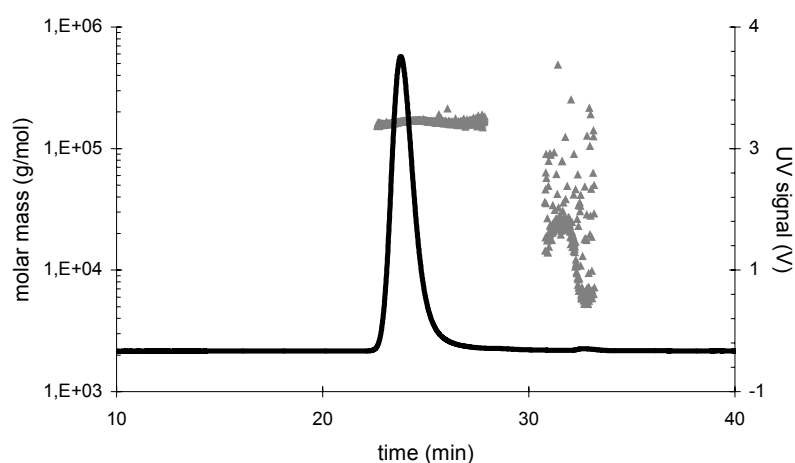


Fig. 57. SE-HPLC analysis of turbid syringe volume. UV_{280} -spectrophotometry (black line) reveals the monomer content to exceed 99.7%. Molar mass calculation of monomer was performed via MALS (grey dots), assigning the monomer 148 kDa. Correct MALS data on fragment MW is deemed to be impractical under the prevalent conditions.

Obviously, PAGE and SE-HPLC ascribe adalimumab solutions identical stability, regardless of the presence/absence of visible particulate matter. Although it is prevalent opinion that even smallest amounts of (insoluble) aggregates – i.e., in the range of nanograms - may be causative for protein solution turbidity with subsequent particulate matter, protein aggregation per se had to be deleted from the register of suspects being accused of particle formation within the syringe volumes (Hoffmann, 2000): the potential corpus delicti – i.e., protein aggregates – was not to be tracked down. However, those facts have been reported before: silicone oil was added to protein solutions and turbidity was induced by mechanical stress. Furthermore, the silicone lubricant in syringes was dispersed in droplets forming a turbid emulsion via vigorous movement of the plunger. In both cases no reduced protein potency, e.g., by denaturation or aggregation, has been monitored (Collier and Dawson, 1985). Pertaining to that, silicone-protein interactions can be exploited in order to stabilize the protein against denaturation at interfaces (Brook and Zelisko, 2001).

Principally, in trying to identify the origin of visible particulate matter with analytical methods not capable of undissolved analyte characterization, the application of SE-HPLC and PAGE may be considered a bad choice. On the contrary, AF4 was shown to separate dissolved and undissolved sample components successfully. Hence, the task to separate particulate matter

of syringe volumes from adalimumab protein and to identify both components by advanced detection methods such as MALS appeared tailor-made. However, AF4 applicability in that very analytical task was first to be screened by means of silicone oil emulsions.

7.4 Development of AF4 application: aqueous silicone oil emulsions

Hitherto, AF4 analysis of silicone oil droplets in μm range has not been performed. In contrast, the chromatographic characterization of silicone oils in organic media is well established. Molecular weight distribution analysis of silicones was performed as well as the specification and quantification of organosilicone compounds at sub-ppm level (Muller and Opila, 1988; Dorn et al., 1994). Conversely, running HPLC with aqueous media normally leads to irreversible deposition of siloxane polymer on the columns (Sible, 1996).

Bearing in mind the low inner surface area of an AF4 channel – usually $<30\text{ cm}^2$ and therefore reducing potential adsorption incidents - and the successful separation of supermicrometer polystyrene latex particles by AF4 recently, the development of an AF4 application targeting the characterization of silicone oil droplets/emulsions should have promise (Wahlund and Zattoni, 2002).

Since silicone oil DC 360 is used as syringe lubricant, that grade was used to produce aqueous emulsions (DC 360, 12,500 cSt, Dow Chemicals, Midland, MI, USA). Facing a maximum degree of 0.38% syringe siliconization - i.e., $\sim 3.4\text{ mg}$ silicone oil per syringe –, 0.5% w/w emulsions were generated in 50 mL Falcon-tubes using PBS pH 7.2 medium at ambient temperatures. The addition of surfactants such as SDS in incipient experiments in order to enhance emulsion stability due to reduction of silicone oil coalescence subsequent to dispersion proved to render no significant gain in stability of μm sized droplets. Moreover, surfactants may impair detector signal-noise ratios, facilitate base-line artifacts and generally change the adsorption behavior of samples (Schimpf et al., 2000). Hence, SDS was omitted.

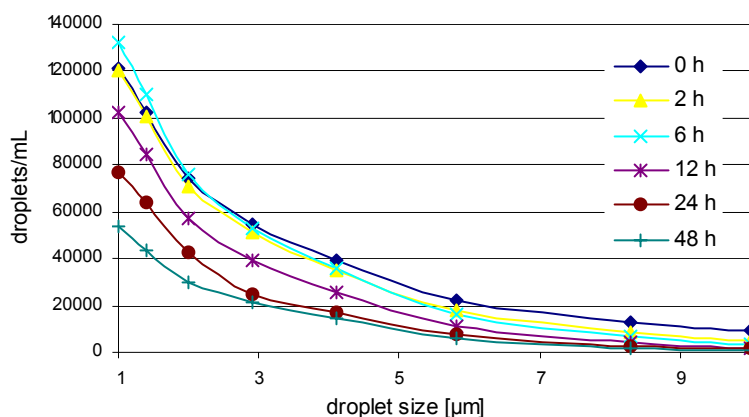


Fig. 58. Size-distribution of silicone oil droplets in a 0.5% w/w aqueous emulsion depending on storage time (cumulative view). Due to coalescence events, the number of silicone oil droplets decreased over the whole size range. Coevally, small visible vesicles of silicone oil deposited at the container wall.

As illustrated in Fig. 58, exerting shear stress by an ultra-turrax (T25 basic, IKA-Werke GmbH, Staufen, Germany) lead to emulsions featuring a criterion generally considered to be

typically for stable emulsions, equivalent conditions provided: the lower the droplet size, the larger the droplet number (van Aken and Zoet, 2000). Because of the lower detection limit of the applied light obscuration technique, droplets $<1 \mu\text{m}$ could not be detected. In contrast to the number of droplets, which rose with increasing of both time of shear and shear intensity, those parameters did not influence the size distribution profile (time intervals 3-6 min, shear intensity 11,000-24,000 r/min). However, subsequent to storage for 6-12 hrs, the number of droplets lessened, regardless of the size. Concomitantly, small transparent vesicles emerged at the surface of the Falcon-tubes, thus uncovering the progression of droplet coalescence. This phenomenon may be explained by monitoring the size distribution in differential way during storage (Fig. 59).

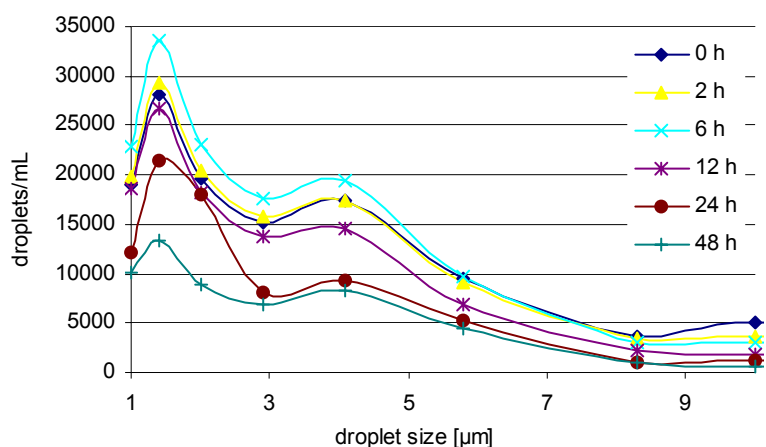


Fig. 59. Size distribution of silicone oil droplets in a 0.5% w/w aqueous emulsion depending on storage time (differential view). Note the bivalent size distribution profile, indicated by maxima droplet quantities around dimensions of $1.5 \mu\text{m}$ and $4 \mu\text{m}$, respectively.

Since the decrease in droplet number affects principally the complete spectrum, silicone oil must be deprived of the dispersed component – via adherence upon the tube surface prior to visible vesicle formation. Thus, the findings merge into a coherent picture.

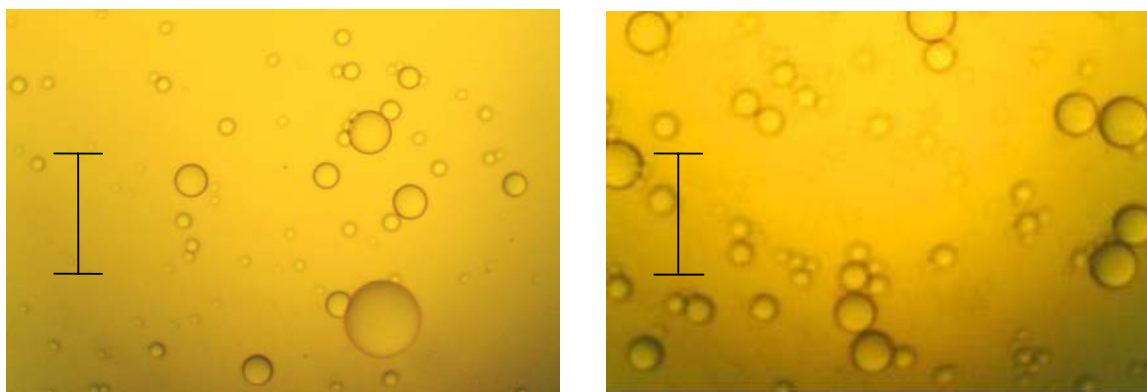


Fig. 60. Silicone oil emulsion characterized by light microscopy; storage time 6 hrs at $25 \text{ }^\circ\text{C}$; scale-bar represents $100 \mu\text{m}$.

It is important to emphasize the intention of droplet formation being targeted on (short-time stable) μm sized droplets to mimic (sub-)visible particulate matter in syringes rather than on long-time stable droplets in nm range. The presence of droplets well in the μm range can be visualized by light microscopy (Fig. 60). Due to the waiving of surfactant use – which would

negatively influence parameters such as stealth signals and signal-noise ratio – the size of the generated droplets increases. Moreover, their size distribution reveals a bivalent profile. This is consistent with latest findings, where the absence of stabilizing surfactants – e.g., proteins – was shown to facilitate the formation of larger μm range droplets in o/w emulsions within 2 hrs storage (van Aken and Zoet, 2000). Furthermore, a bivalent size distribution was assessed dependent on surfactant concentration.

The merger of droplets in the nm range may explain the slight increase of the absolute number of droplets $\geq 1 \mu\text{m}$ after 2 hrs storage (Figs. 58 and 59). However, the emulsions – concerning μm sized droplets – exhibited a stability for at least 6 hrs. Subsequently, silicone oil vesicles emerged upon the tube surface, resembling the situation within turbid siliconized syringes. As practical consequence a maximum 6 hrs time slot was used for AF4 analysis.

UV-spectrophotometry – though a traditional detection method for HPLC or AF4 – is not typically used for silicone characterization due to a lack of absorption in the UV region of the spectrum (Sible, 1996). Nevertheless, the droplets induced a notable UV_{280} response when subjected to AF4/UV analysis (Fig 61). So, how is that?

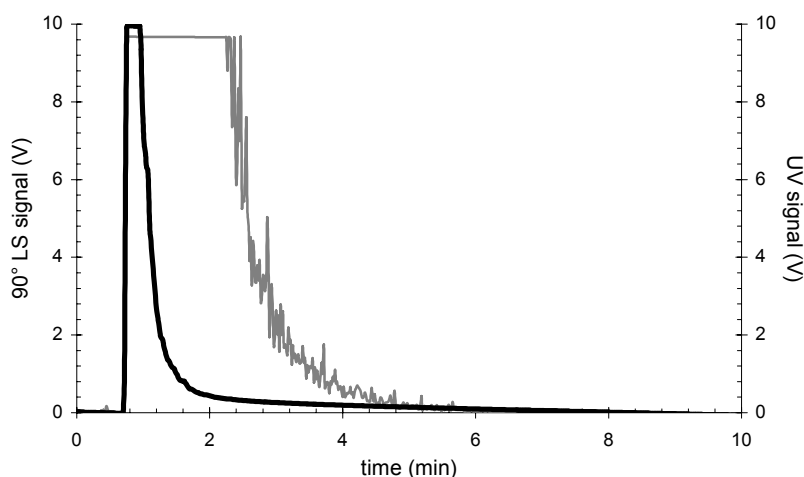


Fig. 61. AF4 fractogram of silicone oil droplets; cross flow 60%; detection via UV_{280} (black line) and MALS (grey line).

On the one hand, the inherent turbidity of the emulsion fraction implies a reduced transmission of light within the UV detector flow cell. More importantly, a notable amount of light will be scattered by the oil droplets, provoking the detector photodiodes to monitor a decreased light intensity. Thus, reduced transmission and scattering phenomena supersede absorption, and the quantification of silicone oil is rendered possible.

The dimension of the droplets implies several consequences: as demonstrated in Fig. 61, the droplets elute according to a steric mode profile. I.e., despite the exerted 65% cross flow – adalimumab monomer would be retained for ~ 15 min – the droplets are detected without notable retention, exhibiting a characteristic elution profile. Furthermore, the intense MALS signal gives evidence of the high sensitivity of MALS detection on large analytes, straightening out UV data, which attribute the droplets to finish elution within the first 2 min of fractionation. Contrarily, MALS demonstrates droplet elution to maintain twice as long. If the injected $100 \mu\text{L}$

droplet amount is reduced by factor 10, the UV signal is no longer overexcited and the matter becomes more straightforward (Fig. 62).

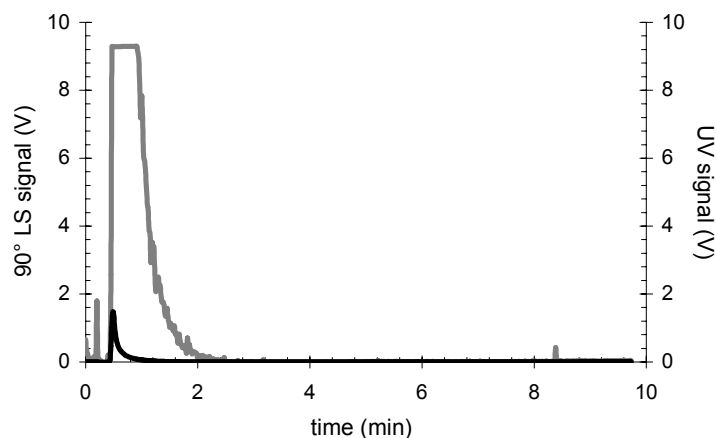


Fig. 62. Fractionation of silicone oil emulsion. Due to the small amount of injected emulsion (10 μ L) the UV signal (black line) is dwarfed by the still overexcited MALS signal (grey line). Note the high signal intensity of MALS compared to UV.

Considering steric mode conditions and a small amount of injected sample, one may ratiocinate the silicone oil droplets to reveal membrane adsorption tendencies: though the droplets commence elution with the void peak, the elution process is maintained for a relatively long time. Anyhow, as the droplets scatter light in anisotropic way, MALS responsivity is on the rise towards smaller angles, exposing droplet elution to continue for ~ 6 min (Fig. 63).

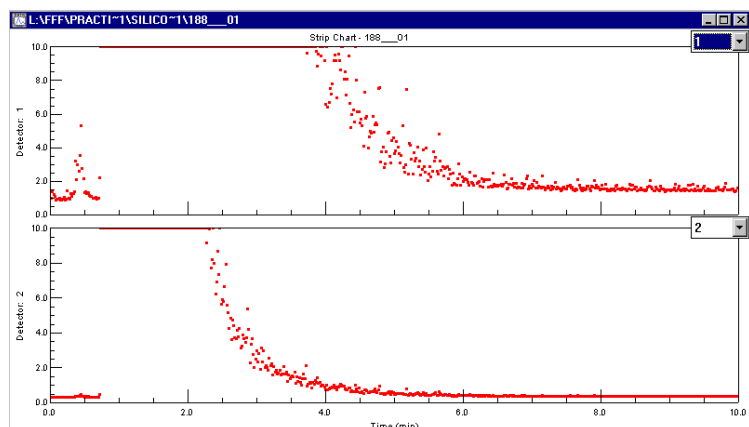


Fig. 63. Monitoring AF4 droplet elution via MALS. The higher responsivity of lower angles (45°, upper profile) demonstrates the droplets to elute within ~ 6 min, indicating adsorption phenomena to interfere with elution. Medium angles (90°, lower profile) pretend the silicone to have left the AF4 channel within ~ 4 min.

Additionally, droplet adherence and immobilization upon the membrane is reflected by a thin, greasy layer of oil covering the membrane surface and being palpable at membrane removal. Hence, the separation power of the system bates, as the area of open membrane pores is downsized by adhering silicone. Unfortunately, this limited membrane reuse for a total of approximately ten AF4 experiments. Since the extent of adsorption remained constant, however, when the membrane was sufficiently “coated”, this drawback was of low effect (Fig. 64).

Compared to UV detection – which is here solely based on obscuration and scattering incidents, applying RI detection for data acquisition renders greater sensitivity, especially at low analyte concentrations, and is therefore frequently used in PDMS analysis (Schunk and Long, 1995). Yet, the responsiveness of RI can not compete with that of MALS. Besides, RI baseline stability was found to be prone to disturbance when subjected to pressure fluctuations induced

by cross flow modulations. Nevertheless, RI detector passage of the droplets is reflected by an distinct inverse-shaped peak (Fig. 65).

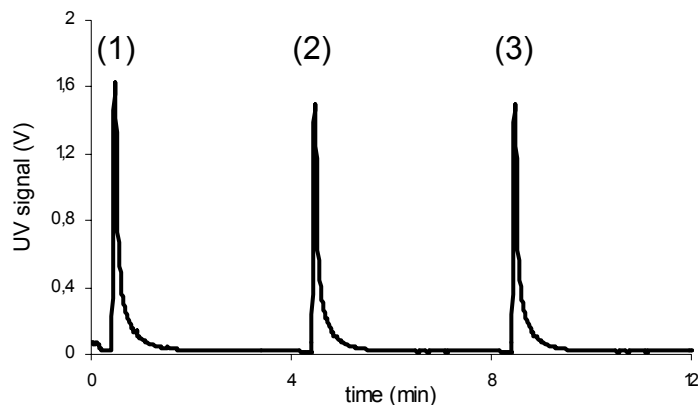


Fig. 64. Successive injection of oil droplets into the AF4 channel. Notwithstanding adsorption events occurred, the detected AUC_{UV280} perpetuated continuity once the membrane was lined with a silicone film: 0.435 (1), 0.426 (2), 0.428 (3).

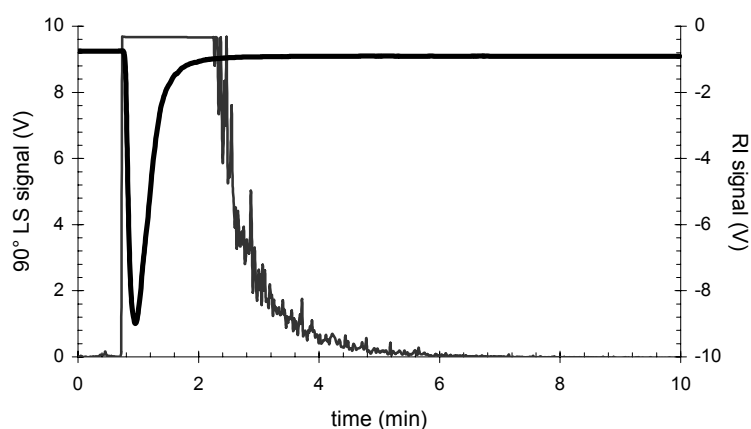


Fig. 65. Detection of silicone oil droplets via RI (black line) and MALS (grey line). Whereas MALS reveals a substantially greater sensitivity, RI signal intensity is proportional to sample concentration.

Theoretically, a calibration curve will result by plotting various masses of injected silicone oil versus pertaining AUC_{RI} values, thereby providing a convenient method for the quantification of detached/dispersed silicone oil. A conditioned membrane assumed, injecting 10 μL of a 0.5% PDMS emulsion – i.e., 50 ng PDMS – made up the lower AF4 analytical limit which provided data with acceptable accuracy ($S_{rel} < 20$), thus representing an alternative method of silicone quantification. Furthermore, the principal applicability of AF4 in the separation of silicone oil droplets in steric mode has been effectually verified. In order to preclude misconceiving: because of its minimal degree, the extent of silicone migration into parenteral formulations is generally unknown. However, conventional silicone determination methods such as IR or atomic absorption spectrometry (AAS) are capable of detecting trace amounts in the ppm and ppb range, and advanced methods like graphite furnace AAS inhere potential for even higher sensitivity (Mundry et al., 2001).

7.5 Analysis of syringe volumes

The attempt to artificially induce silicone oil detachment off syringe surfaces is propelled by one main argument: if the detachment of silicone oil can not be enforced by exerting harsh

stress conditions, a spontaneous detachment in syringes at moderate conditions such as shockless storage at 5 °C seems unlikely. In that case, the syringe particulate matter is not to be ascribed to detachment events.

The removal of oil from solid surfaces in the presence of aqueous solutions was performed earlier by Rowe using a benchtop ultrasonic bath (Rowe et al., 2002). In the style of Row, siliconized placebo syringes were subjected to ultrasound for 30 min (Sonorex RK 510, Bandelin electronic, frequency 35 kHz, Berlin, Germany). The effect of temperature (25 – 50 °C) was found to have no impact on the findings. Within several minutes, a slight turbidity appeared, which intensified and resulted in the formation of whitish, fluffy entities of ~500 µm in size. Subsequent storage at 5 °C did not lead to the coalescence of transparent vesicles at the inner glass surface. However, ultrasound-stressed placebo syringes were consistently attributed a greater turbidity than verum syringes, which developed particulate matter during storage. AF4 analysis of the stressed syringe volumes disclosed the turbidity to be due to seizable particulate matter (Fig. 66).

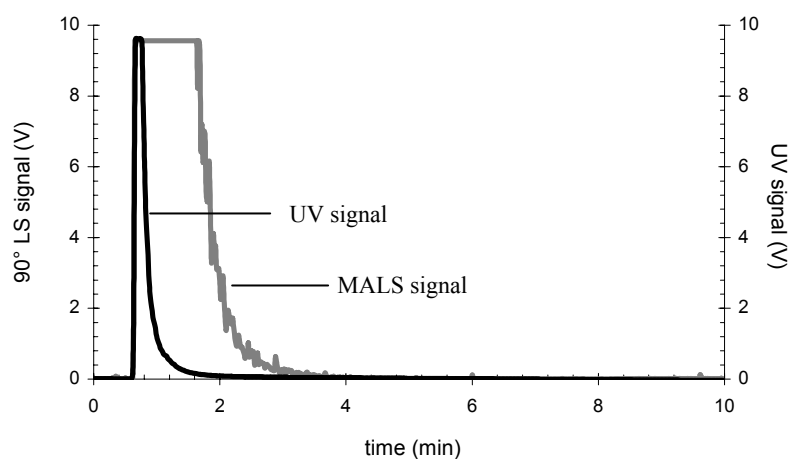


Fig. 66. Characterization of placebo syringe content subsequent to 30 min ultrasound stress. Due to the steric mode elution profile (65% cross flow), the detected specimen are assigned dimensions $>1 \mu\text{m}$; detection with UV_{280} (black line) and MALS (grey line).

The elution profile resembles that of silicone oil emulsions. Consequently, the fractionated sample can present forced-detached silicone. It may be hypothesized that due to the (mechanic) energy supply of ultrasound silicone oil was removed from the glass surface, either by mechanisms of emulsification and solubilization or roll-up, which is responded to later on (Miller and Raney, 1993). The final identification was performed by subjecting a highly concentrated sample of the eluting fraction – i.e., ~1 min after experiment start – to light microscopy (Fig. 67).

In order to prove the principal possibility of oil detachment in verum syringes, adalimumab solution in syringes was replaced by PBS pH 6.8 prior to ultrasound stressing. Otherwise, adalimumab protein may aggregate, resulting in particle formation – thus potentially intervening with the AF4 characterization of detached oil.

The fractogram of PBS volume stored in verum syringe glass containers during ultrasound stress is illustrated in Fig. 68. Subsequent identification of the fractionated component

via light microscopy unveiled silicone oil droplets to cause the turbidity/ particulate matter after 30 min exposure to ultrasound (Fig. 69).



Fig. 67. Light microscopy analysis of components inducing turbidity in placebo syringes after ultrasound stress. Comparing this picture to the image of droplets in silicone oil emulsions verifies the siliconic nature of the particulate matter in placebo syringes; scale bar represents 100 μm .

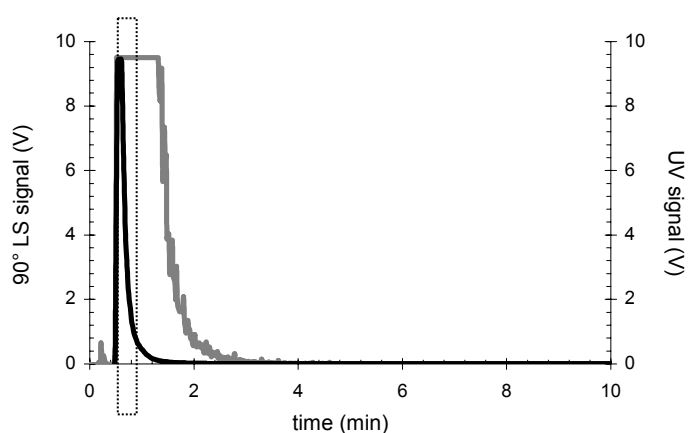


Fig. 68. Buffer-filled verum syringes stressed via ultrasound prior to AF4 analysis. Parameters: 65% cross flow, detection with UV₂₈₀ (black line) and MALS (grey line). Box represents the volume that was sampled and analyzed by light microscopy (Fig. 69).

Interestingly, the question whether syringe plungers may contribute to particulate matter is rarely addressed in the literature. Conversely, it has been repeatedly published that siliconized rubber stoppers can be the source of undesired negative features in the parenteral product, mainly particle formation (Li et al., 1993). Actually, siliconized stoppers do not mandatorily have to come into contact with the product to facilitate particle generation, e.g., in case of the manufacturing of freeze-dried products (Gebhardt et al., 1996).



Fig. 69. Light microscopy picture of a fraction collected during AF4 analysis of buffer-filled verum syringe volume (refer to Fig. 68).

As the plungers of all syringes are coated with silicone oil, however, this topic was evaluated by placing the plungers of 10 placebo syringes in 20 mL PBS, pH 6.8. The batch was exposed to ultrasound for 15 min and analyzed via light microscopy – and no particles could be detected (limit of resolution $\sim 1.8 \mu\text{m}$). On the other hand, placing the remaining barrels into 30 mL buffer medium, the same proceeding yielded silicone oil droplets comparable to those

illustrated in Fig. 69. Obviously, the siliconized inner barrel surface exhibits a greater potential to contingent particle formation than the siliconized plunger surface.

The developed AF4 application is only of value if the separation of silicone oil aside adalimumab protein can satisfactorily be shown. This feat can be jeopardized by the inconsistency of AF4 separation parameters required for the fractionation of droplets, adalimumab monomers and higher-order protein specimen, respectively. Moreover, adalimumab may exhibit an affinity to silicone oil adhering upon the membrane, thus abetting the incident of artifacts. Considering that, to simulate the situation within turbid syringe volumes by adding silicone oil emulsions to adalimumab solutions and to analyze those model samples via AF4 seems reasonable. As the steric mode elution of the droplets proceeds for over 4 min, the in effect optimal separation conditions for adalimumab have to be adapted (Fig. 70): reducing a 30% cross flow level after 2 min in a non-linear way to a 0% level at $t=6$ min enables the separation of adalimumab monomer and higher-order components within 9 min. MW calculation with MALS reflects the elution of an inhomogeneous aggregate fraction at ~ 6.5 min by displaying the molecular weights around 10^7 Da. The void peak – representing non-focused material regardless of the MW – is assigned $\sim 10^6$ Da, what is to be considered as MW average of monomers and aggregates. Bearing in mind a >4 min interval of droplet elution, the 2 min delay of adalimumab monomer elution start is not eligible for analysis of samples containing both oil droplets and protein monomers.

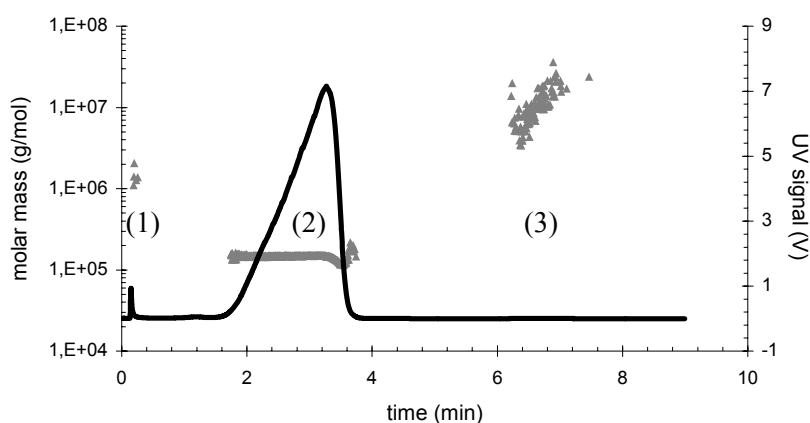


Fig. 70. Optimal AF4 separation of adalimumab monomer (2), keeping distance to void peak (1) and aggregate fraction (3), the latter representing $<0.1\%$ of total protein mass (black curve: UV₂₈₀ signal; grey dots: molar masses, derived via MALS).

Via reduction of both focus time and intensity and slight changes in the cross flow profile, eluting adalimumab monomer can be reflected by an UV₂₈₀ peak with ideal symmetry (Fig. 71). Additionally, the superiority of MALS in detection of hmw specimen (3) is impressively demonstrated: confronted with the task to detect an aggregate fraction which accounts for $<0.1\%$ of total protein – the appendant UV peak can be visualized solely in magnified view – MALS responds to the marginal aggregate portion with an AUC_{LS90° exceeding that of the monomer.

In order to generate a model of turbid syringe volumes, the 800 μ L content of clear syringes were diluted with AF4 elution medium to provide adalimumab sample loads of 100-800

μg . That high sample loads may be associated with low qualities of resolution power is a well-known fact (Schimpf et al., 2000). Subsequently, 200 μL of silicone oil emulsion (0.5%) were added to 800 μL syringe volume and homogenized via vortexing (10 s, 120 rpm, rotation radius 2 cm). Thereby, the resulting 1 mg/mL content of silicone oil aligns with the scope of syringe siliconization degree of ~ 3.4 mg/syringe. Compared to turbid verum syringes, the model volumes exhibited a greater turbidity and were prone to creaming phenomena: after storage for 24 hrs at 5 $^{\circ}\text{C}$ and 25 $^{\circ}\text{C}$ a thin, coherent film of silicone oil was buoying at the surface. Thus, the model volumes were analyzed via AF4 within 6 hrs after creation.

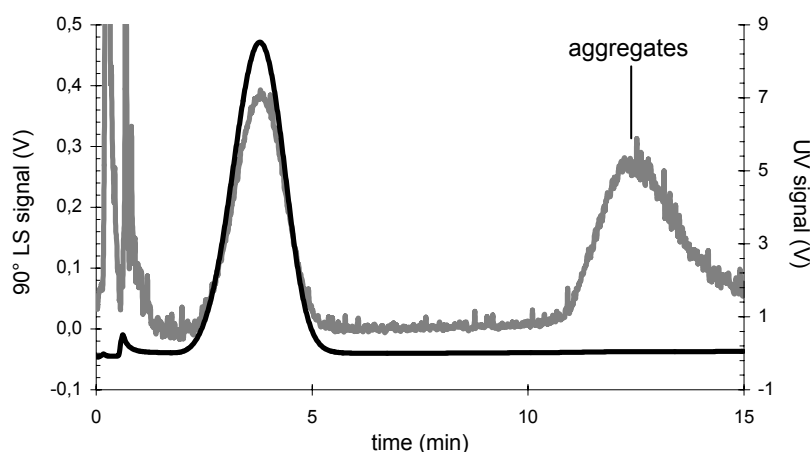


Fig. 71. Sample load identical to the experiment illustrated in Fig. 71. Humble variations of AF4 separation parameters ameliorate peak symmetry, but prolong experiment time. Note the intense respond of MALS (grey line) on aggregates, in contrast to the minimal UV respond (black line).

Pertaining to Fig. 72, droplets and protein monomer can be separated, whereby the droplet fraction is represented by a characteristic acuminate peak. In order to provide a sufficient lag between (post-)eluting oil droplets and the onset of protein elution, the cross flow level was risen to 65% - thus retaining adalimumab for ~ 4 min. However, as UV detection provides a rather ambiguous picture of the droplet elution profile, an alignment of both UV and MALS signal is conducive to clarification of facts (Fig. 73). Furthermore, if the MALS signal of the droplets were to intervene with that of the protein, the adalimumab MW calculation – at present conditions yielding ~ 150 kDa - would be erroneous.

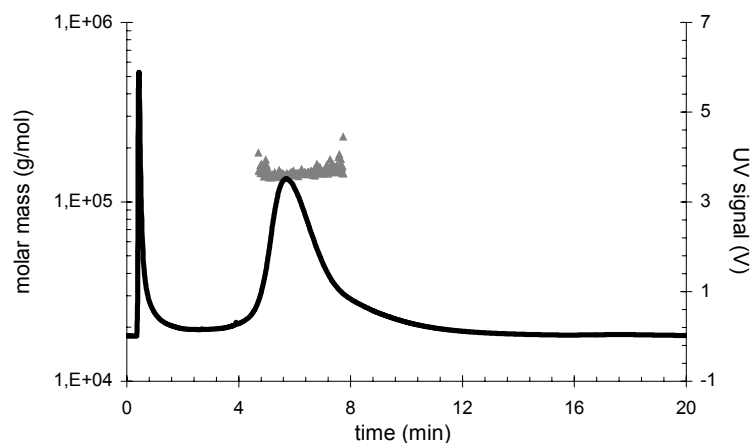


Fig. 72. AF4 separation of adalimumab solution enriched by silicone oil emulsion. The fronting/tailing of the protein UV_{280} peak (black line) is attributed to protein affinity to the silicone oil film covering the membrane surface.

Unfortunately, protein adsorption occurs, reflected by fronting and tailing of the monomer peak (Fig. 73). Referring to this, the affinity of immunoglobulins G with silicone

surfaces was evaluated earlier, demonstrating the antibody adsorbing to silicone surfaces more strongly than proteins that are considered to inhere equal hydrophilicity such as albumine (Ortega-Vinuesa et al., 1998). Thereby, protein adsorption is suggested to be an irreversible process (Wigren et al., 1991). But as the extent of this irreversibility depends on the contact time – and the AF4 experiment being performed apace –, the small time of adalimumab exposure applies the brakes on irreversible protein adsorption (Lundstrom and Elwing, 1990).

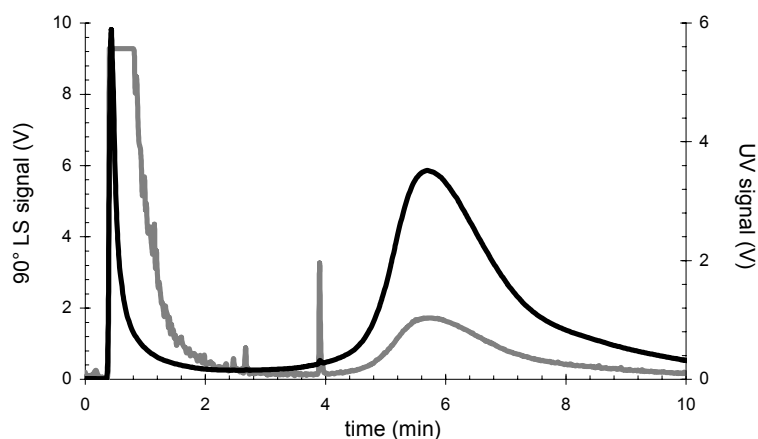


Fig. 73. Fractionation of droplets and protein monomer. Both UV (black line) and $MALS_{90^\circ}$ (grey line) prove system parameters to provide sufficient resolution of droplet fraction and monomers.

The separation of silicone oil droplets and protein specimen via AF4 was successfully demonstrated – what hitherto has never been published - and this application can be employed to elucidate the origin of particulate matter in siliconized verum syringes.

The situation in syringes which appear clear during visual inspection is unambiguous (Fig. 74). Because of the separation conditions (65% cross flow, programmed to reach a 0% level in non-linear manner at $t=13$ min) the first evidence of adalimumab elution can be monitored not until 5 min. Furthermore, the presence of a small aggregate fraction is disclosed, accounting for <2% of total protein and spanning the gamut from 500,000 Da to almost 10^8 kDa. (It will be explained later on why the latter information has to be scrutinized and doubted.)

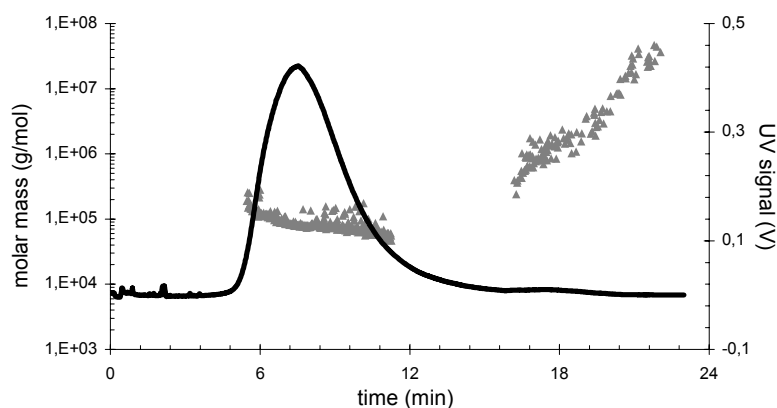


Fig. 74. AF4 analysis of the content of clear verum syringes. Besides monomer, a small aggregate fraction can be detected, visualized by the UV signal (black line) in magnified view and by (arguable) MW data (grey dots) (refer to text).

Focusing step and high initial cross flow rates allow for reducing the void peak to minimal levels. Thus, it can be further embarked on the strategy that visible particulate matter, if present in syringe samples, is assumed to elute in steric mode and to induce detector signals in the first stages of the AF4 experiment.

Even if the visible component inheres no UV activity and is present in minimal concentrations, the sensitivity of MALS on large analytes guarantees to scent out that very visible entity. In case Milli-Q™-water is subjected to AF4 separation conditions identical to those applied in Fig. 74, according to UV₂₈₀ data no analytical entity is to be detected (Fig. 75). However, Homer sometimes nods, and MALS unequivocally verifies the detector passage of one fraction immediately after start of the separation step, whereas a second fraction is identified when the exerted cross flow is zero (t=13 min).

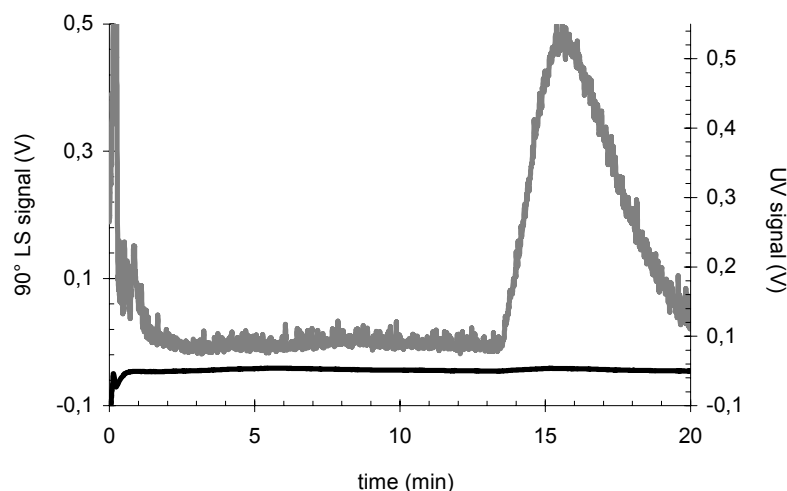


Fig. 75. UV (black line) and MALS_{90°} signal (grey line) of Milli-Q™-water characterization subsequent to a run analyzing silicone oil emulsion. Due to experiment conditions, silicone oil adhering upon the membrane is unhitched and detected solely by MALS (refer to text).

Prior to the experiment, a silicone oil emulsion was characterized. A humble fraction of oil adheres upon the membrane and may leave the channel during the successive experiment, thereby inducing artifact peaks. During the focus step, the membrane is flushed by two opposing flow profiles, and a minute fraction of silicone oil may become dispersed into the channel volume – thus partially being positioned at elevated channel positions and leaving the channel embedded in fast flow laminae. That lowest gravitational or hydrodynamic forces may be sufficient to actuate spontaneous oil detachment off surfaces has been repeatedly described (Thompson, 1994). Conversely, at no cross flow forces effective after 13 min, the mere streaming of elution medium ushers in similar detachment phenomena. As a consequence, it has to be carefully deliberated about the trustability of these data. In worst case, the MALS signal may be misconceived as sluggishly eluting hmw protein aggregates or can superimpose the signals of sample components, then potentially adulterating the values of calculated molar masses (refer to Fig. 74).

The situation within turbid syringes is presented in Fig. 76.

The eye-catching peak at t=0.5 min bears a substantial resemblance to signals of silicone oil emulsions and of syringe volumes with artificially induced detachment incidents. Adalimumab protein is unified by a UV₂₈₀ signal exhibiting considerable tailing – that may be ascribed to system parameters, protein adsorption events and concentration effects of the component eluting before. Assumed that this component represents silicone oil droplets, tiny droplets in nm range

may elute within the protein fraction – or oil drops resolve sporadically from the contaminated membrane and pass the detectors concomitantly with adalimumab. MALS misattributes the scattering of silicone to protein, thus overcalculating molar masses and rendering broad mass distributions. According to Fig. 76, adalimumab is assigned ~ 180 kDa at the UV_{280} maximum (+20% aberration), and at minor protein concentrations the MW data is fringed because of an unfavorable signal (adalimumab) – noise (single particulate specimen) ratio.

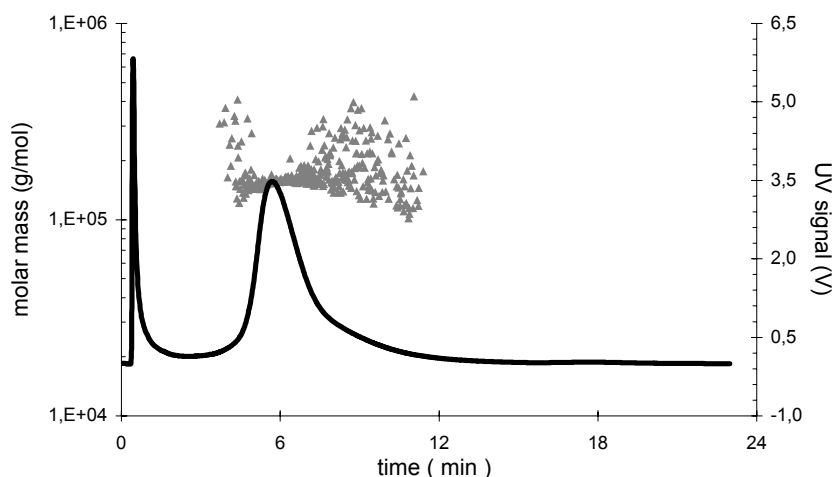


Fig. 76. Analysis of the volume of turbid syringes. The main difference to fractograms of clear syringes is an intense UV peak (black line) preceding the adalimumab monomers (refer to text).

Hence, the component eluting in steric mode may indeed be oil droplets. Due to the affinity of silicone oil to the membrane, the droplet fraction – if really consisting of silicone oil – should reveal a kind of delay in its elution profile, regardless of the theoretical constraints. Anyway, that is easily to be verified by confronting UV and MALS signals (Fig. 77).

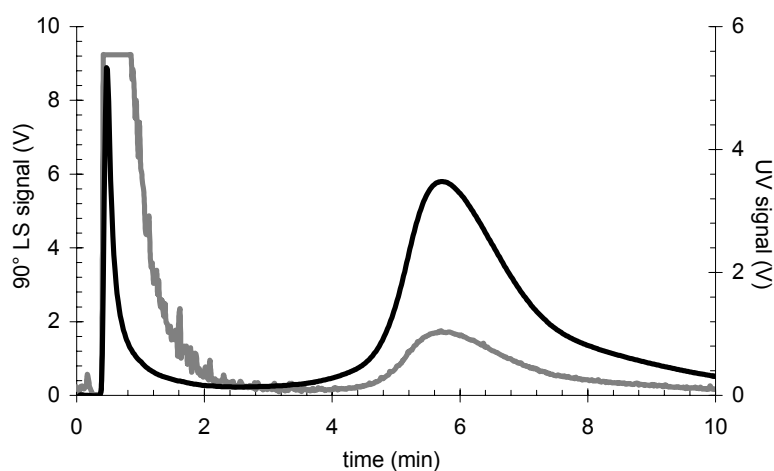


Fig. 77. UV (black line) and $MALS_{90^\circ}$ signal (grey line) of turbid verum syringe content. MALS demonstrates the first fraction - being separated in steric mode - a delayed elution profile, thus indicating analyte adhesion events upon the membrane.

Two causalities can be mentioned in terms of MALS overexcitement in the initial experiment stage: high analyte concentration and ultra-large analyte dimension. Considering the intensity of MALS substantially outnumbering the analogical UV signal in case of the steric mode sector, the latter appears to apply. However, once the challenge of particulate matter separation is performed, the walk through the task of identification is straightforward: one possibility is to

combine AF4 with electrospray mass spectrometry as on-line detector for analyte identification (Hasseloev et al., 1997). Alternatively, the sampled fraction can be subjected to proton nuclear magnetic resonance spectroscopy ($^1\text{H-NMR}$) or AAS, which have both been repeatedly applied in the identification of silicon compounds (Lykissa et al., 1997; Leung and Edmond, 1997). Otherwise, the particles' origin can easily be elucidated by comparing the steric mode fraction to silicone oil emulsions in light microscopy analysis – and detached silicone oil emerges to be the cause of syringe turbidity (Fig. 78). That the sampled AF4 fraction inheres less droplets than a 0.5% silicone oil emulsion is thereby comprehensible.

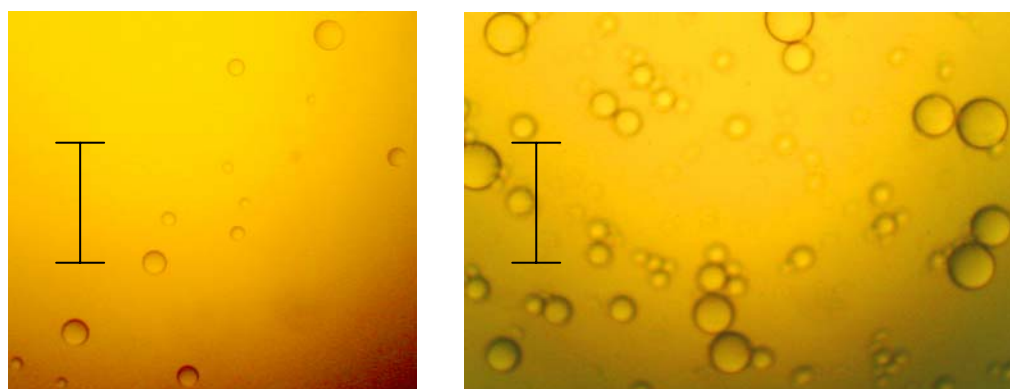


Fig. 78. Light microscopy analysis of a collected AF4 fraction of turbid syringe volume (left image) versus silicone oil emulsion (0.5%, right image); scale-bar represents 100 μm .

The degree of silicone oil detachment in syringes poses the question of the impact on adalimumab stability. The tendency of especially hydrophobic surfaces to denature proteins is deemed a top issue in the literature (Ostuni et al., 2003). Hence, assuming the inner barrel surface area of 690 mm^2 to be multiplied by the droplet formation due to detachment/coalescence, the threat to protein stability is a serious one. The more, as established methods like light obscuration were shown to fail in differentiation between oil droplets and protein precipitates (refer to Table 8). However, according to Fig. 76, no distinct aggregate fraction is detected.

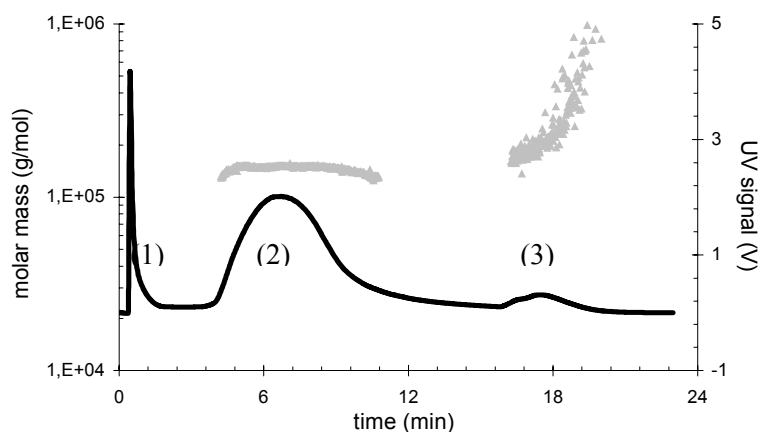


Fig. 79. Subjecting syringes which already experienced detachment to thermal stress (45 $^{\circ}\text{C}$, 10 d) renders three components amenable to AF4 separation: silicone oil droplets (1), adalimumab monomer (2) and hmw aggregates (3).

In order to go further into this issue, adalimumab denaturation was compelled within turbid syringes – i.e., detachment has occurred - via 10 d storage at 45 °C. Subjected to stress, adalimumab obviously has undergone denaturation, and the appendant aggregate fraction can be separated as individual fraction via AF4 (Fig. 79).

In conclusion, via AF4 the visible particulate matter in siliconized adalimumab disposable syringes has convincingly been demonstrated to be due to detachment of silicone oil during storage. Besides, protein aggregates could not be detected. This topic was further elucidated applying analytical techniques like PCS and SEM, thereby corroborating the data presented above (Fraunhofer et al., 2002c).

7.6 The effect of silicone oil detachment on syringe frictional drags

Commercial disposable syringe barrels – regardless if made by polypropylene or glass – are lubricated with silicone oil to reduce the coefficient of friction during plunger motion. Thereby, the plunger movement is determined principally by the interference or squeeze between piston and barrel and the amount of compression set (deformation) a constrained piston takes during sterilization and subsequent storage, but mainly by the type and amount of lubricant (PDA, 1981). In this regard, especially if the siliconization process is not accompanied with a final heat curing process, simple water washes have been shown to flush a proportion of the silicone lubricant from syringes, what leads to increased frictional drags during plunger motion, referred to as syringe stiction (Capes et al., 1996). In general, the matter of potential lubricant detachment has enormous impact on the safety and quality of the emptying process, because due to the then increased frictional drags the drug application is impeded. If syringe pumps are applied, the effects may be dramatic: more than one million Becton Dickinson brand syringes were recalled, because their high breakloose force was causing false alarms with syringe pumps (communication, 1991).

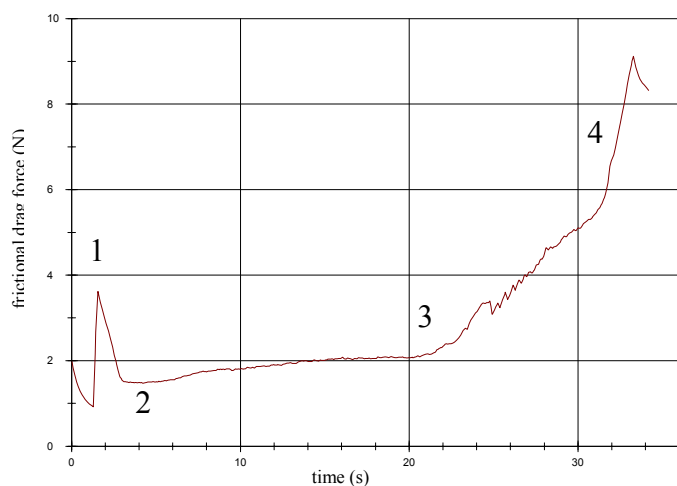


Fig. 80. Monitoring frictional drags during depletion of clear siliconized adalimumab syringes: breakloose force (1), start of average extrusion force (2), end of average extrusion force and force increase due to barrel tapering (3), piston compressed against barrel end (4).

Bearing in mind lubrication being the main function of barrel siliconization, adalimumab syringes which have undergone silicone oil detachment – i.e., a loss of lubrication – should reveal different frictional drags during depletion compared to syringes with intact siliconization. The force required to initiate and maintain syringe plunger motion can be gauged with methods specified by regulatory authorities or professional associations (Fig. 80).

Thereby, the syringes were mounted vertically in the holding system with the needle tip downwards and the plungers were moved automatically at a nominal speed of 70 mm/min (friction transducer WN805687, Boehringer Ingelheim GmbH, Biberach, Germany). The plunger was straightened in the barrel so that the major axes of the plunger, barrel and the force gauge were parallel to prevent lateral forces or rocking of the piston during operation. Initially, the breakloose force – defined as the force required to commence plunger movement against the static frictional drag - has to be overcome (PDA, 1988). For that almost ~ 4 N were required. Subsequently, only the sliding frictional drags have to be opposed. A force of ~ 2 N is sufficient to maintain the average extrusion force. Generally, the upper limit of the force sensor was 8.5 N.

As outlined in Figs. 81 and 82, the extrusion force profile changes dramatically when the barrel lubrication of placebo and verum syringes decreases because of induced silicone oil detachment.

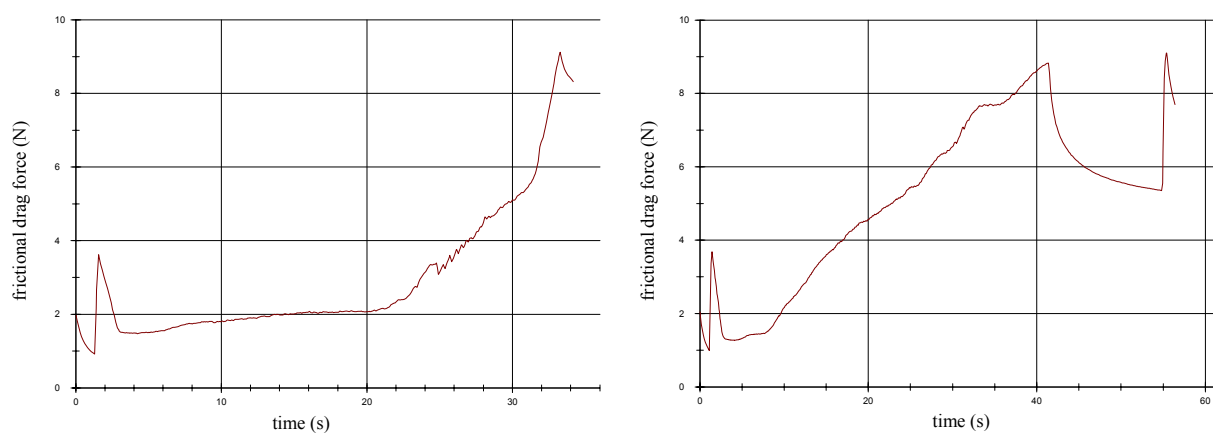


Fig. 81. Frictional drags during depletion of siliconized placebo syringes, prior to (left) and subsequent to (right) induced silicone oil detachment by ultrasound stress. After stressing, the syringe volumes were turbid because of oil detachment and droplet formation. As the lubricating effect is decreased, the average extrusion force for plunger movement steadily increases, indicating non-uniform detachment.

In the course of sample preparation/providing for characterization of syringe volumes, clear and turbid adalimumab syringes were emptied by moving the plunger with a backup piston. As subjective the personal impression may be: the notion that the required forces for manual depletion of turbid syringes exceeded the force necessary for clear syringe depletion by a multiple was corroborated by automatic force monitoring (Fig. 83).

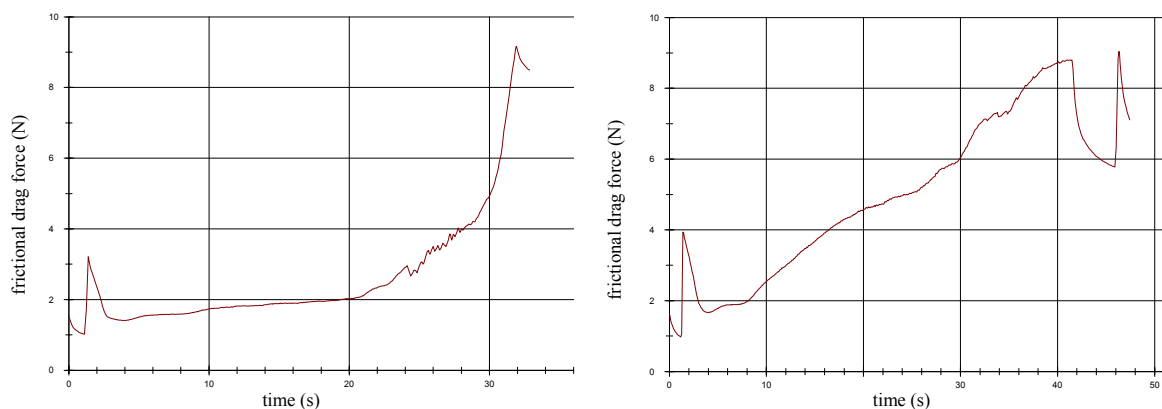


Fig. 82. Frictional drags during depletion of clear siliconized adalimumab verum syringes, prior to (left) and subsequent to (right) induced silicone oil detachment by ultrasound stress. Again, silicone oil detachment impedes plunger movement, demonstrated by rising average extrusion forces up to 8 N.

According to Fig. 83, the migration of silicone oil off the barrel surface into the syringe volume spirits away the lubricating effects. The signals due to primary static friction and subsequent sliding friction merge, and a constant force of at least 6 N is needed to empty the syringes. In conclusion, the data of AF4 analysis countenance the findings illustrated above, ascribing the particulate matter development during syringe storage to oil detachment.

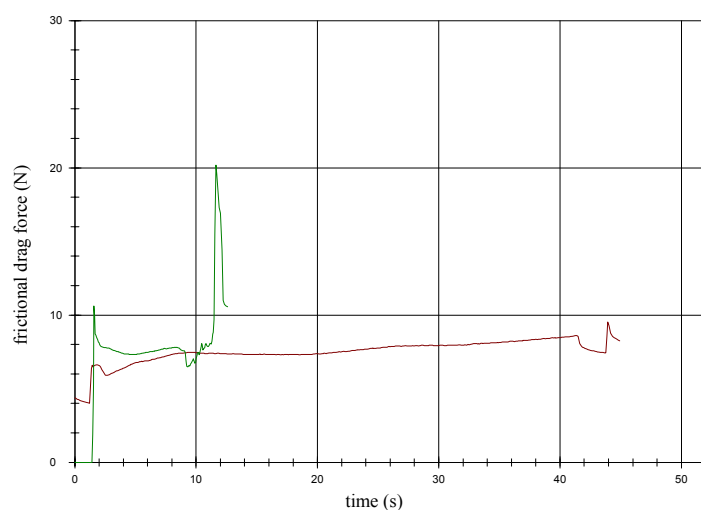


Fig. 83. Depletion of two adalimumab syringes which experienced silicone oil detachment and turbidity during storage. Right from the beginning, forces of >6 N are required for plunger motion (red line), whereas in a second syringe the frictional drags after 7 mm of plunger motion exceeded the upper record limit of the apparatus (8.5 N, green line).

Generally, there are a few requirements limiting the amount of silicone oil – i.e., PDMS – in siliconized containers or medical devices. The European Pharmacopoeia postulates a siliconization degree of <0.25 mg/cm² for disposable syringes (2002 Edition, Monograph 3.2.8: Sterile single-use plastic syringes). Neither the USP24/NF19 nor the Japanese Pharmacopoeia XIII state any requirements for the degree of siliconization of glass and plastic containers or rubber closures. However, one actual limitation for lubricants in food and drugs of 1 ppm is stipulated by the U.S. Food and Drug Administration (FDA) for the use of silicone oils – i.e., dimethylpolysiloxane, viscosity >300 cSt - in 21 CFR § 178.3570, (1998) “Lubricants with incidental food contact”

(Mundry et al., 2001). Still far away from propelling a laissez-faire policy, the FDA nevertheless has eclipsed the mischiefs associated with silicones by the recent general approval for silicone oil (1000 cSt) for intraocular injection (Benedetto and Lewis, 2003).

Conversely, product purity and stability are generally arresting more attention, as those parameters are deemed to directly influence general drug safety. Even for the professional it may be astonishing how closely package siliconization is connected to the issue of general drug safety:

7.7 Can protein drugs vanish within a syringe?

By means of AF4 the turbidity of adalimumab syringe volumes was demonstrated beyond doubt to be caused by silicone oil detachment and not by precipitated protein. Unfortunately, by screening the AF4 data not only qualitatively but also quantitatively, the matter gains intricacy (Table 9).

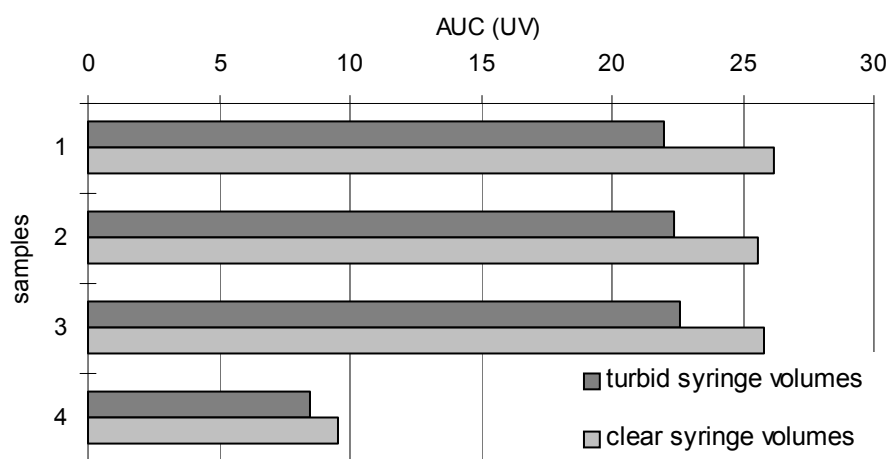


Table 9. Comparison of sample recovery in terms of UV₂₈₀ data: turbid versus clear syringes (sample load of samples 1-3: 2 mg; sample 4: ~0.7 mg).

According to Table 9, there seems to be an indirect correlation between syringe volume turbidity – i.e., silicone oil detachment – and sample recovery. Obviously, clear syringes outnumber turbid syringes in protein content by ~15%. Can the detachment of silicone oil really influence the amount of detectable protein? Two reasons jump the queue – and both are associated with incidents based on oil droplet formation. Here, the protein is confronted with an immensely increased hydrophobic surface, and why should the protein not take the bait and adsorb thereon? In most qualitative pictures of adsorption, processes involving the interaction of a hydrophobic patch on the protein surface and a hydrophobic surface region such as oil droplets are followed by conformational changes in the protein that (partially) exposes its hydrophobic core. Dehydration of hydrophobic sites provides an entropic impetus for adsorption (Ostuni et al., 2003). As denaturation often comes along with fragmentation, adalimumab may have fragmented and the fragments pass the AF4 ultrafiltration membrane, thus avoiding detection.

On the other hand, proteins do not mandatorily have to change their conformation when they adsorb on surfaces (Norde, 1998). However, since the droplet fraction induces UV response

subsequent to AF4 fractionation merely by reduced transmission and scattering phenomena, the UV signal of proteins potentially adhering upon the droplet surface is superseded and eclipsed. As a consequence, in that case protein is underquantified by UV₂₈₀ detection, if ever.

Pertaining to the fragmentation hypothesis, the matter can easily be elucidated by filtration of clear and turbid syringe volumes, revealing the ~15% loss of protein to be ascribed to the removal of oil droplets rather than to fragmentation (0.2 μm, PVDF).

batch	syringe volume	UV ₂₈₀ absorbance
50 μl filtrated syringe content + 3000 μl Milli-Q™ water	turbid	1.033
	clear	1.182

Table 10. UV₂₈₀ absorbance of adalimumab syringe volumes after 0.2 μm filtration (n=3).

The findings above are substantiated by the evaluation of SE-HPLC data. Originally, SE-HPLC analysis was applied in order to investigate whether turbid syringe volumes differ from clear syringe volumes in qualitative terms, i.e., in aggregate content. Via quantitative interpretation of the data, a correlation of turbidity and protein disappearance (~14%) becomes manifest (Table 11).

syringe	sample preparation	sample	AUC UV ₂₈₀	AUC _{UV280} average
clear volume	filtration (0.1 μm, PVDF)	1	8.37	8.47
		2	8.52	
		3	8.51	
clear volume	none	1	8.55	8.56
		2	8.47	
		3	8.65	
turbid volume - oil detachment	ultracentrifugation, 5500 g, 3 min	1	7.25	7.26
		2	7.25	
		3	7.28	
turbid volume - oil detachment	filtration (0.1 μm, PVDF)	1	7.50	7.63
		2	7.66	
		3	7.73	
turbid volume - oil detachment	filtration, twice (0.1 μm, PVDF)	1	7.28	7.35
		2	7.41	

Table 11. Detected AUC UV₂₈₀ of adalimumab during SE-HPLC analysis dependent on syringe volume conditions: turbid due to silicone oil detachment versus clear. Sample preparation did virtually not influence sample recovery, as illustrated.

The possibility of adalimumab adhering irreversibly upon the siliconized barrel surface is to be ruled out – in that case, the assessed protein content should differ from 40 mg, as declared. As a matter of fact, assessed and declared content matched.

To elucidate the adsorption problem, it may be helpful to leave the mere pharmaceutical ken towards other fields of research. In the laundry business, the cleaning of solid surfaces is of considerable interest, as oily contaminants that could otherwise be deleterious to subsequent process steps or for quality purposes have to be removed (Rowe et al., 2002). Thereby, the strong

adhesion of surfactant molecules upon the oil contaminants is considered to be a crucial step. In Food Industries, protein emulsifiers protect finely dispersed droplets against immediate re-coalescence and, during storage, provide long-term stability towards creaming and flocculation – by rapid adsorption at the oil-water interface (Dalglish, 1997). In all those fields, proteins adhere to considerable extent at interfaces in oil-water emulsions. Returning to the syringes: given a siliconization degree of >3mg PDMS per syringe, with a notable amount thereof undergoing detachment, coalescence and droplet formation during storage, turbid syringe volumes may be considered as PDMS-water emulsions. As a consequence, abundant protein emulsifiers – i.e., adalimumab - will adhere at interfaces, thus potentially avoiding detection in AF4 experiments. This hypothesis is fueled by the fact that especially globular β -lactoglobulins are known to adsorb substantially on oil-water interfaces – hence, the risk for globular immunoglobulin to meet a similar fate seems genuine (Dickinson, 1998).

In order to assess the amount of protein adsorbed on the droplet surfaces, if ever, the AF4 droplet fractions leaving the channel within the first 2 min of separations were collected and the quantity of adalimumab incorporated therein was quantified via a protein-specific bio-assay (D_c protein assay, Bio-Rad Laboratories, Hercules, CA, USA). Due to the assay specificity towards protein and the dilution of the collected steric-mode fraction (~ 1.5 mL), artifacts in UV_{595} detection which are based on scattering, refraction and reflectance of light are virtually forestalled. The principal applicability of the assay was scrutinized by generation of a standard calibration row (Fig. 84).

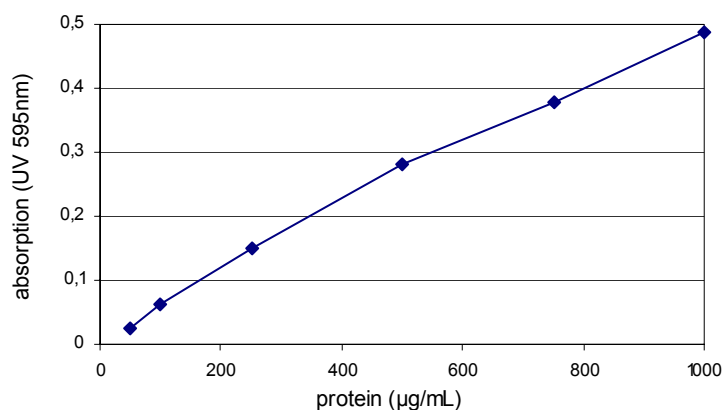


Fig 84. Response of protein-specific Lowry-assay on various adalimumab loads (50-1000 $\mu\text{g/mL}$); R 0.994; $x=2000(y-0.01)$, detection via UV_{595} spectrophotometry.

In theory, the AF4 droplet fraction of turbid syringe volumes – note that only turbid volumes contain silicone oil droplets – should reveal a protein content commensurate with the difference in protein content of clear and turbid syringes. In this realm, the observed $\sim 15\%$ difference in drug load correspond to 6 mg protein.

There is, of course, a substantial flaw in the methodology: the underlying principles of AF4 imply the void peak to comprise sample specimen which circumvented focusing. Although the applied AF4 separation conditions guarantee the adalimumab void fraction to be $<0.2\%$ of the injected sample mass, protein of the void fraction eluting concomitantly with the droplet

fraction will inevitably be recorded subsequently by the assay. Hence, clear syringe volumes – i.e., no oil droplets being present – and placebo syringe volumes were also analyzed in terms of reconciliation (Table 12).

Pursuant to Table 12, via combination of AF4 and bio-assay quantification the amount of adalimumab adsorbing on silicone oil droplets in turbid syringe volumes averages ~6% of total syringe content. Thus, it can be concluded that silicone oil – once migrated into the syringe volume and causing droplet formation – exhibits a great tendency for protein adsorption and subsequent immobilization.

analyzed sample	experiment	protein mass contained in void/ droplet fraction (µg)	protein mass of void/droplet fraction in relation to total syringe load (%)
turbid syringe volume	1	2784	6.96
	2	2344	5.86
	3	2680	6.70
clear syringe volume	1	344	0.86
	2	312	0.78
placebo syringe volume	1	8	0.02
	2	8	0.02

Table 12. Protein masses eluting within the void/droplet fraction of AF4 runs. Samples drawn from turbid syringe volumes exceed notably samples of clear and placebo volumes in protein content – proving the silicone oil droplets to capture a notable amount of protein drug.

Since previous experiments with filtration, SE-HPLC and AF4 assessed the difference in detectable protein between clear and turbid syringe volumes to be ~15%, the question of the protein whereabouts can not be answered completely. Possible explanations therefore are: subsequent to interface adsorption and denaturation, the proteins may fully migrate into the interior of the silicone oil droplets. Complete unfolding provided, the attractive van der Waal contribution would have to be added to the entropic impetus of dehydration of the hydrophobic protein surface, which could be attained thereby (Ostuni et al., 2003). Moreover, the features of the inner barrel surface will alter due to silicone oil detachment. As a consequence, adalimumab may develop a greater tendency towards immobilization upon glass surfaces which lack the shield of covering silicone oil.

The final argument addresses the silicone oil layer adhering the AF4 ultrafiltration membrane – what renders one artifact to become conceivable: because of the cross flow induced close proximity between sample components and the ultrafiltration membrane, an intense interplay between (still) eluting and (already) adsorbed silicone oil specimen appears likely – needless to state that the same applies to eluting protein, too. Hence, a transfer of silicone oil between the eluting fraction and the membrane-covering fraction will occur. Additionally, it was found that emulsion droplets exchange a notable quantity of oil molecules even if immediate vicinity is not provided through the continuous phase, i.e., the elution medium. Processes similar

to Ostwald ripening were demonstrated to foster those events (Taisne et al., 1996). Anyhow, protein-rich droplets of lower stream laminae may swap places with protein-poor silicone oil covering the membrane. In summary, any of the processes outlined will result in an AF4 under-quantification of protein. On this account, the data merge into a coherent picture.

Generally, silicone oil droplets within the syringe volumes are no static entities but amenable to processes of permanent coalescence, re-emulsification incidents and re-migration of droplet appendant silicone oil (Dickinson, 1998) (Fig. 85).

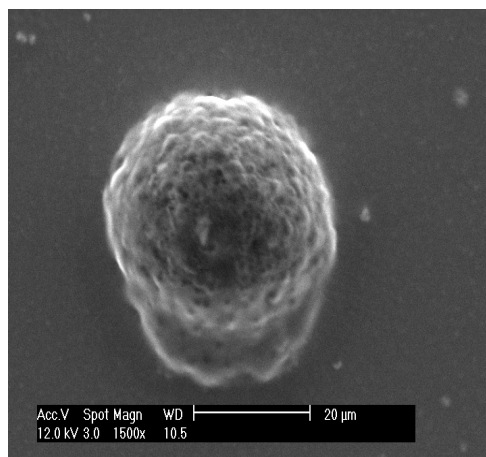


Fig 85. Characterization of a silicone oil droplet of turbid syringe volumes subsequent to separation via AF4 by scanning electron microscopy (XL40ESEM, Phillips GmbH, Germany). Note the agile droplet character reflected by surface bubbling, surface protuberances and vesicle coalescence.

In this realm, also protein adsorption may be deemed a steady process and proteins adhering on the droplet surface may displace and migrate back into the aqueous medium (Bos et al., 1997). Provided that adalimumab maintains the native conformational state, there is no reason to worry. The matter is further complicated since adsorption of proteins is highly competitive with surfactants – mainly proceeding via solubilization in case of ionic surfactants, whereas non-ionic surfactants such as Tweens involve a replacement mechanism (Heertje et al., 1996). As the protein was formulated into the syringes using Tween 80, formulation components – including protein monomers and aggregates - may adsorb and detach even alternately. Therefore, a final statement whether the protein adsorbs onto the dispersed silicone oil droplets exclusively in monomeric form is not possible.

Silicone oil detachment may facilitate protein aggregation and aggregates in general may abscond from detection via immobilization on oil droplets – against the background of the potential of aggregates to trigger adverse immune responses and immunogenicity, respectively, syringes revealing silicone oil detachment are assessed to inhere risks in terms of general drug safety. In a case study proteins were demonstrated to primarily build up a monomeric formation on silicone surfaces, but with increasing adsorption time a rising amount of aggregates was detected (Alemeida et al., 2002). Advanced analytical techniques like front-face fluorescence spectroscopy or atomic force microscopy may provide information about the interfacial composition, but neither technique is capable of general, apodictic statements (Rampon et al.,

2003). Facing a variety of unanswered questions, this field with utmost probability will be the topic of intensive future research.

7.8 Summary

Today, disposable prefilled siliconized syringes for the parenteral application of drugs enjoy a great popularity among both patients and physicians. However, the process of siliconization – if of insufficient quality - is known to potentially give rise to particulate matter contamination. This chapter attends to an analytical case study of protein drug containing siliconized syringes, which sporadically developed visible particulate matter and a slight turbidity during 5 °C storage. Subvisible particulate matter analysis showed those syringes to be substantially contaminated with particles $\geq 1 \mu\text{m}$ (>150.000 per mL). In this regard, the answer of questions aiming at particle source and protein stability was urgently required.

Originally, the embarked strategy appeared straightforward: (a) find an increased ratio of soluble aggregates in the turbid syringe volumes, (b) separate the visible particulate specimen, (c) identify that specimen to reveal a proteinic nature and (d) finally subsume the matter to decreased protein stability due to insufficient formulation composition.

Analysis via SDS-PAGE and SE-HPLC, however, provided no hints towards a satisfying answer – in terms of protein stability, clear and turbid syringe volumes were of equal quality. As a consequence, the protein drug instabilities were not to account for particle origin.

On the other hand, it was found that the manner of syringe depletion was decisive for the number of subvisible particles assessed in the syringe volumes. Traditional emptying via plunger movement through the needles resulted in substantially higher particle numbers than providing the syringe volume via the barrel aperture subsequent to backward plunger removal. Given the background of barrel siliconization without a final heat curing – which is known to increase adhesive strength and inertness of the silicone oil layer -, the observed difference in particle contamination was possibly due to silicone oil, abraded via plunger movement.

In order to translate this hypothesis into syringes – i.e., to verify the processes oil detachment, coalescence and droplet formation -, an AF4 application was developed, targeting at the separation of μm sized silicone oil droplets. Hitherto, no successful characterization of oil droplets via AF4 has been published. The task was approached by the analysis of aqueous silicone oil emulsions, followed by the fractionation of ultrasound-stressed syringe volumes containing detached and coalesced silicone oil after stress exposure. Thereby, a possible scenario of the conditions within turbid syringes was simulated. Finally, a notable fraction of silicone oil could be identified in the volumes of turbid syringes, whereas clear syringe volumes lacked a droplet fraction. These data were corroborated by light microscopy and matched the findings of

syringe frictional drag analysis – which ascribed syringes to exhibit increased frictional drags during depletion when the lubricating effect is diminished because of silicone oil detachment.

Unfortunately, this turned out to be only half of the truth. Because the droplet formation increased the hydrophobic surface based on silicone, adsorption incidents were revealed, leading to a substantial reduction of the detectable protein content in syringes. AF4 provided the analytical fundament for the isolation and semi-quantification of that surface, i.e., the silicone oil droplets. Via protein-specific bioassay the isolated droplets were demonstrated to branch off a considerable fraction (>6%) from the declared protein drug load within the syringes. Thereby, a thorough approach to the question whether protein aggregates contingently adhere – and maybe detach - would be beyond the scope of this chapter. The more, as it was repeatedly shown that due to its complexity the question if proteins adhere upon surfaces exclusively in monomeric or aggregated form can definitively not be answered.

Earmarked to elucidate the visible particulate matter origin in the course of an analytical case study of siliconized syringes, the application of AF4 thereby turned out to provide much more information on a variety of parameters than usually intended. Hence, AF4 proved to be a valuable tool for answering challenging questions, which otherwise would have necessitated to apply a multiplex daedalian array of expensive analytical methods.

8 Characterization of gelatin nanoparticles by AF4

8.1 Introduction

The highly interdisciplinary field of nanoparticles encompasses chemistry, materials research, molecular biotechnology, immunology, medicinal and engineering sciences (Niemeyer, 2001). In the pharmaceutical industry, nanoparticles prepared from a variety of natural or synthetic polymers attracted much attention because of the target-oriented advanced drug delivery features of these systems (Farrugia and Groves, 1999). The research field of nanoparticles is expected to rapidly evolve and gain increasing importance for medicine and pharmaceuticals in the next years (Langer, 1998).

Especially in applications like gene therapy, the design of ideal polymeric carriers, those being able to target specific cell types, is highly desired – the more, as DNA delivery with non-viral vectors is deemed the most important delivery challenge of the new millennium (Kaul and Amiji, 2002). In this regard, via nanoparticles, the sustained parenteral delivery of DNA and oral gene delivery were successfully approached as well as the transfection of stem cells only a few months ago (Roy et al., 1999; Cohen et al., 2000; Corsi et al., 2003). Although the majority of nanoparticles described in the literature is formulated with poly(D,L)-lactide-co-glycolide (PLGA), the use of PLGA in DNA delivery bears one grave drawback: being a hydrophobic slow degrading polymer that results in highly acidic local microenvironment, PLGA is not a very effective polymer matrix for DNA encapsulation (Kaul and Amiji, 2002).

Pertaining to that, nanoparticles based on the natural biopolymer gelatin are very promising, as they enable high transfection rates (Truong-Le et al., 1999). Moreover, gelatin has a long history of safe use with low antigenicity in a wide range of medical and pharmaceutical applications, cosmetics, as well as in food products (Ward and Courts, 1977). The parenteral use of gelatine derivatives over many years provides a sound safety basis for future applications, and there are numerous ways for nanoparticle implementation. Fundamental knowledge of nanoparticle dimensions is of utmost importance as the influence of size on nanoparticle efficacy is still intensively discussed. For instance, 100 nm-sized nanoparticles exceeded 1000 nm-sized nanoparticles considerably in membrane permeability and thus uptake efficiency (Desai et al., 1996). Consequently, the application of new analytical methods in nanoparticle characterization struggles to keep pace.

For nanoparticle size determination, two main techniques are established: Electron Microscopy and Photon Correlation Spectroscopy (PCS), often referred to as Dynamic Light Scattering (DLS) or Quasi-elastic Light Scattering (QELS).

The intensive utilization of Scanning Electron Microscopy (SEM) may be ascribed to both high resolution and ease of sample preparation. The accessible physicochemical parameters

include particle size, porosity and morphology (Li et al., 1999). However, the conditions precedent to SEM analysis are sample conductivity and tolerance of vacuum ambience. Sometimes the presence of surfactants in the preparation may inhibit nanoparticle characterization via SEM due to the formation of a smooth, camouflaging coating on nanoparticle surfaces (Kreuter, 1983). The second microscopic method implemented for nanoparticle characterization is Transmission Electron Microscopy (TEM). The exceeding magnifications of TEM enable accurate particle surface and morphology analysis (Chui and Mumper, 2002). Inherent drawbacks of both methods are random sampling - instead of an overall sample analysis - and time consuming sample preparation and measurement procedures.

In reviewing the literature dealing with nanoparticle characterization, one will come across PCS as the dominating sizing technique. Because of its non-invasive and non-destructive performance, PCS evades artifacts. Dissolved and undissolved matter can be sized within minutes in a reproducible way. The major obstacle in order to achieve veritable results is due to the underlying principles: since PCS measures the effective z average of the diffusion coefficient proportional to the reciprocal particle radius for spherical shapes, the sizes derived are influenced by the presence of dust or agglomerated fractions present in the sample (Wyatt, 1998). Furthermore, a number of assumptions inherent in data analysis also affect particle distributions. However, PCS has become the preferred choice of technique for nanoparticle sizing, provided that size distributions are narrow.

Other sizing techniques play a minor role in nanoparticle characterization. Considering the prevalent dimensions of polymeric nanoparticles used in medicinal and pharmaceutical sciences ranging from 50 to 400 nm, light obscuration and Coulter technique are deemed a poor choice in nanoparticle analysis, due to their low resolution in nm scale. Conversely, the upcoming technique of Scanning Force Microscopy (SCM), also known as Atomic Force Microscopy (AFM), was successfully used in visualizing nanoparticles (Jungmann et al., 2002). Yet, the main area of application lies in the investigation of surface morphologies.

However, without exception the analytical methods outlined above are batch techniques, i.e., the constraints of enlarging the size application range to a maximum due to the presence of inhomogeneous samples - with small components present aside large components – call for a significant loss in resolving power. In this realm, optimal conditions provided, AF4 was shown recently to be capable of analyzing a cellulose derivative over a wide range of molar mass, including hmw components (Andersson et al., 2001). The question arises, whether such an AF4 application can be transferred to the issue of gelatin nanoparticle characterization: (a) starting with the important characterization of basic gelatin raw material, as it was demonstrated that the presence of notable lmw gelatin fractions in the preparation batch detracts from nanoparticle stability (Coester et al., 2000); (b) gelatin nanoparticle characterization per se – since the resolution of FFF/MALS was demonstrated to exceed that of (T)EM measurements for many

classes of particles (Wyatt, 1998); (c) monitoring drug loading efficacy. Herewith, the separation of DNA loaded nanoparticles from unloaded DNA would provide a fast, convenient and accurate possibility of drug loading assessment. Up to now, a successful realization of such an analytical approach has not been published.

8.2 Materials and methods

Gelatin type A from porcine skin (175 Bloom), glutaraldehyde (25%), EDC (N-[3-dimethylaminopropyl]-N'-ethylcarbodiimide hydrochloride) and cholaminchloride hydrochloride ([2-aminoethyl]-trimethylammonium chloride hydrochloride) were purchased from Sigma-Aldrich (Taufkirchen, Germany). Gelatin nanoparticles were prepared via a two-step desolvation method (Coester et al., 2000). Initially, 1.25 g of gelatin was dissolved in water under gentle heating (5% w/w). The first desolvation step was initiated by adding 25 ml acetone. After sedimentation of precipitated gelatin fractions over 60 s, the supernatant was discarded and the sediment was redissolved in water under constant heating and magnetic stirring at 500 rpm (MR 3001K, Heidolph GmbH, Germany). Subsequently, the pH was adjusted to 3.0 using 1 M HCl. By drop-wise addition of acetone the gelatin was desolvated again and stirred for 10 min. Finally, 200 μ l glutaraldehyde (25%) were added in order to stabilize the gelatin nanoparticles by intra-particle crosslinking of gelatin amino groups. Surface Modification: 50 mg EDC and 50 mg cholaminchloride hydrochloride were added and the batch was incubated for 14 hrs. The resulting nanoparticles were purified by triple centrifugation (16,000 g for 20 min) and redispersed in Milli-QTM-water (conductivity < 0.04 mS/cm).

DNA plasmid loading: 20 μ g of DNA plasmid, containing the *Photinus pyralis* luciferase gene (under control of the cytomegalovirus enhancer/promoter) were incubated with surface modified gelatin nanoparticles in water (1.0 mg/ml). After incubation at 37 °C (using a Thermomixer comfort, Eppendorf AG, Hamburg, Germany) the samples were centrifuged (~8,000 g, 20 min) and unbound plasmid was determined by UV₂₆₀ spectrophotometry in the supernatant.

Analytical instrumentation: nanoparticles were characterized using a Zetamaster (Malvern Instruments, Worcestershire, UK); the assigned size, polydispersity index and zeta potential values based on ten individual measurements. Additionally to the on-line detection methods outlined in Chapter 6 – i.e., RI and UV spectrophotometry coupled with MALS via a miniDAWNTM - AF4 was combined with a DAWN EOSTM (MALS, Wyatt Technology Corp., Santa Barbara, USA). Via that apparatus, scattered light is detected by an array of 15 photodiodes arranged at various angles relative to the incoming laser beam. According to light scattering theory, nanoparticles scatter light in anisotropic way (i.e., in a more forward direction). Consequently, the photodiodes placed at lower angles will detect more scattered light than photodiodes placed at higher angles. To enable accurate size determination of the nanoparticles, the sensitivity of eight photodiodes

was dimmed by a factor of 100 (photodiode angles: 14°; 26°; 35°; 43°; 90°; 121°; 142°; 163°). Thus, overexcitement of the photodiodes by huge intensities of light scattered by nanoparticles was avoided. Considering that small analytes (e.g., <10 nm) such as oligonucleotides or proteins with molar masses below 500 kDa scatter light scarcely, the sensitivity of the seven remaining photodiodes was retained unchanged at highest level (appendant angles: 52°; 60°; 69°; 80°; 100°; 132°; 153°). This arrangement measured scattered light intensity concomitantly with dimmed and unattenuated photodiodes and enabled the simultaneous size determination of large analytes like nanoparticles aside small analytes such as proteins or oligonucleotides. For nanoparticle size determination, a detector fit/plotting method according to Debye theory was implemented. For molar mass determination of gelatin and other proteins, the refractive index increment dn/dc was set to 0.174 mL/g and the second virial coefficient was set at 0. SE-HPLC experiments were performed with a TSKgel G 3000 SW column (7.5 mm x 30 cm; Tosoh Biosep GmbH, Stuttgart, Germany). The SE-HPLC system comprised a LKB 2248 pump (Pharmacia Corp., Germany), an autosampling device (Spectra Series AS 100) and a vacuum in-line degaser (both from Thermo Separation Products, Germany). The AF4 and SE-HPLC separation experiments were performed at 24 °C, using a buffer with pH 7.4 (5 mM $\text{Na}_2\text{HPO}_4 \cdot 2\text{H}_2\text{O}$ and 14 mM NaCl) for nanoparticle characterization, whereas gelatin characterization was performed in a buffer at pH 6.0 (2 mM $\text{Na}_2\text{HPO}_4 \cdot 2\text{H}_2\text{O}$ and 14 mM NaCl).

8.3 Analytics of gelatin raw material

The most widely applied method for the analysis of gelatin molecular weight distributions within the pharmaceutical and clinical field is SE-HPLC (Barth et al., 1998). In this realm, the characterization of lmw gelatin specimen is most important. For instance, the mean weight average of succinylated gelatin - an extensively utilized gelatin-based plasma substitute – was found to be 43 kDa (Kaur et al., 2002). As SE-HPLC lacks absoluteness, size calibration standards are necessary for size determination. In case of gelatine, the use of polystyrene sulfonates, denatured globular proteins, standard gelatins and dextrans have been reported for this purpose (Pernigo et al., 1994; PAGI, 1997). Yet, considering the proneness of that procedure when hmw samples are to be analyzed, the use of MALS for absolute size determination of gelatin fractions has demonstrated to render data with higher veracity (Kaur et al., 2002). A typical size distribution profile of gelatin bulk solution is visualized in Fig. 86.

According to the chromatogram, the bulk solution exhibits two fractions of gelatin specimen, which can be defined as hmw and lmw fractions. The borderline between "high molecular weight" and "low molecular weight" was assessed at 100 kDa because of two reasons: (a) hmw gelatin specimen are represented by a sharp, pronounced UV signal peak, enabling the convenient quantification of evidently two different fractions. The end of the peak descent

corresponds to a molar mass of 100 kDa, verified by MALS calculation. Concerning to that, the characterization of a 100 kDa globular protein (monoclonal antibody; F(ab')₂ fragment of isotype G3K) substantiated the accuracy of the SE-HPLC/MALS method. (b) It has repeatedly been reported that the molecular weight of the gelatin α -fraction matches \sim 100 kD (Steckert et al., 1992). Gelatin α -chains are the result of hydrogen-bond breaking and disruption of the triple-helix structure of soluble tropocollagen, and they define the borderline between a sub- α fraction (primarily hydrolysis fragments) and β -, γ - and δ -fractions, with the latter ones being composed of aggregates of the main α -chain fraction (Farrugia and Groves, 1999).

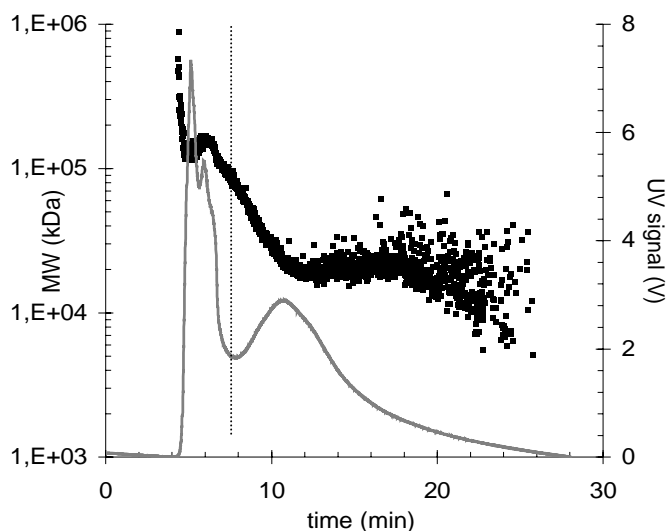


Fig. 86. SE-HPLC analysis of gelatin bulk solution; detection with UV₂₈₀ and MALS. Note that a MW value of \sim 100 kDa clearly marks off two gelatin fractions with molar masses greater and lower than 100 kDa (indicated by dotted line).

It is noteworthy to accent the criterion which assesses the suitability of gelatin batches in terms of nanoparticle preparation – i.e., the more hmw components present, the higher the nanoparticle stability (Coester, 2000). The established 100 kDa benchmark renders the evaluation of gelatin batches straightforward and the efficacy of the desolvation step can be scrutinized.

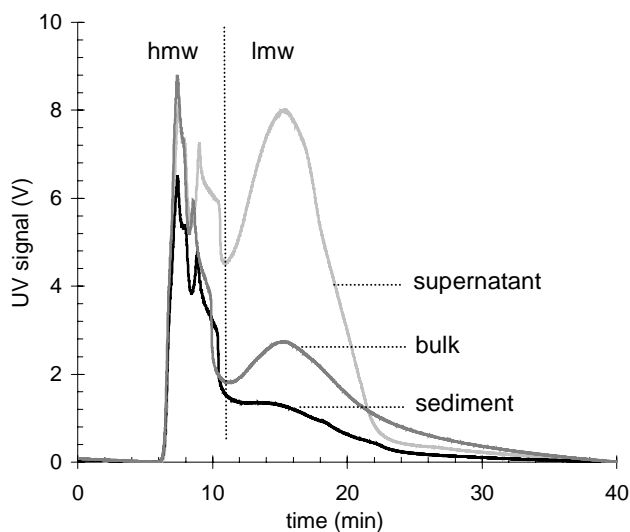


Fig. 87. SE-HPLC analysis of various gelatin fractions associated with the desolvation step process. According to the UV₂₈₀ elution profile, the ratios of hmw specimen $>$ 100 kDa were 29% in supernatant, 38% in bulk and 58% in sediment (flow 0.7 mL/min).

As outlined in Fig. 87, the desolvation by acetone has a great bearing on the elution profile of the various gelatin batches: hmw specimen – i.e., γ - and δ -fractions – account for 58%

of total gelatin mass in the sediment. Conversely, the original 38% ratio decreases within the supernatant by approximately 10%. Apparently, the quantification of hmw components – running the gamut from 100 kDa up to ~500 kDa – via SE-HPLC seems to be faultless.

Since the molecular weight composition of the precipitated gelatin is influenced by several parameters (i.e., organic solvent proportion, pH of the solution, temperature, time available for precipitation/sedimentation), the generation of precipitated gelatin batches with identical molecular weight properties in a reproducible way is difficult (Farrugia and Groves, 1999). Needless to note that different gelatin raw materials will render nanoparticles which vary in size and stability. Therefore, reliable characterization of the molecular weight profile of the desolved gelatin is indispensable. It is well-known that biopolymeric hmw components may be artifact prone, when analyzed by SE-HPLC (due to shear degradation and upper exclusion limitations of the columns). Consequently, variations of separation parameters can have a deep impact on data reproducibility. As illustrated in Fig. 88, decreasing the elution flow volume from 0.7 mL/min to 0.3 mL/min – changing thereby invariably other separation parameters such as sample residence time and system pressure – results in noticeable data change.

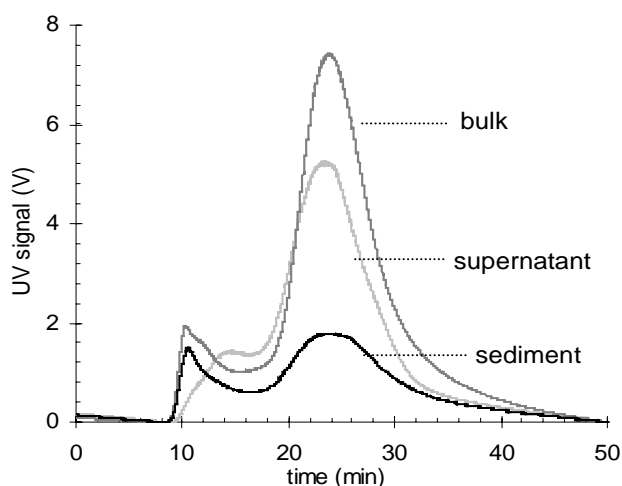


Fig. 88. SE-HPLC analysis of gelatin fractions identical to those illustrated in Fig. 87. Note that the alteration of one separation parameter – i.e., reducing the flow to 0.3 mL/min – has an immense effect on the gelatin elution profile and thus on data concerning hmw ratios.

Maintaining the evaluation criteria applied hitherto – i.e., assigning the first UV_{280} peak to hmw components – leads to a significant reduction of hmw components in all batches, though the order of hmw content remains constant: sediment (24%) > bulk (15%) > supernatant (13%). As the suggested bivalent MW distributions of the batches were verified by analyzing a 100 kDa protein which elutes concomitantly with visualized UV_{280} signal minima at $t=18$ min, the question of the hmw components' whereabouts arises.

Hence, SE-HPLC fractionation conditions have to be selected carefully and should be retained unchanged in order to enable proper comparison of data from experiments performed at different time (Barth et al., 1994). Contrarily, the overall molar mass range of gelatin specimen analyzed by AF4/MALS ranged from about 20 kDa to over 10,000 kDa, outranging maximal molar mass values yielded with SE-HPLC/MALS experiments by more than one order of

magnitude (Fig. 89). Because of low field strengths exerted (5%), the elution profile of the gelatin specimen corresponds to a characteristic molecular weight order without separating individual fractions. Yet, the molecular weight heterogeneity of gelatin is confirmed.

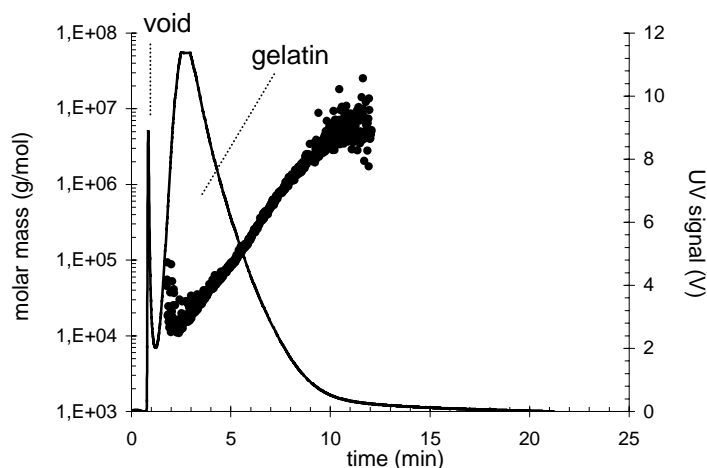


Fig. 89. Analysis of gelatin bulk solution via AF4. Due to a 5% cross flow the gelatin specimen exhibit a characteristic elution profile, with smaller components eluting prior to larger ones. Because of the absence of shear forces, hmw specimen up to molar masses of 10,000 kDa can be detected.

It is to be assumed that the differences in the values of the maximal molar masses are due to minimized sample stress because of the moderate conditions of AF4 experiments – i.e., package material free separation and a 6 bar maximum of hydrostatic pressure within the AF4 systems compared to >20 bar column pressure during SE-HPLC runs. Pertaining to that, it is known that especially hmw polymers in SE-HPLC experiments tend to degradation- advanced by abrasive shear forces exerted by column package material - what may lead to data misinterpretation (Barth et al., 1994). Conversely, because of greatly reduced shear forces, even very shear sensitive proteins can be fractionated via AF4 without running the risk of structural alterations (Li et al., 1997). The results shown above are in good agreement with former studies on molar mass distributions of natural rubbers in microgels, wherein the largest molecules detected via FFF were found to be more than three orders of magnitude greater than indicated by SE-HPLC (White, 1997).

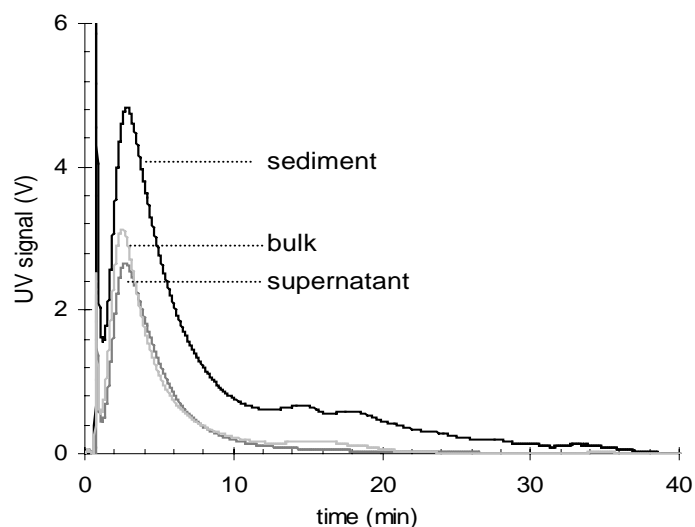


Fig. 90. AF4 fractogram of various gelatin batches. Due to the moderate separation conditions, even a low cross flow exerted (10%) is sufficient to separate hmw components from lmw gelatin in the sediment batch.

Principally, AF4 corroborates the findings of SE-HPLC, as the share of hmw components accumulates in the order gelatin in supernatant < gelatin in bulk < gelatin in sediment. Due to the dimensions of hmw gelatin specimen, the exertion of only 10% cross flow is sufficient to at least double their elution time (Fig. 90). Despite the fact that those components are not separated as individual peaks, the elution profile changes notably, foreshadowing the presence of a substantial hmw fraction mainly in the sediment batch.

The difference of the gelatin batches in their hmw content becomes evident when the samples are exposed to higher cross flow rates (Fig. 91). In case of sediment, 40% initial cross flow is sufficient to separate a hmw fraction revealing minimal molar masses of ~ 450 kDa, accounting for $\sim 27\%$ of total protein. In contrast, supernatant and bulk exhibit lower hmw ratios of 10% and 17%, respectively, thereby backing the purpose of the desolvation step.

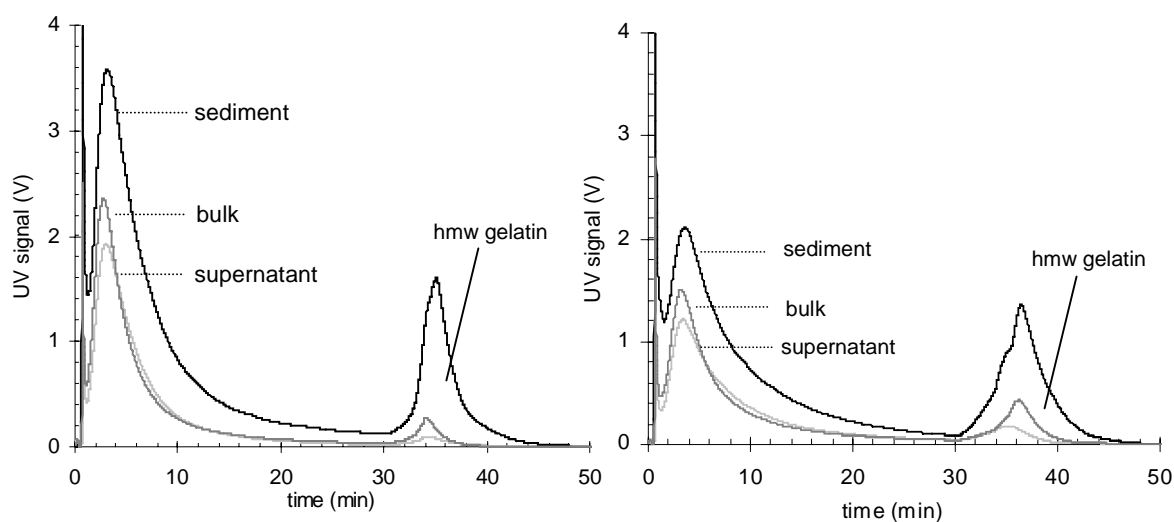


Fig. 91. Separation of hmw fractions of gelatin batches with 40% (left) and 55% cross flow (right). Increasing the AF4 resolution by changing the cross flow intensities did influence data concerning absolute hmw contents. However, the relative proportion of hmw fraction content of the different batches remained constant, affirming the hmw content to increase in the order supernatant < bulk < sediment.

Referring to this, increasing the initial cross flow rates to 55% influenced data solely in absolute way – i.e., the proportions of hmw content of the batches relative to each other remained constant, ascribing the sediment fraction a greater hmw ratio (32%) than bulk (23%) and supernatant (18%). In all AF4 experiments the assessed maximal molar masses of gelatin analytes exceeded those determined via SE-HPLC/MALS, hence indicating the absence of shear forces and reflecting AF4 data veracity. In summary, both SE-HPLC and AF4 proved to be capable of evaluating the efficacy of the acetone desolvation step. Yet, as AF4 separated ultra-hmw gelatin components without running the risk of fostering polymer degradation, AF4 inheres a significant asset compared to SE-HPLC.

8.4 Size determination of unloaded/loaded nanoparticles

Data on nanoparticle size characterization by PCS and zeta-potential measurements are summarized in Table 13. The zeta-potential values of both loaded and unloaded particles indicate the presence of interparticular forces, by this opposing agglomeration tendencies. Emanating from dimensions of ~ 256 nm, the size increase due to plasmid loading is almost negligible. Thereby, the plasmid strands enjoy a great steric freedom, propelling a tight packing of the twisted strands on the particle surface. Furthermore, the remarkably positive zeta potential of unloaded nanoparticles is attracting a diffuse layer of surrounding medium, thus increasing the hydrodynamic layer encasing the particles. Conversely, if the positive surface charge is counterbalanced by negatively charged oligonucleotides, both zeta-potential and thickness of the surrounding diffuse medium layer are decreased, resulting in reduced hydrodynamic diameters determined by PCS (Mueller, 1996).

nanoparticles	unloaded	loaded
size (nm; via PCS)	256 ± 1.80	269 ± 7.37
PI (polydispersity index)	0.028 ± 0.012	0.062 ± 0.038
zeta-potential (mV)	+ 42	+ 29
size (nm, estimated via SEM)	150 - 300	150-300
R_{rms} (nm, via MALS)	60 - 98	68 - 105
size (nm, calc. from R_{rms})	155 - 253	175 - 271

Table 13. Nanoparticle characterization by PCS, SEM and MALS. Note that data derived by PCS is *prima facie* inconsistent with SEM and MALS data, respectively.

SEM images of loaded nanoparticles substantiate this theory, unveiling the surface of the spherical nanoparticles to be smooth and unruffled (Fig. 92).

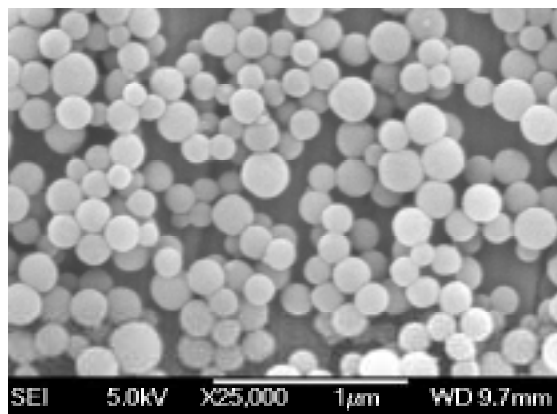


Fig. 92. SEM picture of plasmid loaded nanoparticles, revealing a broad nanoparticle size distribution, as smaller (~ 150 nm) and larger (~ 300 nm) particles are detectable in random quantities.

In contrast to the unimodal size distributions suggested by PCS, SEM analysis – demonstrating smaller and larger nanoparticles to be present at random - provides reason to

critically reconsider PCS data: whereas SEM reveals particle dimensions to encompass 150 – 300 nm, PCS assigns nanoparticle sizes of ~256 nm (unloaded) and 269 nm (loaded), respectively.

Of course, one explanation for the differences can be ascribed to the underlying principles of both methods, exemplified earlier with synthetic polymer-based nanoparticles (Hoffmann et al., 1997; Finsy et al., 1992): the contrast of SEM pictures allows only the visualization of the nanoparticle core – conversely, PCS assesses the hydrodynamic radius of analytes. Anyway, due to the data inconsistency of SEM with PCS, a demand for accessorial sizing techniques appears on the analytical agenda.

Generally, if AF4 experiments aim at providing great resolution, to apply high cross flow intensities is considered to be state-of-the-art (Coelfen and Antonietti, 2000). But great cross flow rates may cause the sample concentration at the ultrafiltration membrane to increase and thereby the risk of inducing artifacts via sample-sample and sample-membrane interactions is growing. Hence, to approach optimal separation conditions by primarily low retention levels and to increase the resolution subsequently run-by-run can be an appropriate procedure in the characterization of ultra-hmw components (Wittgren and Wahlund, 1997) (Fig. 93).

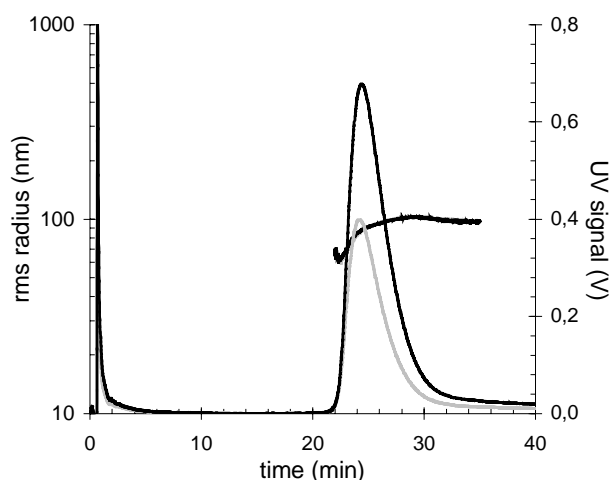


Fig. 93. AF4/MALS analysis of unloaded gelatin nanoparticles. A difference in sample loads - 0.5 mg/mL (grey line) and 0.9 mg/mL (black line), respectively – did not influence the determined sizes, demonstrated by absolute identical size distribution profiles. Substantial void peaks are due to low initial cross flow rates of 20%.

As a consequence, cross flow intensities were increased run by run in 5% intervals, and conditions of initial 20% cross flow rates – which were maintained for 10 min prior to programmed decrease – revealed both the drawback of notable void peaks and the asset of sufficient nanoparticle resolution. Pertaining to that, size distributions of unloaded nanoparticles were determined to span a 155-253 nm hydrodynamic diameter range. In this regard, dimensions yielded by MALS are first to be expressed as root mean square (rms) radii, often referred to as radii of gyration (R_G). However, R_G values can easily be transferred to values expressed as hydrodynamic diameters – e.g., assessed by PCS – via extracting the root of $20/3 (R_G)^2$. Fortunately, raising the injected sample mass by a factor of 1.8 (from 0.5 mg/mL to 0.9 mg/mL) resulted in a commensurate increase in AUC_{UV280} values (from 1.56 to 2.80), did not affect size distribution data and had no effect on the resolution power, hence fostering MALS data veracity. This is the more important, as the polydispersity of hmw specimen such as ethylhydroxyethyl

cellulose was shown to be constantly underestimated, if the resolution of the AF4 system is insufficient (Andersson et al., 2001). The dependency of nanoparticle elution profiles on even slight cross flow modifications is illustrated in Fig. 94.

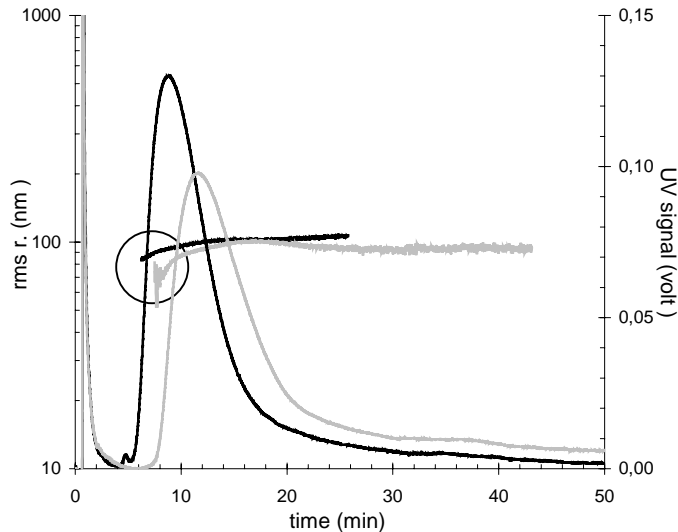


Fig. 94. Characterization of plasmid loaded nanoparticles using 5% cross flow (black line) and 10% cross flow (grey line). Differences in resolution power induced MALS to yield variations in determined sizes, despite samples are identical (highlighted by circle).

Obviously, the exertion of 5% cross flow intensities is insufficient for the accurate measurement of nanoparticle size distributions, as the sample components elute not in total accordance with their size: nanoparticles inhering smallest dimensions elute contemporarily with larger nanoparticles right at the beginning of the elution process. Consequently, the MALS signal of the smallest nanoparticles is superimposed by the signal of larger nanoparticles and, sequentially, MALS averages the dimensions of both eluting fractions to a mean radius of 80 nm. Due to the insufficient resolution at 5% cross flow conditions, nanoparticle aggregation phenomena can not be circumvented. If 10% cross flow rates are applied, the resolution is sufficient to achieve an elution order in strict accordance with particle sizes. Now the MALS signal of the smallest nanoparticles is not superimposed, and the radii of the nanoparticles which elute first are calculated to be 68 nm.

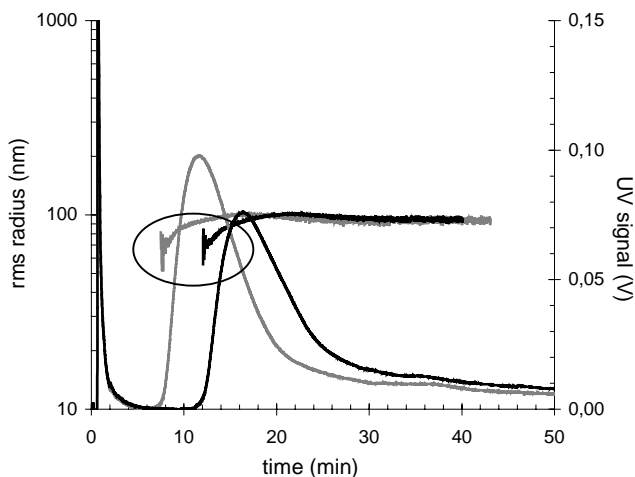


Fig. 95. Characterization of plasmid loaded nanoparticles using 10% cross flow (grey line) and 15% cross flow (black line). Due to sufficient resolution, increasing field strengths do not facilitate MALS to yield different data on size distributions (highlighted by circle).

In order to control, if 10% cross flow rates really provide sufficient resolution, the field strength was increased to a 15% level, what led to a further delay of the nanoparticle elution profile (Fig. 95). However, as far as the calculated nanoparticle size distributions are concerned, there is no data difference, regardless if 10% or 15% field strength is applied. In both cases, the distribution of the nanoparticle radii is calculated to span 68 – 105 nm. Hence, any possibility of latent data ambiguity is eliminated and the separation conditions are considered to be proper, because otherwise, cross flow modulations should influence the calculated size distributions.

In summary, MALS clearly substantiates SEM data: from both analytical techniques, a broad particle size distribution within a diameter range of 150 – 300 nm can be concluded. Thus, PCS data – suggesting unimodal size distributions and being *prima facie* inconsistent with SEM data – is to be scrutinized when used in nanoparticle characterization.

8.5 Determination of nanoparticle loading efficacy via AF4

Hitherto, assessing drug loading efficacy of colloidal drug carriers like gelatin nanoparticles is a time consuming and somewhat tedious procedure. After incubation of drug carrier and designated payload the samples are subjected to several washing and centrifugation steps. Subsequently, the unbound payload share – e.g., plasmid or a designed oligonucleotide – is determined UV spectrophotometrically in the supernatants (Prbha et al., 2002). However, this *modus operandi* is delicate. If the force of gravity exerted upon the sample is too intense, the nanoparticles may be destructed or aggregate, thus opposing proper redispersing. On the other hand, a too gentle centrifugation would inevitably give rise to the possibility of not removing the nanoparticles from the supernatant quantitatively. Generally, the risk of DNA degradation is to be avoided, as fragmentation of DNA is deemed to affect the transfectivity of loaded nanoparticles (Walter et al., 1999).

In this concern, the wide applicability of AF4 provides the prospect of an alternative way to assess loading efficacy. Being capable of separating entities like plasmids, DNA or dissolved drugs from undissolved drug carriers, AF4 may allow almost real-time analysis of sample concentrations in the incubation container. Ideally, after incubation the AUC_{UV} decrease of the DNA fraction designated for loading should comply with the AUC_{UV} increase of the (then loaded) nanoparticles. Consequently, the difference in signal intensities of unloaded and loaded nanoparticles is considered to be due to drug payload. Whereas AF4 was shown to be able to characterize nanoparticles qualitatively – i.e., to assess size and size distributions - the quantification of nanoparticle concentration in reproducible way is a precedent condition for the monitoring of the nanoparticle loading step.

As outlined in Fig. 96, the correlation of nanoparticle concentration with assessed AUC_{UV} values can be performed with AF4 in a reproducible way – i.e., the quantification of

nanocolloidal drug carriers is manageable. This is not to be taken for granted, considering a variety of pitfalls described in the literature associated with the AF4 analysis of samples inhering dimensions of ~ 100 nm.

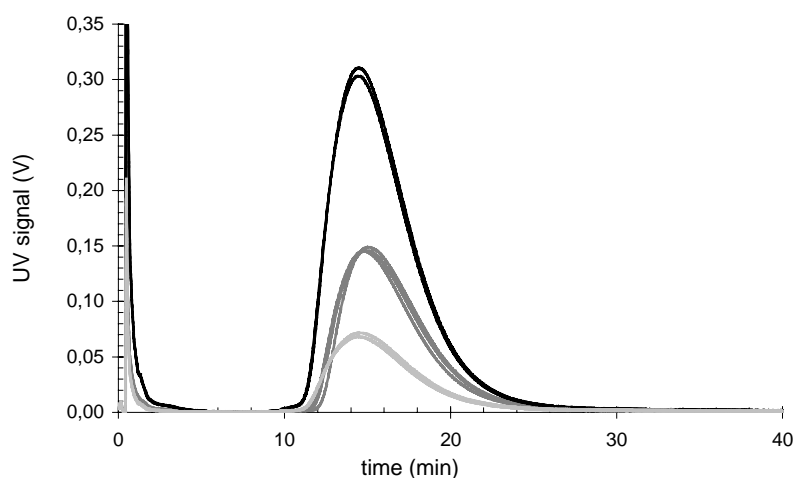


Fig. 96. Quantification of nanoparticle concentration via AF4/UV₂₈₀ (experiments performed in triplicate). The assessed AUC_{UV} values were in sound agreement with the individual sample concentrations: 476 ng/mL – AUC 1.966
238 ng/mL – AUC 0.901
119 ng/mL – AUC 0.459

E.g., the characterization of polyorganosiloxane nanoparticles in aqueous dispersion by AF4 was shown to involve void peaks accounting for $>50\%$ of total UV detector signals (Jungmann et al., 2001). Similarly, the AF4 analysis of Janus micelles – which exhibited dimensions of 40 – 250 nm – was coming along with comparable problems: probably due to a notable sample loss obligatory with both challenging application and arranged separation parameters, the sample recovery was “assumed to be 100%” - but was not verified - to enable weight-average molar mass determination via MALS (Erhardt et al., 2003). In the course of monitoring nanoparticle loading efficacy, conditions such those prevailing in both examples outlined above would prohibit accurate analyte quantification.

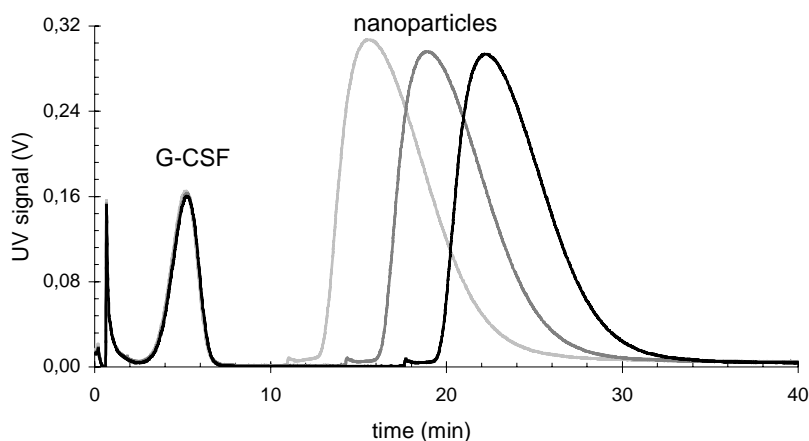


Fig. 97. Separation of G-CSF (~ 20 kDa) from nanoparticles applying a decay of initial 20% cross flow to 1% after 13 min (pale line), 16.3 min (grey line) and 19.7 min (black line), respectively.

The task of separating nanoparticles from unbound DNA drug load was approached by surrogate experiments, e.g., the fractionation of nanoparticle-protein mixtures. Therefore, G-CSF as a model compound (~ 20 kDa) was added to nanoparticle batches and the influence of cross flow variations on the nanoparticle elution pattern was investigated (Fig. 97).

According to the underlying principles of AF4, G-CSF elutes prior to the nanoparticles. Furthermore, the protein is separated from the drug carrier in base-line quality. Of course, variations in field strength also render a modified elution profile of protein possible, giving analytical leeway if a change in sample elution pattern were desired (Fig. 98).

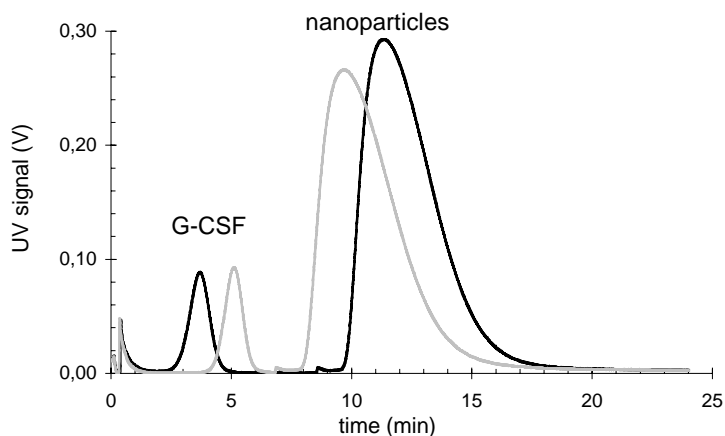


Fig. 98. The possibility to program cross flow intensities in desired way provides a great flexibility in assessing sample elution profiles: initial 30% cross flow conditions (black line) force G-CSF to elute earlier than 50% field strengths (grey line).

This flexibility of AF4 separation parameters is an essential prerequisite for both accurate sample quantification and size determination because superimposing of UV or MALS detector signals would inevitably lead to assessing incorrect concentrations or size distributions.

In case of the fractionation of an oligonucleotide (5.4 kDa) from nanoparticles, the attention is directed towards a sufficient separation of void peak and oligonucleotide (Fig. 99).

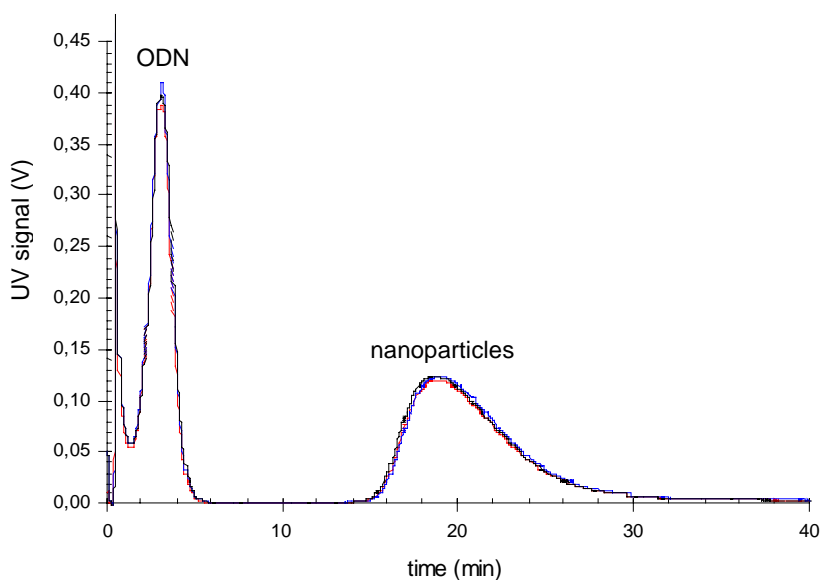


Fig. 99. Fractionation of a sample containing oligonucleotide (ODN, 5.4 kDa) and nanoparticles. The swapping of the depicted three individual fractograms indicates a reproducible manner of quantification ($S_{rel} < 0.3$).

Principally, small analytes tend to elute out of the channel early, adjacent to the void peak. The base-line separation of void peak and low molecular weight samples by exerting intense field strengths is common practice. However, the commitment to eliminate the void peak usually demands AF4 operation conditions which assist potential (irreversible) adhesion phenomena, such as intense focusing or high initial cross flow modes. Hence, providing data on void peak intensity is a must

and considered a cachet, if sample quantification is intended – in contrast to situations where nanoparticle characterization is a priori reduced to qualitative terms (Lao et al., 2002).

At optimal conditions, even demanding separation tasks can be successfully approached, thereby maintaining due distances between each component peak (Fig. 100).

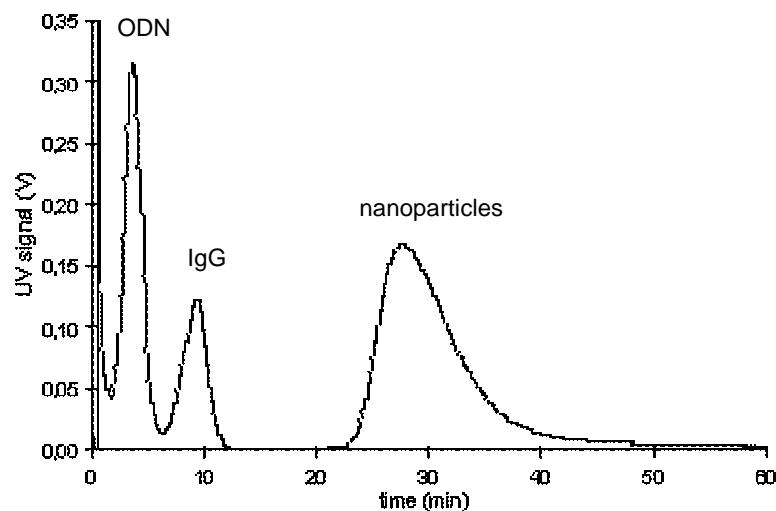


Fig. 100. Exemplifying the broad AF4 application range in the field of nanoparticles by a challenging separation task: oligonucleotides (ODN; 5.4 kDa), immunoglobuline (IgG, 150 kDa) and nanoparticles are fractionated within 50 min.

Providing sufficient resolution in order to reproducibly separate oligonucleotides, immunoglobulins and nanoparticles within one single run, AF4 system parameters may be considered to guarantee an accurate monitoring of nanoparticle loading with plasmid DNA.

Prior to the incubation step, the amount of DNA designated for nanoparticle payload was assessed via AF4. Likewise, unloaded – but surface modified – gelatin nanoparticles were quantified and both components were subjected to incubation. Subsequently, the incubation batch was analyzed using conditions equally to those yielding elution profiles as illustrated in Fig. 99. The fractograms of the particular AF4 separations are visualized in Fig. 101.

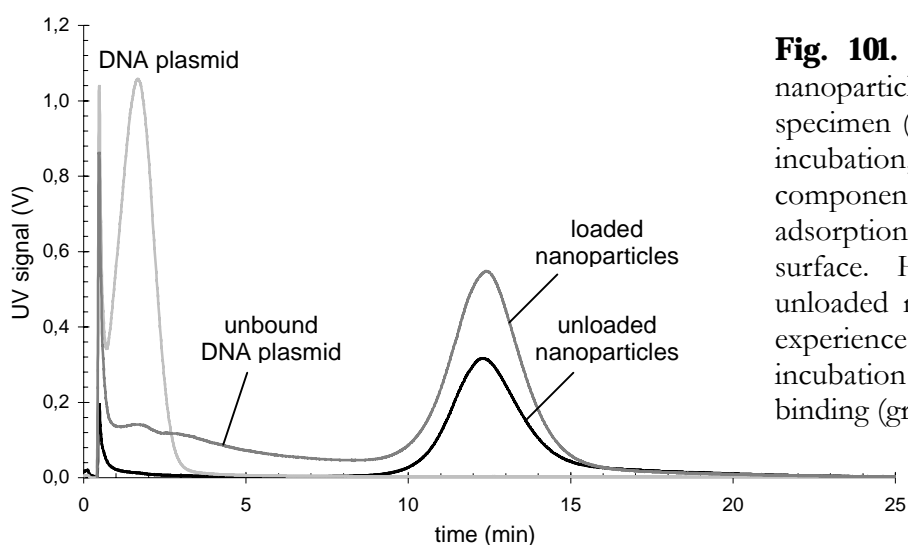


Fig. 101. Fractograms illustrating nanoparticle loading with DNA specimen (pale line). Subsequent to incubation, the AUC_{UV} of the DNA component decreases due to adsorption upon the nanoparticle surface. Hence, the AUC_{UV} of unloaded nanoparticles (black line) experiences a gain after the incubation step due to DNA binding (grey line).

According to Fig. 101, the extensive signal of the DNA plasmid yielded prior to the incubation is downsized – because of binding on nanoparticles - to a humble fraction of

remaining unbound plasmid. Conversely, the nanoparticle UV signal intensity is increased commensurately. Since the AUC values can be transferred to masses of nanoparticles and plasmid, respectively, the loading efficacy can conveniently be determined (Table 14).

	prior to incubation/loading process			after incubation/loading process			
	DNA	nanoparticles	total	unbound DNA	nanoparticles + DNA	DNA load thereof	total
AUC _{UV}	1.536	0.981	2.517	0.797	1.691	0.739	2.488
mass (μg)	20	1000	1020	10.38	1009.62	9.62	1020
AUC _{UV}	1.602	0.996	2.598	0.850	1.807	0.752	2.657
mass (μg)	20	1000	1020	10.61	1009.39	9.39	1020

Table 14. Monitoring of two nanoparticle DNA loading processes with AF4/UV.

The efficacy of two nanoparticle loading processes was assessed by AF4 to be ~50%, as 9.62 μg and 9.39 μg, respectively, out of 20 μg DNA available were bound. Given the possibility of characterizing and quantifying DNA and nanoparticles in one single run, two further reasonable applications arise: monitoring of nanoparticle stability and durability of drug load. During long-term storage, size and size distribution of nanoparticles may alter, and both parameters can conveniently be evaluated by AF4/MALS. On the other hand, bound DNA may detach from the nanoparticle surface during storage, thereby reducing the amount of drug load. In this case, unbound DNA will be accessible to AF4 quantification via inducing a individual peak in the fractogram. Conversely, the nanoparticle UV signal intensity is to be decreased by a commensurate degree.

8.6 Summary

The persisting impediments in efficient delivery of DNA with non-viral vectors can be attributed to three factors: (1) poor in vitro/in vivo correlation, (2) non-decomplexation of (plasmid) DNA from the carrier, (3) and the lack of physico-chemical characterization of formulations (Hussain et al., 2003). If the issue of DNA loaded nanoparticles is indeed relapsing due to the first factor may be deemed a matter of opinion. How to overcome the second is topic of extensive research and approached via adsorption and encapsulation of DNA upon/within nanoparticles (Singh et al., 2000). Contrarily, research on nanoparticle characterization was forced to take a back seat, since methods such as PCS and electron microscopy are considered to be well established – although data are often contradictory.

In this concern, the aim of this chapter was to demonstrate the ability of AF4 to provide an overall characterization of gelatin nanoparticles, from gelatin bulk material analysis to monitoring of nanoparticle drug loading processes.

It was shown that gelatin bulk material can be analyzed by AF4/MALS without inducing artifacts. Bearing in mind the contribution of hmw components to gelatin nanoparticle stability, the feature of AF4 to analyze hmw gelatin without inducing shear degradation is deemed a crucial parameter in evaluating bulk preparation efficacy by desolvation steps. Pertaining to that, SE-HPLC was demonstrated to yield similar results as far as the order of hmw ratios in different gelatin batches is concerned. However, MALS proved the hmw gelatin specimen to be abraded during SE-HPLC analysis. As this phenomenon detracts from data veracity – and thus from accurate bulk evaluation – AF4 is considered to be more suitable in gelatin bulk material assessment. Against the background of (hmw) polymer-based drug delivery systems, the AF4 application performed is of great value to upgrade the spectrum of analytical tools in pharmaceuticals (Langer, 1998).

For the first time, the determination of size and size distribution of gelatin nanoparticles by means of AF4/MALS was performed. Loaded and unloaded nanoparticles were characterized and the data was put into correlation with PCS and SEM results. Because MALS is able to size nanoparticles subsequent to AF4 separation, data accuracy is superior to PCS measurements, where the underlying principles force the samples to be characterized in the whole batch (Wyatt, 1998). On the other hand, SEM is reliant on sample preparation. In conclusion, AF4 was shown to assess nanoparticle size with high confidence. Thus, data derived from other techniques and being *prima facie* inconsistent with each other – e.g., PCS versus SEM - merge into a coherent picture.

This AF4 application was developed further to render a new way of monitoring the drug loading process of nanoparticles possible. AF4 separation parameters were established which enable the separation of colloidal drug carriers and the designated drug load simultaneously in one single run. Moreover, the reproducibility of AF4 in nanoparticle quantification was satisfactorily shown. Based thereon, the amount of DNA binding on the colloidal carrier was quantified aside unbound DNA remaining in the incubation container. It is to be outlined that AF4 is capable to determine the efficacy of nanoparticle drug loading without precedent sample preparation essential in prevalently applied methods (e.g., centrifugation and redispersing).

The suitability of AF4 to conveniently monitor stability of colloidal drug carriers and decomplexation of DNA during storage is additionally valorizing the developed application.

9 Particulate matter in parenterals: a case study

9.1 Introduction

The control of key features of a product and the respective manufacturing processes are essential to quality assurance. With parenteral formulations, important variables influencing product quality are often discussed in absolute terms. While dealing in absolute yes/no statements may be philosophically satisfying, this practice can not accommodate all real world scientific problems – among those are problems of sterility and particle contamination associated with the mass production of parenterals (Knapp, J. Z., 1998). Referring to the latter, particulate matter may be described as insoluble material inevitably present in injectable solutions (Groves, 1991). It is prevalently known that any recipient of parenteral medication such as infusion will receive a significant particle load encountered therein. In the case of infusions, this load was estimated to potentially encompass many thousand individual particles in μm range (Puntis et al., 1992).

In case the particle load contains visible specimen the formulation is to be rejected, since it is not acceptable to hazard the consequences of vascular occlusions subsequent to intravenous application. Pertaining to subvisible particulate matter, there is little evidence of clinically deleterious effects. Nevertheless, studies have identified the presence of particles originating from parenterals in lung tissue, lymph nodes and liver, causing granulomas and inflammatory responses. Additionally, investigations in neonates also have unveiled potentially serious effects linked to particles originating from infusions (Allwood, 2000).

Whereas the absence of visible particulate matter in parenterals is generally considered as a must, the presence of subvisible particulate matter is permitted within narrow margins. Yet, the stated upper limitations in particle size and numbers as well as designated analytical methods for particle characterization vary within the national pharmacopeias (e.g., USP, Ph. Eur., Japanese Pharmacopeia). One reason therefore may be the lack of global harmonization of the results of particle analysis. E.g., there is no commonly accepted framework for the definition or analysis of the outcome of a manual inspection for visible particles (Knapp, 1998).

In this realm, the control of particle contamination in injectable products is a two-fold problem for the pharmaceutical industry, and both issues appear to necessarily conflict with each other: (a) the provision of a contamination-free product at (b) economic costs acceptable to the user. Nowadays, processing conditions for parenteral solutions are designed to substantially minimize the absolute dimensions of particulate components present in the formulation down to $\sim 0.1 \mu\text{m}$. Generally, there are strong recommendations that terminal in-line filtration is deemed best practice, especially for large volume parenterals (Allwood, 1998).

Basically, the source of particulate matter is manifold: packaging material, manufacturing variables such as filters, air flow, equipment and housekeeping procedures as well as the active drug and excipients pose possible sources of particle contamination (Borchert et al., 1986). However, a constant threat to particle-freedom is in conjunction with the main dogma guaranteeing general safety of parenterals: product sterility achieved via sterilization. Unfortunately, the effects of sterilization are two-edged: although glass and metal can withstand the temperatures exerted during heat sterilization (~ 170 °C in case of dry heat and ~ 120 °C with moist heat), there are relatively few “engineering” type plastics and a limited number of rubbers which retain satisfactorily physical properties and, hence, do not facilitate particle contamination (Frampton and Dean, 2000). Additionally, the parenteral product per se may experience a deleterious effect due to sterilization. E.g., bottled dextran solutions for clinical use were reported to be prone to severe insoluble particle formation during sterilization (Veljkovic et al., 1989). Contrarily, protein formulations in primary containers are generally not amenable to sterilization due to their proneness to thermally induced denaturation. As a consequence, package material is to be sterilized prior to filling the sterile filtrated product into the prime container.

In terms of visible particles, quantification is commonly performed via human visual inspection, though mechanic inspection systems - basing on the autoscanning and evaluation of video/camera images – are available (Knapp, 1986). Subvisible particle quantification is approached via microscopic methods, light scattering, Coulter technique, light obscuration and holographic techniques. Similarly, a broad variety of methods is implemented for particulate matter identification, ranging from standard techniques like chromatography, atomic spectroscopy and molecular spectroscopy (e.g., Raman spectroscopy, mass spectrometry) to advanced techniques such as x-ray energy dispersive spectroscopy (Allwood et al., 1998).

In summary, it is noteworthy that despite the variegated spectrum of analytical techniques applied, the final parenteral product quality depends on product quality prior to inspection and the parameters of the inspection process, respectively (Knapp, 1998).

9.2 Background

A pharmaceutical G₁ antibody was formulated in phosphate buffered medium at pH 5.2 (50 mg/mL, 0.8 mL, 2R glass vials). At that time, the protein solution was proved to be free of visible and subvisible particulate matter and conformed to appendant specifications of protein stability, the latter assessed by protein activity assay, SE-HPLC and ion exchange chromatography (IEX). During long-time storage over 12 months at 5 °C within one production lot – encompassing several thousand vials – a visible component emerged in some vials at random after arbitrary storage time. Due to the peculiar feature of that particulate specimen to ostensibly vanish/dissolve during moderate vial shaking, the problem of how to seize the

particles analytically emerged. In this regard, the question of particle origin is of crucial importance. Given the background that – in accordance with empirical knowledge of many pharmaceutical formulators - the development of particulate matter during storage in protein parenterals in many cases is to be ascribed to insufficient protein drug stability, the analytical investigation primarily focused on parameters concerning immunoglobulin stability (Wang, 1999). The more, as the shelf life generally required for economic viability of a typical protein pharmaceutical product is considered to be 18-24 months (Cleland et al., 1993).

It is the aim of this chapter to present a case study of a parenteral product, wherein analytical challenges – though of daunting nature – were approached, combining state-of-the-art methods like light obscuration, SE-HPLC and PAGE with (relatively) new methods such as AF4, MALS and ultra-sensitive microcalorimetry. Various data – even if at first glance inconsistent with each other – are inter-related in order to add up to a final conclusion concerning particulate matter origin.

9.3 Providing evidence of particulate matter

Subjecting numerous (>100) vials to visual inspection revealed the presence of whitish particle specimen accumulating at the center of the container bottoms. Bringing the vial volume into turbulence by a single limp-wristed agitation, a fine particulate haze spiraled and was visible for several seconds before the particles seemed to vanish and to re-dissolve. The particles causing that haze appeared to be crystalline in nature and exhibited maximal dimensions of approximately 100 μm . Analysis by light microscopy substantiated the crystalline impression (Fig. 102).

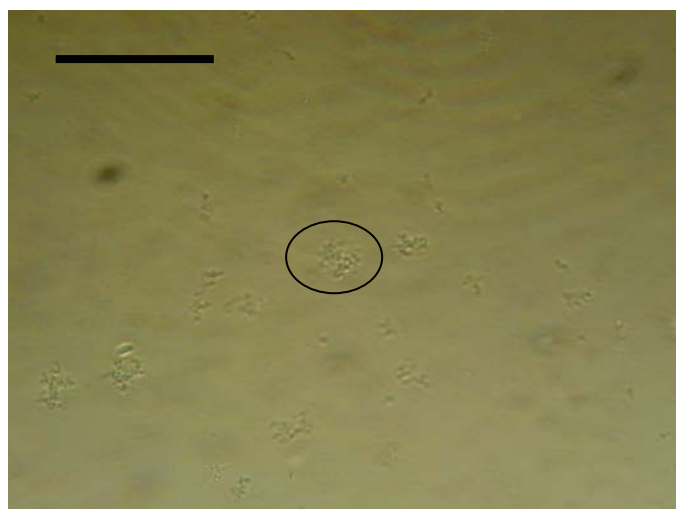


Fig. 102. Light microscopic analysis of a vial volume revealing visible particulate matter, highlighted by black circle (scale bar represents 100 μm).

In case the moderate manual agitation step was repeated, no particles were visible. Conversely, vial shaking had no notable impact on the data of light microscopy (Fig. 103). Whereas subsequent short-time storage of the vials did not result in visible particle recovery,

storage for 6 months at 5 °C enabled the particles in most cases (>80%) to regain visible dimensions exceeding ~50 µm.

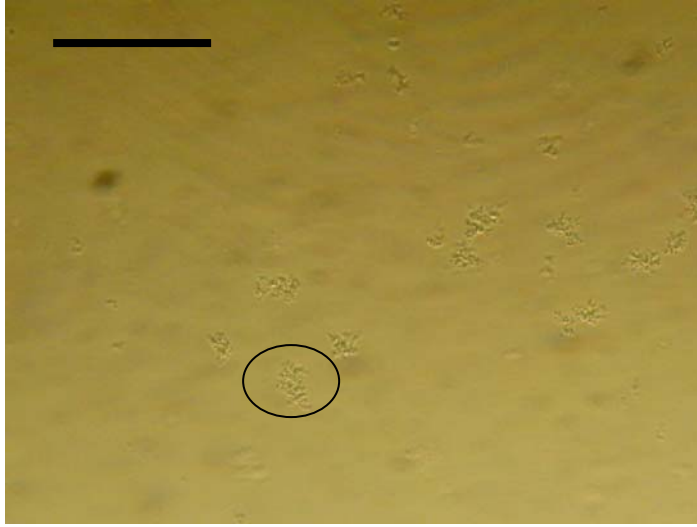


Fig. 103. After manual vial shaking no visible components were to be detected by visual inspection. Nevertheless, analysis by light microscopy verified the presence of particulate matter (highlighted by black circle) in the two-digit µm range (scale bar represents 100 µm).

Although the visible inspection of parenterals renders definite yes/no statements in respect of visible particulate matter contamination, these data are subjective values and not to be expressed in absolute quantitative terms. Furthermore, one should be aware that consistent levels of visible particulate matter does not mandatorily imply consistent quality since the origin of visible and subvisible particles can vary (Knapp, 1986). Almost without exception the detection of visible specimen in parenterals is associated with the presence of subvisible components – the turnaround-statement, however, is not valid. Pertaining to that, the analysis of subvisible particulate matter in parenterals by light obscuration is well-established (Boom et al., 2000; Backhouse et al., 1987).

In order to verify the findings above – i.e., shear stress leads to a reduction of particle size, but does not relieve the particle contamination per se – the vials were subjected to light obscuration analysis (SVSS-C⁴⁰, PAMAS GmbH, Rutesheim, Germany) (Table 15).

number of particles per mL with dimensions of	vials revealing visible particulate matter (no shear stress)	vials revealing visible particulate matter (shear stress via shaking)	vials without visible particulate matter
≥1 µm	137,592	159,717	18,279
≥2 µm	44,389	42,321	8,731
≥10 µm	123	105	291

Table 15. Light obscuration analysis of immunoglobulin solutions (n=9, $S_{rel} < 1.6$; data in cumulative presentation). Note that shear stress has only a humble impact on particle numbers.

According to Table 15, the findings of visible inspection are corroborated: vials exhibiting visible particles contain a considerably greater number of particles with dimensions beyond 1 µm and 2 µm, respectively, than vials without a visible component. Thereby, the exertion of shear

stress via shaking has virtually no impact on the data, i.e., the extent of particle contamination remains constant. Nevertheless, the results are consistent with the outcome of visual and microscopic inspection, inasmuch as shaking induces larger particulate entities – i.e., greater than 2 μm – to disintegrate into smaller particles. Consequently, the number of particles $\geq 1 \mu\text{m}$ increases. It is not to be expected that vial volumes without a visible fraction contain more particles $\geq 10 \mu\text{m}$ than the contaminated batches. Anyway, the discrepancies are too minute to draw an unambiguous deduction. Interestingly, the assessed particle levels are sufficiently low in order not to contravene regulatory standards.

In summary, the precarious issue of the whereabouts of visible particulate matter subsequent to shear stress was clarified: visible particulate specimen disintegrate into smaller entities and are amenable to analytics via light microscopy and light obscuration.

Basically, the size and structure of visible protein entities – i.e., protein precipitates following precipitation, aggregate growth and ageing - in agitated volumes is dependent on the exerted shear (Byrne et al., 2002). In that realm, when protein particles were demonstrated to disappear when subjected to shear stress. It was hypothesized that - once formed - aggregates reach a sufficiently large size, agitation leads to shear induced particle breakage or erosion, which in regimes where particles are smaller than turbulent microscale impellers occurs mainly as a result of fluid-induced stresses (Spicer et al., 1996). In general, the principal reversibility of the formation of protein precipitates back to native state protein is well-documented in the scientific literature (De Young et al., 1993) - and can arrestingly be demonstrated in any laboratory by adding 10 mL acetonitrile to albumin solution (10 mg in 10 mL) and redissolving the generated protein precipitates by adding 10 mL of water. On the other hand, it is known that precipitates of inorganic material such as buffer components or additives are – once formed – highly unlikely to redissolve (FDA, 1994). As a consequence, the information above may facilitate to hypothesize a tendency of the particle origin to be not proteinic.

9.4 Investigations by SE-HPLC and SDS-PAGE

Since the development of particulate matter in solutions as a consequence of protein aggregation is a frequently encountered problem during shelf life studies, manifold analytical methods have been applied in order to elucidate that issue. Two techniques turn out to enjoy a great acceptance, i.e., SE-HPLC and PAGE (Fletcher et al., 1992). Both methods enable the analysis of aggregation and, thus, provide data for clarification of protein precipitates' origin. It is to be outlined that protein aggregation in solution will not necessarily lead to precipitation, as the presence of insoluble aggregates will depend largely on the solubilizing properties of the solvent and the nature of the aggregates formed (Charman et al., 1993).

Consequently, vials revealing no visible particles were subjected to SE-HPLC/MALS analysis to assess the presence of soluble aggregates (Superose 6HR 10/30, Pharmacia, Germany; elution medium PBS pH 7.5, flow 0.5 mL/min) (Fig. 104).

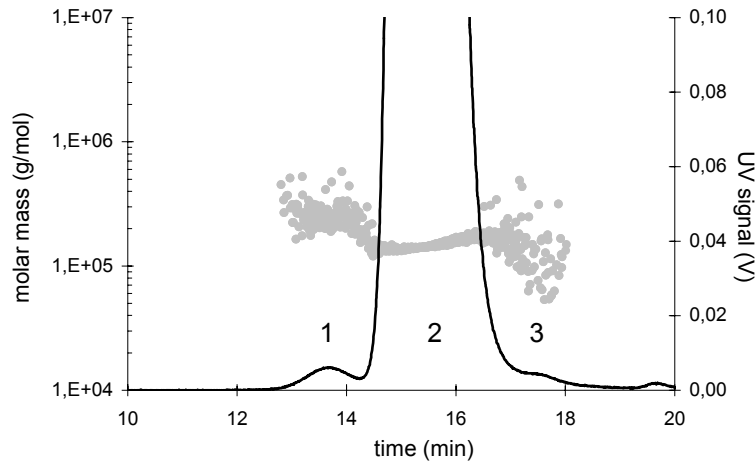


Fig. 104. Analysis of vial volumes without visible particulate matter via SE-HPLC/MALS/UV₂₈₀. Besides monomers (2), remote aggregate (1) and fragment fractions (3) were detected. Assessed MW values were ~150 kDa for the monomers and ~302 kDa for the aggregates, indicating dimers to be the main aggregate specimen.

As illustrated in Fig. 104, vial volumes free of visible specimen exhibited a marginal aggregate fraction (<0.5%). According to MALS, the aggregates are attributed molar masses of ~302 kDa, pointing out the presence of dimer and the absence of higher-order aggregates. Referring to that, the sensitivity of light scattering in terms of detecting even smallest amounts of (hmv) aggregate specimen is known (Wyatt, 1998). In case the visible particulate matter is due to protein aggregation, vials revealing a visible component are expected to differ from inconspicuous vials in aggregate content (Fig. 105).

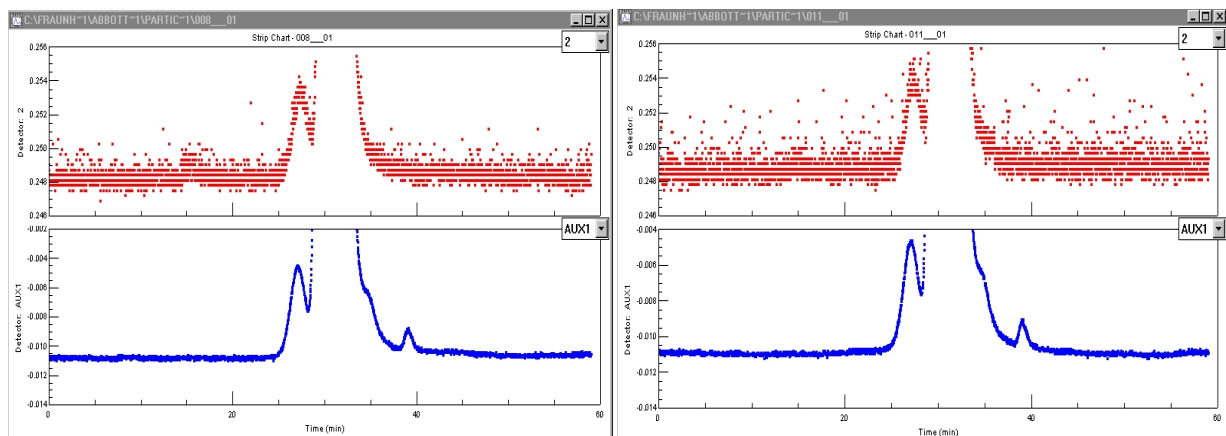


Fig. 105. Comparison of vial volumes with (left) and without (right) visible particles. Note that both samples appear absolute identical according to MALS_{90°} (■) and UV₂₈₀ signals (---).

Because the samples analyzed by SE-HPLC exhibited no discrepancies in MALS and UV₂₈₀ detection, regardless of the findings of visual inspection, a relation of the presence of visible particles with protein instability phenomena is deemed unlikely – the more, as the samples

were not subjected to processes such as filtration or centrifugation prior to analysis. Data of a more comprehensive investigation by means of SE-HPLC are listed in Table 16.

sample	aggregate (%)	monomer (%)
experiment a: vial volume with visible particles	0.440	99.560
---- vial volume without visible particles	0.439	99.561
experiment b: vial volume with visible particles	0.437	99.563
---- vial volume without visible particles	0.436	99.564

Table 16. Data on monomer and aggregate content of various vial volumes, derived by SE-HPLC/UV₂₈₀ experiments (for all data n=3, S_{rel} < 1.1, no sample preparation performed).

Assessing the aggregate content of vials with/without visible particulate matter resulted in identical data. Given the background that the presence of particulate matter had no impact on the values of AUC_{UV280} detection, according to SE-HPLC analysis the particle formation in immunoglobulin solutions is hardly to be put down to protein instability.

On the other hand, case studies were reported where protein solutions underwent severe protein precipitation that was not reflected in a notable increase in soluble aggregates. E.g., G-CSF solutions were shown to develop precipitates though the ratio of soluble aggregates – mainly dimer - remained constant and did not exceed 3% of total protein, according to SE-HPLC data (Bartkowski et al., 2002). It may be hypothesized that lmw aggregates (dimer, trimer, etc.) inhere immense reactivity and undergo further aggregation either between themselves or with monomer specimen. As a consequence, their steady-state concentrations will remain low and SE-HPLC will solely detect a slight decrease in monomer concentration, if any. In the long run, a corresponding gain in hmw aggregates may result in visible particle formation. That even minimal amounts - <0.1% of total protein, depending on the concentration - of insoluble aggregates can cause turbidity and visible particle contamination, matches those phenomena (Hoffmann, 2000). Additionally, small quantities of low soluble aggregates can render the formation of protein crystals as defects (Bondos et al., 2000).

The fact that HPLC analysis yields no results on hmw aggregates does not imply PAGE to fail in detecting those specimen, too. Recent investigations demonstrated SDS-PAGE to be successfully applied in the retrieval of hmw protein specimen (Bondos and Bicknell, 2003). Insoluble protein aggregates are considered to immobilize within the pockets of the gel beds during analysis and to be still amenable to subsequent staining processes. Results of SDS-PAGE analysis of various vial volumes are presented in Fig. 106 (Laemmli method, NU-PAGE 10% Bis-Tris-Gel, colloidal blue staining, Invitrogen GmbH, Karlsruhe, Germany).

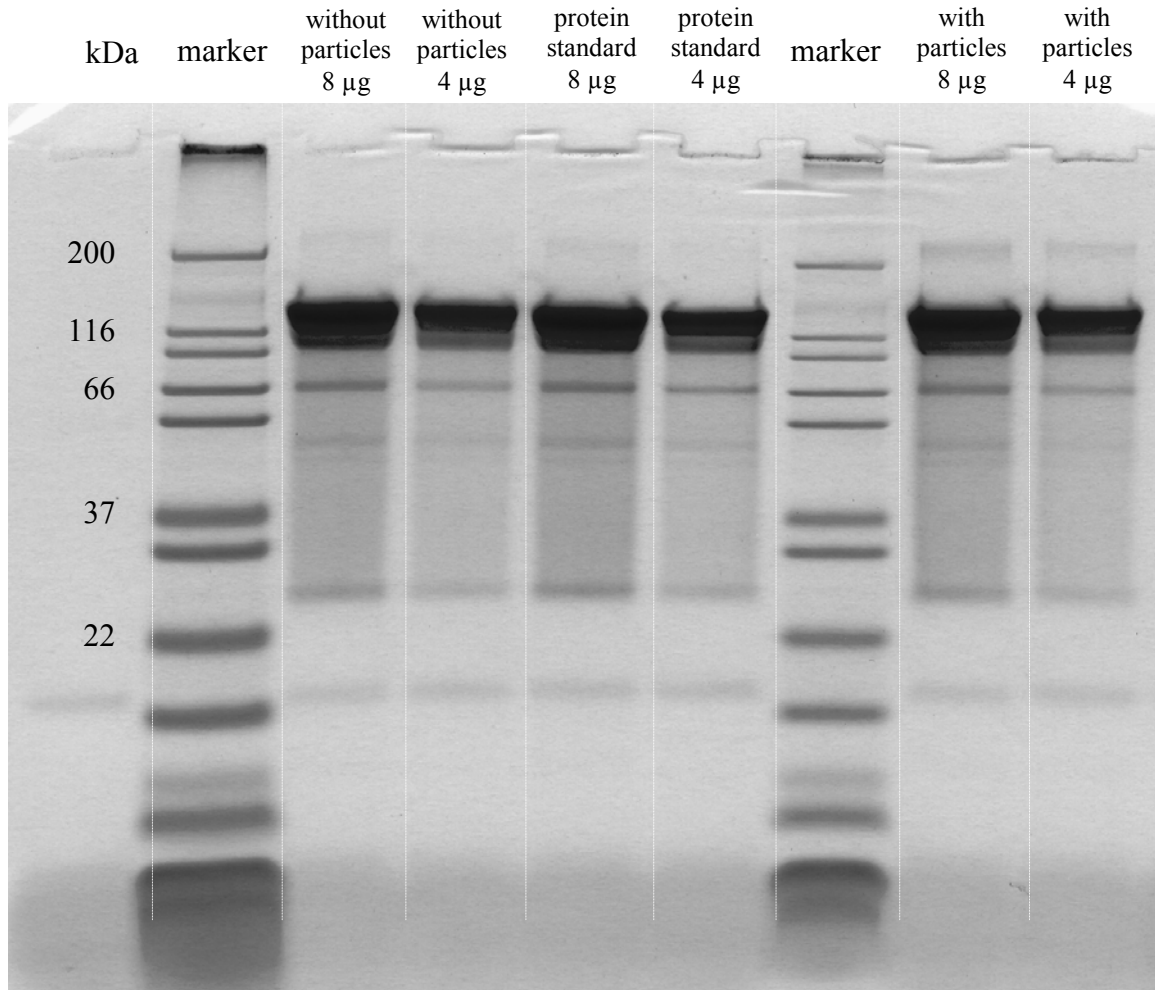


Fig. 106. SDS-PAGE analysis of immunoglobulin solutions revealing visible particulate matter (with particles) and particle-free volumes, resp. (without particles). Molar mass determination is enabled by molecular weight standards (marker); immunoglobulin bulk solution was analyzed to facilitate evaluation (protein standard); protein load per lane was 8 and 4 μg , resp.

Referring to Fig. 106, no notable difference can be detected between the immunoglobulin batches. All samples exhibit an intense monomer band assigned ~ 150 kDa by comparison to molecular weight (MW) standards, matching the theoretical value. Furthermore, three fragment specimen are unveiled to be present in all solutions: two more pronounced bands in the MW sectors of ~ 70 and ~ 30 kDa and a vague band in the range of ~ 50 kDa. Of course, the protein specimen reveal greater staining intensities at higher sample loads (8 versus 4 μg). In terms of higher-order specimen, samples drawn from particle-contaminated solutions carry the impression of revealing slightly higher dimer ratios than particle-free volumes, because the bands accounting for dimer (~ 300 kDa) are more pronounced. Yet, the differences are unimpressive. PAGE data back the findings of SE-HPLC, inasmuch as no differences in protein stability could be detected between immunoglobulin solutions with and without visible particulate matter, respectively – thus disclaiming the particles' nature to be proteinic.

Unfortunately, literature inquiries complicate the circumstances: precipitated pellets of porcine growth hormone were analyzed by reducing and non-reducing SDS-PAGE but neither technique detected the presence of hmw or lmw components, even after subjecting the precipitates to SDS solubilization (Charman et al., 1993). Protein concentrations falling below the minimal detection limit of PAGE or absolute irreversibility of the precipitation process may be cited as explanations therefore.

Nevertheless, in conclusion, data of SE-HPLC and PAGE exonerate the immunoglobulin from inhering insufficient stability – and consequently from being the source of particle formation – as no discrepancies between the investigated vial volumes were to be elucidated.

9.5 Microcalorimetric experiments

Microcalorimetry – often referred to as ultra-sensitive differential scanning calorimetry (DSC) – measures the difference in heat uptake between a sample solution and an appropriate reference such as buffer with increase in temperature. In concerns of protein stability, DSC data are often expressed in T_m values. T_m – effectively termed the transition peak – is defined as the temperature at which 50% of the protein molecules are unfolded or, in an ideal dynamic reversible two-state equilibrium, the temperature at which a protein molecule spends 50% of its time folded and the residual time unfolded (Cooper et al., 2001). Hence, in case the presence of particulate matter in immunoglobulin solutions were due to alterations in the protein's tertiary structure, DSC data may unveil discrepancies between sample batches with and without visible specimen, respectively.

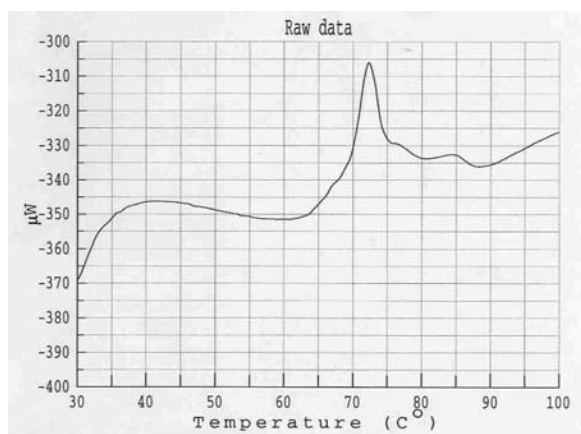


Fig. 107. DSC data for thermal protein unfolding in vial volumes exhibiting no visible particulate matter. T_m was determined at 72 °C.

A thermogram of a particle-free vial volume is depicted in Fig. 107. The assessed T_m value of 72 °C is consistent with T_m data of other dissolved G_1 immunoglobulins, which were determined to be 74 °C (Vermeer et al, 1998). In the course of the experiments (CSC Model 6100, cell volume 299 µL; Calorimetry Sciences Corp., USA; scan rates 0.5-1 °C/min), various vial volumes were ultrafiltrated (Vivaspin 6, polyethersulfone, 20 kDa cut-off, Vivascience AG,

Hannover, Germany) in order to yield protein-free blank solutions and to provide dilution medium, respectively (protein solution from vial volumes diluted down to 0.5-2.5 mg/mL).

In contrast to the unimodal heat transition of particle-free vial volumes, antibody solutions containing visible particulate matter unveiled a different DSC profile (Fig. 108).

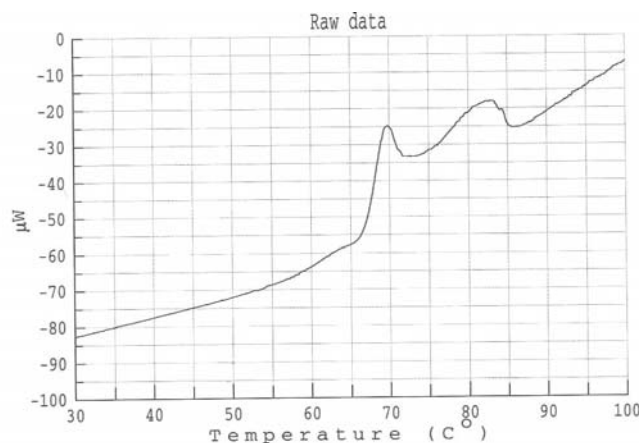


Fig 108. Thermogram of sample vials containing visible specimen. In addition to a T_m of ~ 70 °C, an endothermic transition can be determined, spanning a range from ~ 73 -85 °C.

According to Fig. 108, the presence of visible particulate matter induces the heat transition to exhibit a bimodal pattern: besides the peak representing the unfolding of the immunoglobulin ($T_m \sim 70$ °C), a heat energy uptake - beyond T_m and up to 85 °C – was detected. If that divergency is due to protein precipitates present in the sample is not to be explained plainly: unfolded protein is sticky stuff, and most will aggregate upon thermal denaturation. This aggregation is commonly exothermic and irreversible, causing a distortion of the DSC endotherm, compounded with noisy traces at higher temperatures because of convection of clumpy aggregates in the apparatus cell (Cooper, 2001). Hence, experiment reproducibility is generally low.

In order to scrutinize the origin of the detected bimodal heat transition, antibody bulk solution was subjected to heat stressing (60 °C). After 8 hrs, the solution was clear and appeared to be free of turbidity and particles when analyzed by visual inspection, but revealed an increase in soluble aggregate content by $\sim 4\%$, verified by SE-HPLC and AF4 analysis. DSC data of heat-stressed antibody solution is shown in Fig. 109.

The results are on the main lines in concordance with data of particle-contaminated immunoglobulin solutions: protein unfolding is expressed by a T_m of ~ 71 °C, but the intensity of the appendant peak is considerably lower than the signal detected in particle-free batches. Furthermore, endothermic heat transitions can be monitored at temperatures above T_m , extending to ~ 88 °C. Repeating the experiments – though facing low reproducibility – substantiated the findings, as bimodal heat transitions appeared immanent to the heat-stressed solutions. Generally, even in the absence of a priori aggregation phenomena, thermal unfolding is rarely completely reversible, since exposure of the unfolded protein to elevated temperatures can lead to improper refolding, proline isomerization, deamidation and other chemical changes

(Cooper, 2001). It may be assumed that this is the reason why little is published addressing DSC analysis of protein solutions which have already undergone aggregation prior to the experiments.

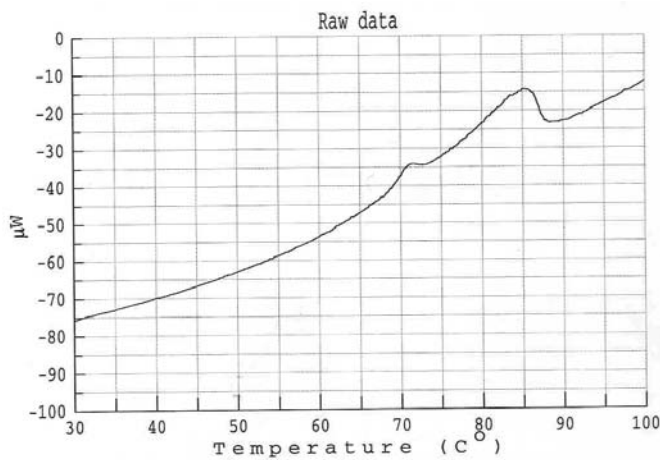


Fig. 109. DSC data of heat-stressed antibody bulk solution. Note the bimodal heat transition and that the peak attributed to thermal unfolding ($T_m \sim 71^\circ\text{C}$) is eclipsed, compared to the results of particle-free solutions (refer to Fig. 109).

Reviewing the DSC results gives rise to the impression the bimodal heat transition of vial volumes containing visible particles may be due to protein instabilities and changes in tertiary structure. Yet, G_1 antibodies were demonstrated to exhibit bimodal heat transitions and multiple transition temperatures, what was ascribed to the build-up of the antibody molecules by various protein units – i.e., heavy and light chains (Hoffmann, 2000). Moreover, the potential presence of molten globule intermediates can affect DSC data, as the kinetically trapped high-energy folded states are considered to be reflected in exothermic processes (Epan and Epan, 2003).

In order to verify a possible influence of changes in protein structure, protein aggregates and proteinic particulates on DSC data, another 150 kDa monoclonal antibody (MAB, targeted on hepatitis B-virus) was driven into protein precipitate formation via short-term stress at 65°C . Thereby, it was attempted to induce particle contamination comparable to the situation within the vial volumes of the immunoglobulin developing visible particulate matter during long-time storage at 5°C (Table 17).

size of particles present per mL	vial volumes without visible particulate matter	(shaken) vial volumes revealing visible particles	MAK solution - unstressed	MAK solution - thermal stress
$\geq 1 \mu\text{m}$	18,279	159,717	11,333	135,142
$\geq 2 \mu\text{m}$	8,731	42,321	6,867	56,942
$\geq 10 \mu\text{m}$	291	105	383	1,992

Table 17. Light obscuration data of two immunoglobulin solutions, subjected to various conditions ($n=9$, S_{rel} for all data < 1.8).

As outlined by Table 17, the particle contamination of MAK solutions was developed by thermal stressing to levels comparable to the situation in particle-containing vial volumes – as far

as particles in the one-digit μm range are concerned. In terms of particles greater than $10\ \mu\text{m}$, the contamination levels differ notably. Pertaining to that, protein solutions were demonstrated to vary substantially in the contamination levels with particles larger than $10\ \mu\text{m}$, although they contained identical amounts of smaller particles (i.e., $<2\ \mu\text{m}$). The main parameters accounting for this phenomenon were found to be protein class and the kind of stress parameter applied for particle generation (Mueck, 2002).

The thermogram of unstressed MAK solution reveals a T_m value of $77\ ^\circ\text{C}$ and an asymmetrical heat transition profile which is typical for immunoglobulins (Fig. 110).

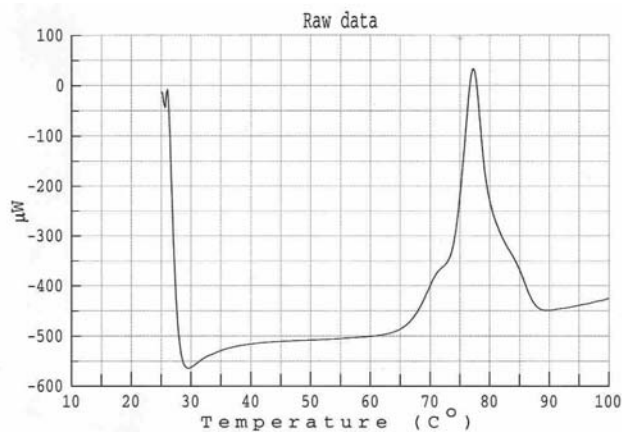


Fig 110. DSC data of an unstressed monoclonal antibody (MAB, 150 kDa, $T_m \sim 77\ ^\circ\text{C}$).

Similarly to the DSC data of the verum immunoglobulin (refer to Fig. 107), the transition peak is flanked by various “shoulders”. This behavior may be attributed to the formation of small aggregates (dimers, etc.), as suggested in previous DSC experiments (Fransson et al., 1997). Since dimerization was found to be the main aggregation pathway of the immunoglobulin when exerted to heat stress, this matches the data derived hitherto. DSC analysis of heat-stressed MAK solutions suffering particulate contamination bears out bimodal heat transitions (Fig. 111).

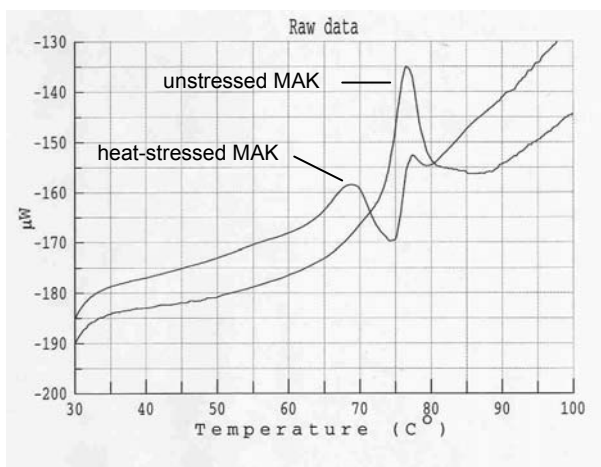


Fig. 111. Thermograms of unstressed MAK solution inhering minimal particle contamination and MAK solution revealing severe particle contamination due to heat stress. Note that heat transition profiles differ considerably.

Similar to the results on the verum immunoglobulin, the presence of particles in MAK solutions reduces the intensity of the unfolding endotherm. Thereby, the value of T_m remains constant ($77\ ^\circ\text{C}$). However, in contrary to the findings of particle containing verum vial volumes,

the additional endotherm signal causing a bimodal heat transition profile emerges at temperatures below T_m , ranging within $\sim 55\text{-}75\text{ }^\circ\text{C}$.

In summary, DSC experiments reveal a tendency to ascribe the presence of visible particulate matter in the vial volumes to changes of the protein's tertiary structure. Subjecting particle-free immunoglobulin solutions to thermal stress induces DSC data to exhibit a characteristic bimodal heat transition profile similar to that derived from vial volumes containing particulate matter. This phenomenon was only partially corroborated by experiments with MAK solutions: though heat-stressed MAK reveals a bimodal heat transition curve, the additional DSC endotherm was developed at temperatures below T_m , thus hampering unambiguous data interpretation.

9.6 Particulate matter analysis by AF4/MALS and filtration

The use of techniques applying light transmission and light scattering for the analysis of particulate specimen is well established. Tests for clarity or transparency – based on light transmission – are aiming to quantify the amount of light which passes through the formulation in the primary container. Some pharmacopoeia tests require a certain level of light transmission to be achieved in order that particulate contamination can be checked, e.g., USP XXXIII (Dean, 2000). Yet, considering that the immunoglobulin solutions reveal an a priori opalescence due to the high protein concentration, the application of light transmission tests for the characterization of visible particulate matter in vial volumes may be deemed futile. Conversely, the detection of even minimal amounts of particles will not be impeded by opalescent solutions, due to the high sensitivity of light scattering on μm sized analytes (Wyatt, 1993).

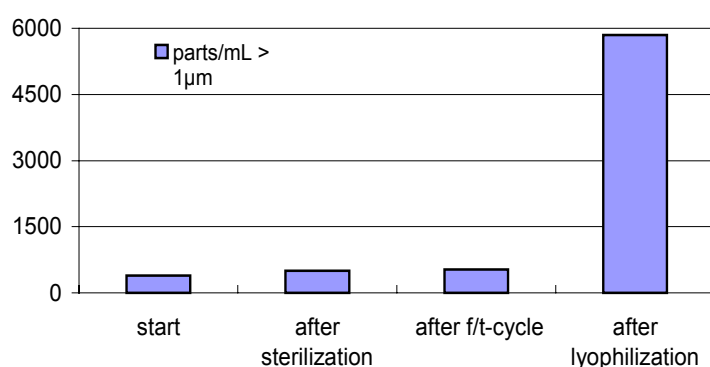


Fig. 112. Particulate matter growth in 20R glass vials according to successive order of manufacturing and production processes (data derived by light obscuration, $n=9$, S_{rel} for all data <2.1 ; refer to text).

In order to scrutinize the sensitivity of MALS in the detection of particulate matter, parenteral package containers were subjected to various processes that package materials normally encounter in the course of manufacturing and production of pharmaceuticals (Fig. 112). To provoke particulate matter generation, 20R glass vials were sterilized by dry heat ($180\text{ }^\circ\text{C}$, 20 min), filled with 5 mL Milli-QTM-water, stored at $-80\text{ }^\circ\text{C}$ for 24 hrs prior to further 24 hrs storage

at 5°C, were exposed to lyophilization applying state-of-the-art process parameters, and finally refilled by adding 5 mL Milli-Q™-water. Referring to this, it is known that besides by drug instability, particulate matter can emerge in parenterals/package materials during processing, e.g., by sterilization, freezing and lyophilization (Gebhardt et al., 1996). According to Fig. 112, the final lyophilization step accounts for the lion's share of particulate contaminates, whereas light obscuration data ascribes sterilization and freeze/thaw processes to induce solely minor particulate contamination. Conversely, AF4/MALS analysis of the sample batches prior/subsequent to the freeze/thaw cycle reveals a notable increase of scattered light intensity due to particles in the higher nm range and μm range, which emerged during freeze/thawing (Fig. 113).

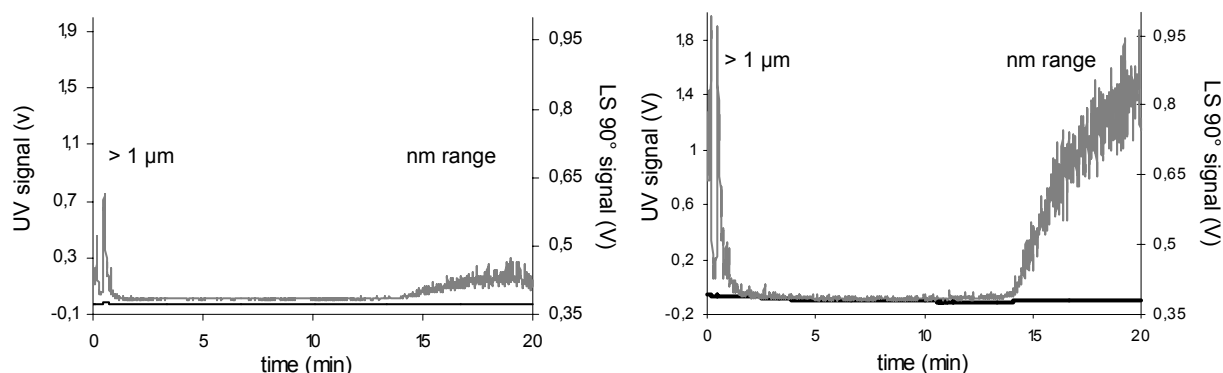


Fig. 113. In contrast to light obscuration, the sensitivity of AF4/MALS proves to be sufficient for detection of particulate matter induced by manufacturing processes: container volume prior (left) and subsequent (right) to freeze/thaw cycle. Since the particles reveal no UV_{280} absorbance, UV spectrophotometry (black curve) fails detection – whereas the sensitivity of MALS_{90° (grey curve) is expressed by intense signals. AF4 parameters: 25% cross flow is reduced to 0% after 13 min, forward flow 1 mL/min.

According to these results, AF4 seems qualified for the analysis of vial volumes revealing particulate matter contamination. Bearing in mind the failure of light obscuration in monitoring particulate entities generated by freeze/thaw processes – but AF4 unveiling substantial particulate matter originating therefrom –, AF4 appears all the more a good choice in analytical challenges where even light obscuration detects notable results – i.e., in the differentiation between immunoglobulin solutions with and without visible particulate matter. Concerning that task, AF4 recently succeeded in the fractionation of particulate samples in the two-digit μm range, thereby approaching sample components coming up to visibility (Wahlund and Zattoni, 2002).

Such micrometer analytes are separated in an elution mechanism referred to as steric- or lift-hyperlayer mode - in contrast to submicrometer components, which are fractionated in normal mode (Caldwell, 2000). As a consequence, visible particulate matter in the immunoglobulin solutions is expected to be separable from dissolved protein specimen. In the first Flow-FFF report addressing steric mode separations applied flow rates of 20-40 mL/min were reported – causing immense hydrostatic pressure within the system (Chen et al., 1988). In

contrast, today's advanced channel set-ups enable steric mode separations to be performed with flow rates below 1 mL/min, thus reducing potential shear stress towards zero. Given the background of the visible particles' proneness to physical degradation due to shear, focus step and intense field strengths were avoided during the AF4 experiments (cross flow 10% for 10 min). However, AF4/MALS could detect no difference between the vial volumes (Fig. 114).

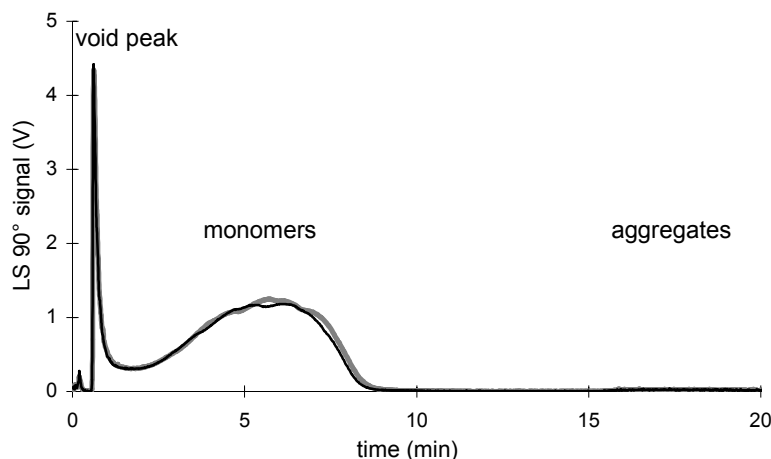


Fig. 114. Analysis of vial volumes with (black line) and without visible particles (grey line) by means of AF4/MALS. The intense void peak is due to moderate AF4 separation conditions.

Even if the intense void peak – due to the absence of focusing – is suspected to superimpose light scattering signals of particulate matter eluting in steric mode, the samples were expected to reveal different void peak intensities, because of varying contents of particulate specimen. These data are substantiated by UV/MALS analysis, where the signal charts are shown to be virtually interchangeable, regardless of the findings of visual inspection (Fig. 115).

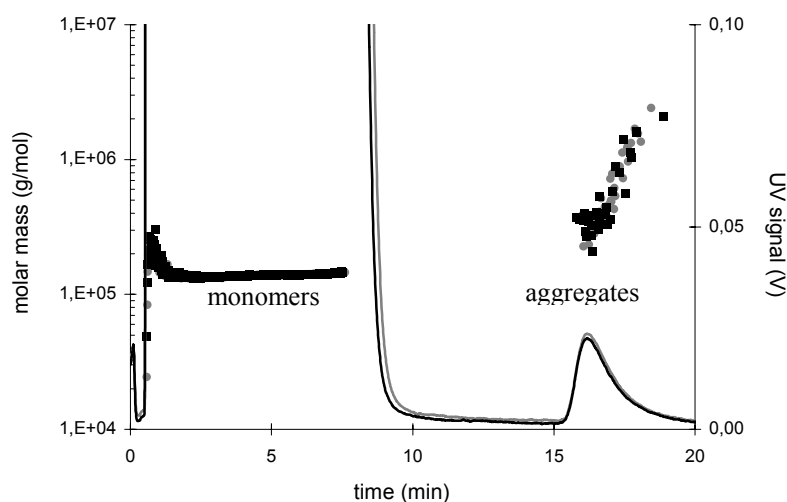


Fig 115. UV₂₈₀ detection (exploded view) proves particle-free (grey curve) and particle-contaminated antibody solutions (black curve) to reveal equal aggregate ratios (0.7%). Similarly, molar masses of monomer (150 kDa) and aggregate fraction (300-1200 kDa) were calculated to be identical in both solutions.

It may be argued that due to the dilution (by factor three) of the vial volumes prior to AF4 analysis the particulate matter may have redissolved, thus avoiding detection. However, the drawbacks of contingent re-dissolution of the particulate specimen are mandatorily associated with (semi)-chromatographic methods such as AF4 and HPLC due to the use of elution media. Another explanation may be that the cross flow – although of moderate intensity – forces μm

sized particles into close proximity to the membrane, thus giving rise to potential adsorption phenomena and consequently burking detection (Schimpf et al., 2000). Pertaining to that, running the risk of potential analyte adsorption can be circumvented by performing AF4 analysis without exerting field strengths, resulting in a separation mechanism referred to as capillary hydrodynamic chromatography (CHDC) (Shiragami, 1991). Thereby, larger analytes are eluting prior to smaller analytes, as exemplified by the analysis of vial volumes containing visible particulate specimen (Fig. 116).

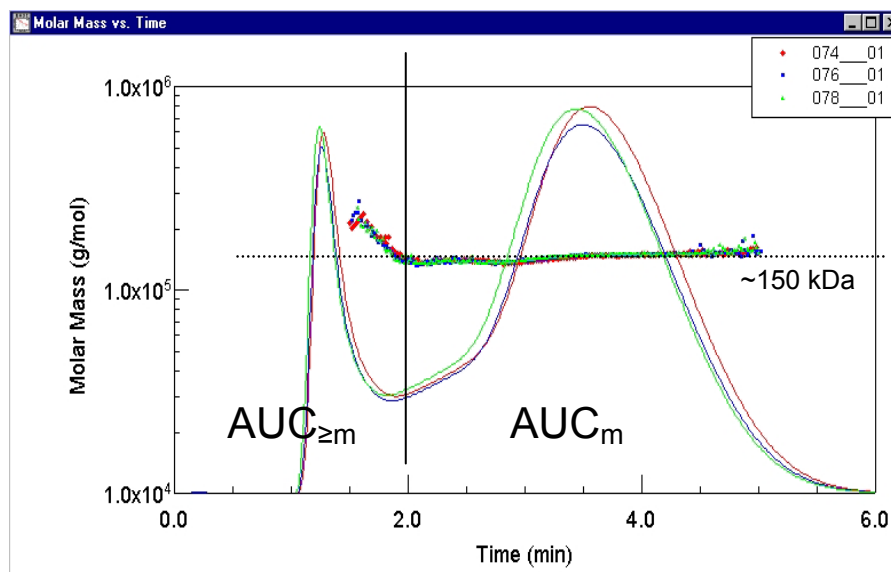


Fig. 116. Performing AF4 separation without exerting field strengths results in a characteristic elution profile: larger analytes are eluting prior to smaller analytes, i.e., particles and higher-order aggregates ($AUC_{\geq m}$) elute earlier than monomers (AUC_m). Due to the pronounced break of the molar mass marks at $t=2$ min, a distinct borderline between the 150 kDa monomer fraction and higher-order analytes can be set.

Due to the accuracy of the molar mass calculation via MALS, the eluting components can be separated into two individual fractions: a fraction containing solely antibody monomers – verified by the unimodal mass distribution throughout that fraction – which elutes subsequent to a fraction encompassing monomers but mainly higher-order specimen (dimer, aggregates, particles, etc.). A quantitative analysis of the different protein solutions is presented in Table 18.

sample	$AUC_{\geq \text{monomer}}$	AUC_{monomer}	$\geq \text{monomer} (\%)$	monomer (%)
vial volume without visible particles	2.16	11.48	15.83	84.17
vial volumes with visible particles	2.29	11.56	16.50	83.50

Table 18. AF4 analysis of vial volumes without exerting field strengths ($n=6$; S_{rel} for all data <2.7).

In vial volumes revealing visible particles the ratio of the fraction “ \geq monomers” exceeds the same fraction detected in particle-free vial volumes by 0.67%. It may be hypothesized the visible components for the most part to remain physically intact during separation, thus

contributing to the AUC_{UV280} of the fraction eluting first. Yet, the difference between both vial batches is humble. In this concern, MALS for all samples demonstrated the components of the fraction “ \geq monomers” to encompass identical molar mass ranges.

In summary, AF4 does not disclose stability discrepancies between immunoglobulin solutions which vary in the outcome of visible inspection. Both protein solutions are attributed identical aggregate ratios by AF4, reaffirming the data derived by SE-HPLC and PAGE. Though AF4 was demonstrated to exceed light obscuration in detection sensitivity of process-induced particulate matter, operating AF4 conventionally yielded no differences between the vial volumes in terms of particle contamination. In contrary, running AF4 in a CHDC-like mode unveiled vial volumes with visible particles to slightly exceed particle-free vial volumes in the content of fractions that unify any sample components larger than monomer. However, the assessed differences remained too low (0.7%) to draw unambiguous conclusions.

In case vial volumes containing visible particulate matter are subjected to sterile filtration (0.2 μm), the filtrate appears to be free of visible components. Furthermore, light obscuration analysis demonstrates the filtration step to notably reduce the amount of subvisible particles – minimizing the number of particles $\geq 1 \mu\text{m}/\text{mL}$ from a 137,592-level down to ~ 2000 . Assumed the particulate matter is of proteinic nature, particles remaining on the filter membrane are expected to re-dissolve when exposed to denaturants such as 2% SDS, 6M urea or 6M GdnHCl (Allison et al., 1996; Brange et al., 1997). Subsequently, the re-dissolved proteins are amenable to analysis by PAGE or UV spectrophotometry. In this realm, the determination of particulate matter in parenteral solutions via 0.2 μm -filtration and successive analysis of the remainder by means of qualified analytical methods such as element analysis and SEM is long established (Winding and Holma, 1976).

Volumes of five vials (with and without visible particulate matter, respectively) were combined and filtered (Minisart[®], 0.2 μm , celluloseacetate, Sartorius AG, Goettingen, Germany). In order to obviate artifacts by adsorption, the filters were washed five times with 10 mL Milli-Q[™]-water. Such washing is considered a state-of-the-art process in protein purification and precipitate isolation by means of filters (Kinekawa and Kitabatake, 1996). Subsequently, the filters were flushed ten times with the identical volume of 5 mL 2% SDS to re-dissolve protein precipitate potentially sticking on the filter membrane. The amount of protein recovered was assessed by UV_{280} spectrophotometry. In order to enable a reasonable data interpretation and to evaluate method efficacy, the same process was applied to protein-free buffer medium and batches inhering protein precipitate. Therefore, immunoglobulin bulk solution was exposed to thermal stress (70 °C, 10 min). The proceedings are summarized in Table 19.

samples	buffer medium	vial volume with visible particles	vial volume without visible particles	heat-stressed IgG bulk solution
UV ₂₈₀ absorption	0.0000	0.0325	0.0315	0.4170

Table 19. UV₂₈₀ quantification of filter remainders, re-dissolved by means of 2% SDS (n=6, S_{rel} for all data <0.9).

According to the data of heat-stressed protein solution, a considerable amount of insoluble protein is retained by the filter membrane and amenable to quantification subsequent to re-dissolution by SDS. Additionally, the absence of protein in the sample derived from buffer volume matches the theory – thus affirming the principal applicability of the experimental set-up. In terms of the immunoglobulin batches, data of samples drawn from visible particle-contaminated solutions are shown to exceed the results of particle-free vial volumes only marginally (~3%). Considering the minimal amounts of protein recovered from batches based on immunoglobulin vial volumes, that difference is attached minor significance.

In order to render the re-dissolved batches more distinguishable and to broaden potential differences in protein concentration, 1 mL of each batch was concentrated to 0.25 mL by ultrafiltration (millipore ultrafree[®], cut-off 10 kDa, Vivascience AG, Hannover, Germany) and analyzed by SDS-PAGE (Fig. 117).

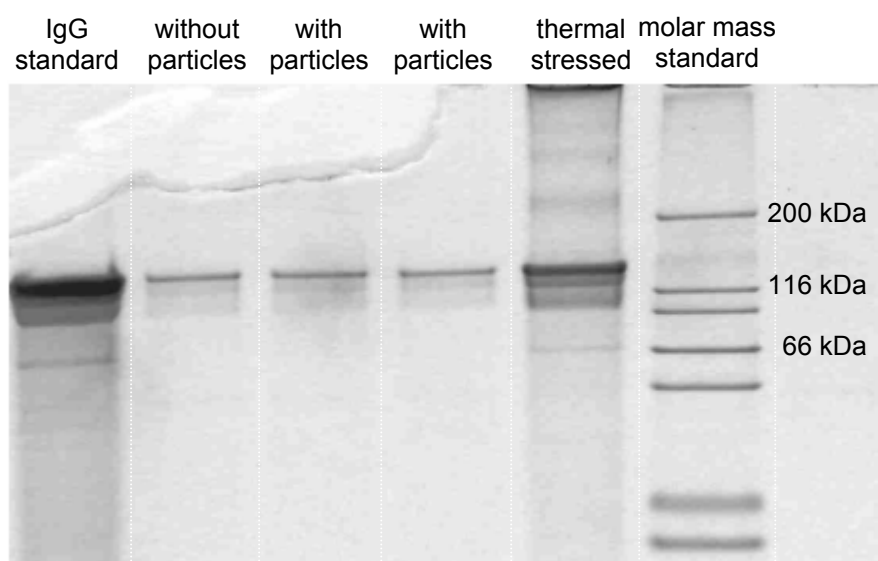


Fig. 117. PAGE analysis of filter remainders re-dissolved in 2% SDS and concentrated by ultrafiltration; staining with colloidal blue. The batch based on thermal-stressed protein solution reveals a pronounced monomer band and weak bands representing fragment (~70 kDa) and dimer (300 kDa). In contrast, the lanes representing vial volumes are deemed identical, exhibiting solely monomer bands.

Basically, the findings derived hitherto are corroborated: because the denaturant solution appendant to thermal-stressed protein solution contained the highest amount of protein, the lane on the gel exhibits bands representing fragment, monomer and dimer. In contrast, the monomer

bands of sample batches basing on immunoglobulin vial volumes appear weak in comparison. Generally, PAGE data of batches based on the vial volumes in dispute are absolutely identical in qualitative and quantitative terms - this was substantiated by further PAGE analysis of the concentrated denaturant solutions, thereby applying silver staining.

In summary, isolation of the particulate matter present in vial volumes was performed by 0.2 μm filtration. Identification of the filter remainders was approached by re-dissolution with 2% SDS. Neither UV_{280} spectrophotometry nor SDS-PAGE analysis unveiled any discrepancies between immunoglobulin solutions with and without visible particulate matter, respectively. As a consequence, the visible particles may not be considered to be of proteinic origin.

9.7 Summary and evaluation

This chapter addresses a case study of an immunoglobulin solution developing visible particulate matter within the glass vials sporadically during long-term storage. Information on the particles' origin is of utmost importance, since the potential presence of any insoluble aggregates in a protein pharmaceutical is generally not acceptable for product release (Wang, 1999).

Evidence of the particulate matter in the vial volumes is definitely provided by visible inspection as well as by light microscopic and light obscuration analysis. Minimal shear stress – e.g., by vial shaking – pretended the visible entities to dissolve, but had virtually no impact on light obscuration data.

In case the particles' origin is due to protein instability, this is expected to be reflected in increased aggregate ratios. However, a comprehensive analysis by SE-HPLC, SDS-PAGE and AF4 demonstrated particle-contaminated antibody solutions to equal particle-free solutions in aggregate content. Furthermore, detection methods known to be sensitive on (hmw) aggregates proved the principal parity of the vial volumes concerning the molar mass dimensions of the aggregates, regardless of the degree of particulate matter contamination.

In contrast, microcalorimetric data of visible particle-contaminated batches resembled those of immunoglobulin solutions containing a notable aggregate fraction, induced by thermal stressing. Both samples featured characteristic bimodal heat transitions, comprising the transition of the unfolding process and a second endotherm at temperatures beyond T_m . Consequently, alterations in protein structure and stability may account for the formation of visible components in immunoglobulin solutions.

AF4 separation parameters were developed that proved AF4/MALS to be superior to light obscuration in the detection of particulate matter. Yet, AF4 failed in the separation of the visible entities applying normal mode conditions. On the other hand, performing AF4 in a separation mode without exerting cross flow enabled to yield a fraction encompassing sample components larger than monomers. In contrast, the ratio of this very fraction was lower in

particle-free vial volumes – matching the findings derived hitherto, but presenting no further information on the particle source.

Finally, the particulate matter was removed from the formulation by 0.2 μm -filtration. Assuming the particles to be constituted by insoluble protein aggregates/precipitates, the protein remaining on the filter membrane was re-dissolved by 2% SDS solution and analyzed by UV_{280} spectrophotometry and SDS-PAGE. However, no differences between each vial volumes could be monitored.

In summary, the visible particulate matter developing in some vials at random during storage is in all probability not of proteinic nature, since the majority of the analytical techniques applied denies any distinctive features in protein stability. Given the fact that precipitates in parenterals can be induced by a variety of sources – e.g., the insolubility of phosphate buffer specimen, the precipitation of trace elements or particle formation due to stopper materials – the identification of particle nature is commonly considered delicate (Allwood, 2000; Allwood et al., 1998; McGoff and Scher, 2000). In general, due to the complexity of the issue, the analytical arsenal may be enlarged with sophisticated techniques such as element analysis or high resolution mass spectrometry (Anderson et al., 2001) – but none technique per se can guarantee to provide unambiguous data.

10 Minimizing aggregation in antibody pharmaceuticals: a laboratory case study

10.1 Introduction

Understanding the principles of protein stabilization and armed with the methods to gauge changes, the formulation scientist can apply chemical or physical methods to provide a pharmaceutical dosage form with acceptable shelf life. Although there is a remarkable move towards alternative routes of administration such as nasal, oral, rectal and aerosol dosage forms, proteins commonly still are formulated as parenteral injectable products. Referring to the latter, ten years ago only few peptides and proteins have demonstrated adequate stability in parenteral solutions to provide marketable pharmaceuticals with shelf lives of one year or more (Hanson and Rouan, 1992).

Contrarily, within the last few years a variety of pharmaceutical proteins have successfully been formulated as solutions, for instance erythropoietin-related darbepoetin alpha (AranespTM), receptor antagonists (anakinra, KineretTM) and monoclonal antibodies (adalimumab, HumiraTM). However, that is not because pharmaceutical formulators suddenly had panaceas to their disposal, but due to the mere fact that protein pharmaceuticals per se took center stage of research in both science and industries (Walsh, 2003).

Still, there is no general valid formulation strategy at hand – so proteins in pharmaceutical solutions have to be stabilized individually, often on a trial-and-error basis (Wang, 1999). It is the aim of this chapter to introduce strategies and pitfalls encountered in the formulation of liquid protein pharmaceuticals by means of a laboratory case study. Thereby, the liquid formulation of a pharmaceutical antibody (adalimumab, 147 kDa, 50 mg/mL) was to be optimized in order to increase stability during long-time storage.

The chapter is precluded by a succinct review, wherein latest options of stabilizing methods are presented. Due to the complexity of the matter, a comprehensive list of investigations and achievements in protein stabilization can not be provided. Yet, common strategies in protein formulation are highlighted and mainstream trends are evaluated. Furthermore, attention was paid to the quoted references - as literature on the topic is plentiful, even the professional may facing difficulties in keeping track of. It is a further intention of 10.2 to leave the mark of protein liquids' formulation to be a challenging realm.

10.2 Formulation/stabilization of liquid protein pharmaceuticals: a short review

Generally, the successful formulation of a protein into a liquid formulation can not be taken for granted. Hence, it is advisable to concomitantly provide a backup formulation by

stabilizing the protein via physical methods, usually lyophilization (Carpenter et al., 2002) or spray-drying (Andya et al., 1999).

In case the formulator wishes to reconcile his strategy with published literature, he can refer to several reviews targeting protein formulation (Patro et al., 2002; McNally, 2002; Wang, 1999; Hanson and Rouan, 1992). Additionally, a number of review articles describing protein instability have been published. Since those articles commonly are focused on unveiling degradation and aggregation pathways - thereby describing parameters opposing protein stability -, they are bound to (unintentionally) provide information on how to circumvent protein instabilities and thus how to stabilize protein liquids (Arakawa et al., 2001; Reubsæet et al., 1998; Kendrick et al., 1998; Constantino et al., 1995; Ó Fágáin, 1995; Chen et al., 1994; Cleland et al., 1993).

For many years, the epitome of protein stabilization was the excipient patch, peer with stabilization via internal changes, i.e., altering the protein's structure. However, one paradigm shift has certainly proceeded, concerning the chemical modification of proteins in order to increase stability. Bearing in mind that many of the 20 amino acids occurring in proteins have reactive functional groups such as thiol groups or amino groups – thus rendering the protein drug amenable to numerous pathways of degradation and inactivation -, the need for efficient conjugation or immobilization procedures has always been an issue in scientific and technical literature, reaching the climax about one decade ago (Ó Fágáin, 1995). Several distinct chemical modification strategies were deemed to inhere potential to take a front seat in protein stabilization techniques, mainly amino acid replacement (Querol et al., 1996), intra- or intermolecular cross-linking (Wong and Wong, 1992), surface group modification and glycosylation (Liu, 1992), and modifications with polyethylene glycol (PEG, PEGylation) (Katre, 1993). However, early has it been in the offing that these modifications are not to be performed at random, and that for the majority of proteins chemical modifications are associated with severe drawbacks concerning long-term stability. Most importantly, these modifications are often related to the decrease, and sometimes the complete loss of biologic activity of the protein pharmaceutical (Zhang et al., 2002). Meanwhile, PEGylation turned out to be the remain of the former array of auspicious approaches and – considering huge research efforts put in that very field (Veronese, 2001) – reciprocation is at hand: e.g., pegfilgrastim (Neulasta™) was approved for treatment of febrile neutropenia by the U.S. Food and Drug Administration (FDA) in February, 2002, and peginterferon alpha-2a (Pegasys™) received FDA approval for treating hepatitis C shortly afterwards, in October, 2002.

As a consequence of the manifold difficulties connected to chemical modifications, today's stabilization of protein liquids is primarily approached by the use of excipients. These excipients are also referred to as co-solvents (Timasheff, 1998), co-solutes (Arakawa et al., 1993) or chemical additives (Li et al., 1995). Thereby, the selection of excipients in parenteral

formulation design is often both rational and empirical. Rational, inasmuch as features and stabilizing effects of excipients are known, and they are added to prevent specific problems which would likely arise in their absence. On the other hand, the choice of the exact excipient used is far from rational – it seems to be driven more by an empirically impetus, satisfying one question: “Has it been used previously in a similar parenteral formulation?” It may be a surprising fact that many prototype formulations have been terminated because one or more of the selected excipients was not applied in a previously approved parenteral product (Powell et al., 1998).

Basically, when proteins are to be used in a clinical setting as a human therapeutic, certain criteria restrict the type of excipients that may be used and the conditions under which the protein is subjected to long-term storage: excipient components must be safe, i.e., non-toxic and non-infective. The solution should be isotonic with respect to the route and mode of administration. Moreover, the pH is to be adjusted in appropriate way (Arakawa et al., 2001). Taking also into account the impact of excipients and osmolalities on felt pain and burning syndroms of the patients during drug administration is considered a matter of course. E.g., sodium citrate enjoys the reputation of being an excellent stabilizing buffer, often used in concentrations of sizeable 20 mM (Remmele et al., 1998). Unfortunately, at higher concentrations sodium citrate is too painful in most instances for subcutaneous use (Powell et al., 1998). Similarly, PEGs – though used in liquid protein formulations in amounts up to 65% – were proved to inhere drawbacks, as the replacement of PEG by components with lower osmolality has effectively reduced the incidence of side effects such as pain and thrombosis (Doenicke et al., 1992). Facing such requirements, the formulator may anticipate failure ante portas.

In this realm, the usual proceeding of the formulating scientist is to screen the array of excipients available for use – selected on the criterion of what has been used previously. To stay with PEGs: the use of lmw PEGs has received approval for numerous parenteral formulations, e.g., VepesidTM and RobaxinTM injectable contain both PEG 300 as excipients, and AtivanTM is formulated with the use of PEG 400, according to information provided by the manufacturer. However, what about PEG 1200, PEG 4000 or hmw PEGs? Concerning to that, it was shown that PEG 4000 inhibits the thermal aggregation of lmw urokinase (Vrkljan et al., 1994). Furthermore, PEGs were demonstrated to contribute to lactate dehydrogenase stability in solution and after freeze-thawing, and the protective effects were maximal with hmw PEGs (Mi et al., 2002). Additionally, hmw PEGs such as PEG 8000 were shown to be able to direct precipitation, once proceeding, in a manner that protein precipitate is essentially native in secondary structures, revealing a virtually identical second-derivative IR spectrum to the native dissolved protein control (Kendrick et al., 1998).

In many cases, problems are associated not only with excipient choice but especially with concentrations. E.g., the stabilizer sucrose was demonstrated to reveal virtually no effect on the (thermal) stability of megakaryocyte growth factor at low protein concentrations, while at higher

protein concentrations (~2 mg/mL) the addition of sucrose increased the protein stability substantially. To confuse the matter further on, sucrose exhibited no effect on the reversibility of the denaturation (Narhi et al., 1999). Vice-versa situations, where stabilization is facilitated by lower excipient concentrations, are also reported. For instance, sorbitol hampers heat-induced aggregation of fibroblast growth factor at 55 °C notably below concentrations of 0.5 M, but inheres considerably less effect at higher concentrations (Tsai et al., 1993).

So, facing such inconsistencies, how to decide which class of excipient is to be prioritized, which specimen in particular, what are the proper concentrations? Two main approaches are prevalently considered state-of-the-art: to apply high-throughput formulation screening (HTS) and to perform accelerated stability studies.

Pertaining to the first, computational HTS can be applied to study the physico-chemical features of proteins, thus providing a sound knowledge on protein characteristics (Luo et al., 2002). Subsequently, various HTS tools may be used in order to identify promising excipients that confer physical stability for a given protein. E.g., in self-interacting chromatography the protein is immobilized on a chromatographic packing material and elutions are performed with the identical protein in mobile phases containing excipients of interest. Compounds that result in shortest retention times correspond to those that minimize protein-protein interactions (Przybycien and Wilcox, 2002). Naturally, autosampling devices which increase the evaluation efficiency of protein liquids are also to be subsumed to HTS, such as autosampling DSC instruments (Plotnikow et al., 2002). However, most pharmaceutical formulators will specify HTS as a tool of preformulation studies, which nowadays may be considered to interdigitate with the virtual formulation process to an increasing extent (McNally and Lockwood, 2002).

On the other hand, accelerated stability studies (ASS) can be employed to assess the influence of excipients – and therefore to predict shelf life of protein formulations. ASS were reported to be performed in isothermal and non-isothermal ways (Reithmeier et al., 2001). Unfortunately, proteins sometimes act idiosyncratic, and the general consensus is that prediction of protein stability based solely on accelerated studies is difficult due to the alleged non-Arrhenius character of protein degradation – because mechanism and route of degradation may depend on temperature (Bartkowski et al., 2002). Yet, dealing successfully with the formulation of protein liquids when tests under accelerated storage conditions (e.g., 40 °C) are not applied has rarely been reported. Conversely, by arranging ASS in proper way outstanding efficacy may be yielded: besides parameters contributing to the stability of recombinant factor VIII, reasons of inactivation and main aggregation pathways were elucidated via ASS. Furthermore, simple analytical techniques such as HPLC were found to be sufficient in order to monitor and predict stability and shelf life, yet in lieu of alternative methods such as one-stage clotting assays (Wang and Kelner, 2003). However, it is to be outlined that even the most ingenious HTS and ASS studies are no surrogate for real-time stability tests.

Evaluation of optimal pH values and buffer components usually accounts for the first step towards a stable protein formulation. Since proteins exhibit a stability optimum in a narrow pH range – often in a scope of <0.5 pH values -, the assessment of the pH of the formulation is a crucial point (Fatouros et al., 1997). In any case, it is advised to distinguish the formulation pH by more than 1 unit from the protein's isoelectric point.

Common buffer systems are based on phosphate, citrate, succinate, acetate, TRIS or histidine, and a variety of other buffer specimen has successfully been applied – but proteins are deemed to normally favor one specific buffer system (Piros et al, 2003). For instance, in phosphate buffer (10 mM) megakaryocyte growth factor irreversibly precipitated upon unfolding under all conditions examined, whereas in imidazole buffer (10 mM) no precipitation was to be detected, and unfolding was shown to be (partially) reversible (Narhi et al., 1999). Besides the compatibility of the buffer system with the protein, the characteristics of the buffer per se have to be scrutinized – as solutions containing components such as sodium phosphate can undergo a dramatic decrease in pH at the eutectic point, making those media potentially a poor choice if freezing during storage or transport were a matter (Arakawa et al., 2001).

The use of surfactants remains an important beacon for the field of stabilizing protein liquids, whereby the utilization of ionic surfactants may be considered out of date because they exhibit a notable affinity to the protein's polar and nonpolar groups, thus facilitating denaturation phenomena (Giancola et al., 1997). Despite a broad variety of nonionic surfactants is at hand, derivatives and modifications of virtually solely three surfactants reap the merits, i.e., Tween (polyoxyethylene sorbitan monooleate), Pluronic (polyoxyethylene polyoxypropylene block polymer) and Brij (polyoxyethylene alkyl ether) (Hillgren et al., 2002; Katakam et al., 1995). The observed stabilization of proteins (e.g., albumins) against heat treatment is due to surfactants altering aggregation behavior rather than inducing considerable stabilization of the native state. In this regard, the binding of nonionic detergents to proteins through hydrophobic surface interaction has been shown (Jones and Randolph, 1995). Stabilization by surfactants often implicates rather than enhancing conformational stability, the prevention of loss from unfolding at air-water or solid-water interfaces, or protection of proteins from aggregation that occurs as a result of unfolding, shaking or shear stress, or freezing. However, it is difficult to distinguish which of these mechanisms is of primary importance in detergent-induced protein stabilization, but nevertheless, due to empiric reasons, the use of surfactants is still on the rise (Arakawa and Kita, 2000).

In contrast to the explicit consent to surfactants, scientists are challenging existing paradigms in terms of salts. Hitherto, the addition of salts to protein formulations was deemed a must – fostered by the fact that the mechanisms of protein stabilization were thought to be elucidated, mainly by sorting things out by means of the Hoffmeister lyotropic series (Timasheff, 1998). Further models addressed parameters like electrostatic shielding, weakening of ionic

repulsion/attraction, an increase of surface tension at water-protein interfaces and preferential hydration of proteins (Kohn et al., 1997). Moreover, salts can stabilize via alternative ways, e.g., fostering ligand-binding: a >500-fold stabilization of starch phosphorylase against irreversible inactivation at elevated temperatures (>50 °C) by adding salts was reported (Griessler et al., 2000). However, the number of case studies where salts stabilize is put into perspective by studies proving salts to have no effect or even to destabilize, what is easily verified by searching the review articles. Recently, a full factorial experiment established that all proteins investigated were insensitive to sodium chloride concentrations, but greatly stabilized by glycerol (Engel et al., 2002). Furthermore, as far as tonicity of formulations is concerned, non-electrolytes are often preferred to salts as tonicity adjusters due to the potential problems salts cause in precipitating proteins (Pikal, 1990). It is to be noted that comprehensive studies - investigating the effect of numerous stabilizing additives - were published, wherein the attempt of stabilization via salts was virtually turned down (Sebeka et al., 2001). Yet, if that will become the rule is to be doubted, but currently the relevancy of protein stabilization via salts struggles to keep pace with other approaches, especially those using sugars and polyols.

Today, sugars and polyols enjoy a great popularity in being used as protein stabilizers. In contrast to salts, sugars and polyols contribute to protein stability not only in a non-specific way, but they additionally can protect proteins from chemical degradations such as oxidation (Li et al., 1996). In the majority of published studies, the stabilizing effect of sugars depends on their concentration, and 0.3 M (5%) sugar and polyol, respectively, has been proposed as a lower concentration limit (Arakawa et al., 1993). The issue is excellently addressed by a comprehensive review attributing the stabilization of proteins in aqueous media to the presence of weakly interacting cosolvents such as sugars and polyols (McClements, 2002). However, since it was published in a field not directly related to pharmaceuticals, the article – at least hitherto – was attracting little response.

The three classes of excipients presented above undoubtedly account for the lion's share of substances used for protein stabilization in liquids. Yet, a plurality of other components are frequently utilized, with amino acids, metal ions and polymers representing those being most widely-used.

Especially the field of protein stabilization by polymers is in rapid move, since in the last decade dramatic improvements in production and purification of tailor-made polymers have been achieved. E.g., cyclodextrins (especially hydroxypropyl- β -cyclodextrin) reveal biocompatibility, stability and solubilizing features and, hence, are frequently employed as stabilizers (Sharma et al., 2000). More importantly, efficient syntheses of new sugar-branched stabilizing cyclodextrins have meanwhile become a habit (Hattori, 2001). Whereas the stabilizing potential of poly(vinylpyrrolidone) – e.g., in terms of antibody solutions - in concentrations of ~1% is known since about one decade (Gombotz et al., 1994), other water-soluble polymers such as

polyethyleneimine have only recently been proved to effectively stabilize various proteins with polymer concentrations down to 0.01% (Andersson and Hatti-Kaul, 1999). Alternatively, polymers can be designed with utmost affinity to either potential destabilizers such as metal ions or to the designated protein. Although the main application of such polymers is deemed to be protein stabilization in gels (Bromberg, 2001) or in aqueous protein analytics (Pessela et al., 2003), rational applications in protein liquids are to be expected.

Of course, protein stability by new excipients can not always be resoundingly successful. Heralded as potent and efficacious stabilizers for instance for the stabilization of antibodies (Vangala et al., 2000), compatible solutes such as ectoin and hydroxyectoin fell short of the formulators' expectations, though further applications have been described (Borges et al., 2002). This is mainly because compatible solutes normally demand to be used in high concentrations (>3 M) and because they are high in price.

Although a general rule of stabilization can not be provided, in many cases proper adjustment of pH as well as an adequate choice of buffer system, surfactant and of one additional excipient such as sugar should provide conditions for sufficient protein shelf life.

10.3 General experimental procedures

A pharmaceutical active immunoglobulin (adalimumab, subclass G₁, 147 kDa) was to be formulated in an adequate solution in order to generate a liquid parenteral dosage form, revealing 50 mg/mL final drug concentration. Due to previous formulation experiments, a phosphate/citrate buffer system was proved to be superior to other buffer systems in terms of protein stabilization. Solution pH values of 5.2 and 6.0, respectively, were found to be favored. Consequently, dosage form (liquid) and drug concentration (50 mg/mL) were enjoined parameters and optimization had to be approached via addition of adequate excipients. All excipients used were of highest purity ("pro analysi" grade) and purchased from Merck KGaA, Darmstadt, Germany. Mannitol was sourced from Mallinckrodt Baker B.V., Deventer, Holland.

Analysis of visible particulate matter was conducted according to the regulation of Ph. Eur. 2002 (§ 2.9.20 Contamination with particulate matter – visible particles). Subvisible particulate matter analysis was realized via light obscuration (SVSS-C⁴⁰, PAMAS GmbH, Rutesheim, Germany). A Superose TM6 10/30 column (Amersham Pharmacia Europe GmbH, Freiburg, Germany) was implemented for SE-HPLC analysis (assessment of protein monomer content), applying a 0.5 mL/min flow rate of a PBS buffer with pH 7.5, and connected to UV₂₈₀ spectrophotometry, refractive index detection and MALS for on-line detection as described in Chapter 6. Analysis of each sample was performed at least in triplicate. Except stated otherwise, for all SE-HPLC data S_{rel} was below 0.13 and for all light obscuration data below 2.3.

Individual protein formulations were prepared via dilution of adalimumab concentrates (~70 mg/mL) with excipient stock solutions. The latter were generated by excipient dissolution in phosphate/citrate buffer medium. Prior to sterile filtration (0.2 μm , Minisart[®], Sartorius AG, Goettingen, Germany), pH adjustment was performed by adding of acid/base specimen of buffer components. All formulations were prepared at least in duplicate, and generated via final sterile filtration of solution batches into heat-sterilized (180 °C, 25 min) 2R glass vials (Schott Glas, Mainz, Germany) under aseptic laminar air flow conditions. Teflon coated butyl-rubber closures were sterilized via moist heat (121 °C) according to Ph. Eur. prior to usage. The formulations were subjected to 3 m-short-time storage at three different temperatures (5 °C, 25 °C, 40 °C).

Adalimumab concentrates were provided by diafiltration of adalimumab bulk solution via Vivaflow 50 units (cut-off 50 kDa, Vivascience AG, Hannover, Germany), using phosphate/citrate buffer medium for buffer exchange. Popular current processes for concentration and buffer exchange of biopharmaceutical solutions are based on IEX, SE-HPLC, ultra-/diafiltration and tangential flow filtration (Christy et al., 2002). Diafiltration was applied because purification, concentration and buffer exchange are rendered possible within a single-unit operation with variable flow dynamics, thus minimizing protein stress (Fig. 118).

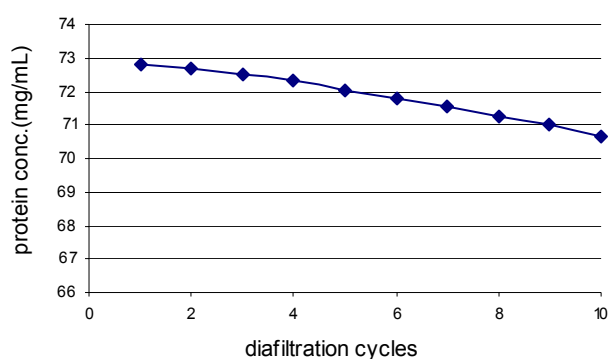


Fig. 118. Exemplified correlation of protein loss and number of diafiltration cycles. Each cycle performed accounted for a protein loss of ~0.25% of total protein. Generally, protein loss did not exceed 7% in the course of concentrate production.

Within one diafiltration cycle, protein concentration was doubled and re-diluted to the original concentration, except for the terminal concentration step. Hence, dissolved substances not intended for presence can effectively be removed (e.g., a 1.00% concentration can be downsized to 0.00098% within ten diafiltration cycles). Subsequent to purification and concentration, the adalimumab concentrates were centrifugated (5 °C, 3000 g, 20 min).

10.4 Evaluation of pH optimum

In order to evaluate the optimal solution pH (i.e., pH 5.2 or pH 6.0), three different adalimumab formulations were analyzed, varying solely in pH. Stability data of formulations containing 1 mg/mL Tween 80 are illustrated in Fig. 119.

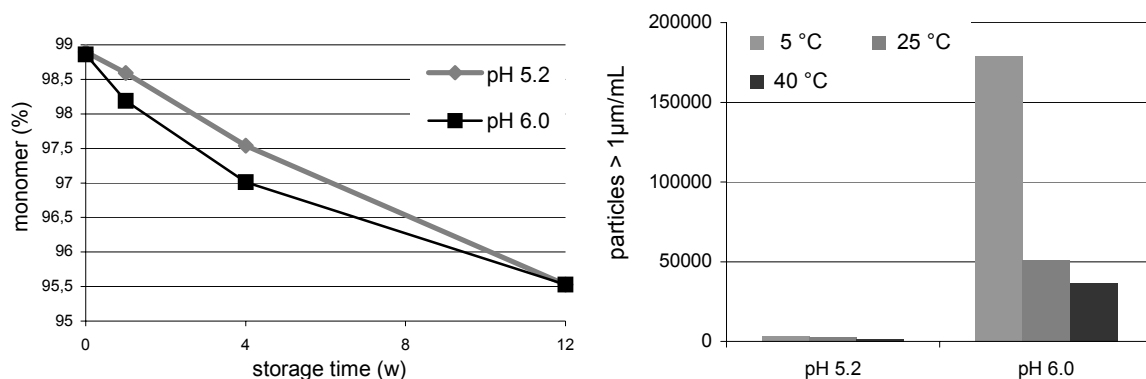


Fig. 119. Formulations containing 1 mg/mL Tween 80. Influence of formulation pH on monomer content (left) and subvisible particulate matter formation (right) during 40 °C storage.

Concerning the monomer content, no pH is to be favored, as both formulations exhibit comparable monomer losses at 40 °C storage, albeit differing slightly in the stability profile. Data of 25 °C storage conditions are similar to 40 °C data, whereas at 5 °C all protein solutions analyzed in the course of this study did virtually undergo no alterations in monomer content. Yet, this is to be expected, since the impact of both thermodynamic forces affecting protein stability (i.e., enthalpic and entropic forces) is shifted towards protein stabilization at lower temperatures (Wang, 1999; Kristjansson and Kinsella, 1991). Contrarily, a 6.0 solution pH did notably facilitate the formation of subvisible particulate matter during 12 w storage, regardless of the storage temperature. As the intensity of particulate matter formation is obviously connected with lower temperatures, the particles' origin is *prima facie* not to be assumed proteinic. In that regard, if severe particulate matter formation were merely due to protein instabilities, this prevalently is associated with exposure to elevated temperatures during storage tests (Constantino et al., 1995).

In case the formulations contained 6.16 mg/mL NaCl instead of Tween 80, the findings were substantiated (Fig. 120).

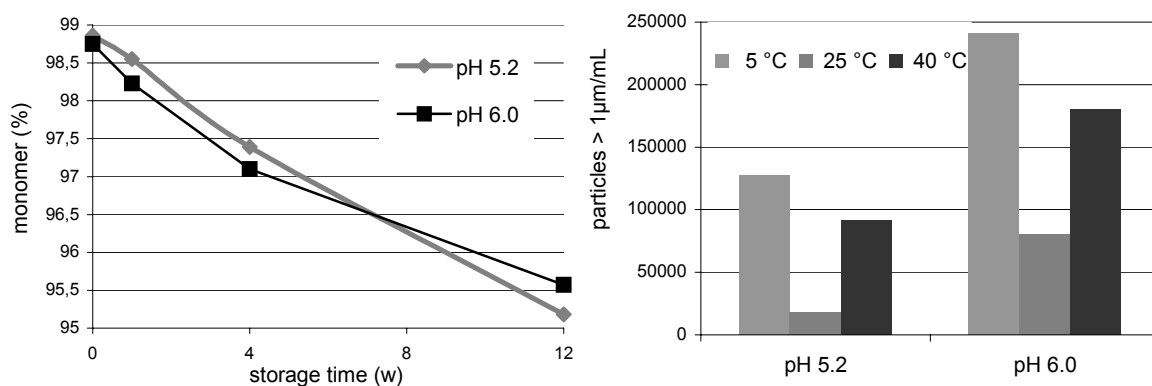


Fig. 120. Formulations containing 6.16 mg/mL NaCl. Influence of formulation pH on monomer content (left) and subvisible particulate matter formation (right) during 40 °C storage.

However, the addition of salt appeared to auxiliarily foster the formation of subvisible particles, since the number of particles greater than 1 μm is increased by a similar degree in both solutions. Furthermore, after 12 w SE-HPLC data ascribed the pH 6.0 solutions a greater monomer content than at pH 5.2 conditions, though the differences were minimal ($\sim 0.3\%$) and not corroborated by 25 $^{\circ}\text{C}$ results.

Hitherto, particle formation appeared to be facilitated by NaCl addition and pH 6.0 storage and to be opposed by Tween 80 addition and a solution pH of 5.2. Consequently, the question arises whether Tween 80 can alleviate particle contamination in solutions containing salts such as NaCl (Fig. 121).

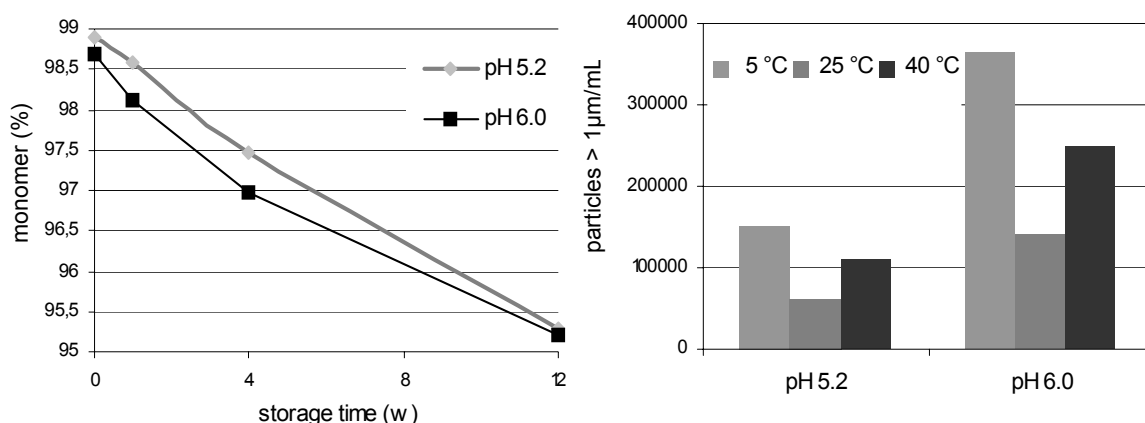


Fig. 121. Formulations containing 6.16 mg/mL NaCl and 1 mg/mL Tween 80. Influence of formulation pH on monomer content (left) and subvisible particulate matter formation (right) during 40 $^{\circ}\text{C}$ storage.

Yet, according to Fig. 121, once the formulations comprised salt, the addition of surfactant had no influence in terms of subvisible particle formation. Interestingly, in all samples particle numbers were maximal at lowest storage temperature (5 $^{\circ}\text{C}$), indicating the particle origin to be potentially due to inorganic material. Moreover, visible inspection of solutions containing salt revealed a slight turbidity after 4 w storage, regardless of the storage temperature. It is known that precipitation of visible inorganic components can be the result of storage at cold temperatures, even if the storage is temporarily. E.g., sodium phosphate buffers may yield the relatively insoluble $\text{Na}_2\text{HPO}_4 \cdot 12\text{H}_2\text{O}$ at 4 $^{\circ}\text{C}$ (Borchert et al., 1986). However, in terms of particulate matter being an evaluating criterion, a solution pH of 5.2 is to be prioritized.

The matter has to be approached differently as far as data of monomer content is concerned – as both solution pH values render identical monomer contents during storage and in case of NaCl-containing formulations (without Tween 80!) a pH of 6.0 appears to reveal even slightly higher stability. Yet, it is commonly accepted that at pH values towards neutral or even basic conditions proteins are prone to a broader variety of potential degradation mechanisms (Wang, 1999). E.g., carbonyl-amine reactions of un-ionized protein amides, (base-catalyzed) β -eliminations and deamidations are facilitated by higher pH values as well as various oxidation reactions (Akers and DeFelippis, 2000).

Hence, in summary, a solution pH of 5.2 is to be considered superior to a 6.0 value in terms of adalimumab long-time stability.

10.5 Stabilization by excipients

10.5.1 Surfactants

Interestingly, in terms of stabilizing protein liquids Tween 20 appears to inhere an absolute competitiveness - if not a minor superiority - on Tween 80 (Bam et al., 1998; Johnston, 1996). Yet, Tween 80 enjoys a by far greater popularity among the pharmaceutical formulators, according to the listings of recently FDA approved parenterals or compendia such as Physicians' Desk Reference. In order to scrutinize the stabilizing potential of surfactants on adalimumab, various amounts of Tween 80 were added to a protein solution containing 6.16 mg/mL NaCl. Generally, Tween 80 is assumed to stabilize proteins – inter alia - via binding through hydrophobic surface interaction. As the protein's surface characteristics are decisively influenced by the presence of salts, the effect of NaCl absence additionally was surveyed (Kheirloom et al., 1998) (Fig. 122).

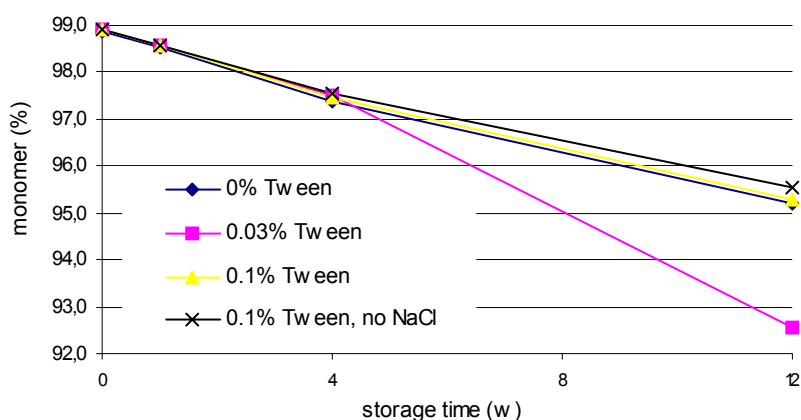


Fig. 122. Influence of Tween 80 on protein formulations containing 6.16 mg/mL NaCl (storage temperature 40 °C).

Pertaining to the data presented in Fig. 122, Tween 80 proved unable to bring any stabilizing influence to bear. If 0.03% Tween 80 was added, this even resulted in decreasing the monomer content after 12 w storage at 40 °C. In this realm, in the majority of articles addressing this topic the stabilizing impact of Tween 80 was shown to be related to increasing concentrations of surfactant, this being valid in the range from 0.001 to 1% (Arakawa et al., 2000). Thus, the data above seem agonizing - the more, as the analysis of the formulations in terms of subvisible particulate matter seemed to meet into a coherent picture (Fig. 123):

At all storage temperatures, the addition of Tween 80 led to a substantial growth of subvisible particle numbers, carried to the extremes at concentrations of 0.03% and, hence, backing the findings of SE-HPLC. Interestingly, the absence of NaCl proved to notably decrease

the formation of subvisible particles, regardless of the storage temperature. Similarly to the findings above, the addition of 0.1% Tween 80 to solutions of interleukin-1 β (100 $\mu\text{g}/\text{mL}$) was demonstrated to have no stabilizing effect in the pH below 7 (Gu et al., 1991). The potential of Tween 80 to destabilize proteins was also reported. E.g., 0.1 and 0.01% Tween 80, respectively, were shown to facilitate precipitation of bovin somatotropin at 54 $^{\circ}\text{C}$, whereas without Tween 80 the protein revealed enhanced stability (Akers and DeFelippis, 2000).

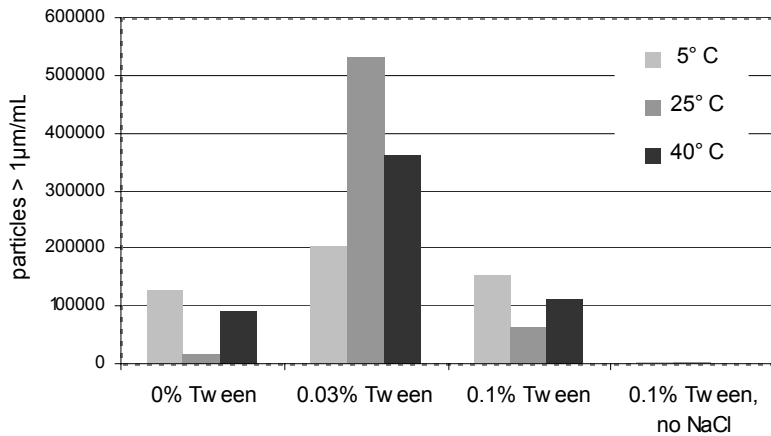


Fig. 123. Influence of Tween 80 on subvisible particulate matter formation during 40 $^{\circ}\text{C}$ storage of solutions containing 6.16 mg/mL NaCl. Note that absence of NaCl impedes particle contamination.

In contrast to the minor stabilizing impact on liquid solutions during storage, Tween 80 proved to confer notable stability towards adalimumab during freeze-thaw cycles (Fig. 124).

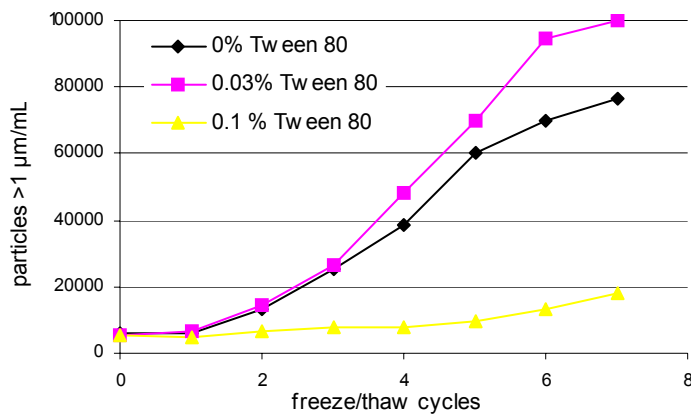


Fig. 124. Stressing protein solutions with varying contents of Tween 80 by means of freeze-thaw cycles led to a considerable increase of particulate matter at concentrations of Tween 80 below 0.1%.

Protein solutions were repeatedly subjected to stress via freezing (-80°C , 12 hrs) and thawing (5°C , 12 hrs), and the effect of Tween 80 was determined. The number of freeze-thaw (f/t) cycles applied was closely correlated to a gain in subvisible particulate matter. However, whereas the exertion of 5 f/t cycles on solutions with 0 or 0.03% Tween 80 content was reflected in a ~ 10 -fold increase in particle contamination (particles $\geq 1\ \mu\text{m}$), the situation virtually remained unchanged in 0.1% Tween 80 solutions. Seconding these findings by SE-HPLC analysis led to similar results (Fig. 125).

In close accordance to the results of numerous studies published where f/t cycles were exerted on other proteins, the stability of adalimumab decreases when exposed to repeated f/t stress and no surfactant is present. Conversely, the addition of surfactant shields the protein

against deleterious parameters associated with freezing/thawing, as the content of native monomer – what was verified with MALS – remained unchanged.

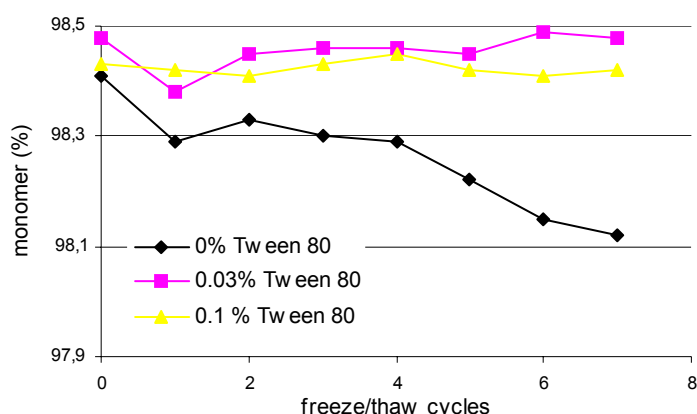


Fig. 125. Loss of monomer in adalimumab solutions varying in Tween 80 content in dependence of number of freeze-thaw cycles exerted.

Until the mid-1990s, this phenomenon was accounted to the protein's exposure to ice-water interfaces, as studies on individual proteins have demonstrated the greater denaturation during f/t cycles when proteins are frozen under conditions assumed to generate a large ice surface area than when conditions leading to less surface area are employed (Hsu et al., 1995). Yet, earlier studies demonstrated Tween 80 to inhere potential to protect adalimumab against f/t stress in concentrations of 0.001%, well below the CMC (Fraunhofer, 2002). Consequently, parameters of ice-water interfaces are not to be considered solely responsible for f/t denaturation of adalimumab, what was corroborated recently in proving sodium phosphate buffers to undergo pH shifts up to 3 pH units due to crystallization of the disodium salt (Pikal-Cleland et al., 2002).

Generally, formulators should be aware of the potential for Tween 80 to affect adversely the oxidative stability of proteins, despite its stabilizing impact on proteins. Unfortunately, it inheres the tendency to produce peroxides which can oxidize methionine and cysteine residues. This phenomenon was reported in studies involving the formulation development of Neupogen[®] (Herman et al., 1996) and recombinant human ciliary neurotrophic factor (Knepp et al., 1996).

In summary, the addition of 0.1% Tween 80 to adalimumab solutions is to be preferred. Though 0.1% Tween was demonstrated to improve the protein stability in stored liquids only marginally, the stabilizing effects during processes such as freezing and thawing are substantial. Anyway, addition of Tween 80 may emerge as great benefit, as freezing is a common unit operation in the production, storage and transport of protein pharmaceuticals (Cao et al., 2003). Additionally, the use of 0.1% Tween 80 in pharmaceuticals is well-accepted, demonstrated by the FDA approval of Orthoclone[™] (murine IgG2a) as early as 1986.

Besides Tween 80, the nonionic surfactant Solutol[®] HS15 was investigated in its potential to stabilize adalimumab. The protecting features of Solutol[®] in concentrations of 0.03 and 0.1% were shown recently in terms of aviscumin parenterals (Steckel et al., 2003). Hence, the influence

of Solutol[®] on adalimumab solutions in terms of particulate matter contamination were compared to protein solutions containing 0.1% Tween 80 (Fig. 126).

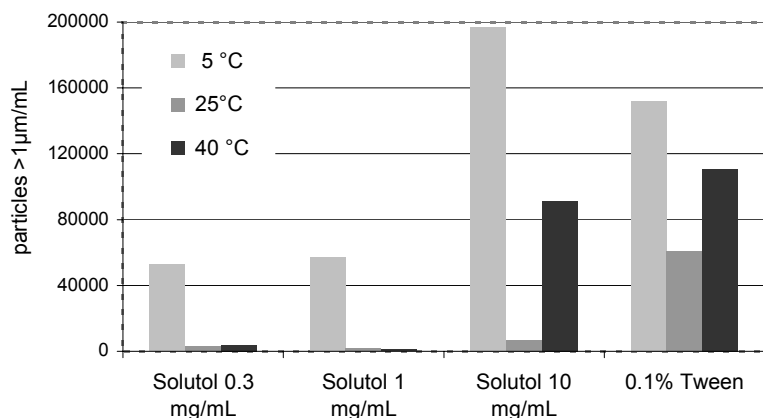


Fig. 126. Influence of various Solutol[®] concentrations on formation of particulate matter after 12 w storage in comparison to a solution containing 0.1% Tween 80.

In contrast to solutions with 0.03% and 0.1% Solutol[®], adalimumab solutions with 1% Solutol[®] and 0.1% Tween 80, respectively, exhibited a notable increase of particulate matter during storage. This positive influence of low Solutol[®] concentrations was not reflected in data of SE-HPLC analysis. After 12 w storage (40 °C), all solutions containing Solutol[®] revealed a loss in monomer content of ~0.5% in comparison to the reference (0.1% Tween 80). Especially the formation of hmw aggregates during storage is to be considered critically, as those are generally deemed as pre-stage specimen of potentially arising visible particulate matter (Fig. 127).

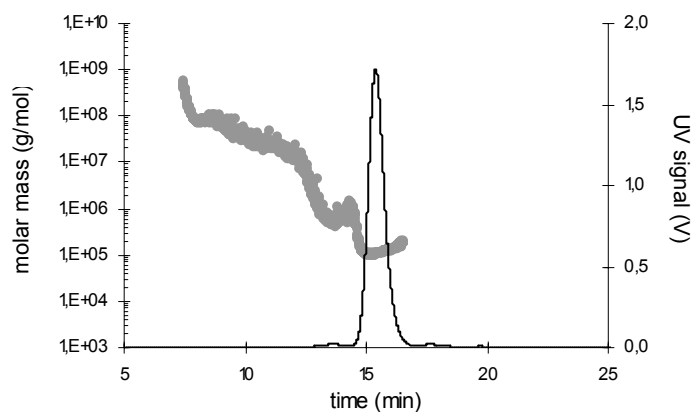


Fig. 127. Visualizing the presence of hmw protein specimen in a solution containing 0.1% Solutol. According to MALS (grey dots), aggregate molar masses equal up to nearly 10^9 Da, accounting for 2.6% of total protein (UV_{280} , black line). Storage at 40 °C for 12 w.

This experiment is suitable to illustrate the great advantages offered by MALS in the early-stage detection of hmw protein aggregates (Fig. 128). Due to its high sensitivity on large analytes, minimal concentrations thereof are sufficient to induce an immense response at the detector. E.g., the formation of hmw aggregates after 1 w storage (40 °C) could be verified by MALS - but was virtually not seizable by UV_{280} -detection.

As a consequence, Solutol has to be deleted from the list of potential stabilizers, as the formation of hmw ranges already in early stages of accelerated shelf life studies is generally not acceptable. The more, as even minimal amounts of protein (<0.1%) are known to contingently account for precipitation (Hoffman, 2000). The findings above fall into place with other data,

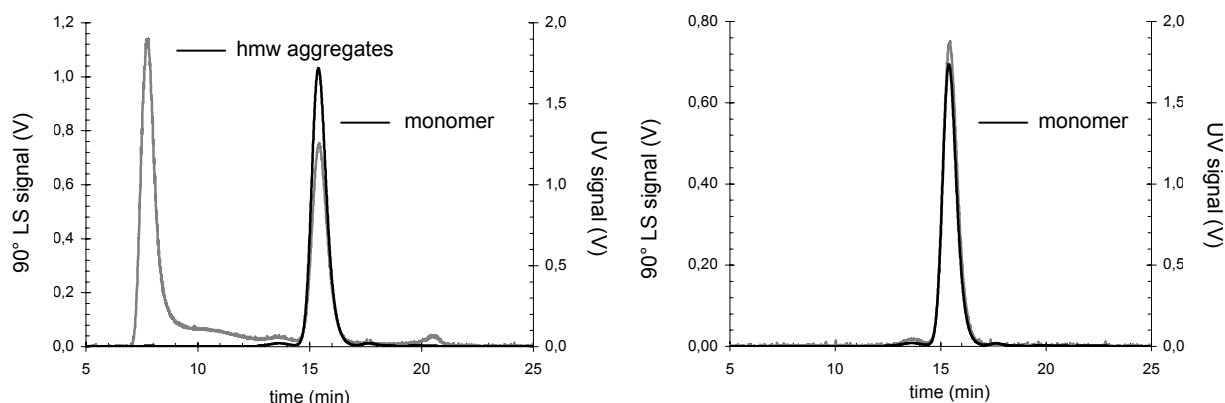


Fig. 128. Early-stage detection of hwm aggregates, emerging during 40 °C storage. Whereas no aggregates could be detected via UV₂₈₀ (black curve), MALS (grey curve) unambiguously proved the presence of hwm specimen. 1 w storage (left) versus original sample (right).

where higher concentrations (>1%) of Solutol[®] HS15 were shown to destabilize solutions of serpine-related protease inhibitor and avail visible particulate matter phenomena (Schmidt, 2003).

10.5.2 Polyols

Many sugars (e.g., sucrose, glucose, raffinose, trehalose) and polyols (e.g., glycerol, sorbitol, mannitol) are subsumed under the category of protein stabilizing co-solvents (Ebel et al., 2000). It is widely believed that those substances act primarily through a steric exclusion mechanism. E.g., polyols such as sorbitol are often used in order to stabilize parenterals, for instance in a number of lyophilized vaccine pharmaceuticals such as Mumps[™], Meruvax[™] II and Attenuvax[™] or intravenous administrable solutions such as Cardene[™].

Yet, in contrast to other excipients such as surfactants, sugars and polyols normally demand to be added in higher concentrations (>0.5 M) in order to deploy their complete stabilizing potential (McIntosh et al., 1998). As a consequence, sorbitol was added to adalimumab solutions in concentrations of 50 and 100 mg/mL, respectively, and subjected to 12 w storage (Fig. 129).

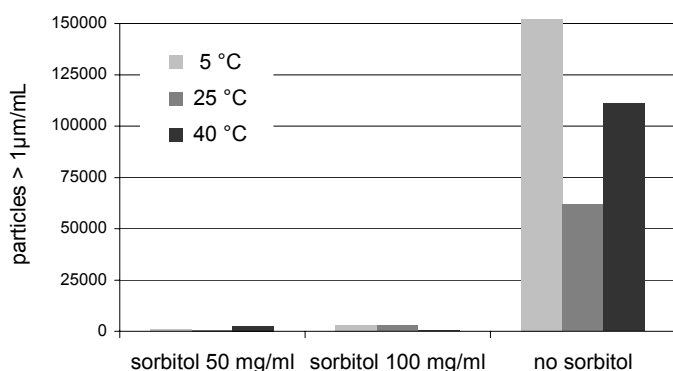


Fig. 129. Influence of sorbitol on particulate matter formation in adalimumab solutions during storage for 12 w.

As far as particulate matter is concerned, sorbitol apparently decreased the tendency for particle formation during storage, compared to solutions where no sorbitol was present. Thereby, the amount of added sorbitol did virtually not result in any differences. In terms of monomer content, the stabilizing effect of sorbitol was found to be closely concentration-dependent (Fig. 130).

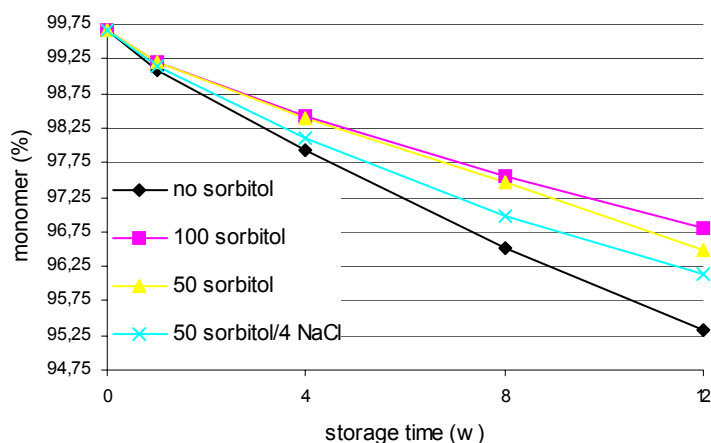


Fig. 130. Adalimumab stability in dependence on sorbitol concentration, reflected by content of protein monomer. Note that the presence of NaCl detracts from protein stability (numbers indicate concentrations in mg/mL; storage at 40 °C).

According to Fig. 130, the addition of 100 mg/mL sorbitol increases the content of monomer by ~1.5% during 12 w storage at 40 °C. Reducing the amount of excipient leads to a reduction of adalimumab stability. The findings are corroborated by recent investigations on the stability of horse immunoglobulins, where 180 mg/mL sorbitol were demonstrated to be superior to the addition of 90 mg/mL in terms of protein stabilization against heat stress (Rodrigues-Silva et al., 1999). That the stabilizing impact of sugars and sugar-derived polyols is concentration-dependent has repeatedly been reported (Chan et al., 1996; Fatouros et al., 1997). Interestingly, the addition of 4 mg/mL salt detracts notably from the stabilizing potential of sorbitol (- 0.25% monomer). However, inasmuch this observation can be correlated to the fact that NaCl was shown to foster the formation of subvisible particles in other adalimumab solutions during storage can – at present – not be explained sufficiently (refer to Fig. 123). On the other hand, the absence of NaCl in adalimumab solutions containing 0.1% Tween 80 leads to only a minimal increase in monomer content during shelf life experiments (refer to Fig. 122).

How does this match to the findings illustrated above? Trying to get to the bottom of the stabilization mechanism prevalently ascribed to polyols and sugars may be helpful: the steric/preferential exclusion mechanism of polyols has already been mentioned. Additionally, recent measurements of the influence of temperature on preferential interaction coefficients hypothesize the stabilization mechanism of some co-solvents to be highly temperature-dependent (Xie and Timasheff, 1997a). In this realm, at higher temperatures it was found that the stabilizing mechanism was due to a greater preferential accumulation of these excipients by the native state than by the denatured state (Xie and Timasheff, 1997b). Can sorbitol be thought to contribute to adalimumab stabilization in a manner to thermodynamically favor native state-sorbitol

interactions more than denatured state-sorbitol interactions? It is to be noted that this is not in complete accordance with the stabilizing mechanism of preferential exclusion, where the majority of stabilizing input is due to thermodynamically unfavorable interactions of hydrophobic protein sites – once denaturation occurred – with the surrounding water molecules.

Now the salt: at low concentrations, salts affect electrostatic shielding (according to Debye-Hueckel), leading to potential stabilization when there are major repulsive interactions leading to protein unfolding (Wang, 1999). At high concentrations salts are inducing preferential hydration of proteins, by keeping hydrophobic protein spots away from the water molecules (Kohn et al., 1997). Bearing in mind the amounts of NaCl added (4 mg/mL), both NaCl and sorbitol may be thought to figuratively compete for the native state adalimumab, with NaCl slightly in the fore. Hence - the stabilizing potential of sorbitol assumed to exceed that of NaCl -, NaCl addition has to be expected to detract from adalimumab stability, as demonstrated. Generally, if the derived hypothesis is to be come into consideration at all, the observations are expected to be continuable with other sugar-derived polyols. Corresponding data in terms of mannitol are presented in Fig. 131.

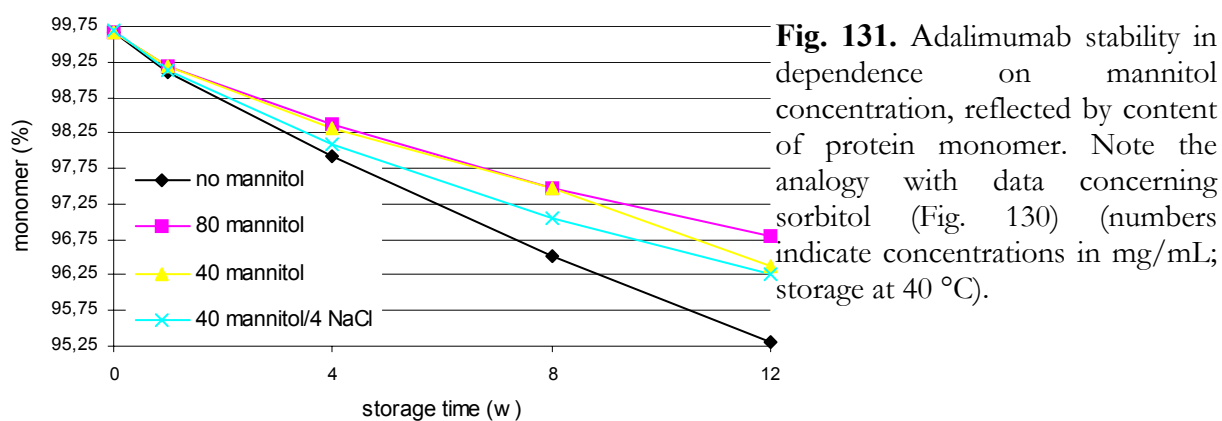


Fig. 131. Adalimumab stability in dependence on mannitol concentration, reflected by content of protein monomer. Note the analogy with data concerning sorbitol (Fig. 130) (numbers indicate concentrations in mg/mL; storage at 40 °C).

Basically, the findings on sorbitol are substantiated by addition of mannitol to adalimumab solutions: (1) solutions enriched by 80 mg/mL mannitol exceed mannitol-free solutions in protein monomer content by ~1.5% after 12 w storage (40 °C), (2) the stabilizing input of mannitol is oriented towards a concentration-dependent profile, (3) and NaCl reduces the forfending features of mannitol. Interestingly, these data are corroborated by identical experiments performed at 25 °C.

In order to prevent misconceiving: the addition of sorbitol or mannitol to protein solutions is not always associated with a gain in protein stability. For instance, sorbitol offered no advantage against precipitation of porcine growth hormone when evaluated during thermal or interfacial stress conditions – in contrast to Tween 20 and hydroxypropyl- β -cyclodextrin, respectively (Charman et al., 1993).

In summary, it may be concluded that adalimumab is stabilized via preferential accumulation of both sorbitol and mannitol by the native state. This mechanism is interfered by

NaCl, which was shown to impede protein stabilization via polyols – the findings that NaCl does not detract from adalimumab stability when added to protein solutions containing 0.1% Tween 80 is consistent with the conclusions above, as in that case the protecting polyol contribution can not be interfered.

excipients (mg/mL)	% monomer	% aggregate	% fragment	aggregate share (%) in the amount of monomer loss
no excipient	95.32	1.68	3.02	35.7
sorbitol 50	96.49	1.40	2.11	39.9
sorbitol 50 NaCl 4	96.13	1.38	2.49	35.7
sorbitol 100	96.80	1.21	1.99	37.8
mannitol 40	96.37	1.42	2.21	39.1
mannitol 40 NaCl 4	96.26	1.40	2.34	37.4
mannitol 80	96.81	1.28	1.91	39.9

Table 20. Impact of excipient addition on adalimumab stability after 12 w storage at 40 °C. Data derived via SE-HPLC.

According to Table 20, the amount of native monomer assessed in each adalimumab formulation is dependent on the addition of polyols and on the excipient composite. Commensurately, the amounts of aggregate and fragment fractions vary. Thereby, the aggregate share in the amount of monomer loss remains constant, regardless of the excipients added, if any. In other words, the ratio of adalimumab aggregates and fragments are in firm balance (i.e., ~38% aggregates and ~72% fragments), and this equilibrium is not influenced by the addition of polyols and salts. In this concern, it is prevalently accepted that the major consequence of protein denaturation is aggregation (Wang, 1999). Then, if sorbitol and mannitol were contributing to adalimumab stability solely via native state stabilization, this should be reflected in alterations of the aggregate share. Since this is not the case, there has to be a further mechanism of adalimumab stabilization by sorbitol/mannitol, resulting in an impediment of fragmentation processes.

In this realm, protein fragmentation is often due to electron transport processes and ion desorption, to be observed in protein oxidation by means of vial headspace O₂ (Goolcharran et al., 2000) or induced during protein analytics, e.g., in electrospray mass spectrometry (Thomson, 1997). It was reported earlier that mannitol in concentrations above ~10 mg/mL is able to inhibit oxidative degradation via complexation of metal ions (Li et al., 1996). Recently, mannitol was demonstrated to reveal free radical quenching features, since the ·OH radical mediated fragmentation of serum albumin was effectively hampered by mannitol (Jaiswal et al., 2002).

In case mannitol/sorbitol were indeed revealing potential to protect adalimumab from oxidative degradation, this were deemed a valorizing characteristic: generally, special care has to

be taken in choosing the right means of protein stabilization against oxidation. E.g., chelates such as Fe(III)-EDTA – commonly used in reducing oxidative fragmentation – were demonstrated to induce rather than prevent oxidation (Zhao et al., 1996).

In conclusion, it was shown that adalimumab can effectively be stabilized by adding mannitol or sorbitol. Besides contributing to protein stability by native state protection, those substances were unveiled to stabilize the protein via a further mechanism, thereby reducing fragmentation during long-term storage.

10.5.3 Salts

Beyond doubt, NaCl is the most-used salt in the formulation of protein parenterals. Whereas NaCl was evidenced to detract from adalimumab stability in the presence of polyols and not to increase protein stability if representing the exclusive excipient, it was often found to prevent proteins from degradation, even in a concentration-dependent manner (Mayr and Schmid, 1993). Generally, in pondering on the potential stabilizing effect of salts acting according to the Hoffmeister lyotropic series provides a rough rule of thumb. Hence, using the anionic acetate instead of chloride as counterion in sodium salts may be promising.

As illustrated in Fig. 132, the individual solutions reveal different protein stability.

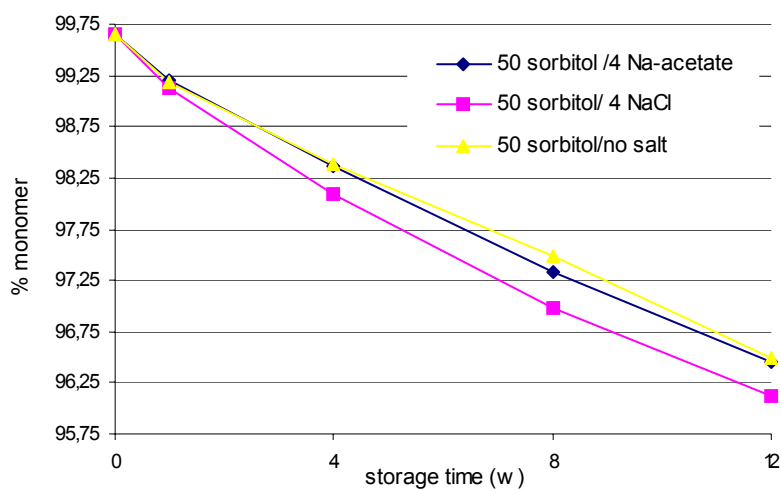


Fig. 132. Stability of adalimumab in solutions containing sorbitol in dependence on salt addition (numbers indicate concentrations in mg/mL; storage at 40 °C).

Obviously, the adalimumab solution containing NaCl is stacked against protein stability, since as early as after 4 w storage (40 °C) formulations containing NaCl and sodium acetate, respectively, exceed the NaCl enriched batch in monomer content by ~0.25%, adding up to a >0.4% difference after 12 w. Consequently, sodium acetate is deemed to contribute more to adalimumab stability than sodium chloride. Due to the Hoffmeister series, acetate ions are attributed a greater ionic strength than chloride ions. Consequently, acetate enhances hydrophobic interactions and reduces solubility of the protein's hydrophobic spots, thus resulting in preferential hydration (Wang, 1999) – providing a sound explanation for the data

above, which are corroborated by the results of 25 °C storage. Nevertheless, the addition of sodium acetate has no share in additional protein stabilization, since the salt-free formulation inheres identical monomer content.

In comparison to both other formulations, acetate containing formulations exhibit a greater number of particles beyond 1 μm ($\sim 180,000/\text{mL}$ versus $<6,000/\text{mL}$).

One main aspect in this realm attends the cationic counterion of the phosphate buffer system, as extreme pH shifts (~ 3 pH units) were reported to occur in sodium phosphate buffer during freezing, what can negatively affect protein stability (Pikal-Cleland and Carpenter, 2001). Yet, an indispensable prerequisite for sodium phosphate buffer use is its basic compatibility with adalimumab in liquid – not frozen – state (Fig. 133).

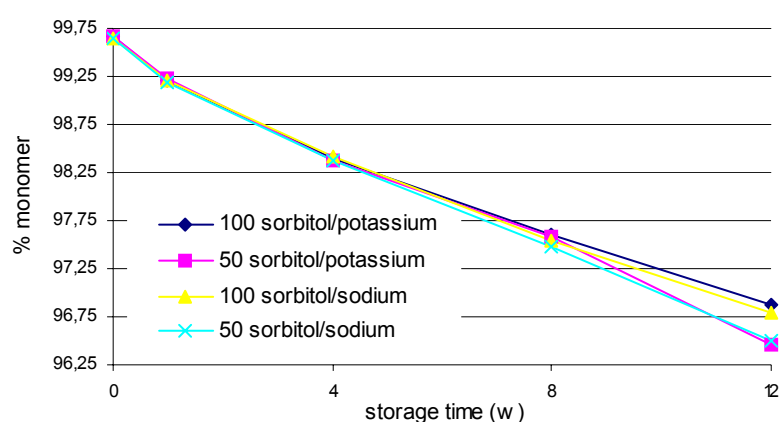


Fig. 133. Adalimumab stability in phosphate buffer systems using sodium and potassium as cationic counterions. Buffer concentration ~ 10 mM, numbers indicate sorbitol concentrations in mg/mL; storage at 40 °C).

As illustrated in Fig. 133, the stability of adalimumab dissolved in potassium phosphate buffer equals that determined in sodium phosphate buffers. Data of storage tests performed at 25 °C substantiated these findings. Additionally, both buffer systems equaled in particulate matter contamination. Hence, potassium phosphate is considered to be preferred in liquid protein formulations.

In summary, it can be concluded that the addition of NaCl should be avoided in case of adalimumab solutions. If the presence of salts is favored – e.g., by reasons of osmolality – the addition of sodium acetate proved to be superior to sodium chloride. Similarly, potassium based phosphate buffer systems equaled sodium phosphate buffer systems in terms of adalimumab stability. Given the background of the substantial pitfalls associated with sodium phosphate buffers in f/t processes, it is to be dissuaded from its use.

10.6 Summary

This chapter was dedicated to the formulation of liquid protein parenterals. Concerning to theory, prevalent strategies in liquid protein formulation were highlighted, actual mainstream

trends were outlined and both assets and drawbacks of the most popular excipients were displayed within a short literature review.

In practical realm, a laboratory case study was demonstrated, encompassing protein bulk preparation and studies on pH optima and stabilizing excipients. Thereby, the influence of processing parameters such as freeze/thawing were taken into consideration, e.g., in case of surfactant concentration and choice of cationic counterion of the phosphate buffer system.

Primarily, a solution pH of 5.2 and the addition of 0.1% Tween 80 were found to be favored against other alternatives. Protein stability and particulate matter contamination after f/t studies and (accelerated) storage tests were evaluating criteria.

Furthermore, polyols such as mannitol and sorbitol were demonstrated to substantially contribute to protein stability with virtually identical potency. Preferential accumulation at the native state protein was found to be not the only stabilization pathway, as both protein aggregation and fragmentation were impeded.

NaCl was evidenced to detract from protein stability, once polyols were present. Yet, the addition of sodium acetate was shown to inhere no deleterious impact on protein stability.

The data merge in a conclusive pattern and can be transferred into the suggestion of a promising formulation, comprising the parameters potassium phosphate buffer, pH 5.2, 0.1% Tween 80 and the addition of ~50 mg/mL mannitol or sorbitol – aiming at final osmolality values of ~300 mosM/kg.

11 Summary, conclusions and prospective

Due to enormous progress in recombinant DNA techniques and methodology, a multitude of biosynthetic, pharmaceutically relevant polypeptides and proteins became available in the past decade and have been employed in numerous pharmaceutical products. Concomitantly, substantial progress was made in pharmaceutical formulation development of peptides and proteins, inasmuch as many challenges in formulating these compounds in products with optimal therapeutic effects and shelf life were successfully approached. Additionally, new drug delivery systems – e.g., based on polymeric materials – will most likely enlarge the spectrum of future proteinic dosage forms, where today solutions and lyophilized products take center stage. Yet, due to the proneness of proteins to degradation - what can affect pharmaceutical relevant features such as biological activity and immunogenicity -, scrutinizing the homogeneity of protein formulations is of utmost importance. Hence, the development and implementation of new analytical techniques in order to keep pace is highly desired. It was the aim of this thesis to evaluate the applicability of asymmetrical flow field flow fractionation (AF4) in pharmaceutical protein analytics, to compare AF4 performance with established state-of-the-art methods and to reveal the effectivity of inherent AF4 characteristics in demanding analytical tasks.

The Theoretical Section encompasses **Chapter 2**, wherein the family of field-flow fractionation techniques is introduced, as well as **Chapter 3** (attending to protein aggregation) and **Chapter 4**, which provides an insight into multi-angle light scattering. The Theoretical Section is summarized in **Chapter 5**.

Chapter 6 attends to the general applicability of (semi-)chromatographic AF4 in protein analysis. The correlation of cross flow progression with increased resolution was exemplified by the separation of human serum albumin (HSA), thereby rendering the (base-line) separation of HSA specimen into monomer, dimer, trimer and tetramer possible. Due to the AF4 feature to discretionarily alter the resolution power within one separation run, the fractionation of higher-order aggregates and insoluble, precipitated protein was successfully performed.

System variables and parameters of fractionation were investigated, revealing that sample loads differing more than two orders of magnitude did not negatively affect data reproducibility. Whereas up to now cross flow intensity was deemed to predominantly account for contingent sample loss during AF4 experiments, analysis of proteins with varying hydrophilicity proved the preceding focusing step to contribute notably for that phenomenon. How to overcome potential drawbacks such as sample-membrane interactions by adequate choice of the ultrafiltration membrane as well as carrier liquid composition was illustrated.

Given the background that effective AF4 fractionations are due to differences in analyte size – i.e., in diffusion coefficients –, the separation of equal-sized proteins is *prima facie* considered to be impractical. Yet, the retaining impact of sample-membrane interaction was evidenced to decrease the effective diffusion coefficient, resulting in successful fractionations of proteins differing ~1% in size (i.e., G-CSF, 19.6 kDa versus IFN- α 2a, 19.4 kDa). In this realm, the normal mode elution order of smaller analytes eluting prior to larger ones was shown to be invertible, exemplified by the elution of a 40 kDa analyte prior to IFN- α 2a.

AF4 potency in analysis of insoluble high molecular weight (hmw) aggregates was compared with data derived by established methods such as light obscuration and Coulter technique, verifying the competitiveness of AF4.

A comparative study of AF4 with size exclusion chromatography (SE-HPLC) unveiled SE-HPLC to inhere higher recovery rates and AF4 to exhibit greater resolution. Coupling both techniques with multi-angle light scattering (MALS) detection systems disclosed SE-HPLC to induce artifacts concerning hmw aggregate quantification. Moreover, in contrast to SE-HPLC, AF4 was capable of seizing undissolved and precipitated protein specimen, thus making AF4 a promising alternative in the analysis of protein pharmaceuticals.

AF4's ability to separate undissolved sample components proved to be an indispensable feature in the analysis of a pharmaceutical protein formulated within siliconized disposable syringes, which was attended to in **Chapter 7**. During long-term storage, visible particulate matter developed sporadically within the syringe volumes, raising the question of the particles' origin. Since protein instabilities were not to be accounted for being the particle source – verified by several analytical methods –, silicone oil detachment and subsequent coalescence came into question, as the barrel siliconization process was lacking a final heat curing step. Thus, an AF4 application was developed, intending to separate μm sized silicone oil droplets. The task was approached by analysis of silicone oil emulsions, followed by the fractionation of ultrasound-stressed syringe volumes containing detached and coalesced silicone oil after stress exertion. Unambiguously, detached silicone oil was evidenced by AF4 to account for visible particulate matter in the syringe volumes, corroborated by MALS and refractive index detection as well as light microscopy and syringe frictional drag analysis. Subsequently to artificially induced protein aggregation of particle-containing syringe volumes, AF4 was able to separate silicone oil droplets, protein monomer and aggregates as individual fractions within one single run. Finally, AF4 enabled access to data on protein drug stability and insights into protein adsorption tendencies on coalesced silicone oil specimen – thereby providing valuable data which otherwise would have required a variety of various analytical techniques.

In **Chapter 8** the suitability of AF4 in overall-characterization of gelatin nanoparticles was explored. The efficacy of providing hmw gelatin bulk material by various desolvation steps was evaluated by SE-HPLC and AF4. Due to the absence of shear degradation phenomena, AF4 was demonstrated to enable more moderate separation conditions than SE-HPLC, verified by on-line determination of analyte molecular weight via MALS.

Gelatin nanoparticles were characterized by means of AF4/MALS with respect to size and size distributions and the data were compared to results of photon correlation spectroscopy (PCS) and scanning electron microscopy (SEM). Because of the precedent separation step via AF4, data derived by MALS revealed a greater veracity than PCS results, where the size assessment of nanoparticles relied on batch experiments. Whereas PCS attributed unloaded and DNA plasmid loaded nanoparticles virtually unimodal size distributions, both AF4/MALS and SEM demonstrated the nanoparticles to span a broad size range. Furthermore, loaded and unloaded nanoparticles were unveiled to exhibit only minimal differences in size, thus providing information on the interplay of nanoparticles and plasmid strands.

For the first time, the separation of nanocolloidal drug carrier and designated pharmaceutical payload was established. Additionally to drug carrier characteristics, data on the loading efficacy could be yielded. Furthermore, nanoparticle shelf life stability and extent of potential drug decomplexation could be determined.

Bearing in mind colloidal, polymer-based drug delivery carriers gaining increasing importance, that very AF4 application is expected to accommodate the demand for accurate analytics, as the pharmaceutical product can be characterized in both qualitative and quantitative terms.

In **Chapter 9** a case study of particulate matter analysis of a pharmaceutical antibody solution is presented, wherein individual vials of one production lot developed visible components at random during long-term storage. In order to (a) provide evidence on the presence of the contamination, (b) to attempt particulate entity quantification and (c) to elucidate particles' nature, a multiplicity of analytical techniques were applied, encompassing particle counting (optical inspection, light obscuration, light microscopy), protein characterization techniques (SE-HPLC, polyacrylamide gel electrophoresis, AF4, microcalorimetry) and particle separation techniques (sterile filtration, AF4).

Attempts to isolate the particulate components by AF4 or filtration techniques provided no further indications of the particle's origin.

Virtually no alterations in protein characteristics were monitored between contaminated and particle-free vial volumes, respectively. Solely, microcalorimetric data of contaminated vial volumes resembled those of immunoglobulin solutions exposed to heat stress prior to analytics.

Consequently, protein instabilities were assumed not to cause the visible contamination.

The topic of liquid protein parenterals, protein instability and particulate matter was completed by presenting a formulation process of an immunoglobulin into a liquid formulation in **Chapter 10**. Prevalent strategies and mainstream trends of liquid protein formulation were introduced by reviewing latest publications on the issue.

Parameters revealing decisive influence on the protein's long-term stability such as solution pH as well as type and concentration of excipients were evaluated by means of accelerated stability studies at various storage temperatures. Additionally, processing parameters, e.g., freeze/thawing, were assessed evaluating criteria in terms of surfactant and buffer choice.

The addition of NaCl was shown to detract from protein stability and to facilitate the formation of particulate matter. Non-deleterious alternatives of salt additives were discovered.

On the other hand, the addition of polyols such as mannitol and sorbitol was demonstrated to notably contribute to the immunoglobulin stability. Preferential accumulation at the native state protein was thought to be the mechanism for reducing aggregation phenomena of the protein. Besides, the extent of fragmentation was reduced by polyols, indicating a second pathway of stabilization, which was hypothesized to be hampering of oxidation processes. Due to detailed investigations, a proposal pertaining an optimal formulation could be made in the course of that case study.

This thesis has shown that asymmetrical flow field-flow fractionation (AF) can effectively be used to monitor protein stability in a broad variety of pharmaceutical formulations. Especially in the characterization of the most common outcome of physical instability – i.e., protein aggregation – the potential of AF4 has comprehensively been demonstrated. Moreover, AF4 applications and separation tasks within pharmaceutical analytics considered hitherto impractical or at least highly challenging were successfully performed. Facing increasingly complex liquid- or colloidal-based formulations, with this knowledge practice and research in pharmaceutical analytics can take a notable step forward.

12 References

- Abbott GmbH & Co. KG, Ludwigshafen, Germany, Department Pharmaceutical Development/ Parenterals; Laboratory report: information on adalimumab; Baust, L.; Schroer, C.; Fraunhofer, W., Ludwigshafen (2000)
- Adam, N.; Gosh, P., Hyaluronan molecular weight and polydispersity in some commercial intra-articular injectable preparations and in synovial fluid, *Inflammation Res.*, 50 (2001) 294-299
- Akers, M. J.; DeFelippis, M. R., Peptides and proteins as parenteral solutions, in *Pharmaceutical formulation development of peptides and proteins*, ed. by Frokjaer, S; Hovgaard, L. (2000) 145-177
- Alkan, S. S.; Braun, D. G., Epitope mapping of human recombinant interferon alpha molecules by monoclonal antibodies, *Ciba Foundation Symposium*, 119 (1986) 264-278
- Allison, S. D.; Dong, A.; Carpenter, J. F., Counteracting effects of thiocyanate and sucrose on chymotrypsinogen secondary structure and aggregation during freezing, drying and rehydration, 71 (1996) 2022-2032
- Allwood, M. C.; *Pharmaceutical aspects of parenteral nutrition: from now to the future*, *Nutrition*, 16 (2000) 615-618
- Allwood, M. C.; Martin, H.; Greenwood, M.; Maunder, M., Precipitation of trace elements in parenteral nutrition mixtures, *Clinical Nutrition*, 17 (1998) 223-226
- Almeida, A. T.; Salvadori, M. C.; Petri, D. F., Enolase adsorption onto hydrophobic and hydrophilic solid surfaces, *Langmuir*, 18 (2002) 6914-6920
- Andersen, S. O., Characteristic properties of proteins from pre-ecdysial cuticle of larvae and pupae of the mealworm *Tenebrio molitor*, *Insect Biochem. and Mol. Biol.*, 32 (2002) 1077-1087
- Anderson, R. R.; Martello, D. V.; Strazisar, B. R.; White, C. M., Qualitative and semi-quantitative analysis of semi-volatile organics from ambient air fine-particulate matter, PM_{2.5}, ACS – Division of Fuel Chemistry, Reprints of symposia, 46 (2001) 604-605
- Anderson, D. E.; Becktel, W. J.; Dahlquist, F. W., pH-induced denaturation of proteins: a single salt bridge contributes 3-5 kcal/mol to the free energy of folding of T4 lysozyme, *Biochemistry*, 29 (1990) 2403-2408
- Andersson, M.; Wittgren, B.; Wahlund, K. G., Ultrahigh molar mass component detected in ethylhydroxyethyl cellulose by asymmetrical flow field-flow fractionation coupled to multiangle light scattering, *Anal. Chem.*, 73 (2001) 4852-4861
- Andersson, M. M.; Hatti-Kaul, R., Protein stabilising effect of polyethyleneimine, *J. Biotechnol.*, 72 (1999) 21-31

- Andya, J. D.; Maa, Y.-F.; Constantino, H. R.; Nguyen, P.-A.; Dasovich, N.; Sweeney, T. D.; Hsu, C. C.; Shire, S. J., The effect of formulation excipients on protein stability and aerosol performance of spray-dried powders of a recombinant humanized anti-IgE monoclonal antibody, *Pharm. Res.*, 16 (1999) 350-358
- Antonsen, K. P.; Gombotz, W. R.; Hoffman, A. S., Attempts to stabilize a monoclonal antibody with water soluble synthetic polymers of varying hydrophobicity, *J. Biomater. Sci. Polymer Edn.*, 6 (1994) 55-65
- Arakawa, T.; Prestrelski, S. J.; Kenney, W. C.; Carpenter, J. F., Factors affecting short-term and long-term stabilities of proteins, *Adv. Drug Deliv. Rev.*, 46 (2001) 307-326
- Arakawa, T.; Kita, Y., Protection of bovine serum albumin for aggregation by Tween 80, *J. Pharm. Sci.*, 89 (2000) 646-651
- Arakawa, T.; Philo, J. S., Applications of analytical ultracentrifuge to molecular biology and pharmaceutical science, *Yaku. Zass.*, 119 (1999) 597-611
- Arakawa, T.; Prestrelski, S. J.; Kenney, W. C.; Carpenter, J. F., Factors affecting short-term and long-term stabilities of proteins, *Adv. Drug Deliv. Rev.*, 10 (1993) 1-28
- Arakawa, T.; Kita, Y.; Carpenter, J. F., Protein-solvent interactions in pharmaceutical formulations, *Pharm. Res.*, 8 (1991) 285-291
- Arakawa, T.; Timasheff, S. N., Mechanism of polyethylene glycol interaction with proteins, *Biochemistry*, 24 (1985) 6756-6762
- Arfvidsson, C.; Wahlund, K. G., Time-minimized determination of ribosome and tRNA levels in bacterial cells using flow field-flow fractionation, *Anal. Biochem.*, 313 (2003) 76-85
- Astefieva, I. V.; Eberlein, G. A.; Wang, Y. J., Absolute online molecular mass analysis of basic fibroblast growth factor and its multimers by reversed-phase liquid chromatography with multi-angle laser light scattering detection, *J. Chromatogr. A*, 740 (1996) 215-229
- Azuaga, A. I.; Dobson, C. M.; Mateo, P. L.; Conejero-Lara, F., Unfolding and aggregation during the thermal denaturation of streptokinase, *J. Biochem.*, 269 (2002) 4121-4133
- Backhouse, C. M.; Ball, P. R.; Booth, S.; et al., Particulate contaminants of intravenous medications and infusions, *J. Pharm. Pharmacol.*, 39 (1987) 241-245
- Balakrishnan, M.; Agarwal, G. P.; Cooney, C. L., Study of protein transmission through ultrafiltration membranes, *J. Membr. Sci.*, 85 (1993) 111-128
- Bam, N. B.; Cleland, J. L.; Yang, J.; Manning, M. C.; Carpenter, J. F.; Kelley, R. F.; Randolph, T. W., Tween protects recombinant human growth hormone against agitation-induced damage via hydrophobic interactions, *J. Pharm. Sci.*, 87 (1998) 1554-1559
- Bam, N. B.; Cleland, J. L.; Randolph, T. W., Molten globule intermediate of recombinant human growth hormone: stabilization with surfactants, *Biotechnol. Prog.*, 12 (1996) 801-809

- Barber, T. A.; Pavek-Hicks, C.; Williams, J., Automated performance of particulate matter testing for parenteral products, *Proc. Int. Symp. Lab. Autom. Rob.*, Meeting Date 1991 (1992) 154-186
- Barman, B. N.; Moon, M. H., Sample preparation and choice of carrier liquid in field-flow fractionation, in *Field-flow fractionation handbook*, ed. by Schimpf, M. E.; Caldwell, C.; Giddings, J. C. (2000) 189-198
- Barth, H. G.; Boyes, B. E.; Jackson, C., Size exclusion chromatography, *Anal. Chem.*, 66 (1994) 595R-620R
- Bartkowski, R.; Kitchel, R.; Peckham, N.; Margulis, L., Aggregation of recombinant bovine granulocyte colony stimulating factor in solution, *J. Protein Chem.*, 21 (2002) 137-143
- Battersby, J. E.; Hancock, W. S.; Connova-Davis, E.; Oeswein, J.; O'Connor, B., Diketopiperazine formation and N-terminal degradation in recombinant human growth hormone, *Int. J. Peptide Protein Res.*, 44 (1994) 215-222
- Beckett, R.; Bigelow, J. C.; Zhang, J.; Giddings, J. C., Analysis of humic substances using field-flow fractionation, in *Influence of aquatic humic substances on fate and treatment of pollutants*, ed. by MacCarthy, P.; Suffet, I. H., ACS Advances in Chemistry Series, 219 (1988) Chapter 5
- Beckton-Dickinson, Market research conducted by an independent source for BD Pharmaceutical Systems, New Jersey, USA (1998)
- Benedetti, M.; Ranville, J. F.; Ponthieu, M.; Pinheiro, J. P., Field-flow fractionation characterization and binding properties of particulate and colloidal organic matter from the Rio Amazon and the Rio Negro, *Org. Geochem.*, 33 (2002) 269-279
- Benedetto, A. V.; Lewis, A. T., Injecting 1000 centistoke liquid silicone with ease and precision, *Dermatol. Surg.*, 29 (2003) 211-214
- Benincasa, M. A.; Cartoni, G.; Imperia, N., Effects of ionic strength and electrolyte composition on the aggregation of fractionated humic substances studied by flow field-flow fractionation, *J. Sep. Sci.*, 25 (2002) 405-415
- Benincasa, M. A.; Giddings, J. C., Separation and molecular weight distribution of anionic and cationic water-soluble polymers by flow field-flow fractionation, *Anal. Chem.*, 64 (1992) 790-798
- Bennett, M. J.; Choe, S.; Eisenberg, D., Domain swapping: entangling alliances between proteins, *Proc. Natl. Acad. Sci. USA*, 91 (1994) 3127-3131
- Berg, H. C.; Purcell, E. M., A method for separating according to mass a mixture of macromolecules or small particles suspended in a fluid, 3. experiments in a centrifugal fluid, *Proc. Natl. Acad. Sci. USA*, 58 (1967) 1821-1818
- Bernstein, R. K., Clouding and deactivation of clear (regular) human insulin: association with silicone oil from disposable syringes?, *Diabetes Care*, 10 (1987) 786-787

- Betts, S.; Speed, M.; King, J., Detection of early aggregation intermediates by native gel electrophoresis and native western blotting, *Methods Enzymol.*, 309 (1999) 333-350
- Bohren, C. F.; Hirleman, E. D., *Applied Optics*, 30 (1991)
- Bondos, S. E.; Bicknell, A., Detection and prevention of protein aggregation before, during and after purification, *Anal. Biochem.*, 316 (2003) 223-231
- Bondos, S. E.; Sligar, S.; Jonas, J., High pressure denaturation of apomyoglobin, *Biochim. Biophys. Acta*, 1480 (2000) 353-364
- Boom, F. A.; van der Veen, J.; Verbrugge, P.; van de Vaart, F. J.; Paalman, A. C.; Vos, T., Particulate matter determination in LVPs produced in Dutch hospital pharmacies. Part 2: overview of the results, *PDA J. Pharm. Sci. Technol.*, 54 (2000) 343-358
- Borchert, S. J.; Abe, A.; Aldrich, D. S.; Fox, L. E.; Freeman, J. E.; White, R. D., Particulate matter in parenteral products: a review, *PDA J. Pharm. Sci. Technol.*, 40 (1986) 212-241
- Borcovec, M., Measuring particle size by light scattering, in *Handbook of applied surface and colloidal chemistry*, ed. by Holmberg, K. (2002)
- Borges, N.; Ramos, A.; Raven, N. D.; Sharp, R. J.; Santos, H., Comparative study of the thermostabilizing properties of mannosylglycerate and other compatible solutes on model enzymes, *Extremophiles*, 6 (2002) 209-216
- Bos, M.; Nylander, T.; Arnebrant, T.; Clark, D. C., *Food emulsifiers and their applications*, ed. by Hasenhuettl, G. L.; Hartel, R. W., New York, USA (1997) p. 95
- Bos, J.; Tijssen, R., Hydrodynamic chromatography of polymers, *J. Chromatogr. Libr.*, 56 (1995) 95-126
- Botana, A. M.; Ratanathanawongs, S. K.; Giddings, J. C., Field-programmed flow field-flow fractionation, *J. Microcolumn Sep.*, 7 (1995) 395-402
- Bowman, W. A.; Rubinstein, M.; Tan, J. S., Polyelectrolyte-gelatin complexation: light scattering study, *Macromolecules*, 30 (1997) 3262-3270
- Brange, J., Physical stability of proteins, in *Pharmaceutical formulation development of peptides and proteins*, ed. by Frokjaer, S.; Hovgaard, L., (2000) 89-112
- Brange, J.; Andersen, L.; Laursen, E. D.; Meyn, G.; Rasmussen, E., Toward understanding insulin fibrillation, *J. Pharm. Sci.*, 86 (1997) 517-525
- Brennan, T.V.; Clarke, S., Deamidation and isoaspartate formation in model synthetic peptides. The effects of sequence and solution environment, in *Deamidation and isoaspartate formation in peptides and proteins*, ed. by Asward, W., 1995, p.65
- Brennan, T. V.; Clarke, S., Spontaneous degradation of polypeptides at aspartyl and asparaginyl residues: effects of the solvent dielectric, *Protein Sci.*, 2 (1993) 331-338
- Bromberg, L. E., Interactions among proteins and hydrophobically modified polyelectrolytes, *J. Pharm. Pharmacol.*, 53 (2001) 541-547

- Brook, M. A.; Zelisko, P., Exploiting silicon-protein interactions: stabilization against denaturation at interfaces, *Polym. Prep.*, 42 (2001) 97-98
- Brot, N.; Weissbach, H., Biochemistry of methionine sulfoxide residues in proteins, *Biofactors*, 3 (1991) 91-96
- Brown, W., *Dynamic light scattering: the method and some applications*, Clarendon Press, Oxford (1993)
- Buchholz, B. A.; Barron, A. E., The use of light scattering for precise characterization of polymers for DNA sequencing by capillary electrophoresis, *Electrophoresis*, 22 (2001) 4118-4128
- Bummer, P. M.; Koppenol, S., Chemical and physical considerations in protein and peptide stability, in *Protein formulation and delivery*, ed. by McNally, E. J. (2000) 5-69
- Byrne, E. P.; Fitzpatrick, J. J.; Pampel, L. W.; Titchener-Hooker, N. J., Influence of shear on particle size and fractal dimension of whey protein precipitates: implications for scale-up and centrifugal clarification efficiency, *Chemical Engineer. Sci.*, 57 (2002) 3767-3779
- Caldwell, K. D., Electrical field-flow fractionation, in *Field-flow fractionation handbook*, ed. by Schimpf, M. E.; Caldwell, C.; Giddings, J. C. (2000a) 295-312
- Caldwell, K. D., Steric field-flow fractionation and the steric transition, in *Field-flow fractionation handbook*, ed. by Schimpf, M. E.; Caldwell, C.; Giddings, J. C. (2000b) 79-94
- Caldwell, K. D.; Gao, Y.-S., Electrical field-flow fractionation in particle separation, *Anal. Chem.*, 65 (1993) 1764-1772
- Caldwell, K. D.; Brimhall, S. L.; Gao, Y.; Giddings, J. C., Sample overloading effects in polymer characterization by field-flow fractionation, *J. Appl. Polym. Sci.*, 36 (1988) 703-719
- Caldwell, K. D.; Nguyen, T. T.; Myers, M. N.; Giddings, J. C., Observations on anomalous retention in steric field-flow fractionation, *Sep. Sci. Technol.*, 14 (1979) 935-946
- Cao, E.; Chen, Y.; Cui, Z.; Foster, P. R., Effect of freezing and thawing rates on denaturation of proteins in aqueous solutions, *Biotechnol. Bioeng.*, 82 (2003) 684-690
- Capasso, S.; Mazzarella, I.; Zagar, A., Deamidation via cyclic imide of asparaginyl peptides: dependence of salts, buffers, and organic solvents, *Peptide Res.*, 4 (1991) 234-238
- Capes, D. F.; Herring, D.; Sunderland, V. B.; McMillan, D.; McDonald, C., The effect on syringe performance of fluid storage and repeated use: implications for syringe pumps, *J. Pharm. Sci. Technol.*, 50 (1996) 40-50
- Carpenter, J. F.; Chang, B. S.; Garzon-Rodriguez, W.; Randolph, T. W., Rational design of stable lyophilized protein formulations: theory and practice, *Pharmaceutical Biotechnology*, 13 (2002) 109-133
- Casassa, E. F.; Tagami, Y., Equilibrium theory for exclusion chromatography of branched and linear polymer chains, *Macromolecules*, 2 (1969) 14-26

- Chahine, J.; Nymeyer, H.; Leite, V. B.; Socci, N. D.; Onuchic, J. N., Specific and nonspecific collapse in protein folding funnels, *Phys. Rev. Let.*, 88 (2002) 1681011-1681014
- Chan, H. K.; Au-Yeung, K.-L.; Gonda, I., Effects of additives on heat denaturation of rhDNase in solutions, *Pharm. Res.*, 13 (1996) 756-761
- Chang, B. S.; Beauvais, R. M.; Arakawa, T.; Narhi, L. O.; Dong, A.; Aparisio, D. I.; Carpenter, J. F., Formation of an active dimer during storage of interleukin-I receptor antagonist in aqueous solution, *Biophys. J.*, 71 (1996) 3399-3406
- Charman, S. A.; Mason, K. L.; Charman, W. N., Techniques for assessing the effects of pharmaceutical excipients on the aggregation of porcine growth hormone, *Pharm. Res.*, 10 (1993) 954-962
- Chehin, R.; Thorolfsson, M.; Knappskog, P. M.; Martinez, A.; Flatmark, T.; Arrondo, J. L.; Muga, A., Domain structure and stability of human phenylalanine hydroxylase inferred from infrared spectroscopy, *FEBS Lett.*, 422 (1998) 225-230
- Chen, B.; Beckett, R., Development of SdFFF-ETAAS for characterising soil and sediment colloids, *Analyst*, 126 (2001) 1588-1593
- Chen, B. L.; Arakawa, T., Stabilization of recombinant human keratinocyte growth factor by osmolytes and salts, *J. Pharm. Sci.*, 85 (1996) 419-426
- Chen, B. L.; Arakawa, T.; Morris, F. C.; Kenney, W. C.; Wells, C. M.; Pitt, C. G., Aggregation pathway of recombinant human keratinocyte growth factor and its stabilization, *Pharm. Res.*, 11 (1994a) 1581-1587
- Chen, B. L.; Arakawa, T.; Hsu, E.; Narhi, L. O.; Tressel, T. J.; Chien, S. L., J. Strategies to suppress aggregation of recombinant human keratinocyte growth factor during liquid formulation development, *Pharm. Sci.*, 83 (1994b) 1657-1661
- Christy, C.; Adams, G.; Kuriyel, R.; Bolton, G.; Seilly, A., High-performance tangential flow filtration: a highly selective membrane separation process, *Desalination*, 144 (2002) 133-136
- Chu, B.; Liu, T., Characterization of nanoparticles by light scattering, *J. Nanoparticle Res.*, 2 (2000) 29-41
- Chui, Z.; Mumper, R. J.; Plasmid DNA-entrapped nanoparticles engineered from microemulsion precursors: in vitro and in vivo evaluation, *Bioconjugate Chem.*, 13 (2002) 1319-1327
- Claes, P.; Dunford, M.; Kenny, A.; Vardy, P., in *Laser light scattering in biochemistry*, ed. by Harding, S. E. et al., Cambridge (1992) p. 66
- Cleland, J. L.; Lam, X.; Kendrick, B.; Yang, J.; Yang, T.-H.; Overcashier, D.; Brooks, D.; Hsu, C.; Carpenter, J. F., A specific molar ratio of stabilizer to protein is required for storage stability of a lyophilized monoclonal antibody, *J. Pharm. Sci.*, 90 (2001) 310-321

- Cleland, J. L.; Powell, M. F.; Shire, S. J., The development of stable protein formulations: a close look at protein aggregation, deamidation, and oxidation, *Crit. Rev. Ther. Drug Carrier Syst.*, 10 (1993) 307-377
- Corsi, K.; Chellat, F.; L'Hocine, Y.; Fernandes, J. C., Mesenchymal stem cells, MG63 and HEK293 transfection using chitosan-DNA nanoparticles, *Biomaterials*, 24 (2003) 1255-1264
- Coelfen, H.; Antonietti, M., Field-flow fractionation techniques for polymer and colloid analysis, *Adv. Polym. Sci.*, 150 (2000) 67-187
- Coester, C., Entwicklung peptidischer oberflächen-modifizierter nanopartikulärer Trägersysteme für Antisense-Wirkstoffe und präklinische Testung gegen HIV, Dissertation, Frankfurt/Main (2000)
- Coester, C. J.; Langer, K.; von Briesen, H.; Kreuter, J., Gelatin nanoparticles by two-step desolvation – a new preparation method, surface modifications and cell uptake, *J. Microencapsul.*, 17 (2000) 187-193
- Cohen, H.; Levy, R. J.; Gao, J.; Fishbein, I.; Kousaev, V.; Sosnowski, S.; Slomkowski, S.; Golomb, G., Sustained delivery and expression of DNA encapsulated in polymeric nanoparticles, *Gene Therapy*, 7 (2000) 1896-1905
- Collier, F. C.; Dawson, A. D., Insulin syringes and silicone oil, *Lancet*, 14 (1985) 611
- Communication, anonymous; Syringes may cause infusion pump alarm: more than 1 million recalled, *Biomedical Safety and Standards*, Jan 1 (1991) 5
- Constantino, H. R.; Langer, R.; Klibanov, A. M., Moisture-induced aggregation of lyophilized insulin, *Pharm. Res.*, 11 (1994a) 21-29
- Constantino, H. R.; Langer, R.; Klibanov, A. M., Solid-phase aggregation of proteins under pharmaceutically relevant conditions, *J. Pharm. Sci.*, 83 (1994b) 1662-1669
- Cooper, A., DSC interpretation notes, Glasgow, UK, 25/04/2001
- Cooper, A.; Nutley, M. A.; Wadood, A., Protein-ligand interactions, in *Differential scanning microcalorimetry*, ed. by Harding, S. E.; Chowdhry, B. Z., Oxford, UK (2001) 287-318
- Covan, D. A., Thermophilic proteins: stability and function in aqueous and organic solvent, *Comp. Biochem. Physiol.*, 118A (1997) 429-438
- Dalgleish, D. G., Adsorption of protein and the stability of emulsions, *Trends in Food Sci. & Technol.*, 8 (1997) 1-6
- Daniel, R. M.; Dines, M.; Petach, H. H., The denaturation and degradation of stable enzymes at high temperature, *Biochem. J.*, 317 (1996) 1-11
- D'Auria, S.; Barone, S.; Rossi, M., Effects of temperature and SDS on the structure of beta-glycosidase from the thermophilic archaeon *Sulfolobus solfataricus*, *Biochem. J.*, 323 (1997) 833-840

- Dean, D. A., Development and approval of a plastic pack, in *Pharmaceutical packaging technology*, ed. by Dean, D. A.; Evans, E. R.; Hall, I. H., London, New York (2000)
- Debye, P., Molecular weight determination by light scattering, *J. Phys. Colloid Chem.*, 51 (1947) 18-27
- Debye, P., Light scattering in solutions, *J. Applied. Phys.*, 15 (1944) 338-342
- De Decker, B. S.; O'Brian, R.; Fleming, P. J.; Geiger, J. H.; Jackson, S. P.; Soigler, P. B., The crystal structure of a hyperthermophilic archeal TATA-box binding protein, *J. Molec. Biol.*, 264 (1996) 1072-1084
- Desai, M. P.; Labhasetwar, V.; Amidon, G. L.; Levy, R. J., Gastrointestinal uptake of biodegradable microparticles: effect of particle size, *Pharm. Res.*, 13 (1996) 1838-1845
- Desilets, C. P.; Rounds, M. A.; Regnier, F. E., Semipermeable surface reversed-phase media for high-performance liquid chromatography, *J. Chromatogr.*, 544 (1991) 25-39
- De Young, L. R.; Dill, K. A.; Fink, A. L., Aggregation and denaturation of apomyoglobin in aqueous urea solutions, *Biochemistry*, 32 (1993a) 3877-3886
- De Young, L. R.; Fink, A. L.; Dill, K. A., Aggregation of globular proteins, *Acc. Chem. Res.*, 26 (1993b) 614-620
- Dickinson, E., Proteins at interfaces and in emulsions, *Faraday Trans.*, 94 (1998) 1657-1669
- Dill, K. A.; Alonso, D. O.; Hutchinson, K., Thermal stabilities of globular proteins, *Biochemistry*, 28 (1989) 5439-5449
- Dobson, C. M., Protein misfolding, evolution and disease, *Trends in Biochem. Sci.*, 24 (1999) 329-332
- Doenicke, A.; Nebauer, A. E.; Hoernecke, R.; Mayer, M.; Roizen, M. F.; *Anesthesia & Analg.*, 75 (1992) 431-435
- Dong, A.; Maatsura, J.; Allison, S. D.; Chrisman, E.; Manning, M. C.; Carpenter, J. F., Infrared and circular dichroism spectroscopic characterization of structural differences between beta-lactoglobulin A and B, *Biochemistry*, 35 (1996) 1450-1457
- Dong, A.; Prestrelski, S. J.; Allison, S. D.; Carpenter, J. F., Infrared spectroscopic studies of lyophilization- and temperature-induced protein aggregation, *J. Pharm. Sci.*, 84 (1995) 415-424
- Dorn, S. B.; Frame, E. M.; Skelly, E. M., Development of a high-performance liquid chromatography-inductively coupled plasma method for specification and quantification of silicones: from silanols to polysiloxanes, *Analyst*, 119 (1994) 1687-1694
- Dos Ramos, J. G.; Silebi, C. A., Submicron particle size and polymerization excess surfactant analysis by capillary hydrodynamic fractionation (CHDF), *Polymer Int.*, 30 (1993) 445-450
- Duenas, E. T.; Keck, R.; DeVos, A.; Jones, A. J.; Cleland, J. L., Comparison between light induced and chemically induced oxidation of rhVEGF, *Pharm. Res.*, 18 (2001) 1455-1460

- Duval, C.; le Cerf, D.; Picton, L.; Muller, G., Aggregation of amphiphilic pullulan derivatives evidenced by on-line flow field-flow fractionation/multiangle laser light scattering, *J. Chromatogr. B*, 753 (2001) 115-122
- Dycus, P.; Healy, K. D.; Stearman, G. K.; Wells, M. J., Diffusion coefficients and molecular weight distributions of humic and fulvic acids determined by flow field-flow fractionation, *Sep. Sci. Technol.*, 30 (1995) 1435-1453
- Einstein, A., Theory of the opalescence of homogeneous and of mixed liquids in the neighborhood of the critical region, *Ann. Physik*, 33 (1911) 1275-1298
- Einstein, A., The nature and constitution of radiation, *Zurich Physik. Z.*, 10 (1910) 817-826
- Epanand, R. F.; Epanand, R. M., Irreversible unfolding of the neutral pH form of influenza hemagglutinin demonstrates that it is not in a metastable state, *Biochemistry*, 42 (2003) 5052-5057
- Erhardt, R.; Zhang, M.; Boeker, A.; Zettl, H.; Abetz, C.; Frederik, P.; Krausch, G.; Abetz, V.; Mueller, A. H., Amphiphilic janus micelles with polystyrene and poly(methacrylic acid) hemispheres, *J. Am. Chem. Soc.*, 125 (2003) 3260-3267
- Fahraeus, R., The suspension stability of the blood, *Physiol. Rev.*, 9 (1929) 241-274
- Farrugia, C. A.; Groves, M. J., Gelatin behaviour in dilute aqueous solution: designing a nanoparticulate formulation, *J. Pharm. Pharmacol.*, 51 (1999) 643-649
- Fatouros, A., Oesterberg, T.; Mikaelsson, M., Recombinant factor VIII SQ – influence of oxygen, metal ions, pH and ionic strength on its stability in aqueous solution, *Int. J. Pharm.*, 155 (1997a) 121-131
- Fatouros, A., Oesterberg, T.; Mikaelsson, M., Recombinant factor VIII SQ – inactivation kinetics in aqueous solution and the influence of disaccharides and sugar alcohols, *Pharm. Res.*, 14 (1997b) 1679-1684
- FDA, Food and Drug Administration, Safety alert: hazards of precipitation associated with parenteral nutrition, *Am. J. Hosp. Pharm.*, 51 (1994) 1427
- Fields, G. B.; Alonso, D. O.; Stigter, D.; Dill, K. A., Theory for the aggregation of proteins and copolymers, *J. Phys. Chem.*, 96 (1992) 3974-3981
- Filenko, A. M., Detection and characterization of protein oligomeric species by light scattering methods: myosin light chain kinase supramolecular structures, *Biopolimery i Kletka*, 16 (2000) 369-379
- Finke, J. M.; Jennings, P. A., Early aggregates states in the folding of interleukin-1 β , *J. Biol. Physics*, 27 (2001) 119-131
- Finsky, R., Particle sizing by quasi-elastic light scattering, *Adv. Colloid Interface Sci.*, 52 (1994) 79-143

- Finsy, R.; de Jaeger, N.; Sneyers, R.; Gelade, E., Particles sizing by photon correlation spectroscopy. Part III. Mono- and bimodal distributions and data analysis, Part. III., Systems Characterization, 9 (1992) 125-137
- Fleming, P. J.; Richards, F. M., Protein packing: dependence of protein size, secondary structure and amino acid composition, J. Mol. Biol., 299 (2000) 487-498
- Fletcher, M. A.; Morrison, T. K.; Williams, T. J., Early in vitro lipopolysaccharide-induced serum protein aggregation in tolerant serum, Gov. Rep. Announce. Index (U. S.), 93 (1993) No. 313, 246
- Frampton, N.; Dean, D. A., Sterile products and rubbers, in Pharmaceutical packaging technology, ed. by Dean, D. A.; Evans, E. R.; Hall, I. H., London and New York (2000) 492-516
- Frankema, W.; van Bruijnsvoort, M.; Tijssen, R.; Kok, W. Th., Characterisation of core-shell latexes by flow field-flow fractionation with multi-angle light scattering detection, J. Chromatogr. A, 943 (2002) 251-261
- Franks, F., Protein stability: the value of old literature, Biophys. Biochem., 96 (2002) 117-127
- Fransson, J.; Hallén, D.; Florin-Robertsson, E., Solvent effects on the solubility and physical stability of human insulin-like growth factor I, Pharm. Res., 14 (1997) 606-612
- Fraunhofer, W.; Winter, G.; Zillies, J.; Coester, C., Asymmetrical flow field-flow fractionation as new analytical tool in pharmaceutical biotechnology, New Drugs, 2 (2003) 16-19
- Fraunhofer, W.; Krause, H.-J.; Winter, G., Separation of particulate matter into detached silicone oil and denatured protein drug in siliconized parenteral packages: considered as yesterday's problem?, Meeting of the American Association of Pharmaceutical Scientists, AAPS, Toronto, Canada (2002a)
- Fraunhofer, W., Asymmetrical flow field-flow fractionation combined with multi-angle laser light scattering: new applications of an upcoming analytical method; plenary presentation throughout 4th World meeting on pharmaceuticals, biopharmaceuticals and pharmaceutical technology, Florence, Italy (2002b)
- Fraunhofer, W.; Krause, H.-J.; Winter, G., Identification of particulate matter in siliconized disposable syringes with asymmetrical flow field-flow fractionation, 4th World meeting on pharmaceuticals, biopharmaceuticals and pharmaceutical technology, Florence, Italy (2002c)
- Fraunhofer, W.; Krause, H.-J.; Winter, G., Latest developments in asymmetrical flow field-flow fractionation: a separation method with wide applicability in pharmaceuticals, Meeting of the American Association of Pharmaceutical Scientists, AAPS, Toronto, Canada (2002d)
- Fraunhofer, W.; Schroer, C.; Tschoepe, M.; Winter, G., Asymmetrical flow field-flow fractionation: a new approach to analysis of high-molecular weight protein aggregates, 28th Int. Symp. Controlled Release Bioact. Mater., San Diego (2001)

- Froment, M.-T.; Lockridge, O.; Masson, P., Resistance of butyrylcholinesterase to inactivation by ultrasound: effects of ultrasound on catalytic activity and subunit association, *Biochim. Biophys. Acta.*, 1387 (1998) 53-64
- Gebhardt, J.; Grumbridge, N. A.; Knoch, A., Particulate contamination from siliconized rubber closures for freeze-drying, *PDA J. Pharm. Sci. Technol.*, 50 (1996) 24-29
- Giancola, C.; De Sena, C.; Fessas, D.; Graziano, G.; Barone, G., DSC studies on bovine serum albumin denaturation: effects of ionic strength and SDS concentration, *Int. J. Biol. Macromol.*, 20 (1997) 193-204
- Giddings, J. C., Field-flow fractionation: analysis of macromolecular, colloidal, and particulate materials, *Science*, 260 (1993) 1456-1465
- Giddings, J. C.; Williams, P. S.; Benincasa, M. A., Rapid break-through measurement of void volume for field-flow fractionation channels, *J. Chromatogr.*, 627 (1992) 23-35
- Giddings, J. C., *Unified separation science*, ed. by J. Wiley & Son, New York (1991)
- Giddings, J. C., Hydrodynamic relaxation and sample concentration in field-flow fractionation using permeable wall elements, *Anal. Chem.*, 62 (1990) 2306-2312
- Giddings, J. C.; et al., Analysis in fundamental obstacles to the size exclusion chromatography of polymers of ultra-high molecular weight, *Advances in Chromatography* 20, (1982) 217-258
- Giddings, J. C., Displacement and dispersion of particles of finite size in flow channels with lateral forces: field-flow fractionation and hydrodynamic chromatography, *Sep. Sci. Technol.*, 13 (1978) 241-245
- Giddings, J. C.; Marin, M.; Myers, M. N., High-speed separations by thermal field-flow fractionation, *J. Chromatogr.*, 158 (1978a) 419-435
- Giddings, J. C.; Lin, G.-C.; Myers, M. N., Fractionation and size analysis of colloidal silica by flow field-flow fractionation, *J. Colloid Inter. Sci.*, 65 (1978b) 67-78
- Giddings, J. C.; Lin, G.-C.; Myers, M. N., Fractionation and size distribution of water soluble polymers by flow field-flow fractionation, *J. Liq. Chromatogr.*, 1(1) (1978c) 1-20
- Giddings, J. C.; Yang, F. J.; Myers, M. N., Flow field-flow fractionation as a methodology for protein separation and characterization, *Anal. Biochem.*, 81(2) (1977) 395-407
- Giddings, J. C.; Yang, F. J.; Myers, M. N., Flow field-flow fractionation: a versatile new separation method, *Science*, 193 (1976) 1244-1245
- Giddings, J. C., A new separation concept bases on a coupling of concentration and flow nonuniformities, *Sep. Sci.*, 1 (1966) 123-125
- Giddings, J. C., Eddy diffusion in chromatography, *Nature*, 187 (1960) 1023-1024
- Glatz, C. E., Modeling of aggregation-precipitation phenomena, in *Stability of protein pharmaceuticals*, ed. by Ahern, T.J.; Manning, M. C. (1992) 135-166

- Gombotz, W. R.; Pankey, S. C.; Phan, D.; Drager, R.; Donaldson, K.; Antonsen, K. P.; Hoffman, A. S.; Raff, H. V., The stabilization of a human IgM monoclonal antibody with poly(vinylpyrrolidone), *Pharm. Res.*, 11 (1994) 624-632
- Goolcharran, C.; Khossravi, M.; Borchardt, R. T., Chemical pathways of peptide and protein degradation, in *Pharmaceutical formulation development of peptides and proteins*, ed. by Frokjaer, S.; Hovgaard, L., 70-88 (2000a)
- Goolcharran, C.; Stauffer, L. L.; Cleland, J. L.; Borchardt, R. T., The effects of a histidine residue on the C-terminal side of an asparaginyl residue on the rate of deamidation using model pentapeptides, *J. Pharm. Sci.*, 89 (2000b) 818-825
- Goolcharran, C.; Cleland, J. L.; Keck, R.; Jones, A. J.; Borchardt, R. T., Comparison of the rates of deamidation, diketopiperazine formation, and oxidation in recombinant human vascular endothelial growth factor and model peptides, *Pharm. Sci.* (online computer file) 2 (2000c)
- Goormaghtigh, E.; Cabiaux, V.; Ruyschaert, J.-M., Determination of soluble and membrane protein structure by Fourier transform infrared spectroscopy III. Secondary structures, *Subcell. Biochem.*, 23 (1994) 405-450
- Goto, Y.; Fink, A. L., Conformational states of beta-lactamase: molten-globule states at acidic and alkaline pH with high salt, *Biochemistry*, 28 (1989) 945-952
- Granger, J.; Dodds, J.; Leclerc, D.; Midoux, N.; Flow and diffusion of particles in a channel with one porous wall: polarization chromatography, *Chem. Eng. Sci.*, 41 (1986) 3119-3128
- Griessler, R.; Dáuria, S.; Tanfani, F.; Nidetzky, B.; Thermal denaturation pathway of starch phosphorylase from *Corynebacterium callunae*: oxyanion binding provides the glue that efficiently stabilizes the dimer structure of the protein, *Prot. Sci.*, 9 (2000) 1149-1161
- Groves, M. J., Particulate contamination in parenterals: current issues, *Bollettino Chimico Farmaceutico*, 130 (1991) 347-354
- Gu, L. C.; Erdoes, E. A.; Chiang, H.-S.; et al., Stability of interleukine 1 beta in aqueous solution: analytical methods, kinetics, products, and solution formulation implications, *Pharm. Res.*, 8 (1991) 485-490
- Gunderson, J. J.; Giddings, J. C., Comparison of polymer resolution in thermal field-flow fractionation and size-exclusion chromatography, *Anal. Chim. Acta*, 189 (1986) 1-15
- Ha, E.; Wang, W.; Wang, Y. J., Peroxide formation in polysorbate 80 and protein stability, *J. Pharm. Sci.*, 91 (2002) 2252-2264
- Hallett, F. R., Size distributions from static light scattering, *Monographs on the physics and chemistry of materials*, 53 (1996) 477-493
- Halliwell, B.; Gutteridge, J. M., The chemistry of oxygen radicals and other oxygen derived species, in *Free radicals in biology and medicine*, 2nd edn, Oxford (1989) 22-85

- Hansen, M.; Klein, T., Field-flow fractionation – the best guarded secret in bioanalysis?, *GIT Labor-Fachzeitschrift*, 45 (2001) 506-510
- Hanson, M. A.; Rouan, S. K., Introduction to formulation of protein pharmaceuticals, in *Stability of protein pharmaceuticals*, ed. by Ahern, T. J.; Manning, M. C., 3 (1992) 209-233
- Harris, D. A., Size-exclusion high-performance chromatography of proteins, in *Methods in Molecular Biology*, ed. by Kenney, A.; Fowell, S., 11 (1992) 223-236
- Hasseloev, M.; Hulthe, G.; Lyvén, B.; Stenhagen, G., Electrospray mass spectrometry as online detector for low molecular weight polymer separations with flow field-flow fractionation, *J. Liq. Chrom. & Rel. Technol.*, 20 (1997) 2843-2856
- Hattori, K., Synthesis of sugar-branched cyclodextrins and their dual association with proteins and drugs observed by SPR assay, *Biologicheskii Zhurnal Armenii*, 53 (2001) 82-94
- Hecker, R.; Jefferson, A.; Fawell, P. D.; Farrow, J. B., The characterization of polyacrylamide flocculants by flow field-flow fractionation combined with multi-angle laser light scattering, *Bi-annual Int. Symp. on Fundamentals of Mineral Proc.*, Quebec City, Canada (1999) 107-121
- Hecker, R.; Fawell, P. D.; Jefferson, A., The agglomeration of high molecular mass polyacrylamide in aqueous solutions, *J. Appl. Polym. Sci.*, 70 (1998) 2241-2250
- Heertje, I.; van Aalst, H.; Blonk, J. C.; Don, A.; Nederlof, J.; Lucassen-Reynders, E. H., Observations on emulsifiers at the interface between oil and water by confocal scanning light microscopy, *Food Sci. Technol.*, 29 (1996) 217-226
- Herman, A. C.; Boone, T. C.; Lu, H. S., Characterization, formulation, and stability of Neupogen[®] (Filgrastim), a recombinant human granulocyte-colony stimulating factor, in *Formulation, characterization, and stability of protein drugs*, ed. by Pearlman, R.; Wang, Y. J., New York (1996) 303-328
- Hillgren, A.; Lindgren, J.; Aldén, M., Protection mechanism of Tween 80 during freeze-thawing of a model protein, LDH, *Int. J. Pharm.*, 237 (2002) 57-69
- Himel, D.; Norwood, D. P.; Reed, W. F., Enzymatic degradation of polyester urethanes studied by multi-angle laser light scattering, *Biocatalytics in Polymer Sci.*, 840 (2003) 286-296
- Hoepfner, E.-M.; Reng, A.; Schmidt, P. C., *Fiedler – encyclopedia of additives*, Kirchheim (2002)
- Hodgson, R. J., Genetic algorithm approach to particle identification by light scattering, *J. Coll. Interface Sci.*, 229 (2000) 399-406
- Hoffmann, H., Analytical methods and stability testing of biopharmaceuticals, in *Protein formulation and delivery*, ed. by McNally, E. J., 3 (2000) 71-110
- Hoffmann, F.; Cinatl, J.; Kabickova, H.; Kreuter, J.; Stieneker, F., Preparation, characterization and cytotoxicity of methylmethacrylate copolymer nanoparticles with a permanent positive surface charge, *Int. J. Pharm.*, 157 (1997) 189-198

- Honig, B., Protein folding: from the Levinthal paradox to structure prediction, *J. Mol. Biol.*, 293 (1999) 283-293
- Hsu, C.C.; Nguyen, H. M.; Yeung, D. A.; Brooks, D. A.; Koe, G. S.; Bewley, T. A.; Pearlman, R., Surface denaturation at solid-void interface – a possible pathway by which opalescent particulates form during the storage of lyophilized tissue-plasminogen activator at high temperatures, *Pharm. Res.*, 12 (1995) 69-77
- Huang, S. S., Molecular weight separation of macromolecules by hydrodynamic chromatography, *Column handbook for size exclusion chromatography*, ed. by Wu, S. (1999) 597-610
- Hussain, N.; Singh, B.; Sakthivel, T.; Florence, A. T., Formulation and stability of surface-tethered DNA-gold-dendron nanoparticles, *Int. J. Pharm.*, 254 (2003) 27-31
- ICH, Draft Consensus Guideline, for consultation step II of ICH process, ICH steering committee, february 7, 2002
- Ikai, A., Extraction of the apo B cluster from human low density lipoprotein with Tween 80, *J. Biochemistry*, 88 (1980) 1349-1357
- Jaeger, J.; Sorensen, K.; Wolff, S. P., Peroxide accumulation in detergents, *J. Biochem. Biophys. Methods*, 29 (1994) 77-81
- Jaenicke, R., Stability and folding of domain proteins, *Progr. Biophys. Mol. Biol.*, 71 (1999) 155-241
- Jaenicke, R., Protein misassembly in vitro, *Adv. Protein Chem.*, 50 (1997) 1-60
- Jaenicke, R., Glyceraldehyde-3-phosphate dehydrogenase from *Thermotoga maritima*: strategies of protein stabilization, *FEMS Microbiol. Rev.*, 18 (1996) 215-224
- Jaenicke, R., Folding and association versus misfolding and aggregation of proteins, *Philos. Trans. R. Soc. London B*, 348 (1995) 97-105
- Jaenicke, R., Protein stability and molecular adaptation to extreme conditions, *Eur. J. Biochem.*, 202 (1991) 715-728
- Jaenicke, R., Protein structure and function at low temperatures, *Philos. Trans. R. Soc. London B*, 326 (1990) 535-551
- James, E. L.; Bottomley, S. P., The mechanism of α_1 -antitrypsin polymerization probed by fluorescence spectroscopy, *Arch. Biochem. Biophys.*, 356 (1998) 296-300
- Janca, J., Micro-channel thermal field-flow fractionation: new challenge in analysis of macromolecules and particles, *J. Liq. Chrom. Rel. Technol.*, 25 (2002) 683-704
- Janca, J., Field-flow fractionation, *J. Chromatogr. Libr.*, 51A (1992) 449-479
- Jeandidier, N.; Boullu, S.; Busch-Brafin, M.-S.; Chabrier, G.; Sapin, R.; Grasser, F.; Pinget, M., Comparison of antigenicity of Hoechst 21PH insulin using either implantable intraperitoneal pump or subcutaneous external pump infusion in type I diabetic patients, *Diabetes Care*, 25 (2002) 84-88

- Jensen, K. D.; Williams, S. K.; Giddings, J. C., High-speed particle separation and steric inversion in thin flow field-flow fractionation channels, *J. Chromatogr.*, 746 (1996) 137-145
- Jiang, Y.; Miller, M. E.; Li, P.; Hansen, M. E., Characterization of water-soluble polymers by flow FFF-MALS, *American Lab.*, 32 (2000) 98-108
- Jiang, Y., Ph.D. Thesis, University of Utah (1994)
- Joensson, B.; Lindman, B.; Holmberg, K.; Kronberg, B., *Surfactants and polymers in aqueous solution*, ed. by John Wiley and sons, Chichester (1998)
- Johnson, B. A.; Aswad, D. W., Deamidation and isoaspartate formation during in vitro aging of purified proteins, in *Deamidation and isoaspartate formation in peptides and proteins*, ed. by Aswad, D. W. (1995) p.91
- Johnston, T. P., Adsorption of recombinant human granulocyte colony stimulating factor (rhG-CSF) to polyvinyl chloride, polypropylene, and glass: effect of solvent additives, *PDA J. Pharm. Sci. Technol.*, 50 (1998) 238-249
- Jones, L. S.; Randolph, T. W., Purification of recombinant hepatitis B vaccine: effect of virus/surfactant interactions, in *The 25th Annual Biochemical Engineering Symposium*, ed. by Rakesh, Columbia, MO, USA (1995) 75-82
- Jonsson, J. A., *Trends Anal. Chem.* 20, *Field-flow fractionation handbook*, ed. by Schimpf, M. E.; Caldwell, C.; Giddings, J. C. (2000)
- Jumel, K.; Mei, M.; Bolgiano, B., Evaluation of meningococcal C oligosaccharide conjugate vaccines by size-exclusion chromatography/multi-angle laser light scattering, *Biotechnol. Applied Biochem.*, 36 (2002) 219-226
- Jungmann, N.; Schmidt, M.; Maskos, M.; Weis, J.; Ebenhoch, J.; Synthesis of amphiphilic poly(organosiloxane) nanospheres with different core-shell architectures; *Macromolecules*, 35 (2002) 6851-6857
- Jungmann, N.; Schmidt, M.; Maskos, M., Characterization of polyorganosiloxane nanoparticles in aqueous dispersion by asymmetrical flow field-flow fractionation, *Macromolecules*, 34 (2001) 8347-8353
- Kandori, K.; Uoya, Y.; Ishikawa, T., Effects of acetonitrile on adsorption behavior of bovine serum albumin onto synthetic calcium hydroxyapatite particles, *J. Coll. Interface Sci.*, 252 (2002) 269-275
- Karaiskakis, G.; Koliadima, A.; Farmakis, L.; Gavril, D., Potential-barrier field-flow fractionation: potential curves and interactive forces, *J. Liq. Chrom. & Rel. Technol.*, 25 (2002) 2153-2172
- Katakam, M.; Bell, L. N.; Banga, A. K., Effect of surfactants on the physical stability of recombinant human growth hormone, *J. Pharm. Sci.*, 84 (1995) 713-716

- Katre, N. V., The conjugation of proteins with polyethylene glycol and other polymers altering properties of proteins to enhance their therapeutic potential, *Adv. Drug. Del. Rev.*, 10 (1993) 91-114
- Kaul, G.; Amiji, M., Long-circulating poly(ethylene glycol)-modified gelatin nanoparticles for intracellular delivery, *Pharm. Res.*, 19 (2002) 1061-1067
- Kauzmann, W., Some factors in the interpretation of protein denaturation, *Adv. Prot. Chem.*, 14 (1959) 1-63
- Kelley, D.; McClements, D. J., Interactions of bovine serum albumin with ionic surfactants in aqueous solutions, *Food Hydrocoll.*, 17 (2002) 73-85
- Kendrick, B. S.; Cleland, J. L.; Lam, X.; Nguyen, T.; Randolph, T. W.; Manning, M. C.; Carpenter, J. F., Aggregation of recombinant human interferon gamma: kinetics and structural transitions, *J. Pharm. Sci.*, 87 (1998) 1069-1076
- Kheirilomoom, A.; Ardjmand, M.; Vossoughi, M.; Kazemeini, M., The stability analysis and modeling of pH- and ionic strength inactivation of penicillin G acylase obtained from various species of *Escherichia coli*, *Biochem. Eng. J.*, 2 (1998) 81-88
- Kim, Y. S.; Wall, J. S.; Meyer, J.; Murphy, C.; Randolph, T. W.; Manning, M. C.; Solomon, A.; Carpenter, J. F., Thermodynamic modulation of light chain amyloid fibril formation, *J. Biol. Chem.*, 275 (2000) 1570-1574
- Kinekawa, Y.-I.; Kitabatake, N., Purification of beta-lactoglobulin from whey protein concentrate by pepsin treatment, *J. Dairy Sci.*, 79 (1996) 350-356
- Kirkland, J. J.; Dilks, C. H., Flow field-flow fractionation of polymers in organic solvents, *Anal. Chem.*, 64 (1992) 2836-2840
- Kirkland, J. J.; Dilks, C. H.; Yau, W. W., Sedimentation field flow fractionation at high force fields, *J. Chromatogr.*, 255 (1983) 255-271
- Kirkland, J. J.; Yau, W. W.; Doerner, W. A.; Grant, J. W.; Sedimentation field flow fractionation of macromolecules and colloids, *Anal. Chem.*, 52 (1980) 1944-1954
- Kleijn, M.; Norde, W., The adsorption of proteins from aqueous solutions on solid surfaces, *Heterogeneous Chem. Rev.*, 2 (1995) 157-172
- Klein, T.; Huerzeler, C., Characterization of biopolymers, proteins, particles and colloids by means of field-flow fractionation, *GIT Laborfachzeitschrift*, 11 (1999) 1224-1228
- Knapp, J. Z., Absolute sterility and absolute freedom from particle contamination, *PDA J. Pharm. Sci. Technol.*, 52 (1998) 173-181
- Knapp, S.; Mattson, P. T.; Christova, P.; Berndt, K. D.; Krshikoff, A.; Vihinen, M.; Smitth, C. I.; Ladenstein, R., Thermal unfolding of small proteins with SH3 domain folding pattern, *Proteins: Struct. Funct. Gen.*, 31 (1998) 309-319
- Knepp, V. M.; Whatley, J. L.; Muchnik, A.; Calderwood, T. S., Identification of antioxidants for prevention of peroxide-mediated oxidation of recombinant human ciliary neurotrophic

- factor and recombinant human nerve growth factor, *PDA J. Pharm. Sci. Technol.*, 50 (1996) 163-171
- Kobo, B., Intravenous (I.V.) fluid administration systems and incompatibility of injections, *Yakugaku Zasshi*, 110 (1990) 1-15
- Koch, M. H.; Svergun, D. I.; Gabriel, A.; Goderis, B.; Unruh, T., Recent developments in synchrotron radiation X-ray scattering on (bio)-polymers, *Polymeric Mat. Sci. Engineer.*, 85 (2001) 173
- Kock, H. J.; Schmit-Neuerburg, K. P.; Hanke, J.; Terwort, A.; Rudofsky, G.; Hirche, H., Implementing ambulatory prevention of thrombosis with low molecular weight heparin in plaster immobilization of the lower extremity, *Unfallchirurgie*, 20 (1994) 319-328
- Kohn, W. D.; Kay, C. M.; Hodges, R. S., Salt effects on protein stability: two-stranded alpha-helical coiled-coils containing inter- or intrahelical ion pairs, *J. Mol. Biol.*, 267 (1997) 1039-1052
- Kosa, T.; Maruyama, T.; Otagiri, M., Species differences of serum albumins: II chemical and thermal stability, *Pharm. Res.*, 15 (1998) 449-454
- Krapp, S.; Mimura, Y.; Jefferis, R.; Huber, R.; Sonderrmann, P., Structural analysis of human IgG-Fc glycoforms reveals a correlation between glycosylation and structural integrity, *J. Molecular Biol.*, 325 (2003) 979-989
- Kreuter, J., Physicochemical characterization of polyacrylic nanoparticles, *Int. J. Pharm.*, 14 (1983) 43-58
- Kristjánsson, M. M.; Kinsella, J. E., Protein and enzyme stability: structural, thermodynamic, and experimental aspects, *Adv. Food Nutr. Res.*, 35 (1991) 237-216
- Kuhlman, B.; Yang, H. Y.; Boice, J. A.; Fairman, R.; Raleigh, D. P., An exceptionally stable helix from the ribosomal protein L9: implications for protein folding and stability, *J. Mol. Biol.*, 270 (1997) 640-647
- Kundu, B.; Guptasarma, P., Use of a hydrophobic dye to indirectly probe the structural organization and conformational plasticity of molecules in amorphous aggregates of carbonic anhydrase, *Biochem. Biophys. Res. Commun.*, 293 (2002) 572-577
- Kunitani, M.; Wolfe, S.; Rana, S.; Apicella, C.; Levi, V.; Dollinger, G., Classical light scattering quantitation of protein aggregates: off-line spectroscopy versus HPLC detection, *J. Pharm. Biomedical Analysis*, 16 (1997) 573-586
- Lam, X. M.; Yang, J. Y.; Cleland, J. L., Antioxidants for prevention of methionine oxidation in recombinant monoclonal antibody HER2, *Pharm. Sci.*, 86 (1997) 1250-1255
- Langer, R., Drug delivery and targeting, *Nature* 392 (1998) 5-10
- Lao, A. I.; Trau, D.; Hsing, I.-M., Miniaturized flow fractionation device assisted by a pulsed electric field for nanoparticle separation, *Anal. Chem.*, 74 (2002) 5364-5369

- Lecomte, J.-P.; Meyrueix, R.; Soula, O.; Bloy, C.; Claverie, J. P.; Soula, G., Adsorption and desorption of interferon onto colloidal hydrophobic surfaces, 223rd ACS National Meeting, Orlando, USA, 413 (2002)
- Lee, S.; Kwon, O. S., Determination of molecular weight and size of ultrahigh molecular weight polymers using thermal field-flow fractionation and light scattering, in *Chromatographic characterization of polymers: hyphenated and multidimensional techniques*, ed. by Provder, T., et al. (1995) 93-107
- Lee, H.L.; Lightfoot, E. N., Preliminary report on ultrafiltration-induced polarization chromatography – an analog of field-flow fractionation, *Sep. Sci.*, 11 (1976) 417-440
- Leung, F. Y.; Edmond, P., Determination of silicone in serum and tissue by electrothermal atomic absorption spectrometry, *Clin. Biochem.*, 30 (1997) 399
- Li, J.; Caldwell, K. D.; Maechtle, W., Particle characterization in centrifugal fields: comparison between ultracentrifugation and sedimentation field-flow fractionation, *J. Chromatogr.*, 517 (1990) 361-376
- Li, L. C.; Parasrampur, J.; Tian, Y., Particulate contamination of siliconized rubber stoppers – a statistical evaluation, *J. Parenter. Sci. Technol.*, 47 (1993) 270-273
- Li, M.; Schnablegger, H.; Mann, S., Coupled synthesis and self-assembly of nanoparticles to give structures with controlled organization, *Nature*, 402 (1999) 393-395
- Li, P.; Hansen, M., Protein complexes and lipoproteins, in *Field-flow fractionation handbook*, ed. by Schimpf, M. E., Caldwell, K.; Giddings, J. C. (2000) 433-470
- Li, P.; Giddings, J. C., Isolation and measurement of colloids in human plasma by membrane-selective flow field-flow fractionation: lipoproteins and pharmaceutical colloids, *J. Pharm. Sci.*, 85 (1996) 895-898
- Li, P.; Hansen, M. E.; Giddings, J. C., *J. Liq. Chromatogr. & Rel. Tech.*, 20 (1997) 2777-2802
- Li, S.; Patapoff, T. W., Inhibitory effect of sugars and polyols on the metal-catalyzed oxidation of human relaxin, *J. Pharm. Sci.*, 85 (1996) 868-872
- Li, S.; Schoeneich, C.; Borchardt, R. T., Chemical instability of protein pharmaceuticals: mechanisms of oxidation and strategies for stabilization, *Biotechnol. Bioeng.*, 48 (1995a) 490-500
- Li, S.; Nguyen, T. H.; Schoeneich, C.; Borchardt, R. T., Aggregation and precipitation of human relaxin induced by metal-catalyzed oxidation, *Biochemistry*, 34 (1995b) 5762-5772
- Liu, D. T.-J., Glycoprotein pharmaceuticals: scientific and regulatory considerations, and the US Orphan Drug Act, *Trends Biotechnol.*, 10 (1992) 114-120
- Liu, I.-C.; Tsiang, R. C., Method of determining the absolute molecular weight from gel permeation chromatograms for star-shaped styrenic block copolymers, *J. Polymer Sci.*, 41 (2003) 976-983

- Liu, J.; Shire, S. J., Analytical ultracentrifugation in the pharmaceutical industry, *J. Pharm. Sci.*, 88 (1999) 1237-1241
- Liu, M.-K.; Li, P.; Giddings, J. C., Rapid protein separation and diffusion coefficient measurement by frit inlet flow field-flow fractionation, *Prot. Sci.*, 2 (1993) 1520-1531
- Litzén, A.; Garn, M. B.; Widmer, H. M., Determination of acid phosphatase in cultivation medium using asymmetrical flow field-flow fractionation, *J. Biotechnol.*, 37 (1994) 291-295
- Litzén, A.; Walter, J. K.; Krischollek, H.; Wahlund, K. G., Separation and quantitation of monoclonal antibody aggregates by asymmetrical flow field-flow fractionation and comparison to gel permeation chromatography, *Anal. Biochem.*, 212 (1993) 469-480
- Litzén, A.; Wahlund, K. G., Zone broadening and dilution in rectangular and trapezoidal asymmetrical flow field-flow fractionation channels, *Anal. Chem.*, 63 (1991) 1001-1007
- Lou, J., Salt effect on separation of polyvinylpyridines by thermal field-flow fractionation, *J. Liq. Chrom. & Rel. Technol.*, 26 (2003) 165-175
- Lumry, R.; Biltonen, R.; Brandts, J., Validity of the „two-state“ hypothesis for conformational transitions of proteins, *Biopolymers*, 4 (1966) 917-944
- Lundstrom, I.; Elwing, H., Simple kinetic models for protein exchange reactions on solid surfaces, *J. Coll. Interface Sci.*, 136 (1990) 68-84
- Luo, P.; Hayes, R. J.; Chan, C.; et al., Development of a cytokine analog with enhanced stability using computational ultrahigh throughput screening, *Prot. Sci.*, 11 (2002) 1218-1226
- Lura, R.; Schrich, V., Role of peptide conformation in the rate and mechanism of deamidation of asparaginyl residues, *Biochemistry*, 27 (1988) 7671-7677
- Lykissa, E. D.; Kala, S. V.; Hurley, J. B.; Lebovitz, R. M., Release of low molecular weight silicones and platinum from silicone breast implants, *Anal. Chem.*, 69 (1997) 4912-4916
- Madorin, M.; van Hoogevest, P.; Hilfiker, R.; Langvost, B.; Kresbach, G. M.; Ehrat, M.; Leuenberger, H., Analysis of drug/plasma protein interactions by means of asymmetrical flow field-flow fractionation, *Pharm. Res.*, 14 (1997) 1706-1712
- Manning, M. C.; Patel, K.; Borchardt, R. T., Stability of protein pharmaceuticals, *Pharm. Res.*, 6 (1989) 903-918
- Martin, M.; Williams, P. S., Theoretical advancement in chromatography and related separation techniques, NATO ASI Series C, ed. by Dondi, F.; Guiochon, G., 383 (1992) 513-580
- Matthews, B. W., Structural and genetic analysis of protein stability, *Annual Rev. Biochem.*, 62 (1993) 139-160
- Maxwell, K. L.; Davidson, A. R., Mutagenesis of a buried polar interaction in an SH3 domain; sequence conservation provides the best prediction of stability effects, *Biochemistry*, 37 (1998) 16172-16182

- Mayr, L. M.; Schmid, F. X., Stabilization of a protein by guanidinium chloride, *Biochemistry*, 32 (1993) 7994-7998
- McClements, D. J., Modulation of globular protein functionality by weakly interacting cosolvents, *Crit. Rev. Food Sci. Nutrition*, 42 (2002) 417-471
- McLeod, A. G.; Walker, I. R.; Hayward, C. P., Loss of factor VIII activity during storage in PVC containers due to adsorption, *Haemophilia*, 6 (2000) 89-92
- McNulty, S. E.; Sharkey, S. J.; Schieren, H., Bedside hemoglobin measurements: sensitivity to changes in serum protein and electrolytes, *J. Clin. Monit.*, 10 (1994) 377-381
- Mes, E. P.; Kok, W. Th.; Tijssen, R., Sub-micron particle analysis by thermal field-flow fractionation and multi-angle light scattering detection, *Chromatographia*, 53 (2001) 697-703
- Mi, Y.; Wood, G.; Thoma, L.; Rashed, S., Effects of polyethylene glycol molecular weight and concentration on lactate dehydrogenase activity in solution and after freeze-thawing, *PDA J. Pharm. Sci. Technol.*, 56 (2002) 115-123
- Miller, M.; Ph.D. Thesis, Department of Chemistry, University of Utah (1996)
- Miller, C. A.; Raney, K. H., Solubilization emulsification mechanisms of detergency, *Colloids Surf. A.*, 74 (1993) 169-215
- Millet, I. S.; Doniach, S.; Plaxco, K. W., Toward a taxonomy of the denatured state: small angle scattering studies of unfolded proteins, *Adv. Prot. Chem.*, 62 (2002) 241-262
- Min, B. R.; Kim, S. J.; Ahn, K.-H.; Moon, M. H., Hyperlayer separation in hollow fiber flow field-flow fractionation: effect of membrane materials on the resolution and selectivity, *J. Chromatogr. A*, 950 (2002) 175-182
- Moon, M. H.; Williams, P. S.; Kang, D.; Hwang, I., Field and flow programming in frit-inlet asymmetrical flow field-flow fractionation, *J. Chromatogr. A*, 955 (2002) 263-272
- Moon, M. H.; Hwang, I., Hydrodynamic vs. focusing relaxation in asymmetrical flow field-flow fractionation, *J. Liq. Chrom. & Rel. Technol.*, 24 (2001) 3069-3083
- Moon, M. H., Sedimentation field-flow fractionation, in *Field-flow fractionation handbook*, ed. by Schimpf, M. E.; Caldwell, C.; Giddings, J. C. (2000) 225-237
- Moon, M. H.; Myers, M. N., Experimental field-flow fractionation: practises and precautions, in *Field-flow fractionation handbook*, ed. by Schimpf, M.; Caldwell, C.; Giddings, J. C., (2000) 225-237
- Moon, M. H.; Kim, K.-M.; Byun, Y.; Pyo, D., *J. Liq. Chrom. & Relat. Technol.*, 22 (1999) 2729
- Moreira, T.; Cabrera, L.; Gutierrez, A., Role of temperature and moisture on monomer content of freeze-dried human albumin, *Acta Pharm. Nord.*, 4 (1992) 59-60
- Moss, B. A., Peptide synthesis, in *Pharmaceutical formulation development of peptides and proteins*, ed. by Frokjaer, S.; Hovgaard, L., London, UK (2000)

- Mueck, C., Analytics of protein aggregation via Coulter-principle: comparison with light obscuration technique, Diploma thesis, Albstadt-Sigmaringen, Germany (2002)
- Mueller, R. H.; Zetapotential und Partikelladung in der Laborpraxis, Wissenschaftliche Verlagsgesellschaft Stuttgart (1996)
- Muller, A. J.; Opila, R. L.; A new rapid screening method for silicones by size-exclusion chromatography, *Electr. Contacts*, 34 (1988) 289-300
- Mundry, T.; Surmann, P.; Schurreit, T., Trace analysis of silicone oil in aqueous parenteral formulations and glass containers by graphite furnace atomic absorption spectrometry, *Pharm. Ind.*, 63 (2001) 301-311
- Mundry, T.; Surmann, P.; Schurreit, T., Surface characterization of polydimethylsiloxane treated pharmaceutical glass containers by X-ray-excited photo- and Auger electron spectroscopy, *Fresenius' J. Anal. Chem.*, 368 (2000) 820-831
- Mundry, T., Heat curing siliconization of pharmaceutical glass containers, Dissertation, Humboldt-University Berlin (1999)
- Nagaki, M.; Hughes, R. D.; Lau, J. Y.; Williams, R., Removal of endotoxin and cytokines by adsorbents and the effect of plasma protein binding, *Artificial Organs*, 14 (1991) 43-50
- Narhi, L. O.; Arakawa, T.; Aoki, K. H.; Elmore, R.; Rohde, M. F.; Boone, T.; Strickland, T. W., The effect of carbohydrate on the structure and stability of erythropoietin, *J. Biol. Chem.*, 266 (1991) 23022-23026
- Naughton, C. A.; Duppong, L. M.; Forbes, K. D.; Sehgal, I., Stability of multidose, preserved formulation epoetin alfa in syringes for three and six weeks, *American J. Health-System Pharm.*, 60 (2003) 464-468
- Nguyen, T. H.; Ward, C., Stability characterization and formulation development of Alteplase, a recombinant tissue plasminogen activator, in *Stability and characterization of protein and peptide drugs, case histories*, *Pharmaceutical Biotechnology*, ed. by Wang, Y. J.; Pearlman, R., 5 (1993) 91-134
- Nichols, M. R.; Moss, M. A.; Reed, D. K.; Lin, W.-L.; Mukhopadhyay, R.; Hoh, J. H.; Rosenberry, T. L., Growth of beta-amyloid(1-40) protofibrils by monomer elongation and lateral association. Characterization of distinct products by light scattering and atomic force microscopy, *Biochemistry*, 41 (2002) 6115-6127
- Niemeyer, C. M., Nanoparticles, proteins, and nucleic acids: biotechnology meets materials science, *Angew. Chem. Int. Ed.*, 40 (2001) 4128-4185
- Nilsson, M.; Birnbaum, S.; Wahlund, K.-G., Determination of relative amounts of ribosome and subunits in *Escherichia coli* using asymmetrical flow field-flow fractionation, *J. Biochem. Biophys. Methods*, 33 (1996) 9-23
- Nishimura, K.; Goto, M., Occurrence of sauce separation in white sauce with added bovine serum albumin, *Food Sci. and Technol. Inter.*, 3 (1997) 97-100

- Norde, W., Driving forces for proteins to adsorb at solid surfaces, ed. by Dekker, M., New York (1998) 27-54
- Ò Fágáin, C., Understanding and increasing protein stability, *Biochim. Biophys. Acta*, 1252 (1995) 1-14
- Olivia, A.; Llabrés, M.; Farina, J. B., Comparative study of protein molecular weights by size-exclusion chromatography and laser-light scattering, *J. Pharm. Biomed. Anal.*, 25 (2001) 833-841
- Oliyai, C.; Borchardt, R. T., Chemical pathways of peptide degradation. IV. Pathways, kinetics, and mechanism of degradation of an aspartyl residue in a model hexapeptide, *Pharm. Res.*, 11 (1993) 95-110
- Opatrny, K.; Krouzecky, A.; With, J.; Vit, L.; Eiselt, J., The effects of a polyacrylonitrile membrane and a membrane made of regenerated cellulose on the plasma concentrations of erythropoietin during hemodialysis, *Artificial Organs*, 22 (1998) 816-820
- Ortega-Vinuesa, J. L.; Tengvall, P.; Lundstroem, I., Aggregation of HSA, IgG, and fibrinogen on methylated silicon surfaces, *J. Coll. Interface Sci.*, 207 (1998) 228-239
- Ostuni, E.; Grzybowski, B. A.; Mrksich, M.; Roberts, C. S.; Whitesides, G. M., Adsorption of proteins to hydrophobic sites on mixed self-assembled monolayers, *Langmuir*, 19 (2003) 1861-1872
- Ota, I. M.; Clarke, S., Calcium affects the spontaneous degradation of aspartyl/asparaginyl residues in calmodulin, *Biochemistry*, 28 (1989) 4020-4027
- Pace, C. N., Polar group burial contributes more to protein stability than nonpolar group burial, *Biochemistry*, 40 (2001) 310-313
- Pace, C. N.; Shirley, B. A.; McNutt, M.; Gajiwala, K., Forces contributing to the conformational stability of proteins, *FASEB J.*, 10 (1996) 75-83
- Pace, C. N.; Laurents, D. V., A new method for determining the heat capacity change for protein folding, *Biochemistry*, 28 (1989) 2520-2525
- PAGI, Commission on methods for testing photographic gelatin, in *Photographic and gelatin industries of Japan (PAGI)*, Tokyo, Japan (1997) p. 32
- Palkar, S. A.; Schure, M. R., Mechanistic study of electrical field flow fractionation. 1. Nature of the internal field, *Anal. Chem.*, 69 (1997a) 3223-3229
- Palkar, S. A.; Schure, M. R., Mechanistic study of electrical field flow fractionation. 2. Effect of sample conductivity on retention, *Anal. Chem.*, 69 (1997b) 3230-3238
- Park, I.; Paeng, K.-J.; Yoon, Y.; Song, J.-H.; Moon, M. H., Separation and selective detection of lipoprotein particles of patients with coronary artery disease by frit-inlet asymmetrical flow field-flow fractionation, *J. Chromatogr. B*, 780 (2002) 415-422

- Patel, K.; Borchardt, R. T., Chemical pathways of peptide degradation. II. Kinetics of deamidation of an asparaginyl residue in a model hexapeptide, *Pharm. Res.*, 7 (1990) 703-711
- Patro, S. Y.; Freund, E.; Chang, B. S., Protein formulation and fill-finish operations, *Biotechnol. Ann. Rev.*, 8 (2002) 55-84
- Patro, S.; Przybycien, T. M., Simulations of reversible protein aggregate and crystal structure, *Biophys. J.*, 70 (1996) 2888-2902
- Patton, J. S., Deep-lung delivery of therapeutic proteins, *Chemtech*, 27 (1997) 34-38
- Pauck, T.; Coelfen, H., Hydrodynamic analysis of macromolecular conformation. A comparative study of flow field-flow fractionation and analytical ultracentrifugation, *Anal. Chem.*, 70 (1998) 3886-3891
- PDA Parenteral Drug Association, Technical Report No. 12, Siliconization of parenteral drug packaging components, *J. Parent. Sci. Technol.*, 42 (1988) 1-13
- PDA Parenteral Drug Association, Technical Methods Bulletin No. 2, Elastomeric closures: evaluation of significant performance and identity characteristics, Philadelphia, PA, USA (1981)
- Pearlman, N.; Nguyen, T., Pharmaceutics of protein drugs, *J. Pharm. Pharmacol.*, 44 (1992) 178-185
- Pernigo, N.; Bottura, M.; Ravizza, R., Definition of the mean molecular weight of a gelatin lysate used as a plasma substitute, by means of size-exclusion gel-permeation chromatography, *Riv. Tossicol. Sper. Clin.*, 24 (1994) 63-72
- Pessela, B. C.; Mateo, C.; Carrascosa, A., One-step purification, covalent immobilization, and additional stabilization of a thermophilic poly-his-tagged beta-galactosidase from *thermus* sp. strain T2 by using novel heterofunctional chelate-epoxy sephabeads, *Biomacromolecules*, 4 (2003) 107-113
- Petrucelli, S.; Anon, M. C., Soy protein isolate components and their interactions, *J. Agric. Food Chem.*, 43 (1995) 1762-1767
- Pikal, M. J.; Dellerman, K. M.; Roy, M. L.; Riggin, R. M., The effects of formulation variables on the stability of freeze-dried human growth hormone, *Pharm. Res.*, 8 (1991) 427-436
- Pikal, M. J.; Freeze-drying of proteins II: formulation selection, *Biopharm.*, 3 (1990) 26-30
- Pikal-Cleland, K. A.; Carpenter, J. F., Lyophilization-induced protein denaturation in phosphate buffer systems: monomeric and tetrameric beta-galactosidase; *J. Pharm. Sci.*, 90 (2001) 1255-1268
- Pikal-Cleland, K. A.; Rodriguez-Hornedo, N.; Amidon, G. L.; Carpenter, J. F., Protein denaturation during freezing and thawing in phosphate buffer systems: monomeric and tetrameric beta-galactosidase, *Arch. Biochem. Biophys.*, 384 (2000) 398-406

- Piros, N.; Cromwell, M. E.; Bishop, S., Differential stability of a monoclonal antibody in acetate, succinate, citrate, and histidine buffer systems, 225th ACS National Meeting, New Orleans, LA, USA (2003) March 23-27
- Plotnikov, V.; Rochalski, A.; Brandts, M.; Brandts, J. F.; Williston, S.; Frasca, V.; Lin, L.-N., An autosampling differential scanning calorimeter instrument for studying molecular interactions, *Assay and Drug Dev. Technol.*, 1 (2002) 83-90
- Poepplmeyer, M., Nadir Filtration GmbH, Wiesbaden, Germany, oral information, 2002
- Powell, M. F., A compendium and hydrophathy/flexibility analysis of common reactive sites in proteins: reactivity at Asn, Asp, Gln and Met motifs in neutral pH solution, in *Formulation, characterization and stability of protein drugs*, ed. by Pearlman, R.; Wang, Y. J. (1996) 1-140
- Prabha, S.; Zhou, W.-Z.; Panyam, J.; Labhasetwar, V., Size-dependency of nanoparticle-mediated gene transfection: studies with fractionated nanoparticles, *Int. J. Pharm.*, 244 (2002) 105-115
- Privalov, P. L.; Gill, S. J., Stability of protein structure and hydrophobic interaction, *Adv. Protein Chem.*, 39 (1988) 191-234
- Przybycien, T. M.; Wilcox, A., High-throughput tools for the development of physically stabilized protein formulations, 224th ACS National Meeting, Boston, MA, USA (2002) August 18-22
- Puntis, J. W.; Wilkins, K. M.; Ball, P. A.; Rushton, D. I.; Booth, I. W., Hazards of parenteral treatment: do particles count?, *Ach. Dis. Child.*, 67 (1992) 1475-1477
- Querol, E.; Pervez-Pons, J. A.; Mozo-Villarias, A., Analysis of protein conformational characteristics related to thermostability, *Protein Eng.*, 9 (1996) 265-271
- Raman, C. V., Relation of Tyndall effect to osmotic pressure in colloidal solutions, *Indian J. Physics*, 2 (1927) 1-6
- Ramm, K.; Gehrig, P.; Plueckthun, A., Removal of the conserved disulfide bridges from the scFv fragment of an antibody: effects on folding kinetics and aggregation, *J. Molec. Biol.*, 290 (1999) 535-546
- Rampon, V.; Genot, C.; Riaublanc, A.; Anton, M.; Axelos, M. A.; McClements, D. J., Front-face fluorescence spectroscopy study of globular proteins in emulsions: displacement of BSA by a nonionic surfactant, *J. Agric. Food Chem.*, 51 (2003) 2482-2489
- Randolph, T. W.; Seefeldt, M.; Carpenter, J. F., High hydrostatic pressure as a tool to study protein aggregation and amyloidosis, *Biochim. Biophys. Acta*, 1595 (2002) 224-234
- Ratanathanawongs, S. K.; Giddings, J. C., Dual-field and flow-programmed lift hyperlayer field-flow fractionation, *Anal. Chem.*, 64 (1992) 6-15

- Reithmeier, H.; Dickes, M.; Winter, G., Accelerated isothermal and non-isothermal stability studies of aqueous protein formulations, 28th Int. Symp. Control. Bioact. Mater., San Diego, CA, USA (2001) June 23-27
- Remmele, R. L.; Bhat, S. D.; Phan, D. H.; Gombotz, W. R., Minimization of recombinant human Flt3 ligand aggregation at the T_m plateau: a matter of thermal reversibility, *Biochemistry*, 38 (1999) 5241-5247
- Remmele, R. L.; Nightlinger, N. S.; Srinivasan, S.; Gombotz, W. R., Interleukin-I receptor (IL-IR) liquid formulation development using differential scanning calorimetry, *Pharm. Res.*, 15 (1998) 200-208
- Reschiglian, P.; Zattoni, A.; Roda, B.; Casolari, S., Bacteria sorting by field-flow fractionation. Application to whole-cell escherichia coli vaccine strains, *Anal. Chem.*, 74 (2002) 4895-4904
- Reubsaet, J. L.; Beijnen, J. H.; Bult, A.; van Maanen, R. J.; Marchal, J. A.; Underberg, W. J., Analytical techniques used to study the degradation of proteins and peptides: physical instability, *J. Pharm. Biomed. Anal.*, 17 (1998) 979-984
- Richards, F. M.; Protein stability: still an unsolved problem, *Cell. Mol. Life Sci.*, 53 (1997) 790-802
- Riesz, P.; Kondo, T., Free radical formation induced by ultrasound and its biological implications, *Free Radical Biol. Med.*, 13 (1992) 247-270
- Robertson, A. D.; Murphy, K. P., Protein structure and the energetics of protein stability, *Chem. Rev.*, 97 (1997) 1251-1267
- Robinson, A. B.; Rudd, C. J., Deamidation of glutamyl and asparaginyl residues in peptides and proteins, *Curr. Top. Cell. Regul.*, 8 (1974) 247-295
- Roefs, S. P.; De Kruif, K. G., A model for the denaturation and aggregation of beta-lactoglobulin, *Eur. J. Biochem.*, 226 (1994) 883-889
- Roessner, D.; Kulicke, W. M., On-line coupling of flow field-flow fractionation and multi-angle laser light scattering, *J. Chromatogr. A*, 687 (1994) 249-258
- Roger, P.; Baud, B.; Colonna, P., Characterization of starch polysaccharides by flow field-flow fractionation-multi-angle laser light scattering-differential refractometer index, *J. Chromatogr. A*, 917 (2001) 179-185
- Rohani, S.; Chen, M., Aggregation and precipitation kinetics of canola protein by isoelectric precipitation, *Canadian J. Chem. Engineer.*, 71 (1993) 689-698
- Rosenqvist, E.; Jossang, T.; Feder, J., Thermal properties of human IgG, *Molecular Immunology*, 24 (1987) 495-501
- Rowe, A. W.; Counce, R. M.; Morton, S. A.; Hu, M.; dePaoli, D. W., Oil detachment from solid surfaces in aqueous surfactant solutions as a function of pH, *Ind. Eng. Chem. Res.*, 41 (2002) 1787-1795

- Roy, K.; Mao, H.-Q.; Huang, S.-K.; Leong, K. W., Oral gene delivery with chitosan-DNA nanoparticles generates immunologic protection in a murine model of peanut allergy, *Nature Med.*, 5 (1999) 387-391
- Russel, W.; Saville, D.; Schowalter, W., *Colloidal dispersions*; Cambridge University Press (1989)
- Ruzgas, T.; Razumas, V.; Kulys, J., Sequential adsorption of γ -interferon and bovine serum albumin on hydrophobic silicon surfaces, *J. Colloid Interface Sci.*, 151 (1992), 136-143
- Saltzman, W. M., Diffusion and drug dispersion, in *Drug delivery – engineering principles for drug therapy* (2001) 23-49
- Saltzman, W. M.; Radomsky, M. L.; Whaley, K. J.; Cone, R. A., Antibody diffusion in human cervical mucus, *Biophys. J.*, 66 (1994) 508-515
- Satoru, M.; Moto, K.; Yukitaka, U.; Hiroshige, H.; Kunio, N., Spermine induces cataract and 43-kDa protein that binds spermine possibly participates in the cataract formation, *Biochim. Biophys. Acta*, 1637 (2003) 70-74
- Schimpf, M. E., Thermal field-flow fractionation, in *Field-flow fractionation handbook*, ed. by Schimpf, M. E.; Caldwell, K.; Giddings, J. C. (2000a) 239-256
- Schimpf, M. E., Resolution and fractionating power, in *Field-flow fractionation handbook*, ed. by Schimpf, M. E.; Caldwell, K.; Giddings, J. C. (2000b) 71-78
- Schimpf, M. E., Optimization, in *Field-flow fractionation handbook*, ed. by Schimpf, M. E., Caldwell, K.; Giddings, J. C. (2000c) 95-102
- Schimpf, M. E.; Caldwell, K.; Giddings, J. C., *Field-flow fractionation handbook* (2000)
- Schmidt, R., Department for Pharmaceutical Technology and Biopharmaceutics, Ludwig-Maximilians-University Munich, Germany (2003) oral communication
- Schnablegger, H.; Glatter, O., Simultaneous determination of size distribution and refractive index of colloidal particles from static light-scattering experiments, *J. Colloid Interface Sci.*, 158 (1993) 228-242
- Schoeneich, C.; Hageman, M. J.; Borchardt, R. T., Stability of peptides and proteins, in *Controlled Drug Delivery Challenges and Strategies*, ed. by Park, K. (1997) 205-228
- Schunk, T. C.; Long, T. E., Compositional distribution characterization of poly(methyl methacrylate)-graft-polydimethylsiloxane copolymers, *J. Chromatogr. A*, 692 (1995) 221-232
- Schure, M. R.; Schimpf, M. E.; Schettler, P. D., Retention – normal mode, in *Field-flow fractionation handbook*, ed. by Schimpf, M. E.; Caldwell, K.; Giddings, J. C. (2000) 31-48
- Sendo, T.; Otsubo, K.; Hisazumi, A.; Aoyama, T.; Oishi, R., Particle contamination in contrast media induced by disposable syringes, *J. Pharm. Sci.*, 84 (1995) 1490-1491
- Serpell, L. C.; Berriman, J.; Jakes, R.; Goedert, M.; Crowther, R. A., Fiber diffraction of synthetic alpha-synuclein filaments shows amyloid-like cross-beta conformation, *Proc. Natl. Acad. Sci. USA*, 97 (2000) 4897-4902

- Sharokh, Z.; Strantton, P.R.; Eberlein, G. A.; Wang, Y. J., Approaches to analysis of aggregates and demonstrating mass balance in pharmaceutical protein (basic fibroblast growth factor) formulations, *J. Pharm. Sci.*, 83 (1994) 1645-1649
- Shiragami, N.; Particles size analysis for micro-particles by capillary hydrodynamic chromatography, *Kona*, 9 (1991) 13-18
- Shortle, D., The denatured state (the other half of the folding equation) and its role in protein stability, *FASEB J.*, 10 (1996) 27-34
- Shortt, D. W.; Roessner, D.; Wyatt, P. J., Absolute measurement of diameter distributions of particles using a multiangle light scattering photometer coupled with flow field-flow fractionation; *Am. Lab.*, 28 (1996) 21-28
- Sibbald, M.; Lewandowski, L.; Mallamaci, M.; Johnson, E., Multidisciplinary characterization of novel emulsion polymers, *Macromol. Symp.*, 155 (2000) 213-228
- Sible, V. S., Quantitative analysis of a biocide in silicone emulsions using high performance liquid chromatography, *J. Liq. Chrom. & Rel. Technol.*, 19 (1996) 1353-1367
- Singh, M.; Briones, M.; Ott, G.; O'Hagar, D., Cationic microparticles: a potent delivery system for DNA vaccines, *Proc. Natl. Acad. Sci. USA*, 97 (2000) 811-816
- Sivars, K.; Bergfeldt, K.; Piculell, L; Tjerneld, F., Protein partitioning in weakly charged polymer-surfactant aqueous two-phase systems, *J. Chromatogr. B*, 680 (1996) 43-53
- Skjelkvale, R.; Duncan, C. L., Characterization of enterotoxin purified from *Clostridium perfringens* type C, *Infect. Immunity*, 11 (1975) 1061-1068
- Southan, M.; MacRitchie, F., Molecular weight distribution of wheat proteins, *Cereal Chemistry*, 76 (1999) 827-836
- Speed, M. A.; Wang, D. I.; King, J., Specific aggregation of partially folded polypeptide chains: the molecular basis of inclusion body composition, *Nat. Biotechnol.*, 14 (1996) 1283-1287
- Spicer, P. T.; Keller, W.; Pratsinis, S. E., The effect of impeller type on floc size and structure during shear-induced flocculation, *J. Colloid. Interface Sci.*, 184 (2002) 112-122
- Stadtman, E. R., Oxidation of free amino acids and amino acid residues in proteins by radiolysis and by metal-catalyzed reactions, *Ann. Rev. Biochem.*, 62 (1993) 797-821
- Steckel, H.; Eskandar, F.; Witthohn, K., The effect of formulation variables on the stability of nebulized aviscumine, *Int. J. Pharm.*, 257 (2003) 181-194
- Steinbach, H; Sucker, C., Water association on spreaded films-IV: polyorganosiloxanes, *Colloid Polym. Sci.*, 252 (1975) 306-316
- Stephenson, R. C.; Clarke, S., Succinimide formation from aspartyl and asparaginyl peptides as a model for the spontaneous degradation of proteins, *J. Biol. Chem.*, 264 (1989) 6164-6170
- Stevenson, S. G.; Preston, K. R., Effects of surfactants on wheat protein fractionation by flow field-flow fractionation, *J. Liq. Chrom. & Rel. Technol.*, 20 (1997) 2835-2842

- Straub, J. A.; Akiyama, A.; Parma, P.; Musso, G. F., Chemical pathways of degradation of the bradykinin analog RMP-7, *Pharm. Res.*, 12 (1995) 305-308
- Stuting, H. H.; Krull, I. S., Complete on-line determination of biopolymer molecular weight high-performance liquid chromatography coupled to low-angle laser light scattering, ultraviolet, and differential refractive index detection, *Anal. Chem.*, 62 (1990) 2107-2114
- Sunde, M.; Blake, C., The structure of amyloid fibrils by electron microscopy and X-ray diffraction, *Adv. Prot. Chem.*, 50 (1997) 123-159
- Taisne, L.; Walstra, P.; Cabane, B., Transfer of oil between emulsion droplets, *J. Colloid Interface Sci.*, 184 (1996) 378-390
- Takeda, N.; Kato, M.; Taniguchi, Y., Pressure- and thermally-induced reversible changes in the secondary structure of ribonuclease A studied by FT-IR spectroscopy, *Biochemistry*, 34 (1995) 5980-5987
- Thompson, G.H.; Myers, M. N.; Giddings, J. C., Thermal field-flow fractionation and polystyrene samples, *Anal. Chem.*, 41 (1969) 1219-1222
- Thompson, G. H.; Myers, M. N.; Giddings, J. C., Observation of a field-flow fractionation effect with polystyrene samples, *Sep. Sci.*, 2 (1967) 797-800
- Thompson, L., The role of oil detachment mechanisms in determining optimum detergency conditions, *J. Coll. Interface Sci.*, 163 (1994) 61-73
- Timasheff, S. N., Control of protein stability and reactions by weakly interacting co-solvents: the simplicity of the complicated, *Adv. Prot. Chem.*, 51 (1998) 355-432
- Timmins, P.; Jackson, I. M.; Wang, Y. J., Factors affecting captopril stability in aqueous solution, *Int. J. Pharm.*, 11 (1982) 329-336
- Tomizawa, H.; Yamada, H.; Tanigawa, K.; Imoto, T., Effect of additives on irreversible inactivation of lysozyme at neutral pH and 100 °C, *J. Biochem.*, 117 (1995a) 364-369
- Tomizawa, H.; Yamada, H.; Wada, K.; Imoto, T., Stabilization of lysozyme against irreversible inactivation by suppression of chemical reactions, *J. Biochem.*, 117 (1995b) 635-639
- Towns, J. K.; Regnier, F. E., Capillary electrophoretic separations of proteins using nonionic surfactant coatings, *Anal. Chem.*, 63 (1991) 1126-1132
- Truong-Le, V. L.; Walsh, S. M.; Schweibert, E.; Mao, H.-Q.; Guggino, W. B.; August, J. T.; Leong, K. W., Gene transfer by DNA-gelatin nanospheres, *Arch. Biochem. Biophys.*, 361 (1999) 47-56
- Tsai, P. K.; Volkin, D. B.; Dabora, J. M., Formulation design of acidic fibroblast growth factor, *Pharm. Res.*, 10 (1993) 649-659
- Tyler-Cross, R.; Schrich, V., Effects of amino acid sequence, buffers, and ionic strength on the rate and mechanisms of deamidation of asparagine residues in small peptides, *J. Biol. Chem.*, 266 (1991) 22549-22556
- Tyrell, H. J., Diffusion and heat flows in liquids, ed. by Butterworths, London, UK (1961)

- Ueno, T.; Stevenson, S. G.; Preston, K. R.; Nightingale, M. J.; Marchylo, B. M., Simplified dilute acetic acid based extraction procedure for fractionation and analysis of wheat flour protein by size exclusion HPLC and flow field-flow fractionation, *Cereal Chem.*, 79 (2002) 155-161
- Uversky, V. N.; Li, J.; Fink, A. L., Evidence for a partially folded intermediate in alpha-synuclein fibril formation, *J. Biol. Chem.*, 276 (2001) 10737-10744
- van Aken, G. A.; Zoet, F. D., Coalescence in highly concentrated coarse emulsions, *Langmuir*, 16 (2000) 7131-7138
- van Asten, A., An exploration of thermal field-flow fractionation, Dissertation, Amsterdam (1995)
- van Bruijnsvoort, A.; Kok, W. T.; Tijssen, R., Hollow-fiber flow field-flow fractionation of synthetic polymers in organic solvents, *Anal. Chem.*, 73 (2001) 4736-4742
- van de Hulst, H. C., Scaling laws in multiple light scattering under very small angles, *Reviews in Modern Astronomy*, 9 (1996) 1-16
- van den Berg, L.; Rose, D., Effect of freezing on the pH and composition of sodium and potassium phosphate solutions: the reciprocal system $\text{KH}_2\text{PO}_4\text{-Na}_2\text{HPO}_4\text{-H}_2\text{O}$, *Arch. Biochem. Biophys.*, 81 (1959) 319-329
- Vangala, M. D.; Schwarz, T.; Kaufmann, M., Stabilization of antibodies and antibody conjugates through compatible solutes, *Bioforum*, 23 (2000) 760-762
- Veljkovic, V. B.; Lazic, M. L.; Cakic, M. D., Stability of bottled dextran solutions with respect to insoluble particle formation: a review, *Pharmazie*, 44 (1989) 305-310
- Vermeer, A. W.; Bremer, M. G.; Norde, W., Structural changes of IgG induces heat treatment and by adsorption onto a hydrophobic Teflon surface study by circular dichroism spectroscopy, *Biochim. Biophys. Acta*, 1425 (1998) 1-12
- Veronese, F. M., Peptide and protein Pegylation: a review of problems and solutions, *Biomaterials*, 22 (2001) 405-417
- Vrkljan, M.; Foster, T. M.; Powers, M. E., Thermal stability of low molecular weight urokinase during heat treatment. Part 2. Effect of polymeric additives, *Pharm. Res.*, 11 (1994) 1004-1008
- Wahlund, K. G.; Wittgren, B.; Andersson, M.; van Bruijnsvoort, M., Water-soluble polymer molar mass distributions by field-flow fractionation and light scattering, 223rd ACS Nat. Meeting, Orlando, USA (2002)
- Wahlund, K. G.; Zattoni, A., Size separation of supermicrometer particles in asymmetrical flow field-flow fractionation. Flow conditions for rapid elution, *Anal. Chem.*, 74 (2002) 5621-5628
- Wahlund, K. G., Asymmetrical flow field-flow fractionation, in *Field-flow fractionation handbook*, ed. by Schimpf, M. E.; Caldwell, C.; Giddings, J. C (2000) 279-294

- Wahlund, K. G.; Litzén, A., Application of an asymmetrical flow field-flow fractionation channel to the separation and characterization of proteins, plasmids, plasmid fragments, polysaccharides and unicellular algae, *J. Chromatogr.*, 461 (1989) 73-87
- Wahlund, K. G.; Giddings, J. C., Properties of an asymmetrical flow field-flow fractionation channel having one permeable wall, *Anal. Chem.*, 59 (1987) 1332-1339
- Walsh, G., Pharmaceutical biotechnology products approved within the European Union, *Eur. J. Pharm. Biopharm.*, 55 (2003) 3-10
- Walsh, D. M.; Lomakin, A.; Benedek, G. B.; Condrón, M. M.; Teplow, D. B., Amyloid beta-protein fibrillogenesis, *J. Biol. Chem.*, 35 (1997) 22364-22372
- Walstra, P.; Smulders, I., Food colloids: proteins, lipids and polysaccharides, ed. by Dickinson, E.; Bergenstahl, B., Cambridge, UK (1995) ch.2
- Walter, E.; Moelling, K.; Pavlovic, J.; Merkle, H. P.; Microencapsulation of DNA using poly(DL-lactide-co-glycolide): stability issues and and release characteristics; *J. Control. Release*, 61 (1999) 361-374
- Wang, K.; Singh, A. K.; van Zanten, J. H., Aggregation rate measurements by zero-angle time-resolved multi-angle laser light scattering, *Langmuir*, 18 (2002) 2421-2425
- Wang, P.-L.; Udeani, G. O.; Johnston, T. P., Inhibition of granulocyte colony stimulating (G-CSF) adsorption to polyvinyl chloride using a nonionic surfactant, *Int. J. Pharm.*, 114 (1995) 177-184
- Wang, W.; Kelner, D. N., Correlation of rFVIII inactivation with aggregation in solution, *Pharm. Res.*, 20 (2003) 693-700
- Wang, W., Lyophilization and development of solid protein pharmaceuticals, *Int. J. Pharm.*, 203 (2000) 1-60
- Wang, W., Instability, stabilization, and formulation of liquid protein pharmaceuticals, *Int. J. Pharm.*, 185 (1999) 129-188
- Wang, Y. J.; Shahrokh, Z.; Vemuri, S.; Eberlein, G.; Beylin, I.; Busch, M., Characterization, stability, and formulation of basic fibroblast growth factor., in *Formulation, characterization, and stability of protein drugs*, ed. by Pearlman, R.; Wang, Y. J. (1996) 141-180
- Ward, A. G.; Courts, A., *The science and technology of gelatin*, Academic Press, New York, USA (1977)
- Weber, S. G.; Carr, P. W., in *High Performance Liquid Chromatography*, ed. by Brown, P. R.; Hartwick, R. A., New York, USA (1989) Chapter 1
- Wen, J.; Arakawa, T.; Philo, J. S., Size-exclusion chromatography with on-line light-scattering, absorbance, and refractive index detectors for studying proteins and their interactions, *Anal. Biochem.*, 240 (1996) 155-166

- White, R. J., FFF-MALS – a new tool for the characterization of polymers and particles, *Polymer Internat.*, 43 (1997) 373-379
- Whittingham, J. L.; Scott, D. J.; Chance, K.; Wilson, A.; Finch, J.; Brange, J.; Dodson, G. G., Insulin at pH 2: structural analysis of the conditions promoting insulin fibre formation, *J. Mol. Biol.*, 318 (2002) 479-490
- Wigren, R.; Elwing, H.; Erlandsson, R.; Welin, S.; Lundstroem, I.; Structure of adsorbed fibrinogen obtained by scanning force microscopy, *FEBS Letters*, 280 (1991) 225-228
- Will, S.; Leipertz, A., Thermophysical properties of fluids from dynamic light scattering, *Int. J. Thermophys.*, 22 (2001) 317-338
- Williams, P. S.; Giddings, M. C.; Giddings, J. C., A data analysis algorithm for programmed field-flow fractionation, *Anal. Chem.*, 73 (2001) 4202-4211
- Williams, P. S.; Giddings, J. C., Theory of field-programmed field-flow fractionation with corrections for steric effects, *Anal. Chem.*, 66 (1994) 4215-4228
- Williams, S. K.; Giddings, J. C., Sample recovery, in *Field-flow fractionation handbook*, ed. by Schimpf, M. E.; Caldwell, C.; Giddings, J. C. (2000) 325-343
- Williams, S. K., Flow field-flow fractionation, in *Field-flow fractionation handbook*, ed. by Schimpf, M. E.; Caldwell, C.; Giddings, J. C. (2000) 257-277
- Williams, S. K.; Butler-Veytia, B.; Lee, H., Determining the particle size distributions of titanium dioxide using sedimentation field-flow fractionation and photon correlation spectroscopy, *ACS Symposium Series*, 805 (2002) 285-298
- Wilson, G.; Hecth, L.; Barron, L. D., Residual structure in unfolded proteins revealed by raman optical activity, *Biochemistry*, 35 (1996) 12518-12525
- Winding, O.; Holma, B.; Method for determination and element analysis of particulate contamination in injectable solutions, *American J. Hosp. Pharm.*, 33 (1976) 1154-1159
- Wittgren, B.; Borgstroem, J.; Piculell, L.; Wahlund, K. G., Conformational change and aggregation of kappa-carrageenan studied by flow field-flow fractionation and multiangle light scattering, *Biopolymers*, 45 (1998) 85-96
- Wittgren, B.; Wahlund, K. G., Effects of flow-rates and sample concentration on the molar mass characterisation of modified celluloses using asymmetrical flow field-flow fractionation - multi-angle light scattering, *J. Chromatogr. A*, 791 (1997a) 135-149
- Wittgren, B.; Wahlund, K. G., Fast molecular mass and size characterization of polysaccharides using asymmetrical flow field-flow fractionation-multiangle light scattering, *J. Chromatogr. A.*, 760 (1997b) 205-218
- Wittgren, B.; Wahlund, K. G.; Dérand, H.; Wesslén, B., Aggregation behaviour of an amphiphilic graft copolymer in aqueous medium studied by asymmetrical flow field-flow fractionation, *Macromolecules*, 29 (1996) 268-276

- Wolfbeis, O. S.; Bohmer, M.; Durkop, A.; Enderlein, J.; Gruber, M.; Klimant, I.; Krause, C.; Kurner, J.; Liebisch, G.; Lin, Z.; Oswald, B.; Wu, M., *Advanced luminescent labels, probes and beads and their application to luminescence bioassay and imaging*, Springer Series on Fluorescence, 2 (2002) 3-42
- Wong, S. S.; Wong, L. J., *Chemical crosslinking and the stabilization of proteins and enzymes*, *Enz. Microb. Technol.*, 14 (1992) 866-874
- Wright, S.; Ranville, J.; Amy, G., *Relating complex solute mixture characteristics to membrane fouling*, *Water Science & Technology*, 1 (2001) 31-38
- Wyatt, P. J., *Submicrometer particle sizing by multiangle light scattering following fractionation*, *J. Colloid. Interface Sci.*, 197 (1998) 9-20
- Wyatt, P. J.; Villalpando, D. N., *High-precision measurement of submicrometer particle size distributions*, *Langmuir*, 13 (1997) 3913-3914
- Wyatt, P. J., *Light scattering and the absolute characterization of macromolecules*, *Anal. Chim. Acta*, 272 (1993) 1-40
- Wyatt, P. J.; *Absolute measurements with FFF and light scattering*, *Polym. Mat. Sci. Eng.*, 65 (1991) 198-199
- Wyatt Technology, *Separation and characterization of macromolecules and colloidal particles*, *Lab Plus Inter.*, 10 (2002) 20-21
- Xie, G. F.; Timasheff, S. N., *Mechanism of the stabilization of ribonuclease A by sorbitol: preferential hydration is greater for the denatured than for the native protein*, *Prot. Sci.*, 6 (1997) 211-221
- Yang, F. J.; Myers, M. N.; Giddings, J. C., *Programmed sedimentation field-flow fractionation*, *Anal. Chem.*, 46 (1974) 1924-1930
- Zhang, J.; Peng, X.; Jonas, A.; Jonas, J., *NMR study of the cold, heat, and pressure unfolding of ribonuclease A*, *Biochemistry*, 34 (1995) 8631-8641
- Zhang, M.; Breiner, T.; Mori, H.; Muller, A. H., *Amphiphilic cylindrical brushes with poly(acrylic acid) core and poly(n-butyl acrylate) shell and narrow length distribution*, *Makromolekulare Chemie II*, 44 (2003) 1449-1458
- Zhang, W.; Czupryn, M. J.; Boyle, P. T.; Amari, J., *Characterization of asparagine deamidation and aspartate isomerization in recombinant human interleukin-11*; *Pharm. Res.*, 19 (2002) 1223-1231
- Zhu, G.; Schwendeman, S. P., *Stabilization of bovine serum albumin encapsulated in injectable poly(lactide-co-glycolide) millicylinders*, *Proc. Int. Symp. Control. Release Bioactive Mater.*, 25th (1998) 267-268
- Zimm, B. H.; *The scattering of light and the radial distribution function of high-polymer solutions*, *Chem. Phys.*, 16 (1948) 1093-1099

Zimm, B. H., Molecular theory of the scattering of light in fluids, J. Chem. Phys., 13 (1945) 141-145

13 Publications and presentations associated with this work

Original Research Articles

1. **Fraunhofer**, W.; Winter, G.; Zillies, J.; Coester, C., Asymmetrical flow field-flow fractionation as new analytical tool in pharmaceutical biotechnology, *New Drugs*, 2 (2003) 16-19
2. **Fraunhofer**, W.; Mueck, C.; Winter, G., Characterization of proteinic particulate matter in parenterals by Coulter technique and light obscuration, *J. Pharm. Sci. Technol.*, to be submitted in 2003
3. **Fraunhofer**, W.; Winter, G., Asymmetrical flow field-flow fractionation: general and new applications of an upcoming method in pharmaceutical analysis, *J. Chromatogr. A*, to be submitted in 2003
4. **Fraunhofer**, W.; Coester, C.; Winter, G., Characterization of size and loading efficacy of gelatin nanoparticle carrier systems by means of asymmetrical flow field-flow fractionation and multi-angle light scattering, *Anal. Chem.*, to be submitted in 2003

Oral presentations

1. **Fraunhofer**, W., Asymmetrical flow field-flow fractionation combined with multi-angle laser light scattering: new applications for an upcoming method, 4th World Meeting on Pharmaceutics, Biopharmaceutics and Pharmaceutical Technology, Florence, Italy, 2002

Poster presentations

1. **Fraunhofer**, W.; Schroer, C.; Tschoepe, M.; Winter, G., Asymmetrical flow field-flow fractionation: a new approach to analysis of high-molecular weight protein aggregates?, 28th International Symposium on Controlled Release of Bioactive Materials, San Diego, USA, 2001
2. **Fraunhofer**, W.; Krause, H.-J.; Winter, G., Identification of particulate matter in siliconized disposable syringes with asymmetrical flow field-flow fractionation, 4th World Meeting on Pharmaceutics, Biopharmaceutics and Pharmaceutical Technology, Florence, Italy, 2002

3. **Fraunhofer**, W.; Krause, H.-J.; Winter, G., Towards overall quantification of protein instability outcome: fragments, aggregates, precipitates, Colorado Protein Stability Conference, Breckenridge, USA, 2002
4. Willmann, M.; **Fraunhofer**, W.; Winter, G., Reversible aggregation of G-CSF during vacuum drying from aqueous solutions, Colorado Protein Stability Conference, Breckenridge, USA, 2002
5. **Fraunhofer**, W.; Krause, H.-J.; Winter, G., Separation of particulate matter into detached silicone oil and denatured protein drug in siliconized parenteral packages: considered as yesterdays' problem?, Meeting of the American Association of Pharmaceutical Scientists, AAPS, Toronto, Canada, 2002
6. **Fraunhofer**, W.; Krause, H.-J.; Winter, G., Latest developments in asymmetrical flow field-flow fractionation: a separation method with wide applicability in pharmaceuticals, Meeting of the American Association of Pharmaceutical Scientists, AAPS, Toronto, Canada, 2002
7. Willmann, M.; **Fraunhofer**, W.; Winter, G., Vacuum drying of protein solutions: new results in evaluation of vacuum concentration processes, Meeting of the American Association of Pharmaceutical Scientists, AAPS, Toronto, Canada, 2002

14 Curriculum Vitae

Wolfgang Fraunhofer

Date of birth 03/22/1973
Place of birth Weiden i.d. Opf., Germany
Marital status unmarried

Education

79 - 83 elementary school, Pleystein, Germany
83 - 92 comprehensive secondary school, Neustadt a.d. Waldnaab, Germany
07/92 - 09/93 basic military service: clinical and paramedical service, Germany
11/93 - 04/98 Study at Regensburg University, College of Pharmacy,
Regensburg, Germany
05/98 - 10/98 Practical education in pharmacy (retail),
Maximilians-Apotheke, Regensburg, Germany
11/98 - 04/99 Practical education in pharmacy (industry),
Department of Fine Chemicals, BASF AG, Ludwigshafen, Germany
10/99 Approbation as pharmacist
08/99 - 10/99 Scientific freelance, College of Pharmacy, Free University Berlin,
Berlin, Germany
03/00 to present Ph.D. thesis: Department for Pharmaceutical Technology and
Biopharmaceutics, Ludwig-Maximilians-University, Munich, Germany,
supervisor: Prof. Dr. G. Winter;
in research cooperation with
Department of Pharmaceutical Development and Parenterals,
Abbott GmbH & Co. KG, Ludwigshafen, Germany

Professional Experience

11/99 – 02/00 Deputy head pharmacist (retail), Kreuzberg-Apotheke,
Pleystein, Germany